Fundação Homem do Mar – FHM

Brazilian Simulation Center

Final Report

Maneuverability Analysis in Panama Canal New Locks

Responsible people of the Project:

Mario Calixto

Sérgio Sphaier

Jeferson Carvalho

Ernesto Sá

Tamara Di Maria

Rio de Janeiro, Brazil – April 2016

Final Report

Register Number: CS 034 – International Transport Workers' Federation (ITF)

Rio de Janeiro, Brazil – April, 2016

Project: To assess the Vessel Type seaworthiness, in a safe way, and the tugboats to employ with the Vessel Type at the entrance and exits maneuvers from the new locks of the Panama Canal.

Contractor: International Transport Workers'Federation (ITF)

Carvalho, Jeferson Ferreira de Almeida

Panama Canal: Maneuverability Analysis in Panama Canal New Locks

102f.

Final Report

Fundação Homem do Mar (FHM)

Brazilian Simulation Center (CSA)

1. Maneuverability Simulation.
2. Panama Canal
3. International Transport Workers' Federation (ITF)
I. Title

REVISION INDEX	
REV.	DESCRIPTION AND/OR AFFECTED PAGES
00	ORIGINAL
01	TEXTUAL REVISION
02	TEXTUAL REVISION
03	TEXTUAL REVISION

	REV. 0	REV. 1	REV. 2	REV. 3	REV. 4	REV. 5
DATE	04.13.2016	04.19.2016	04.21.2016	04.25.2016		
EXECUTION	JFC	JFC	JFC	JFC		
AUTHORS	JFC	JFC	JFC	JFC		
VERIFICATION	JMC	JMC	JMC	JMC		
APPROVAL	JBF	JBF	JBF	JBF		

RESUME

Aiming safety in operations, the International Transport Workers' Federation (ITF), hereinafter called contractor, hired the Fundação Homem do Mar, hereinafter called FHM, for perform manoeuvrability studies, in mathematical modelling, using a Manoeuvring Simulator Class A. A scenario and a Vessel Type, with the charachteristics informed and requested by the contractor, were developed in mathematical modelling so that the studies were to be carried out according to the projects' needs.

Fulfilling the comercial proposal Nº CSA_2015_14_Rev._03, was developed the report, which provides the results of own ships' manoeuvrability simulations in the new locks of Panama Canal.

The simulations occurred on February 18th and 19th, 2016 by the contractor. Having the own ship approximately 145 thousand tonnes and being fully loaded, the objective of simulations were analyze the seaworthness of Vesel Type, in a secure way, in manoeuvres of entrance and exit the new locks at Panama Canal and evaluate the use of tugs that assist the manoeuvres of this own ship.

It was taking in account the environment conditions prevailing of the local according to the indicate in technical reports HID-011-2011, HID-2013-06, Hydrodynamic Modeling Study – North East Breakwater Open Water Disposal e Feasibility Study of Palo Seco – Technical Appendices, provides by the contractor.

For this study it has been taken into consideration the international specifications of operational safety, taking into account only the nautical matters.

The data source for areas' and vessels' modelling were derived of informations given by the contractor and are reported in this report. In all simulations, were created scenarios according to datas provided by the contractor.

INDEX

LIST OF FIGURES

LIST OF TABLES

1. INTRODUCTION

This final report presents the results obtained in simulations, in real-time, performed to analyse, under environment conditions indicated by the contractor and in day period, the navigability, in a secure way, of own ship and the use of tugs that are going to be needed in manoeuvres of entrance and exit the new locks at Panama Canal.

The locks utilized in this study are from the Project which consists in elaboration of third set of locks which is being built in Pacific entries (Cocolí Lock) and Atlantic (Agua Clara Lock). Each complex of locks is formed by 3 levels, 3 chambers (427 meters in length), internal gap between gates, 55 meters of width, breadth, 18.3 meters each of operational depth and 4 pairs of gate, in a total of about 1400 meters extension, without counting the approach structures. Each chamber is nourished by an adjacent pool which saves up to 60% of water, preventing the wear of Gatun Lake, which had his level increased in 45cm to the nourishment of locks.

The simulations, in mathematical modeling, also have been performed by representatives of contractor to contractor. In this study have been taken into consideration the prime elements which can affect on navigability conditions and manouevre of a vessel, such as: environmental factors (wind, current and waves), depth and canals' width, own ship's manoeuvrability characteristics, tugs, navigation assistance and interaction effect with banks and proximities. In this way, it was possible analysing the inherent risks to these variables and verify the safest way to navigate and execute all manoeuvres.

The accomplishment of this study and the results presented serve the international specifications of operational safety, valid up to issue date of this report, taking into account only nautical aspects.

This document was prepared with the best information available to FHM and to authors during their performance.

2. DECLARATION

FHM and the authors of this report make no warranties, expressed or implied, as to any matter whatsoever, concerning the inappropriate use of this document for any particular project use.

The user of this report should carefully review our suggestions before executing them; he may propose or suggest any additional information that may contribute to the safety and reliability of this project. FHM team ensures that the analysis meets the requirements, standards and regulations national and international. Therefore, industrial requirements as well as rules may be subject to other interpretations, and FHM cannot guarantee how they will be interpreted in the future.

In this case, FHM does not take any responsibility for any accident or incident that may involve the new locks of Panama Canal, and its adjacent channel access.

The parties commit to maintain strict confidentiality and secrecy of any data or information obtained in reason of this project recognize that they cannot be disclose or provide to third party, except with authorization, in writing, of Contractor.

3. SIMULATION FACILITIES VALIDATION

FHM is the entity responsible for Brazilian Simulation Centre (CSA) administration. CSA has several simulators, which are in activity since November, 2006. Among these Ship Manoeuvring Simulators, two of them are "Full-Mission", having as basis NTPro 5000 software.

The following information outlines the development process of the hydrodynamic modelling of vessels developed for simulation, executing the Vessel Type passage through the new locks of Panama Canal, with the assistance of tugs. Still, what becomes evident is the way that the simulator calculates diverse interactions with the scenario, as well as the capacity of software on managing manoeuvres characteristics.

3.1. VESSEL TYPE

In marine simulation, the term "Vessel Type" is used to describe the computer programming needed to simulate vessel behaviour. The "Vessel Type" database contains the parameters and hydrodynamic coefficients needed to calculate vessel behaviour in a dynamic environment. The source of the data is sea trial data and input from experienced ship's masters and pilots. Note: the more accurate the data provided by the client, the more accurate the Vessel Type in simulation.

The library of software manufacturer owns approximately 200 different Vessel Type, of several types of vessels and of most known projects and applied worldwide in maritime sector.

The Vessel Type takes into account:
- Main Propulsion (steam turbines, gas turbines and diesel/electro engines);
- RPM for each engine variable between full ahead and full astern.
- Vibration effect.
- Propeller (Fixed and variable pitch, Voith-Schneider, nozzles, Azipods, Jets, Z-drives, etc.).
- Thrusters of different types (multiple bow and stern);
- Rudder (single, twin, four, and high lift rudders);
- Autopilot;
- Stranding and grounding;
- Squat;
- Bank interaction effect and proximities;
- Passing ship interaction effect;
- Collision interaction effect (ownship to ownship);
- Resilient wharf interaction effect.
- Anchor dropping and dredging effect.
- Lines;
- Berthing lines and winches effect.
- Towing and pushing effect.

- Shadow area;
- Hull hydrodynamics (shallow water and bank effects);
- Several ships' areas, such as transversal, sail area, longitudinal, midship session area, etc.

The "motion" experienced within a simulation exercise is based on a continuous computation of control data into the Vessel Type. FHM system is capable of interacting with up to eight Vessel Types and over one hundred target ships, all with the same complexity level. The difference between Vessel Type and target ships is that the first one is the human interaction that controls the ship steering, while target ships can only be controlled by the instructor or by the simulator.

The images of ships viewed in Full Mission bridge and in several 3D visualizations are generate from the Virtual Shipyard 2 program that uses others auxiliaries softwares, such as Photoshop, 3D Studio Max and AutoCAD®. The visuals are then "connected" to the Vessel Type hydrodynamic model within the Simulator. The visuals are what the student/operator "sees" in the simulation. However, the behaviour is based on the hydrodynamic model.

All the ships' visual is developed in proportionately way, which means that the distance notions and depth are maintained, offering the maximum of possible reality.

3.2. MODELING SCENARIOS

The FHM have their own development and modelling team, which is responsible for develop and insert on Simulator any modelling scenarios to be used in simulation. This work is held using Model Wizard 5 software, along with others visual tools.

The making of a scenario includes planning of port constructions, bathymetric survey, and modelling of the navigation situation. CSA data base includes magnetic deviations, racons, beacon, IALA standard buoys, and several templates to create models and objects. The Development and Modelling Team incorporates an editor to create and modify 3-D models of shore objects, besides visual models of the region. The scene created may be supplemented with 3-D models (prototypes) from the Object Library or may be built using AutoCAD and 3D Studio Max, and they may be textured in Photoshop from photographs collected from the scene by the team. Lightning effects may be defined (as for example, at any time of the day or night and weather conditions).

The scenarios developed by FHM is based on its constructions electronic nautical charts, updated weekly with official data from Hydrographic Local Authority and complemented with information given by contracting party. It is also possible to work with future situations, for example, using the project of a dredged channel even before they actually start dredging it.

The work of the development team with the scenarios is usually focused on:

- Piers for berthing and unearthing operations;
- Navigational resources;
- Landmarks or conspicuous points;
- Cultural characteristics;
- Landscapes

A high level of details is required to facilitate manoeuvring and berthing and unearthing operations. The scenarios used provide visual details and depth perception to enable the manoeuvres to be conducted. Berthing wharfs are displayed with as much detail as possible without any significant degradation of the visual refresh rate. The sounds are created by the wide range of depths and heights. The navigation features receive a special attention during the development of the visual scene and are designed to accurately represent the actual size, shape and characteristic colours according to the official publications of aids to navigation. Landmarks are developed with accuracy in actual size and shape. The landscape near the banks is developed with the highest level of accuracy, recognizable appearance and depth perception. Cultural characteristics, which are not specified as landmarks, are developed in a recognizable scale and with characteristic texture. They will be visually correct when viewed from any point within area. Wharfs and piers, not designed for anchoring, are correctly positioned and appropriately detailed to the level of awareness they need.

3.3. Vessel Type Calculations

The NTPro 5000 uses six degrees of freedom (6 DOF) differential equations to calculate the Vessel Type behaviour. All hydro-forces and moments are calculated in terms of coefficients. These equations formulate the motion of the model on the basis of the following:

- Longitudinal force balance on the Vessel Type.
- Transverse force balance on the Vessel Type.
- Horizontal force balance on the Vessel Type.
- Roll momentum on the Vessel Type.
- Heave/pitch forces and moments induced by waves.

All forces and/or moments cause appropriate accelerations. The integration of accelerations provides the velocity components. The double integration of these values gives the momentary position and course of the Vessel Type. The movement of the model is calculated from the balance of all forces and moments acting on the ship's hull. The resultant forces X and Y, and the momentum, N and K, will depend on the model's current situation. Accordingly, a non-linear differential equation system of higher order describes the Vessel Type dynamics. This differential equation system is numerically integrated in steps (Euler-Cauchy) until the track of the model over ground is determined.

The Vessel Type motion limiting values are as follows:

Maximum Speed	100 knots
Maximum Rotation	120 degrees/minute

The response of the Vessel Type within the simulation exercise is dependent on the force components that are inputted into the Vessel Type model. The exercise database provides depth, current, wind/wave, and object data. Ship interaction data is provided by other targets and Vessel Types within the exercise.

3.3.1. Wind Forces

Wind forces are defined as X, Y, K, and N (4 DOF) components (constant values, plus gusting and time variable components) over the sea surface. They do become 6 DOF components if the Vessel Type has heave and pitch during navigation. The wind heave and pitch components are usually negligible, as compared to the hydrostatic forces heave/pitch equations of motion, in relation to displacement of Vessel Type.

3.3.2. Wave Forces

Wave forces are computed accurately for all 6 DOF. Accurate wave force computation is critical for modelling dynamic positioning, along with wind and current forces.

3.3.3. Current

Current effects are modelled on the underwater profile and empirical (model tests derived) coefficients for each force components.

3.3.4. Bottom Interaction

Bottom effect forces are modelled on empirical (test data) coefficients as a fraction of the depth/draft ratio multiplied by the deep water value.

3.3.5. Bank and Ship to Ship Interaction

Interaction effects are modelled using twelve (or more) points of force/pressure velocity vectors distributed along the hull and changing their values if the channel or bank configuration changes along the ship path (which gives its new force values). This is one of the most advanced methodologies used in simulation today.

3.3.6. Miscellaneous

Anchor and chain forces, mooring and fender forces, pushing/towing effects, and ship collisions are all modelled as 6 DOF units with its force/moment components defined by their location and 6 DOF ship motion parameters.

3.4. Vessel Model Editing

Mathematical models of the ships and ship equipment can be edited using the Model Wizard® 5 Editing Tool and Virtual Shipyard®. The program allows the user to adjust the mathematical model and create individual models for specific needs.

3.5. Simulators Vessel Types used in the simulations

With the use of the *Virtual Shipyard ®,* which is a vessel editing tool of the Model Wizard, it was hydrodynamically modelled the Vessel Type Heavy Lift (model in ballast) according to data given to FHM by contracting party.

Each model was undergone through validation tests conducted by Marine Consultants and by FHM Development and Modelling Team.

3.6. FHM Source Data and Tests

FHM team developed the models based on data already existent in software library and compared it against ships that are currently in service. The data also included information on the sail area of each vessel.

3.5.1. FHM Validation Tests

FHM Team compared the manoeuvring characteristics of existing and inspected vetted hydrodynamic models.

The parameters that were checked and verified during FHM Validation Tests included the following:

- Engine RPM ahead and astern settings.
- Engine RPM running up time (example – stop to full ahead).
- Engine RPM running down time (example – full ahead to stop and full astern).
- Acceleration and deceleration.
- Wind and current effect.
- Thruster's effect.
- Turning circle.
- General manoeuvring.
- Model visuals.

Final Report

4. MANOEUVRABILITY TECHNICAL ASPECTS IN CHANNELS AND RESTRICTED WATERS

4.1. Interaction effects between vessels

When the vessels are in navigation or in manoeuvres close to each other, in each vessel is perceptible the presence of the others, being in a bigger or smaller way. This is due to the pressure difference in fluid, which can be manifest in several ways, such as induction of undesirable speeds, heading involuntary changes, which can lead to accidents of high magnitude, as stranding, collisions and allisions. Hydrodynamic phenomenon responsible for this vessels' performance, in proximity of others, it's called interaction.

The interaction between vessels varies:
- With the speed squared. It means that as quicker the vessels are, stronger will be the interaction.
- Inversely with the distance between vessels. Thus, the bigger the distance between vessels, the smaller will be the effects of interaction.
- In the inverse proportion of square root in ratio between UKC (Under keel Clearance) and the draft. So, the smaller the UKC, the bigger will be the interaction.

4.2. Tug-Ship Interaction

The tug is generally much smaller than the ship it is attending and while a given depth of water may be deep for the tug, it may well be shallow for the ship. This means that, whereas the ship will have a big interactive effect on the tug, the tug will, naturally, have virtually no effect on the ship.

Modern tractor or reverse-tractor tugs have enough power and manoeuvrability to be in less danger from the effects of interaction than their conventionally propelled counterparts. This is not to say that they are unaffected. Figure 1 shows measurements of the interaction sway force and yaw moment felt by a tractor tug model keeping pace with a large ship; it is seen that large forces develop. However, the fast response and enhanced manoeuvrability of such tugs means that they are much more able to manoeuvre out of difficulty.
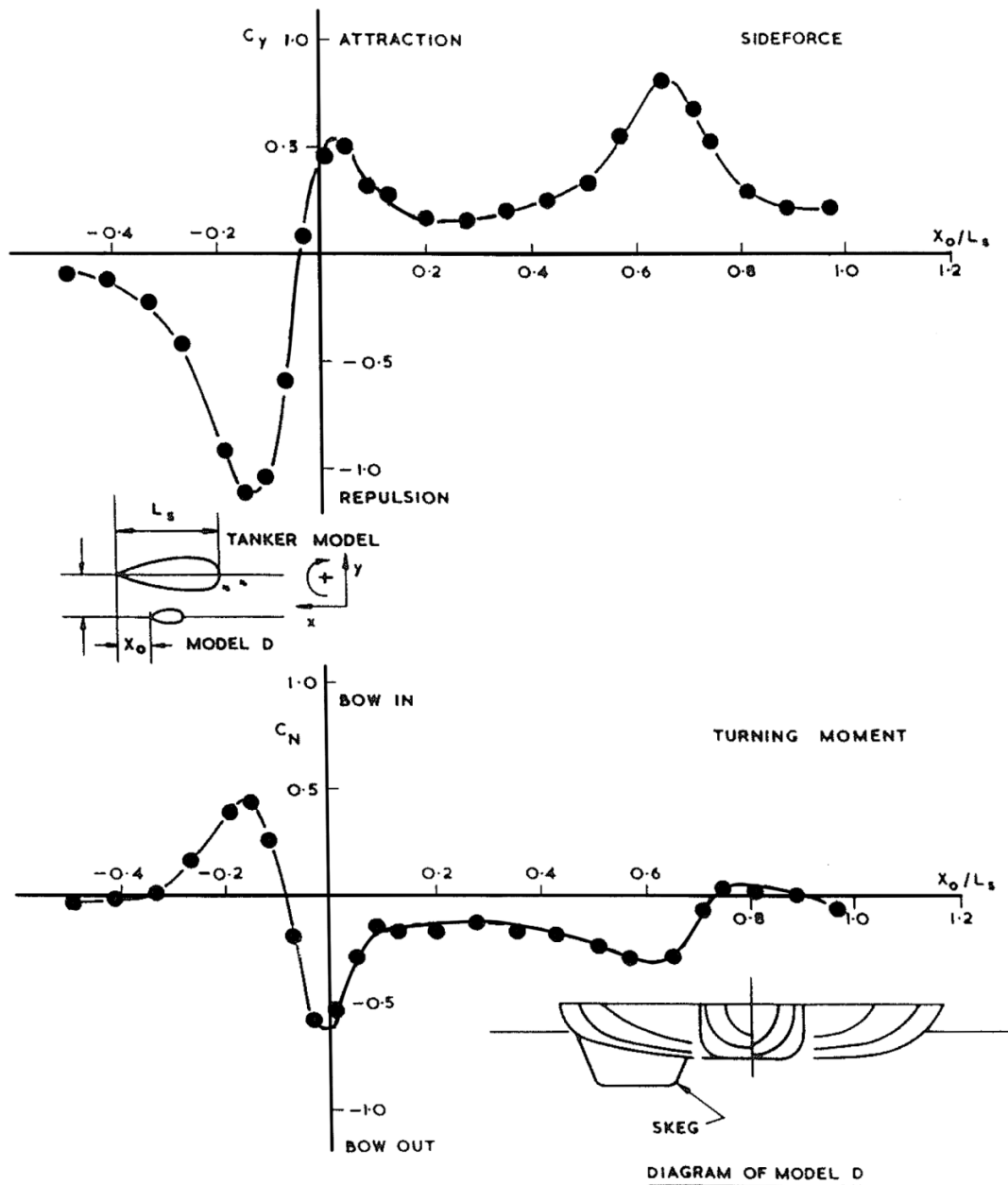
Figure 1: Interaction Forces and Moments Induced on Tractor Tug Model By Tanker Model.

For any conventionally powered (and steered) tugs and other vessels similarly equipped, Figure 2 shows diagrammatically the sort of interaction forces and moments they will experience when they come alongside. Clearly there are areas near the bow and stern those are best avoided because the control that the rudder exerts adds to, rather than subtracts from, the effects of interaction. Of particular interest is the tendency to turn under the bow of the larger vessel brought about by interaction. This has caught a number of conventional tugs unawares over the years with disastrous consequences. The sudden changes in the interaction forces and moments acting on the vessel as it alters its fore and aft position alongside the bigger ship are largely to blame; if they are not anticipated by helmsman, the smaller vessel will drive itself under the bow of the bigger ship.
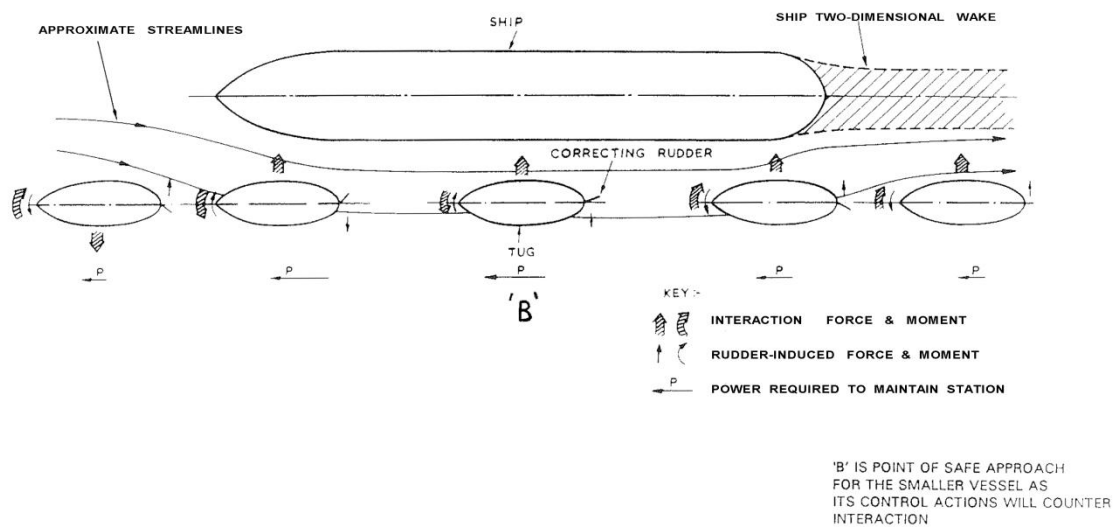
Figure 2: Tug-Ship Interaction.

4.3. Interaction Effects Influencing

Vessels moving in shallow or enclosed areas can generate interaction-like effects. There are different kinds of interaction. Some influence tug performance, others affect tug safety, some both. A few are now considered.

4.3.1. Swinging and Manoeuvring

A vessel manoeuvring unaided in an enclosed area may use a combination of propellers and thrusters. This may cause the water in the area to move and the resultant swinging of the ship (which acts as a form of 'paddle') will cause further movement and pressure changes.

4.3.2. Tug Pumping

The modern harbor tug is usually powered by one or more propellers or, more generally nowadays, by two powerful thrusters. Not only are these good propulsion devices, but in the confined space of an area they act as effective pumps, setting water in motion. In a very confined space (especially if the tugs are on short lines), they can cause the ships they are attending to move in unexpected ways. Figure 3 shows a situation which was modelled physically; it shows how the flow induced by tug wash causes local pressure changes which affect the ship. Notice how the ship moves bodily toward the tug even though the direction in which the tug is pulling does not suggest such behaviour. Similar effects have been experienced in lock-bell-mouths when tug action has inadvertently caused ships to move in an unexpected direction. In extreme cases tug wash can cause and effect which is directly contrary to that expected. Figure 4 shows the turning moment measured on a ship model when 'towed' by a tug in the manner shown. Notice how the turning moment on the ship actually changes sign (i.e. acts in a direction opposite to the expected) at the shallowest water depth. This is yet

another example of the powerful effect of shallow water, and suggests that care should be taken when using powerful tugs on short lines in enclosed areas.
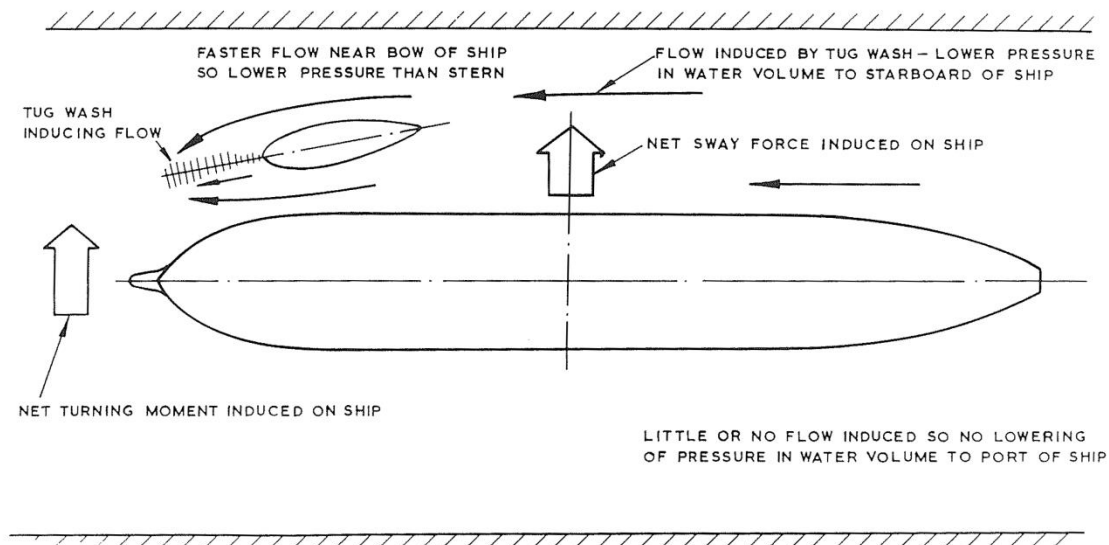
Figure 3: Indirect Effect of Tug Wash in Confined Water.
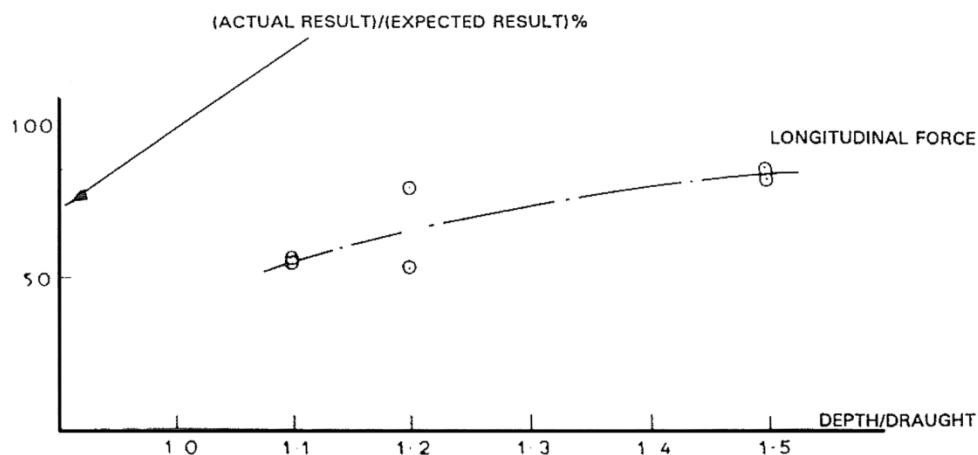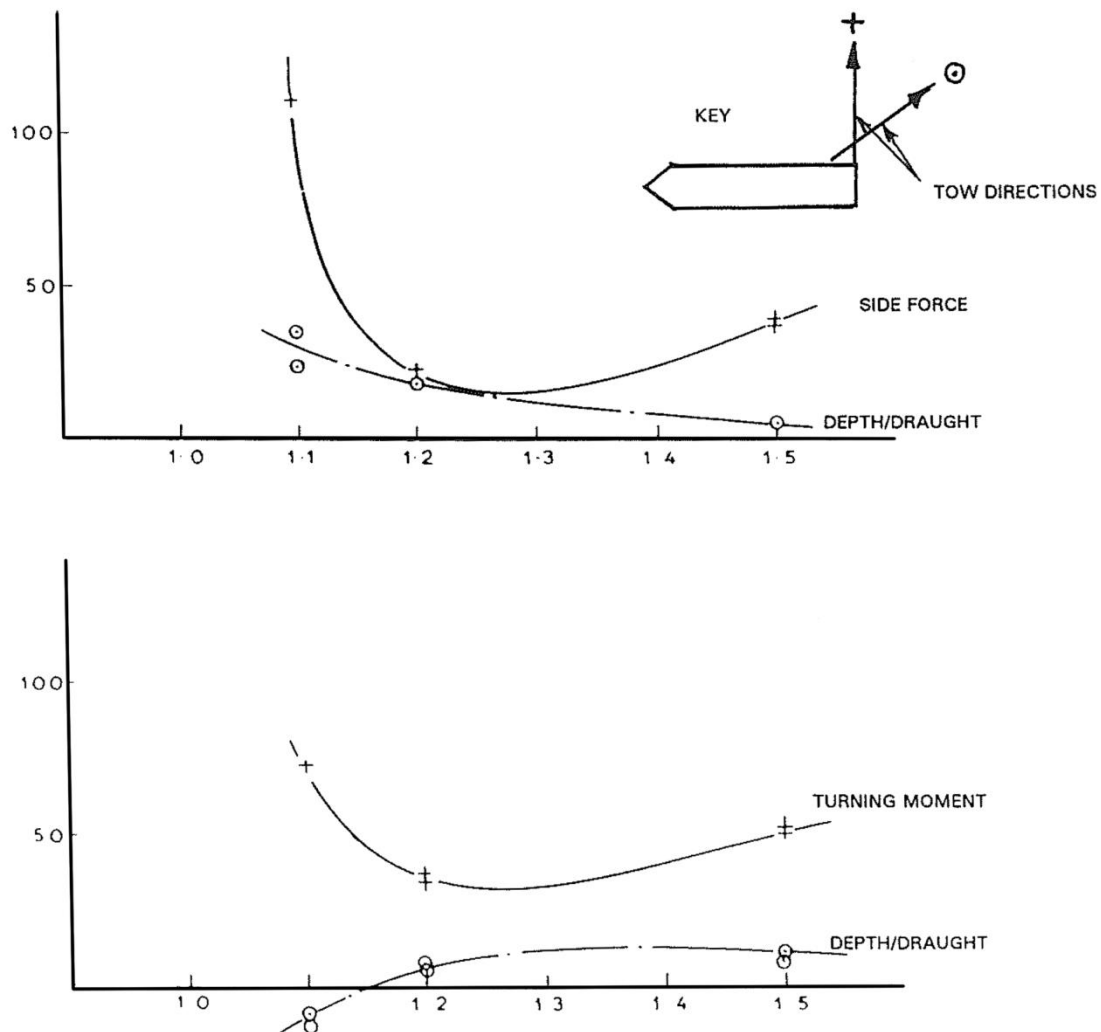
Figure 4: Tug Wash Effects in a Confined Space.

4.3.3. The Following Wake

When a ship slows down too abruptly, the water moving with it may not be so obliging. The ship's wake takes time to slow down and, in shallow, confined alters it should be remembered that the body of water which moves with the ship takes time to slow down and in so doing, will overtake the ship. This may often affect the vessel and can move it ahead or, in extreme cases, turn it in an uncontrolled manner, see Figure 5. The lesson is clearly to reduce speed or a swinging manoeuvre gradually.
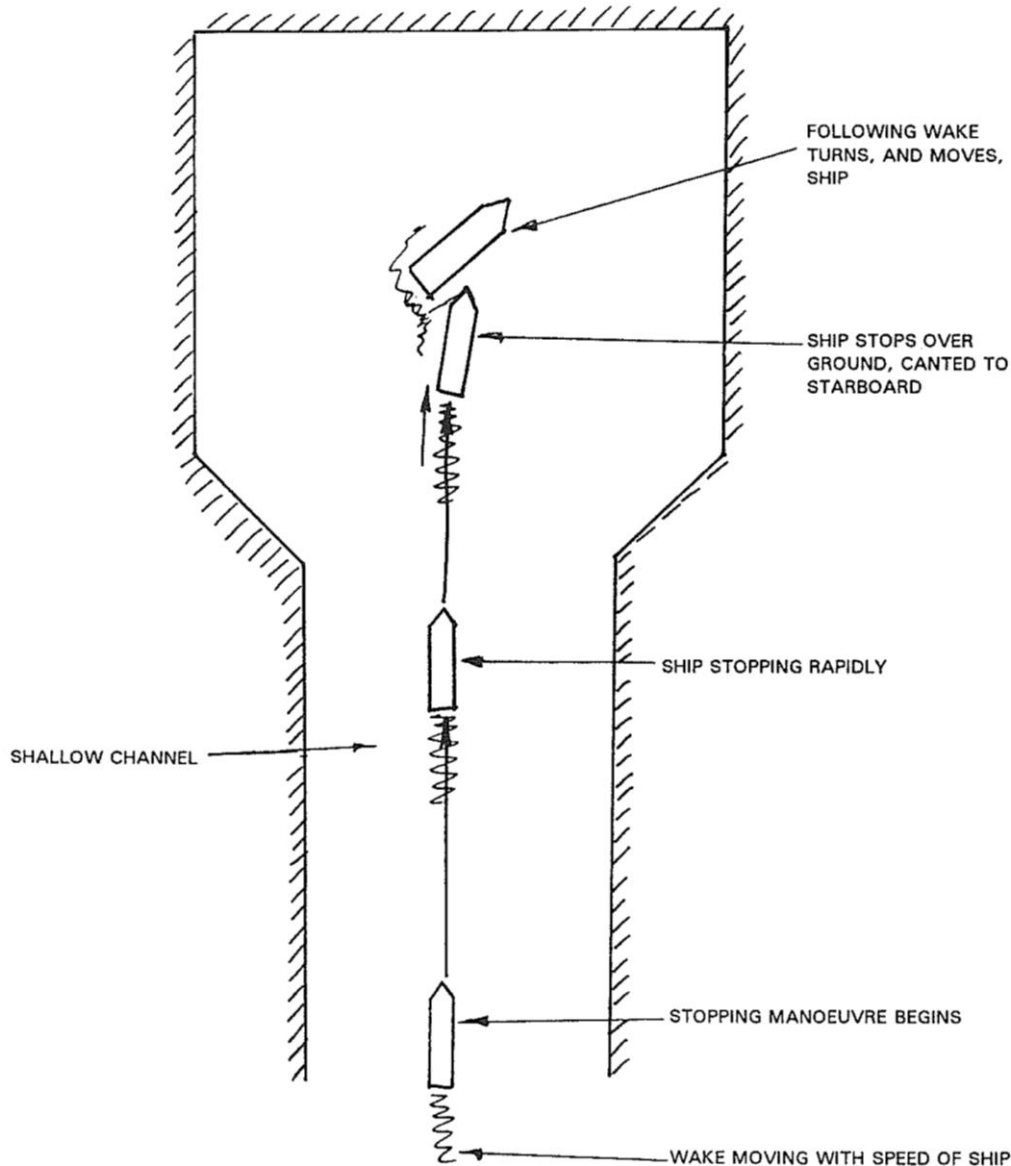
Figure 5 : The Following Wake

4.3.4. Tug Propeller – Tug Hull Interaction

For example, the astern thrust of a reverse-tractor tug/ ASD-tug is 5-10% less than ahead thrust, as a result of a propeller wash hitting the afterbody of the tug and so reducing bollard pull when astern thrust is applied.

4.3.5. Interaction of a Tug Propellers

This is especially the case with azimuth thrusters and VS propellers. Depending on thrust direction, the two propellers of tractor and ASD/reverse-tractor tugs interact to a certain extent and affect a tug's performance.

4.3.6. Tug – Ship Interaction Due to Tug Fendering

Fender characteristics such as energy absorption capabilities and friction coefficients influence the interaction of forces between tug and ship and also tug performance.

4.3.7. Tug – Towline Interaction

Tug reactions such as tug list and consequently tug performance are influenced by towline characteristics, especially by its dynamic load absorption capabilities.

4.3.8. Tug Propeller – Ship Hull Interaction

The reduction in pulling performance due to tug propeller wash hitting a ship's hull has been dealt with in a previous chapter. In the case of small underkeel clearance this effect is more pronounced. Pushing tugs are also affected by this type of interaction when propellers are close to a ship's hull, due to interrupted water flow towards the propellers.

4.3.9. Ship Propeller/Ship Hull – Tug Interaction

These interactions affect performance when operating as stern tug in the propeller slipstream or ship's wake. The effect of ship's wake increases in shallow and narrow waters.

4.4. Interaction and Tug Safety

A very important aspect is the risks harbor tugs may encounter when rendering assistance. It is an essential point when engaged in shiphandling operations. Essential because the main risk of tug acting in a manoeuvre is for stability and it is not only the safety of a tug and vessel that could be at risk, but also the safety of their crew. When rendering assistance tug captains and pilots should be fully aware of the risk involved. Since a number of unsafe situations can be traced back to interaction effects, attention is first paid to this subject and also the influence of shallow water on several interaction effects and the tug assistance required. The more knows about risks, the better can anticipate and take the right measures.

Critical situations a tug may be involved in can simply be divided as follows:

- While passing a towline; and
- While the towline is secured.

The interest in this study, at the time, is the risk that the tug runs when secured in the Vessel Type inside the new locks of Panamá Canal. Therefore, it will be discussed critical situations with tugboat tied to the ship.

4.4.1. Tug Made Fast Overtaking a Bow

A tug with propulsion aft has the risk to capsize when, with the tied line in bow, the ship's speed becomes extreme in relation to tug's limitations (position 1). This can happen when the thruster is pulling too much to the starboard, due to improve the rudder effect in order to make the turn properly. In this situation it is very likely that the tug will come abeam of the ship's bow (position 2) and even in a position further aft with the towline coming under high tension (position 3), see figure 6-A. It is almost impossible for the tug captain to manoeuvre his tug back in line with the ship and the tug is liable to capsize. This may not only be caused by the strong athwartships forces in the towline, but while trying to bring the tug back in the line with the ship, the tug captain applies high steering forces, adding to the heeling forces. With a reliably working quick release system the tug captain can release the towline, avoiding capsizing. On the other hand, if the pilot recognizes the dangerous situation arising in the time he may be able to reduce ship's speed. In doing so the towline force reduces, creating the possibility for the tug captain to come back in line with the ship. It is obvious the more manoeuvrable tugs are, the less likely they are to get involved in similarly dangerous situation.

The above situation is less dangerous to the tractor tug because of the aft lying towing point. A tractor tug swings around on the towline and comes alongside an attended ship unless the towline is released in time – so-called "tripping", see figure 6-C.

Similar situation can arise with a tractor tug when the towing angle – the angle between ships's heading and direction of the towline – is getting too large with respect to the forward speed of a ship. The tug is unable to come back in line with the ship and swings around.

The dangerous of girting can arise in situations like shown in figure 6-B. A ship is making a turn to port, because the tug captain has not been informed that the ship has to enter head first, he starts pulling to starboard to control ship's heading, assuming the ship is veering off course. If the pilot is aware of this, the same dangerous situation for the tug as described above develops, in particular when the pilot observes a decrease in rate of turn due to the tug captain's action and increase engine power while applying a large rudder angle. This situation shows how important it is for tug captains to be well informed about a pilot's intentions. On the other hand, the tug could have asked the pilot what his intentions were.
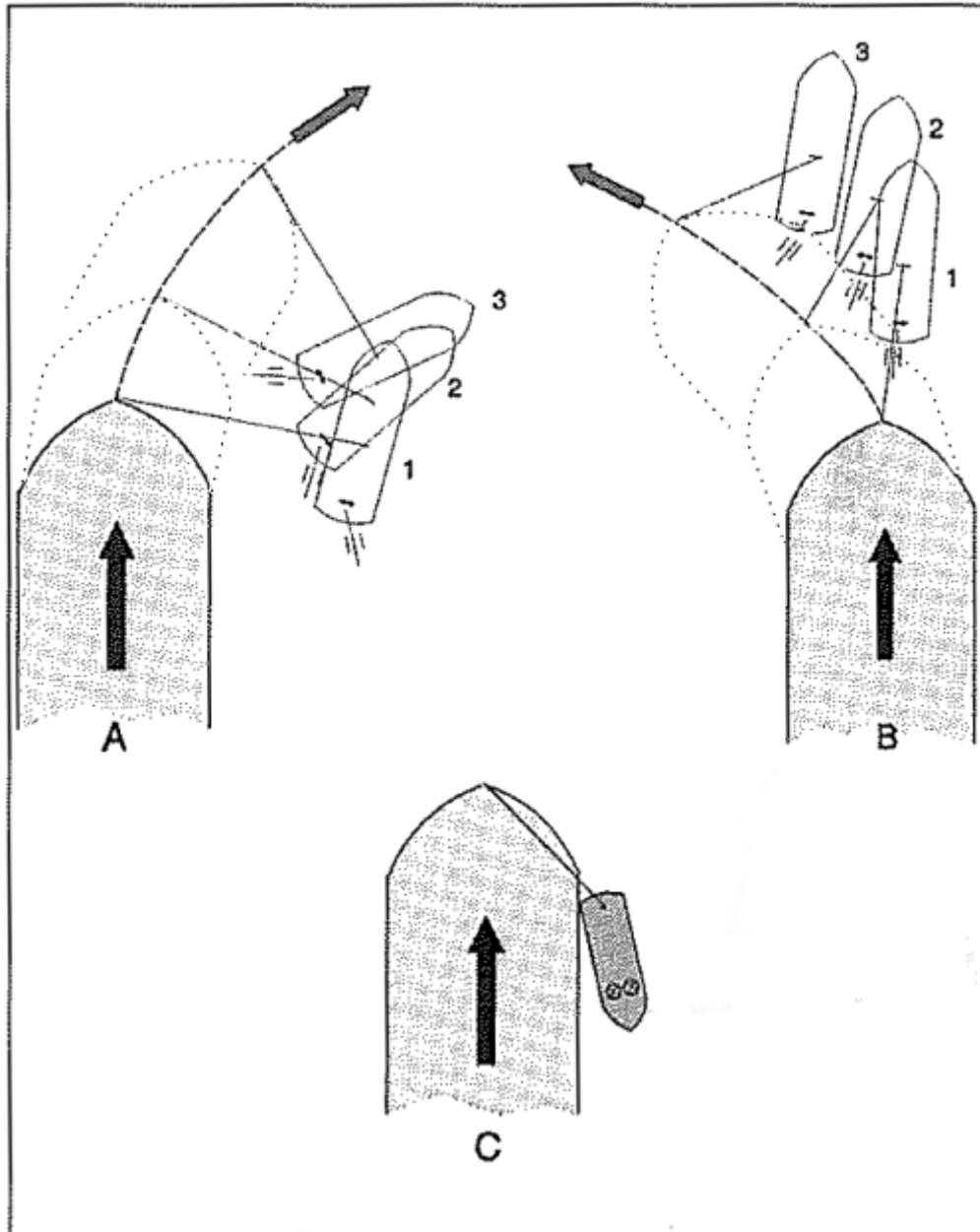
Figure 6: Girting and Tripping

4.4.2. Stern Tug Steering

The stern tug can acting as a drogue steering the ship affectively by going ahead on the engine and so applying steering forces to port or starboard, see Figure 7-A. The tug usually uses a gob rope, although with twin screw tugs this is not always the case.

A dangerous situation arises when a tug's capabilities and limitations are not sufficiently taken into account. When the ship's speed is becoming too high, tug heel caused by high athwart ships towline forces may increase until the tug capsizes. This may not only be caused by the large transverse resistance of the tug as it is pulled bodily through up by the water, but also by the water acting on the tug speeded up by the wash of the ship's propeller. In this situation tug is close of the ship's propeller

and ship generally has a very low forward speed. However, it is essential that the ship's propeller is handled with the almost care. A very dangerous situation arises if the engine is suddenly set to half ahead, the water flow on the tug together with the wild propeller wash may cause the tug to list severely and in the most serious case the tug may capsize. Tug stability, freeboard and deck equipment determine the limits of safe operation.

Care should be taken when using the engine ahead. A ship should take care not to gather headway; otherwise she will collide with the tug due to the small distance between bow and tug.

See Figure 7-B. During a certain phase of manoeuvring it may be necessary for a ship with headway to have the port or starboard position tug (position 1) move astern of the ship (position 3 or 4) to assist in steering or for speed control. This manoeuvre is dangerous to conventional tugs when carried out at too high a ship's speed. This is at speeds of more than about three knots and depends on tug manoeuvrability, stability and freeboard. In situations 2 and 3 risk of girting exists due to the high athwart ships towline forces that may occur.

The manoeuvre just described is no problem for tractor or reverse-tractor tugs, even with a fairly high ship's speed. Conventional tugs with a gob rope system, whereby the towing point can be transferred towards a far aft position, can also swing around at a higher speed. The god rope system should be strong enough and fully reliable otherwise such a manoeuvre becomes really dangerous for the tug.

A conventional tug manoeuvring from a position astern of the ship (e.g. position 3) to a position on the starboard or port quarter can only do this at minimum ship's speed, otherwise risk of girding is arise.

See Figure 7-C. Sometimes it is necessary for a conventional after tug to move from a position on the port to starboard quarter or vice versa. The ship passing through a channel or canal may need to have the after tug stand by on port or starboard quarter to compensate for wind or current forces. It may be also necessary to compensate for the transverse effect of the ship's propeller when she uses engine astern. The tug has to manoeuvre from port to starboard quarter, close underneath the stern. Because of the risk of girding this manoeuvre should be carried out while the ship is nearly stopped in the water. This kind of manoeuvre also involves great risk due to the ship's propeller. A pilot not aware of the tug manoeuvre could go ahead on the engine or apply ahead pitch while the tug is near position 2. The conventional tug comes in to danger. This kind of tug manoeuvre, whenever considered necessary, should always be carried out with the utmost care.
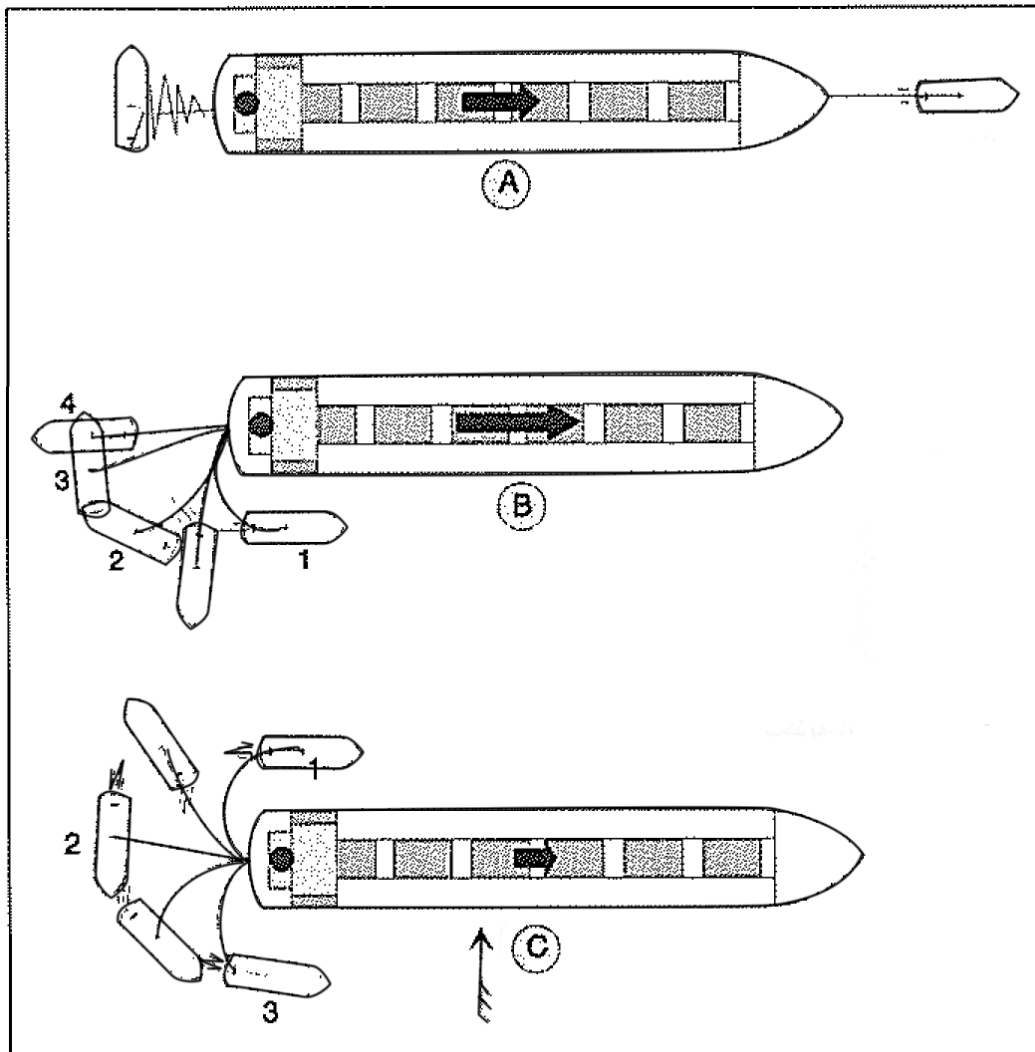
Figure 7: Some Specific Manoeuvres by Tugs Towing on a Line Including Risk of Girding or Capsizing When a Ship's Speed is too high with Respect to Tug limitations.

4.4.3. Bulbous Bows

Although there is a mark on a ship's bow indicating that it has a bulbous bow, tug captains can't see the bulbous bow when it is underwater. Even when only partly submerged the exact position is difficult to determine. This is a problem for forward tugs when taking position to pass or take a towline or when they are assisting using a very short towline. It is most dangerous when the stern of the tugs touches the bulbous bow, and the ship has a rather high forward speed. The tug may be severely damaged and lives may be lost. Tug captains have to be particularly careful when operating close to a bulbous bow, especially during fog and darkness.

4.4.4. Underestimating Wind and Current Forces

Underestimating wind and current forces can create risky situations for a ship and have resulted in accidents. Tugs operating at a ship´s side can also be endangered, see Figure 8. Tugs can be jammed between ship and shore when they don´t get out in time. The situation is particularly dangerous when tugs are secured by towlines. The bollard pull of tugs to compensate for wind and current forces should be more than sufficient to avoid such situations.
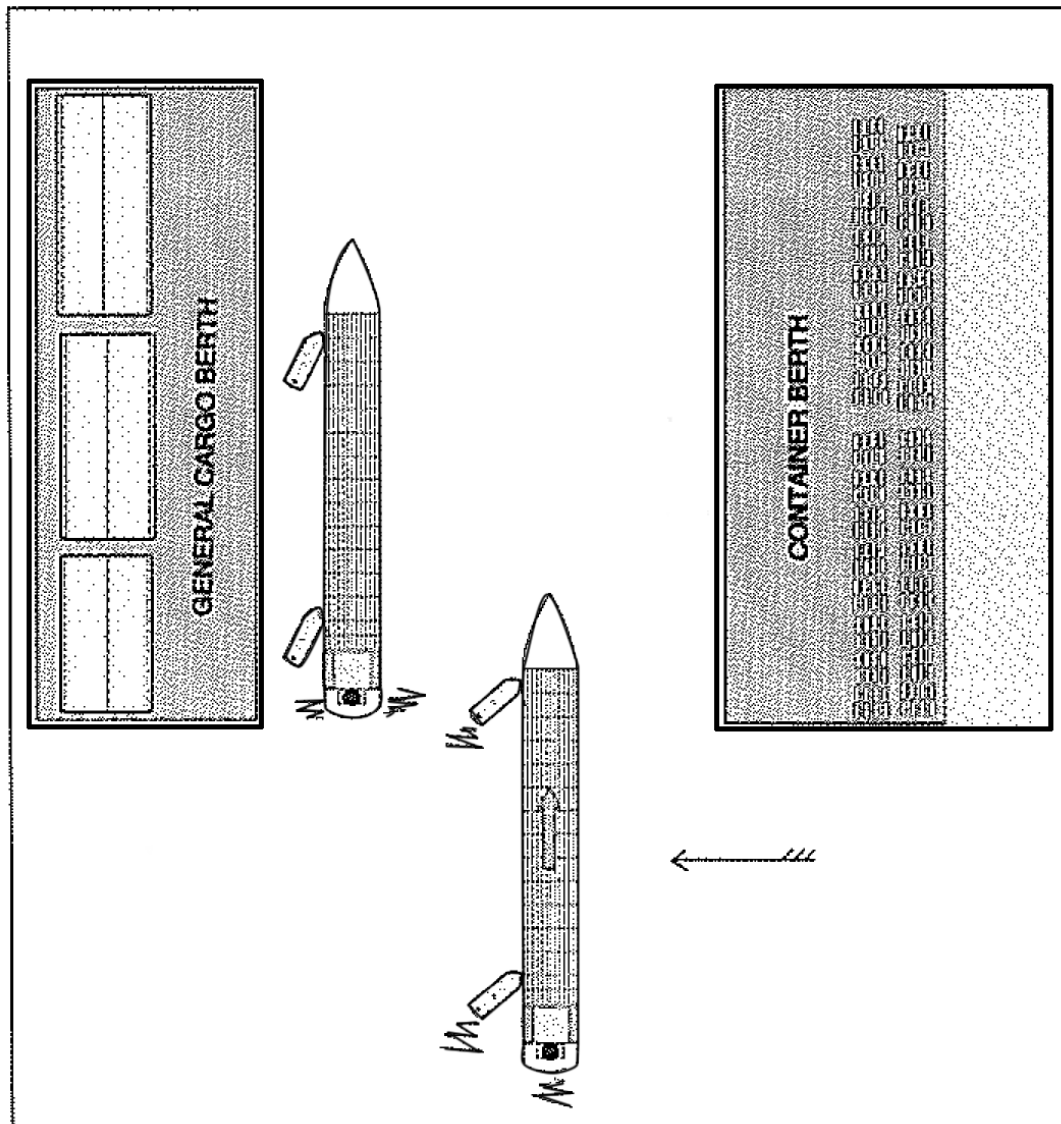
Figure 8: Due to Low Powered Tugs and Strong Beam Wind, a Container Ship Is Drifting and the Tugs Are Getting Jammed Between the Ship and the General Cargo Berth

4.4.5. Information Exchange

Pilots, ship masters and tug captains should know each other's capabilities and limitations regarding ship and tug manoeuvres. Informing to them about everything regarding the manoeuvre in understandable English is the basis of a good cooperation and understanding between them. Tug captains should be properly informed by the pilot about the intended ship manoeuvres. A proper information exchange between pilot, ship captain and tug master is needed for a safe and smooth handling of the ship by attending tugs.

Information for the ship captain to be provided by the pilot may include the number, type and bollard pull of tugs to be used (including, if necessary, the reason why the specific number and/or total bollard pull of tugs has been advised), the rendezvous position and time of the tug(s); where at the ship and how tug(s) to be fastened; when tug(s) to be released and how to be done; transit speeds and intended manoeuvres. If the ship has special manoeuvring devices or limitations regarding manoeuvring, tug, securing, mooring and anchoring equipment, the ship captain should inform the pilot. With respect to the information exchange the reader is also referred to the OCIMF publication 'Recommendations for ship´s fittings for use with tugs'.

4.4.6. Operating Bow-to-Bow

The relatively low effectiveness of tractor tugs, reverse-tractor tugs and ASD-tugs (when operating as reverse-tractor) as bow tug towing on a line with a ship having headway, including the reasons why and the risks involved, is due to their capabilities and limitations.

For reverse-tractor tugs and ASD-tugs this way of operating is generally called 'bow-to-bow'. When operating in this way with a ship having headway the tugs are sailing astern. Directional stability of these tugs types when sailing astern is generally rather low, particularly at higher speeds. Pulling straight astern at a relative high speed might not immediately present a problem, but as soon as the tug deviates from the straight line, for instance, to give steering assistance to the ship, position keeping becomes difficult. It may easily result in a loss of control.

A high underwater resistance, e.g. a large skeg, worsens the situation, while a bow skeg may improve the situation to some extent. The restriction in movement of the bow by the tow rope increases the difficulties in maintaining a safe position and direction relative to the ship under tow. Furthermore, if the tug is working on a short towline, tug-ship interaction effects may play a role, destabilizing the tug´s position, while time left to react is minimal. A comparable situation has led to accidents, amongst others in a severe collision between ship and tug. This incident resulted in a speed restriction for bow-to-bow operations. A maximum speed of five knots was introduced.

4.5. Squat Effect

Squat effect is the vessel tendency to sink and acquire trim when in forward movement, due to the pressure difference between sea bed and vessel keel, with hull suction in towards the bottom, decreasing the UKC. Squat is the sum of vertical sinking called sinkage, with a bow rotational movement called trim. This last movement of the vessel bow upwards or downwards, according to the vessel block coefficient (Cb), as follows:

Vessels that when stopped are in even keel:

- Trim by the head, if its Cb is greater than 0.700; e
- Trim by the stern, if its Cb is less than 0.700.

Vessels in Cb equal to 0.700 do not have bow rotational movement; therefore, its squat is understood as sinkage. Vessels in Cb equal to 0.700 do not have bow rotational movement; therefore, its squat is understood as sinkage.
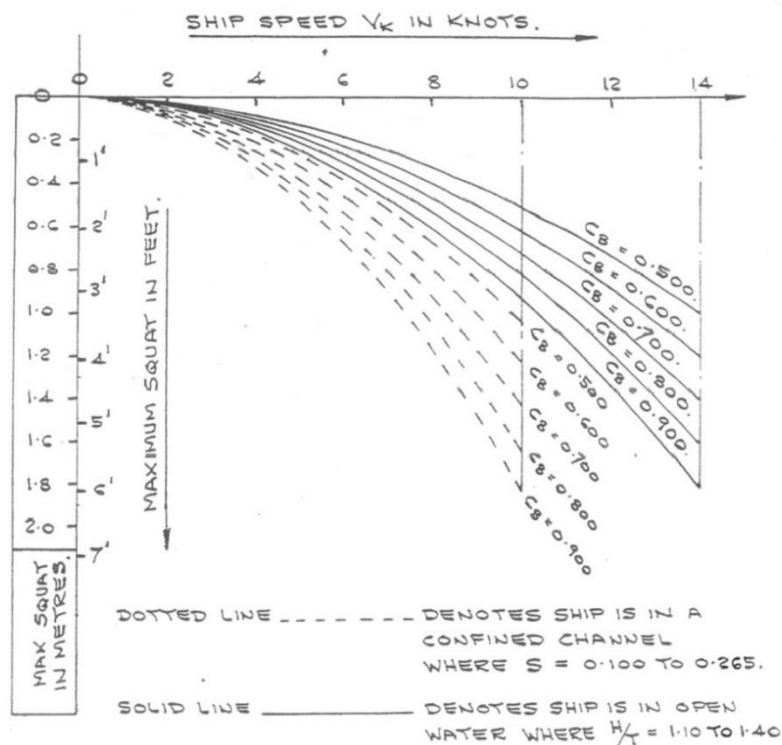
Figure 9: Maximum Ship Squat in Confined Channels and in Open Water Conditions.

Table 1 - Coefficients of types of vessels fully loaded

Ship Type	Typical C_B, Fully-loaded
ULCC	0.860
Supertanker	0.825
Oil Tanker	0.800
Bulk Carrier	0.750
General Cargo	0.700
Passenger Liner	0.625
Container Ship	0.565
Coastal Tug	0.500

The squat can be estimated through several formulas, as the ones utilized by Tuck (1996), Hooft (1974), Huuska (1976), Millward (1990 and 1992), etc. However, for a rapid estimate of the squat, it may be used the ICORELS (*International Commission for the Reception of Large Ships*) expression, which can be utilized for open waters, as restricted waters.

$$\boldsymbol{Squat}\ (\mathbf{m}) = \ \boldsymbol{2,4}. \frac{\nabla}{Lpp^2} . \frac{Fnh^2}{\sqrt{1 - Fnh^2}}$$

In which:

- ∇: Volume of displacement, the immersed volume of the vessel, obtained by multiplication
  $\nabla = \mathrm{Cb. Lpp. B. T}$
- C_b: is the Block Coefficient of vessel
- Lpp: Ship's length between perpendiculars
- B: Ship beam
- T: Ship draught
- *Fnh*: Froude Depth Number

The Block Coefficient (Cb) is the relation between the volume of displacement and parallelepiped's volume. See Figure 10.
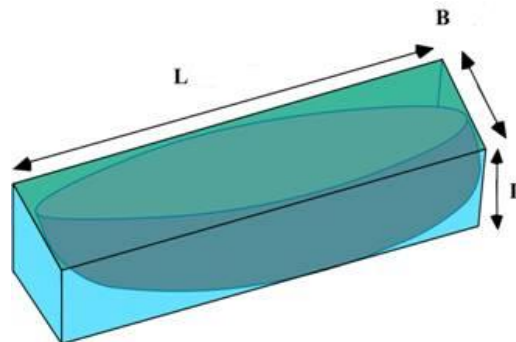
Figure 10: Block Coefficient of a Vessel

The value of Block Coefficient can be obtained through the formula:

$$C_b = \frac{\nabla}{Lpp. B. T}$$

In which:

- Lpp: Ship's length between perpendiculars (m);
- B: Ship beam (m);
- T: Ship draught (m); and
- ∇: Volume of displacement. (m^3).

The Volume of displacement can be obtained through the follow relation:

$$\Delta = \nabla \ . \ \delta_{water}$$

The Froude Depth Number (*Fnh*) is a dimensionless value widely used in hydrodynamics, which measures the relationship between speed and depth, providing a value that informs high or low hydrodynamic resistance to vessels' movement in shallow waters. This value is defined through the relation:

$$Fnh = \frac{V}{\sqrt{gh}}$$

In which:

- V: is the speed through the water in meters/second;
- g: is the acceleration due to gravity (about 9,81 m/sec^2);
- h: is the water depth in meters.

When *Fnh* approximates to the unit or is equal to the unit, the resistance to the vessels' movement reaches very high values, which vessels of greater displacement don't have enough power to overcome. Indeed, it's unlikely that these vessels are capable of overcome values of *Fnh* between 0,6 or 0,7, which form real barriers to the development of speed. This means that is advisable to utilize the Froude Depth Number to verify an ideal parameter of speed in channel.

Still for squat calculation, the Barass formula, created in 1981, can also be applied because it's utilized for open waters and restricted waters:

$$\boldsymbol{Squat}\ (\mathbf{m}) = \frac{\boldsymbol{Cb}}{\boldsymbol{30}} \cdot \boldsymbol{S_2^{2/3}} \cdot \boldsymbol{V_k^{2,08}}$$

In which:

- Cb: is the block coefficient of the vessel;
- S_2: is the blockage ratio, that can be calculated as $A_s = A_w$;
- A_s: midship section area (m^2);
- A_w: wetted cross-section area of waterway (m^2): $A_w = A_{ch} - A_s$
- A_{ch}: equivalent wetted cross-section area of channel with slopes extrapolated to the water surface (m^2); e
- V_k: Vessel speed (knots).

The following conditions are where there is an increase of squat effect:

- Crossing and overtaking;
- Decentralized course in relation to Center line of channel if there is influence of edges;
- Silting up and transients shallow waters;
- Bottom sludge, which creates interaction between the keel and mud-water interface;
- Drift due to environmental forces – wind, waves and current – and deflection.
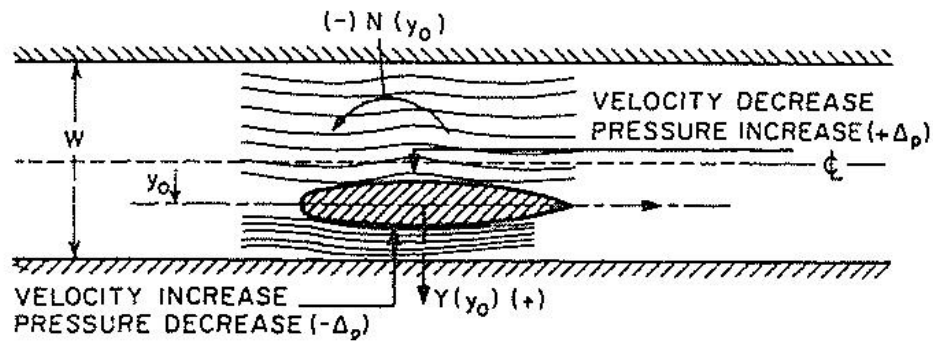
Figure 11: Flow diagram in canal with ship and its velocity vector parallel to canal wall

Since there are no accurate methods of squat calculation out of the conditions above, it may mitigate the effect reducing the vessel's speed.

Using the calculation formula of squat effect presented in this topic and having as base the information from Vessel Type presented in this report, it is possible to utilize the block coefficient of this Vessel Type, which is going to traffic in the new locks of the Panama Canal, and the Froude values to estimate the value of squat effect in this study.

4.6. Depth Considerations

4.6.1. Relation between speed and draft

The hydrodynamic resistance of vessel movement, in shallow waters, is ruled by The Froude Depth Number (*Fnh*), which is the dimensionless reason between speed and depth, as seen in item 4.5 above.

When *Fnh* approximates to the unit or is equal to the unit, the resistance to the vessel's movement reaches very high values, due to the increase of wave-making resistance, resistance formed by irradiated waves by the vessel. In deep waters, the irradiated wave's system by the vessel form, with a diametric plan, a common angle of 19°28', as seen in Figure 12. When the vessel enters in shallow waters, such angle is increased and its value is directly proportional to Fnh value of the vessel, to given speed and depth. In shallow water, the irradiated waves by the vessel also increase in height and decrease in length.
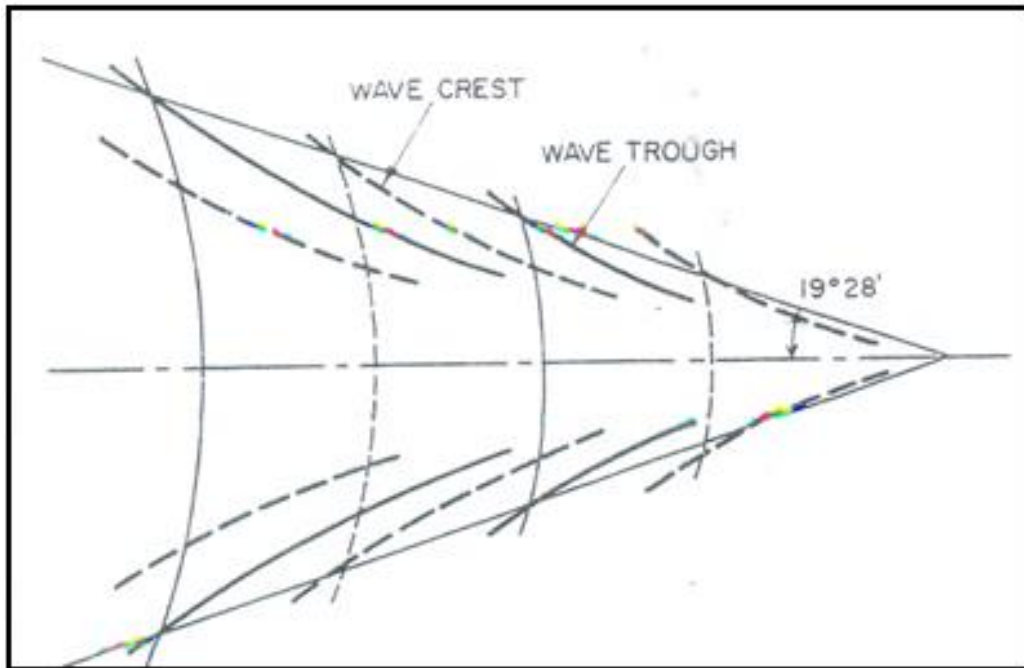
Figure 12: Waves formation in deep waters.

Therefore, as the vessel's speed increases, the *Fnh* also increases, increasing also the resistance formed by irradiated waves.

In fact, it's unlikely that the vessels are capable to overcome *Fnh* values of 0.6 or 0.7, which constitute real speed barriers (suggest speed adjustment in a way that the Fnh value of 0.5 is not exceeded). Alternatively, the Fnh limit can be use as a speed chosen to determine the minimum speed limit.

It's possible to conclude that one of the reasons of decrease vessel's speed when in shallow water is minimize the effects of irradiated waves by the vessel and, in parallel, reduce the effects of these waves in others vessels moored in proximities of harbor.

4.6.2. Water line under keel

The proper study of underkeel clearance, hereinafter UKC, to be considered must be held before enter in restricted waters. This analysis must take into account the value of the vessel's biggest draft, along with the squat effect and the tidal height on time to enter the Canal of harbor access.

The UKC is great interest in security perspective, according to the publication of Ship Channel Design and Operation, from American Society of Civil Engineers (ASCE). According to this publication, a water line of at least 0.6 meters must be kept between the bottom of the vessel in movement and the canal bottom, in order to prevent damage to the vessel's thrusters, incrustation in bombs and capacitors. Depending on the bottom type this water line under the keel must be increased to at least 0.9 meters, when the bottom consists on rocks, sand or consolidated clay.

5. TUGS

When the purpose is to establish the towing device appropriate to a harbour manoeuvre, the first issue to be solved is the calculation of strength needed to move the vessel steered in conditions foreseen to the local where the manoeuvre is held.

Depending on the objective to be attained – towage, mooring, unmooring, rotation, or attendance – the strength needed can be only enough to move a vessel lengthwise or be big enough to rotate in a particular direction and move it crosswise.

Whatever situation, the force required to the towing device must be enough not only to move the vessel, but also to stop its movement and, more than that, must be capable to overcome forces opposed to the intended direction of movement.

The traction force considered is static and longitudinal, therefore must be analysed how it would be this traction force according to the main characteristics from the Vessel Type and from local environmental features characteristics. The main parameters to be considered are:

- Displacement;
- Draft;
- Living and dead works area;
- Intensity and direction of the wind;
- Intensity and direction of the current;
- Waves characteristics.

Then, the total of the calculated force with these requirements will be the value that must correspond to the sum of the forces applicable by the tugs, which are going to form the towing device used in manoeuvre.

Aiming to obtain the Bollard Pull required, it will be applied the formulas presented in publication: *Tug use in Port* – The Nautical Institute. These describe, for each environmental feature, the particular force acting in vessel. The sum of each force will be offset by thrusters when the Bollard Pull corresponds to the sum of wind forces, current and wave.

5.1. Wind force:

To the forces caused by wind, the following formula shall be applied.

Lateral Force

$F_{Ywind} = 0,5 . C_{Ywind} . \rho . V^2 . A_L$ (Newton)

Longitudinal Force

$F_{Xwind} = 0,5 . C_{Xwind} . \rho . V^2 . A_T$ (Newton)

Yaw Moment

$M_{XYwind} = 0,5 . C_{XYwind} . \rho . V^2 . A_L . L_{BP}$ (Newtonmetres)

In which:

C_{Ywind} = Lateral wind force coefficient.

C_{Xwind} = Longitudinal wind force coefficient.

C_{XYwind} = Wind yaw moment coefficient.

ρ = Density of air in kg/m^3.

V = Wind velocity in m/sec.

A_L = Longitudinal (broadside) wind area in m^2.

A_T = Transverse (head-on) wind area in m^2.

L_{BP} = Length between perpendiculars in m.

Use the most conservative data and add a security factor of 25%, to allow a safety margin of 20%, is very reasonable to the calculation of Bollard Pull with thrusters operating wired in the extremities of the vessel.

The forces coefficients and the moment are parameters that can be determinate by means of model tests in wind tunnels. For several ship types the wind coefficients are known for all angles of attack and certain loading conditions.

For ships affected by wind, such as container vessels, ro-ro vessels, car carriers, gas carriers, tankers and bulk carriers in ballast, the bollard pull required can be approximated using this method.

The total value of Bollard Pull needed for the Vessel Type in study, due to the wind, may be calculated utilizing the formulas above.

The current and waves forces may be calculated as well as the wind forces. However, as the intention is analyse the manoeuvres of Vessel Type and of the thrusters, which its assist inside the locks, won't be taken into account the forces related to current and wave.

5.2. Bollard Pull Required

The displacement of the vessel is a characteristic that allow us calculate, by mathematical model, the Bollard Pull needed to move the vessel. To vessels with large displacements (more than 100.000 tons) the following formula also can be used:

$$Required\ Bollard\ Pull\ (tons) = \left(\frac{Displacemaent}{100.000} \times 60\right) + 40$$

For this study, the bollard pull needed is:

$$Required\ Bollard\ Pull = \left(\frac{202,650}{100,000} \times 60\right) + 40$$

$$\boldsymbol{Required\ Bollard\ Pull = 161.59\ tons}$$

The graphs in Figure 13, 14 e 15 gives the minimum, maximum and average total bollard pull used in a number of ports, including the average number of tug. For bollard pull used the upper line of the graph is assumed as the requirement for more difficult situations and the lower line for normal and easier situations. The average bollard pull used show in Figure 14 e 15 for bulk carriers and tankers is more or less comparable with the outcome of the previously mentioned formula based on displacement for ship of deadweight up to about 230,000 tons.

Figure 13: Total Bollard Pull in Tons and Average Number of Tugs for Container and General Cargo Vessel as Used in a number of Ports around the World
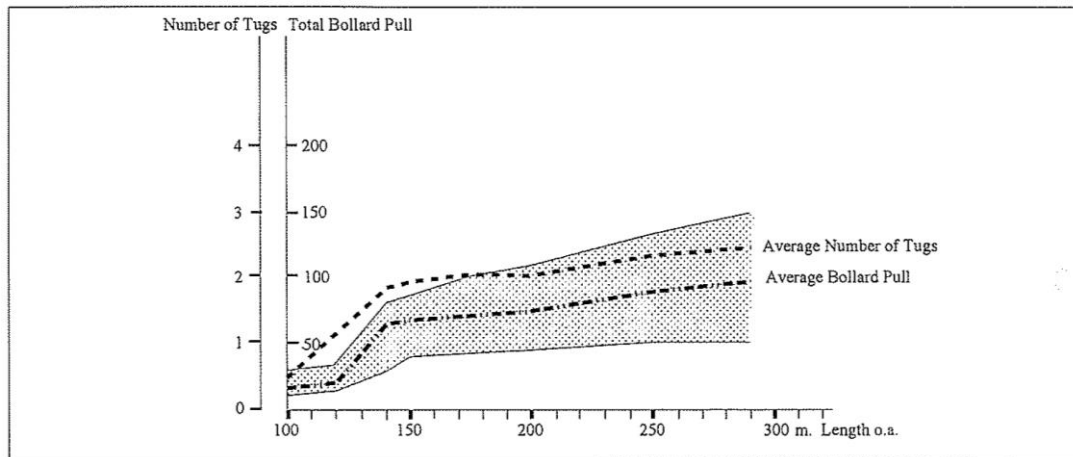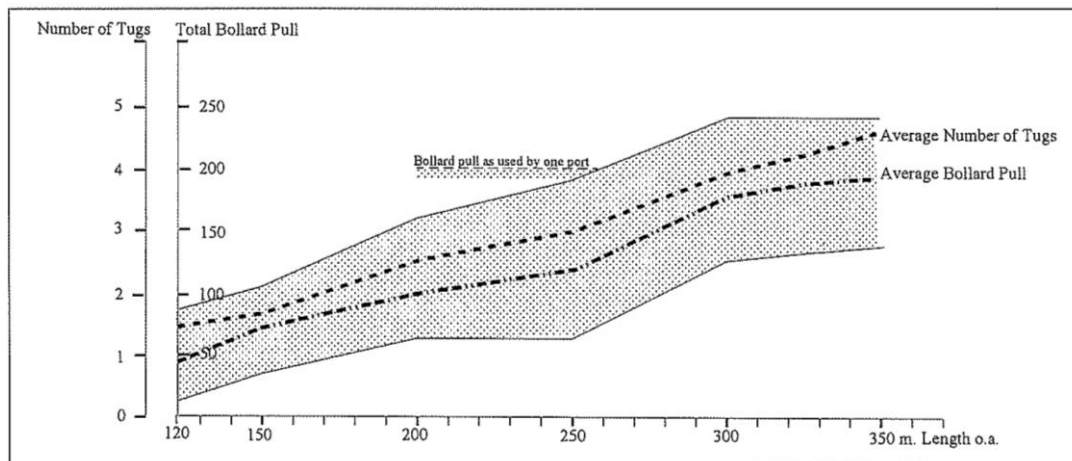

Figure 14: Total Bollard Pull in Tons and Average Number of Tugs for Tankers and Bulk Carriers as Used in a number of Ports around the World
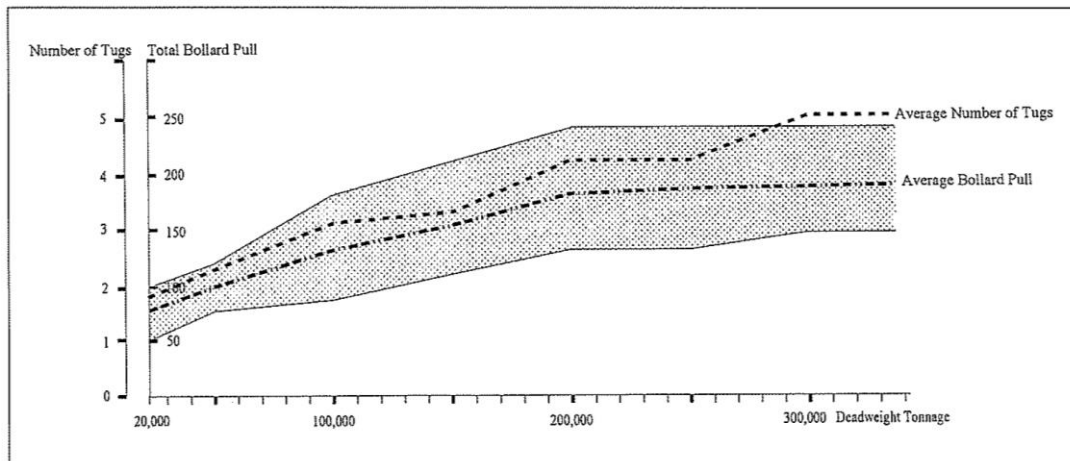
Figure 15: Total Bollard Pull in Tons and Average Number of Tugs for Tankers and Bulk Carriers as Used in a number of Ports around the World

6.   SIMULATION

In this study, conducted by FHM, it was used the *NTPro* 5000 software to simulate the behaviour of the Vessel Type and the port tugs.

It was analysed in simulations the manoeuvres carried out in the new locks of Panama Canal. The basic situation analysed was:

- Vessel Type fully loaded, entering and exiting, with the assistance of tugs, in Panama Canal new locks.

It's important to highlight that all informations used to compose the entire scenario where were carried out the manoeuvrability analyses of Vessel Type and tugs which assisted them, in the quote situation, were given by the contracting party.

Not considering the tide and current inside the locks, the metocean conditions were set up as follows: on the side of Atlantic Ocean, the wind is coming from EAST/NORTHEAST and has intensity of 14.19 knots; the current is 1.3 knots to NORTH/NORTHEAST; on Pacific Ocean side, the wind is coming from NORTH/NORTHWEST and has intensity of 3.9 knots; the current is 2.76 knots to EAST/NORTHEAST. However, in conditions mentioned previously, it was found difficulties to control the Vessel Type and the tugs.

After some experiments in manoeuvres simulations was reached a new configuration of environmental conditions, because it was able to control with less difficulties the Vessel Type and the tugs: not considering the tide and current inside the locks, by Atlantic Ocean side, the wind is coming from EAST/NORTHEAST and intensity of 05.00 knots and current is 0.5 knots to NORTH/NORTHEAST; on Pacific Ocean Side, the wind is coming from NORTH/NORTWEST and intensity of 0.2 knots and current is 03.90 knots to EAST/NORTHEAST. Based on the exposed above and in solicitations of contracting party, when the same came to carry out simulations at FHM, and the configuration of environmental conditions to execute the manoeuvres, were established according to table 2.

The positioning and the dimensions of the Panama Canal new locks are in accordance with the magazine *Programa de Ampliación* (December 2014) and also the files M-6120-30D.pdf and SK-H-1126_WGS84.dwg.

In manoeuvres were used the tugs Azimuth Stern Drive, ZDrive, Azimuth Tractor Drive and Voith Shneider Propeller.

Table 2 – Configurations in carried out manoeuvres

Metocean Manoeuvres Configurations								
	Pacific				Atlantic			
Manoeuvres	Wind		Current (out of locks)		Wind		Current (out of locks)		Executer
	Direction	Speed (knots)	Direction	Speed (knots)	Direction	Speed (knots)	Direction	Speed (knots)	
1	---	00.0	---	0.0	---	---	---	---	Contractor Team
2	---	---	---	---	NNE	20.0	---	---	Contractor Team
3	---	---	---	---	NNE	20.0	---	---	Contractor Team
4	---	---	---	---	NNE	20.0	---	---	Contractor Team
5	NNO	10.0	---	---	---	---	---	---	Contractor Team
6	NNO	10.0	---	---	---	---	---	---	Contractor Team
7	---	---	---	---	NNO	20.0	---	---	Contractor Team
8	---	---	---	---	NNO	20.0	---	---	Contractor Team
9	---	---	---	---	NNO	10.0	---	---	Contractor Team
10	---	---	---	---	NNE	14.2	ENE	1.3	FHM Team
11	---	---	---	---	NNE	14.2	ENE	1.3	FHM Team
12	---	---	---	---	NNE	14.2	ENE	1.3	FHM Team
13	---	---	---	---	NNE	10.0	ENE	1.0	FHM Team
14	---	---	---	---	NNE	05.0	ENE	1.0	FHM Team
15	---	---	---	---	NNE	05.0	ENE	0.5	FHM Team
16	---	---	---	---	NNE	05.0	ENE	0.5	FHM Team
17	---	---	---	---	NNE	05.0	ENE	0.5	FHM Team
18	---	---	---	---	NNE	05.0	ENE	0.5	FHM Team
19	---	---	---	---	NNE	05.0	ENE	0.5	FHM Team
20	NNW	03.9	ENE	2.8	---	---	---	---	FHM Team
21	NNW	03.9	ENE	2.8	---	---	---	---	FHM Team
22	NNW	03.9	ENE	0.5	---	---	---	---	FHM Team
23	NNW	03.9	ENE	0.5	---	---	---	---	FHM Team
24	NNW	03.9	ENE	0.5	---	---	---	---	FHM Team
25	NNW	03.9	ENE	0.3	---	---	---	---	FHM Team
26	NNW	03.9	ENE	0.2	---	---	---	---	FHM Team
27	NNW	03.9	ENE	0.2	---	---	---	---	FHM Team
28	NNW	03.9	ENE	0.2	---	---	---	---	FHM Team
29	NNW	03.9	ENE	0.2	---	---	---	---	FHM Team
30	NNW	03.9	ENE	0.2	---	---	---	---	FHM Team
31	NNW	03.9	ENE	0.2	---	---	---	---	FHM Team
32	NNW	03.9	ENE	0.2	---	---	---	---	FHM Team
33	---	---	---	---	NNE	05.0	ENE	0.5	FHM Team
34	---	---	---	---	NNE	05.0	ENE	0.5	FHM Team
35	---	---	---	---	NNE	05.0	ENE	0.5	FHM Team

6.1. Models used

For this study, it was developed by FHM modelling team, the Vessel Type CSA CS New Panamax I (Container Ship) and the tugs Chiriqui III, Tonosi, Los Santos, Cerro Azul and Cacique. The models and some data about them can be verified in tables 3 and 4.

Los Santos it's an Azimuth Stern Drive with 54 tons of bollard pull. It has stern propeller, bow winches and has stern hooks. It's excellent to work in stern and also can be use in astern, having a behaviour similar with a conventional tug, but with better manoeuvrability.

Chiriqui III it's an Azimuth Stern Drive with 61 tons of bollard pull. It has stern propeller and bow winches. It's excellent to work in stern. Because it's without stern hooks, is not usually used in bow.

Cerro Azul it's an Azimuth Stern Drive with 82 tons of bollard pull. It has head propeller, winches, hook or bollards in stern. It's excellent to work in bow.

Cacique It's a tug with Voith Schneider Propeller with 32 tons of bollard pull. It has head propeller, winches, hook or bollards in stern. It's excellent to work in bow.

Tonosi it's a tug with 65 tons of bollard pull. It has stern propeller and bow winches. It's excellent to work in stern. It doesn't have stern hooks.

Considering that Vessel Type moves ahead and having in mind the characteristics described above, and according to the book *Tug Use in Port*, we worked in manoeuvres considering the best way to use the tugs. Thus, we reach the following configuration:

a) Best Scenario ➔ Higher bollard pull

Cerro Azul (ATD) Tug of 82t bollard pull working in bow with two passed lines and Tonosi (ZDrive) Tug of 65t bollard pull working with one passed line.

b) Worst Scenario ➔ Smaller bollard pull

Cacique (VSP) Tug of 32t bollard pull working in bow with two passed lines and Los Santos (ASD) Tug of 54t bollard pull working with one passed line.

Table 3 – Vessel models used in Simulations

Model	DWT (TPB)	Displacement (t)	Loa (m)	Breadth (m)	Draft (m)
	145,000	202,650	366	49.0	15.2

Table 4 – Tugs models used in Simulations

Model	Bollard Pull (t)	Displacement (t)	Loa (m)	Breadth (m)	Draft (m)
	32	563	28.95	10.36	2.98
	61	563	27.4	11.65	3.65
	54	926.75	30.8	11.14	4.95
	82	805	28.9	13.5	3.3
	65	649	27.4	12.2	3.85

6.2. New Locks

Regarding to the new locks, FHM modelling team virtually developed, for studies purposes, the third set of locks which is being built in Pacific entrance (Cocolí Lock) and Atlantic entrance (Agua Clara Lock).

Each lockage is formed by 3 levels, being 3 chambers of 427 meters in length, internal distance between gates, 55 meters wide, breadth, 18.3 meters operational deep each and 4 pairs of gate, in a total about 1400 meters long, without counting the approach structures.

6.3. Simulation Detailment

With the intention to carry out the manoeuvres, in a safe way, during all Vessel Type track in new locks of Panama Canal, it was analysed tecnically the possibilities, having as base the sources of bibliographic reference in this report.

6.3.1 Manoeuvres Carried out in the Presence of Representatives of the Contracting Party.

Manoeuvres simulations in Panama Canal new locks were carried out on February 18th and 19th 2016 in Fundação Homem do Mar (FHM). President of Consejo de los Metalurgicos del Canal de Panama, the vice president of Area Atlantica de la Union de Ingenieros Marinos and the representative of Area del Pacifico Union de Capitanes y Oficiales de Cubierta were present.

The manoeuvres carried out in the presence of representatives Contracting Party were nine, being three Pacific side entrance and six Atlantic side entrance, daytime and with the Vessel Type fully loaded. The environmental conditions considered to manoeuvres are in table 2.

Manoeuvre 01

The simulated situation was:

Manoeuvre	Wind (knots)	Current (knots)	Tugs
Pacific Entrance	00	0.0	2 de 82t

Manoeuvre 01 – The Cerro Azul Tug was used head and stern, with two tied lines in the bow and two tied lines in the stern. They were controlled by Bridges 1 and 2, as Own Ship.

The Vessel Type was controlled by the instructor, also as Own Ship.

The Vessel Type ran aground in third chamber exit due to its high speed to that occasion, 1.0 knot. Therefore, it happened several occasions of near miss with the tug used in bow.

The tugs were widely used with its maximum power, forcing its machinery.

There was great difficulty to control the Vessel Type and tugs in environmental conditions configured, even using all power from tugs.
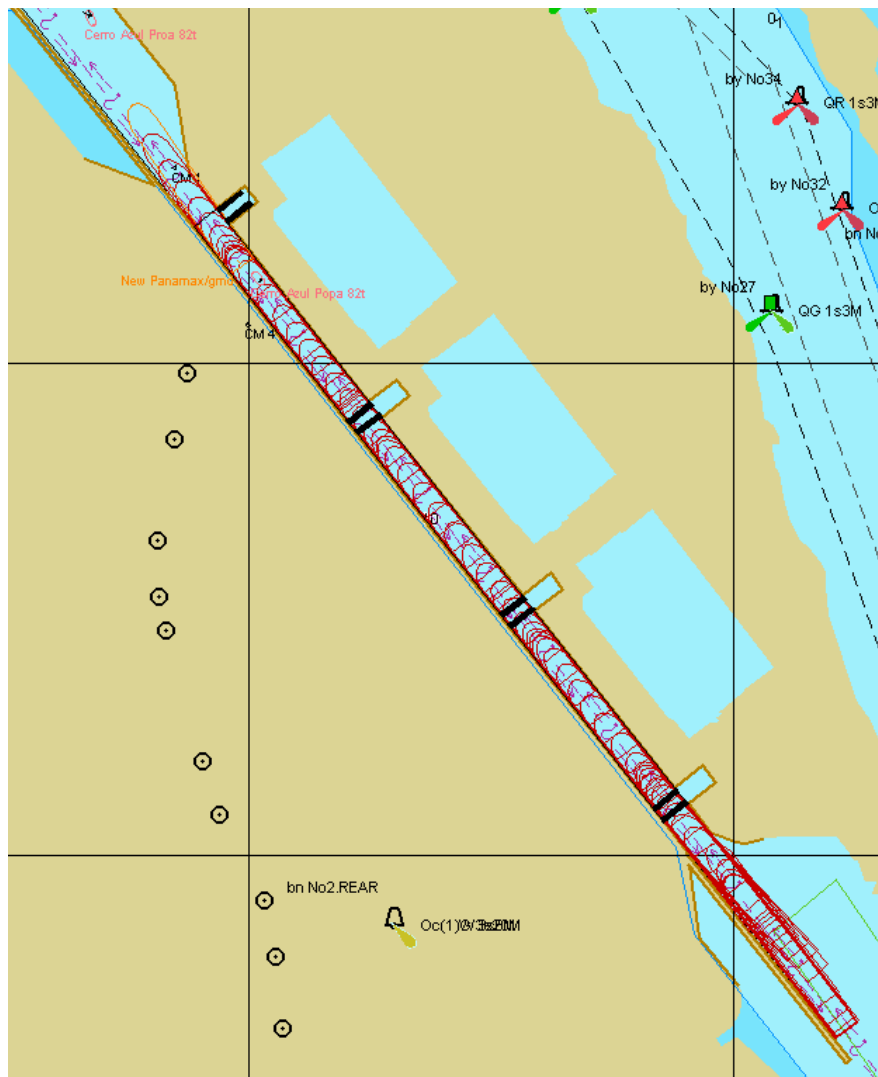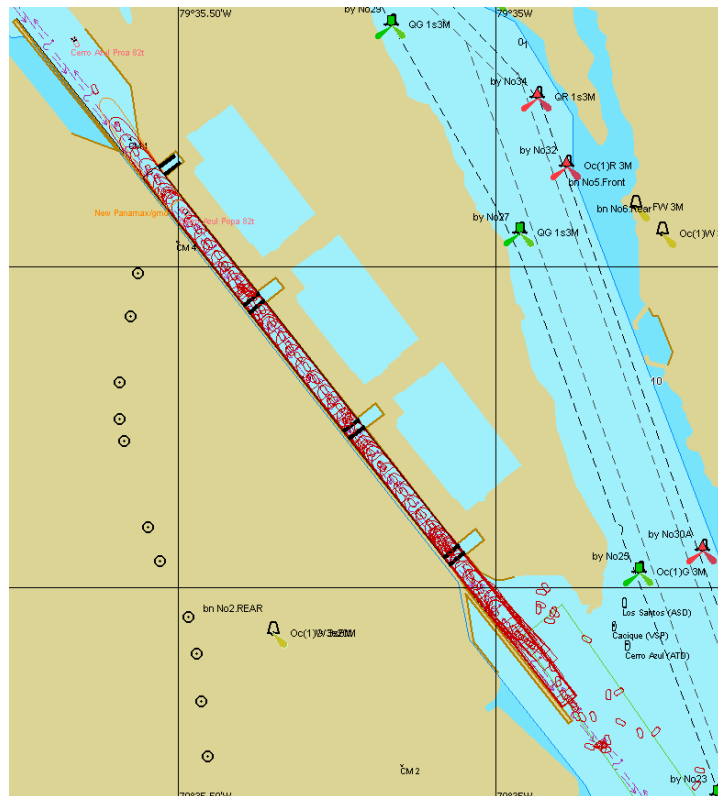

Figure 16: Vessel Type tracking in Manoeuvre 1

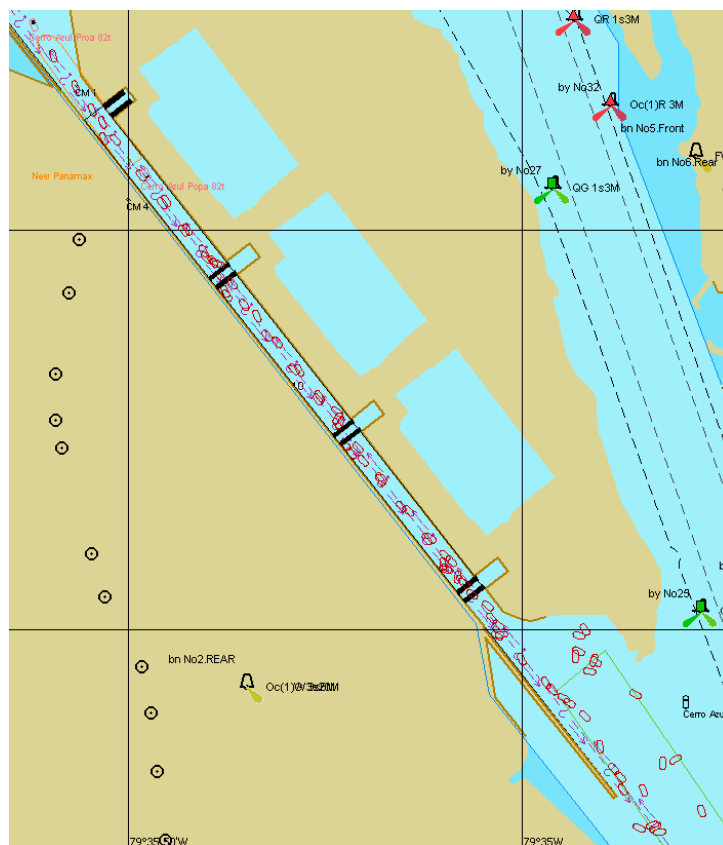Figure 17: Vessel Type and tugs tracking in Manoeuvre 1

Figure 18: Tugs tracking in Manoeuvre 1

Manoeuvre 02

The simulated situation was:

Manoeuvre	Wind (knots)	Current (knots)	Tugs
Atlantic Entrance	20 from NNE	0.0	1 de 82t 1 de 65t

Manoeuvre 02 – The Cerro Azul Tug was used in the bow, with two tied lines, and the tug Tonosi was used in the stern, with two tied lines. The tugs were controlled by Bridges 1 and 2, as Own Ship.

The Vessel Type was controlled by the instructor, also as Own Ship.

It was experienced an entrance manoeuvre in the lock, demanding about one nautical mile of distance and with inicial speed of 5.6 knots. The purpose was trying to obtain a greater manoeuvrability of Vessel Type.

Even with that attempt the Vessel Type collided in approaching zone of lock entrance and the tugs, even used frequently with its maximum power, forcing its machinery weren't able to provide enough bollard pull to control the Vessel Type.

There was great difficulty to control the Vessel Type and tugs in environmental conditions configured.

Figure 19: Vessel Type tracking in Manoeuvre 2

Figure 20: Vessel Type and Tugs tracking in Manoeuvre 2

Figure 21: Tugs tracking in Manoeuvre 2

Manoeuvre 03

The simulated situation was:

Manoeuvre	Wind (knots)	Current (knots)	Tugs
Atlantic Entrance	20 from NNE	0.0	1 de 82t 1 de 65t

Manoeuvre 03 – The Cerro Azul Tug was used in the bow, with two tied lines, and the tug Tonosi was used in the stern, with two tied lines. The tugs were controlled by Bridges 1 and 2, as Own Ship.

The Vessel Type was controlled by the instructor, also as Own Ship.

It was experienced an entrance manoeuvre in the lock, demanding about 1.5 nautical miles of distance and with inicial speed of 5.6 knots. The purpose was trying to obtain a greater manoeuvrability of Vessel Type.

Even with that attempt the Vessel Type ran aground in approaching zone of lock entrance and the tugs, even used frequently with its maximum power, forcing its machinery weren't able to provide enough bollard pull to control the Vessel Type.

There was great difficulty to control the Vessel Type and tugs in environmental conditions configured.
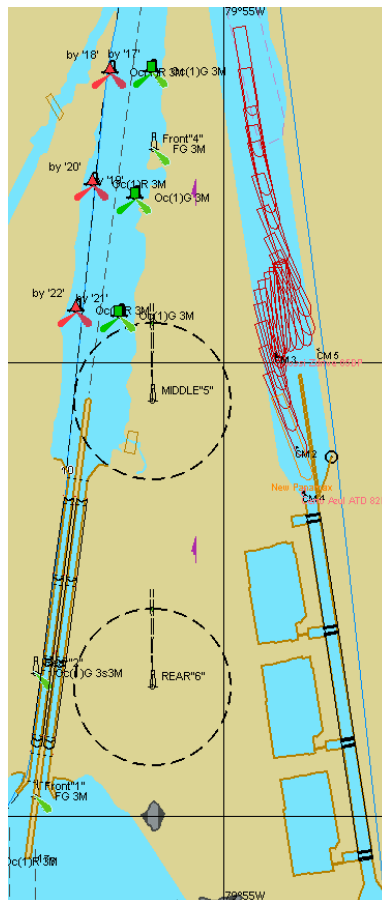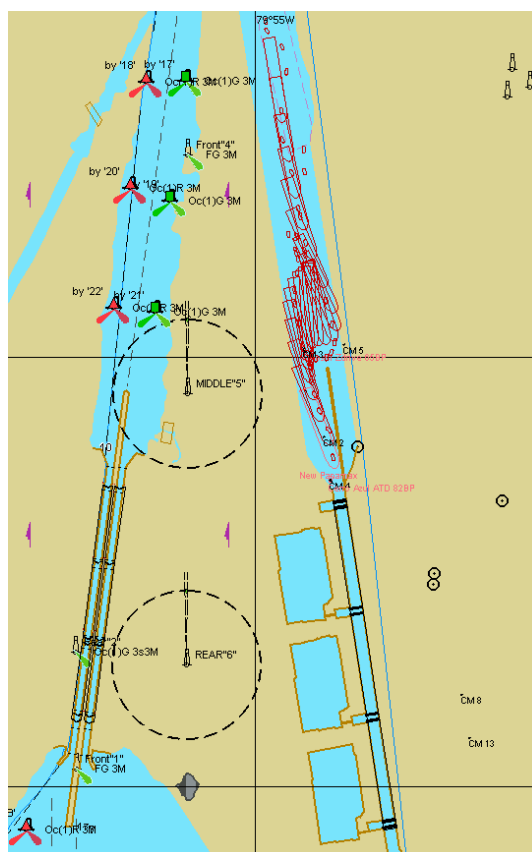

Figure 22: Vessel Type tracking in Manoeuvre 3

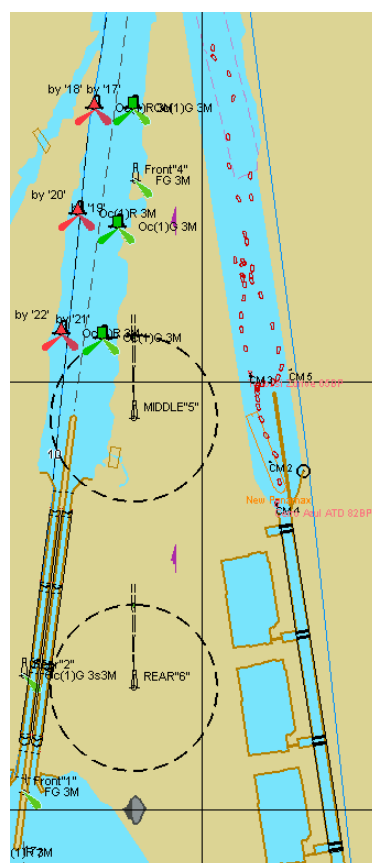Figure 23: Vessel Type and Tugs tracking in Manoeuvre 3
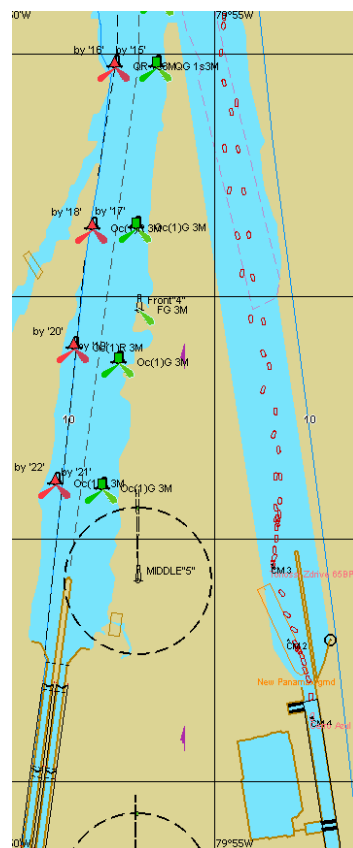
Figure 24: Tugs tracking in Manoeuvre 3

Manoeuvre 04

The simulated situation was:

Manoeuvre	Wind (knots)	Current (knots)	Tugs
Atlantic Entrance	20 from NNE	0.0	1 de 82t 1 de 65t

Manoeuvre 04 – The Cerro Azul Tug was used in the bow, with two tied lines, and the tug Tonosi was used in the stern, with two tied lines. The tugs were controlled by Bridges 1 and 2, as Own Ship.

The Vessel Type was controlled by the instructor, also as Own Ship.

In the first chamber entrance the Vessel Type collided with the stern. Even with the tugs used frequently with its maximum power, forcing its machinery weren't able to provide enough bollard pull to control the Vessel Type.
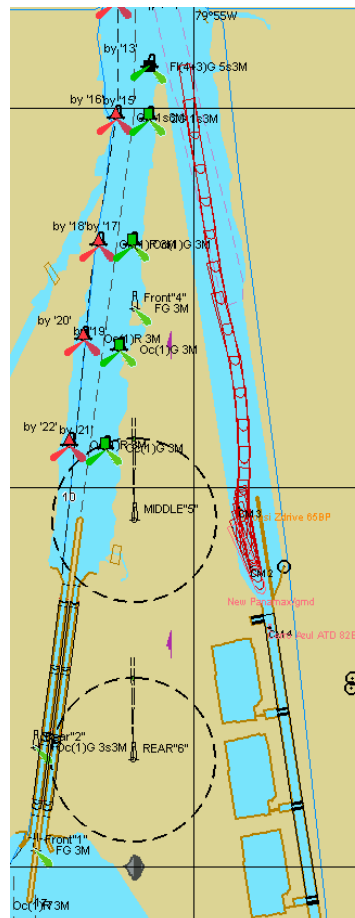

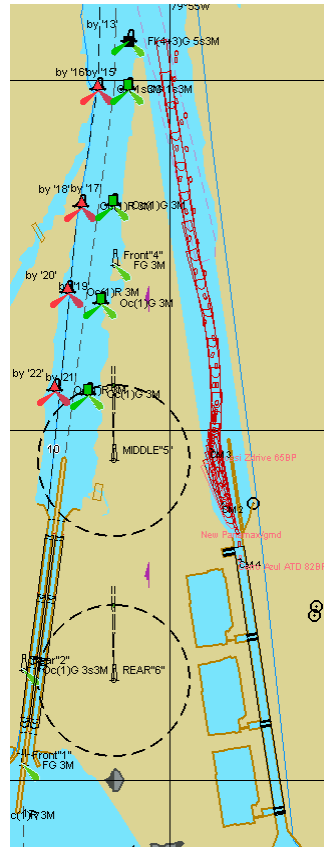Figure 25: Vessel Type tracking in Manoeuvre 04

Figure 26: Vessel Type and Tugs tracking in Manoeuvre 04

Figure 27: Tugs tracking in Manoeuvre 04.

Manoeuvre 05

The simulated situation was:

Manoeuvre	Wind (knots)	Current (knots)	Tugs
Pacific Entrance	10 from NNO	0.0	1 de 82t 1 de 65t

Manoeuvre 05 – The Cerro Azul Tug was used in the bow, with two tied lines through the centre, and the tug Tonosi was used in the stern, with two tied lines. The tugs were controlled by Bridges 1 and 2, as Own Ship.

The Vessel Type was controlled by the instructor, also as Own Ship.

The tug used in bow was in near miss situation inside the first chamber. The situation occurred due to the difficulty on controlling Vessel Type and Tugs in environmental conditions configured, even if in some moments using full power of tugs.
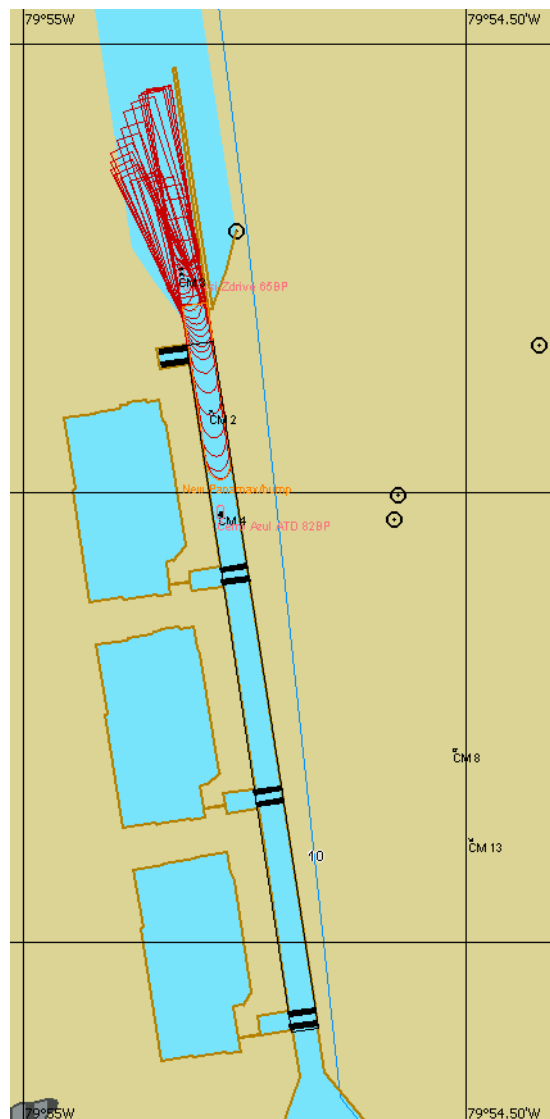

Figure 28: Vessel Type tracking in Manoeuvre 05.

Figure 29: Vessel Type and Tugs tracking in Manoeuvre 05.
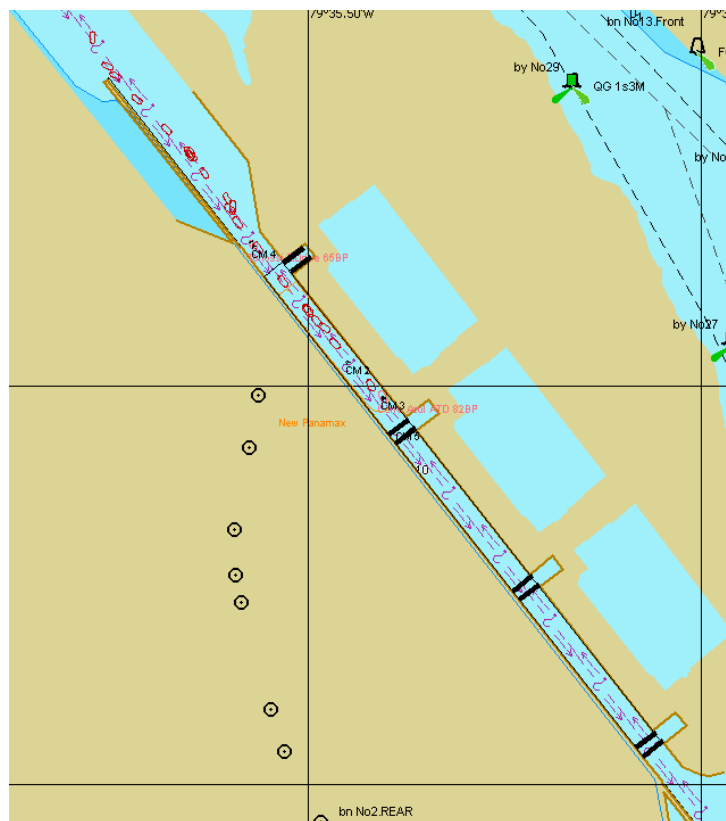
Figure 30: Tugs tracking in Manoeuvre 05.

Manoeuvre 06

The simulated situation was:

Manoeuvre	Wind (knots)	Current (knots)	Tugs
Pacific Entrance	10 from NNO	0.0	1 de 82t 1 de 65t

Manoeuvre 06 – The Cerro Azul Tug was used in the bow, with two tied lines through the centre, and the tug Tonosi was used in the stern, with two tied lines. The tugs were controlled by Bridges 1 and 2, as Own Ship.

The Vessel Type was controlled by the instructor, also as Own Ship.

The Vessel Type ran aground in the first chamber entrance.

Even in some moments using full power of tugs used in stern, it wasn't possible to control the Vessel Type in environmental conditions configured.

Figure 31: Vessel Type tracking in Manoeuvre 06.
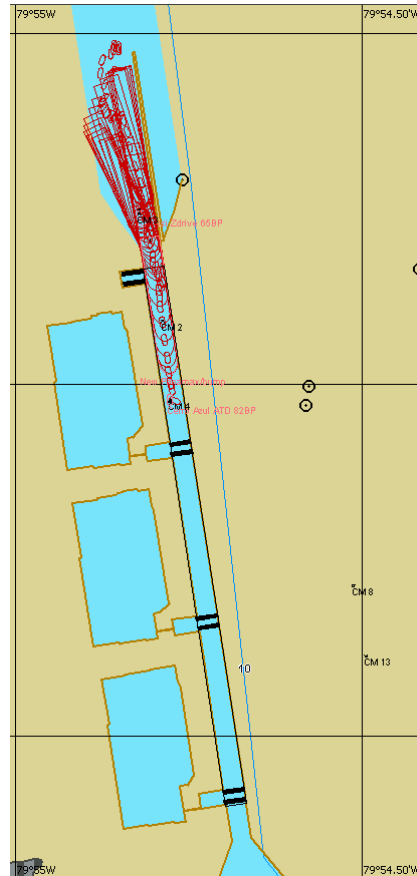
Figure 32: Vessel Type and Tugs tracking in Manoeuvre 06.
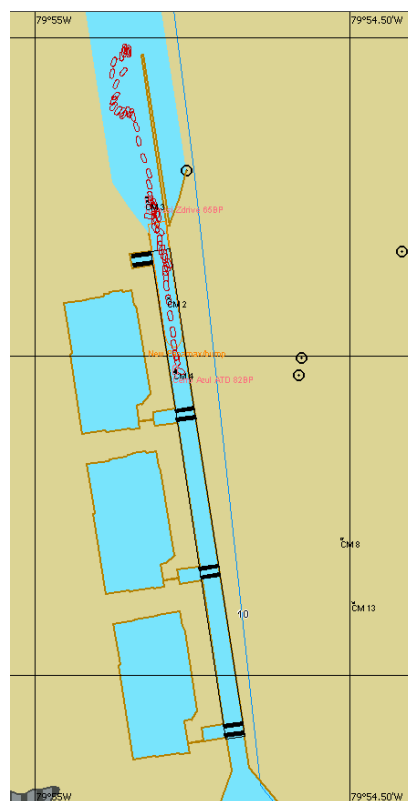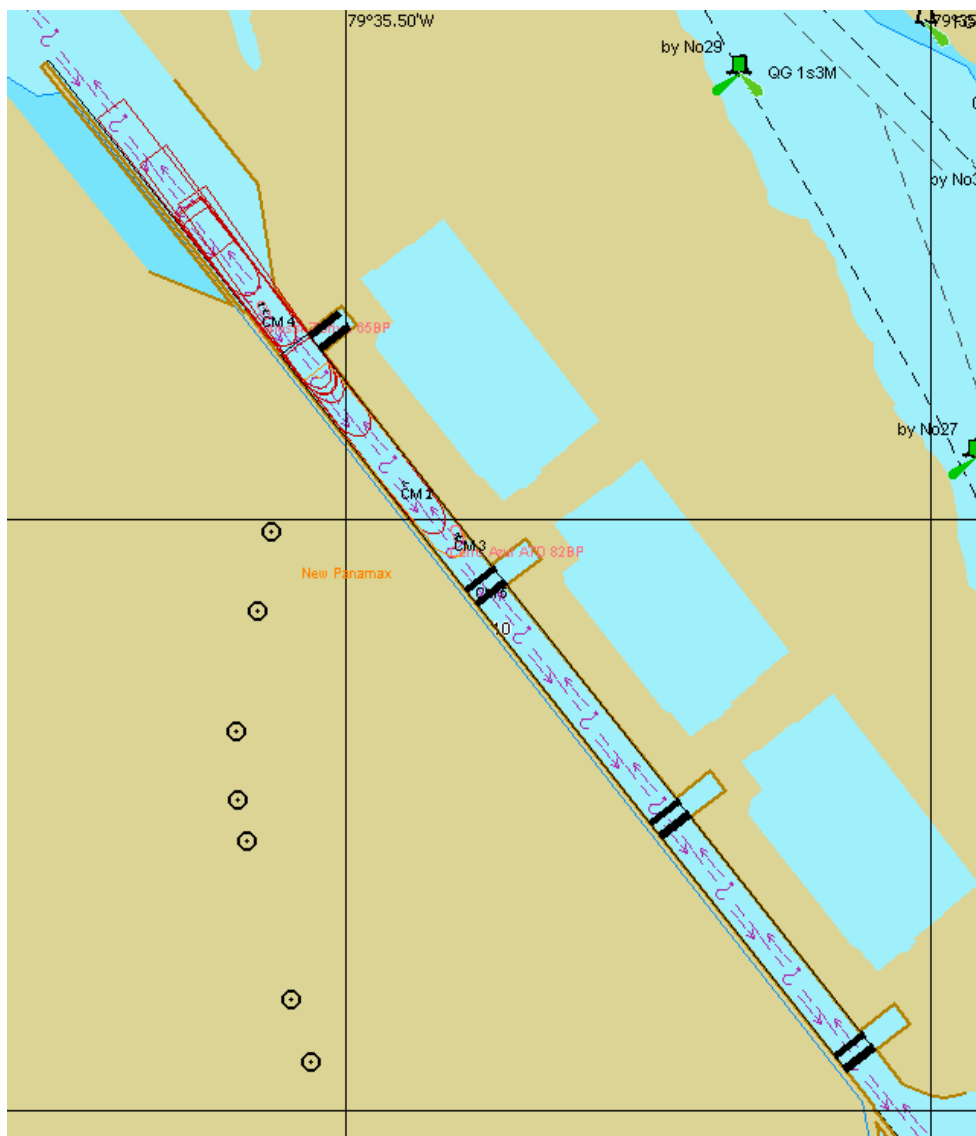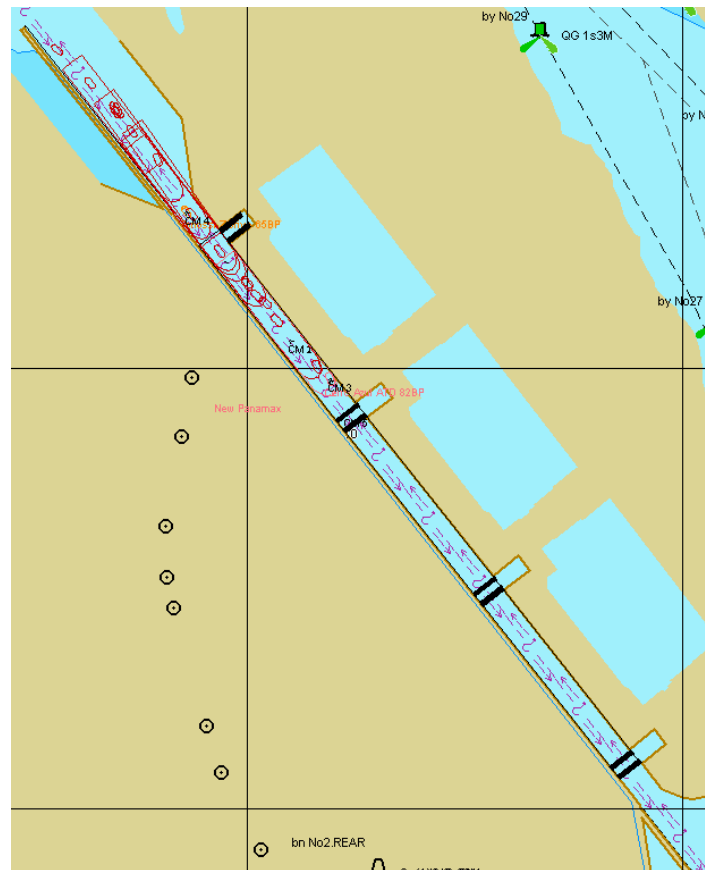

Figure 33: Tugs tracking in Manoeuvre 06.

Manoeuvre 07

The simulated situation was:

Manoeuvre	Wind (knots)	Current (knots)	Tugs
Atlantic Entrance	20 from NNO	0.0	1 de 65t 1 de 65t

Manoeuvre 07 – The Cerro Azul Tug was used in the bow, with two tied lines through the centre, and the tug Tonosi was used in the stern, with two tied lines. The tugs were controlled by Bridges 1 and 2, as Own Ship.

The Vessel Type was controlled by the instructor, also as Own Ship.

It was tried an entrance in locks sailing astern.

The difficulty in control the Vessel Type sailing astern, in environmental conditions configured was higher than with the ship sailing ahead.

The conclusion was that is much more stable sailing ahead as astern, being, in this case, more difficult to maintain control of Vessel Type and tug use in stern.
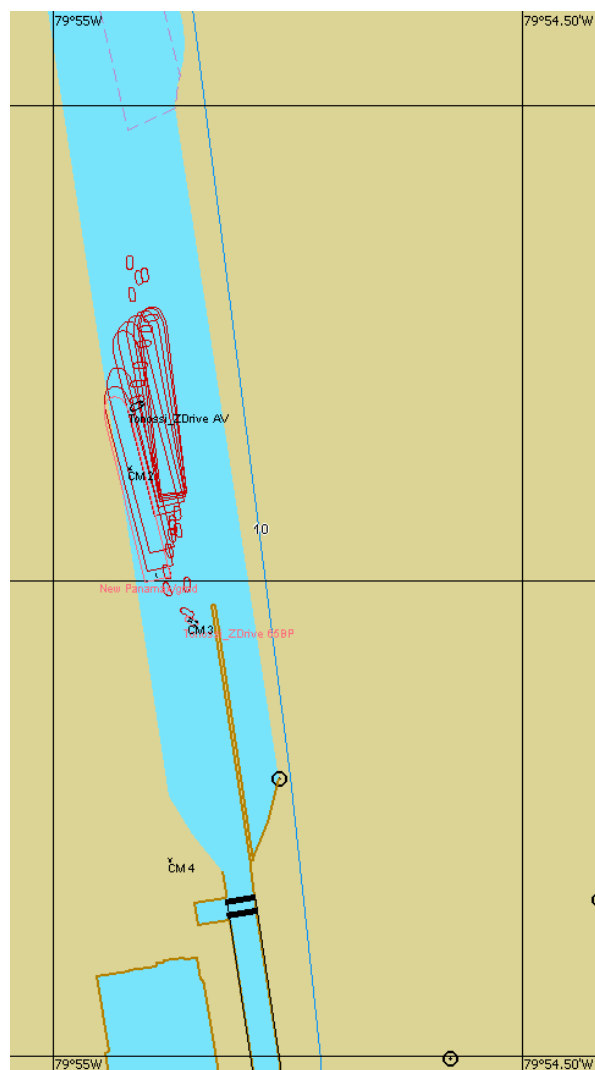
Figure 34: Vessel Type tracking in Manoeuvre 07.

Manoeuvre 08

The simulated situation was:

Manoeuvre	Wind (knots)	Current (knots)	Tugs
Atlantic Entrance	20 from NNO	0.0	1 de 65t 1 de 65t

Manoeuvre 08 – The Cerro Azul Tug was used in the bow, with two tied lines through the centre, and the tug Tonosi was used in the stern, with two tied lines. The tugs were controlled by Bridges 1 and 2, as Own Ship.

The Vessel Type was controlled by the instructor, also as Own Ship.

It was tried an entrance in locks sailing in astern.

The difficulty in control the Vessel Type sailing astern, in environmental conditions configured was higher than with the ship sailing ahead.

The conclusion was that is much more stable sailing ahead as astern, being, in this case, more difficult to maintain control of Vessel Type and tug use in stern.

Inside the first chamber the Vessel Typed collided with the chamber internal wall due to its high speed, 1.2 knots.
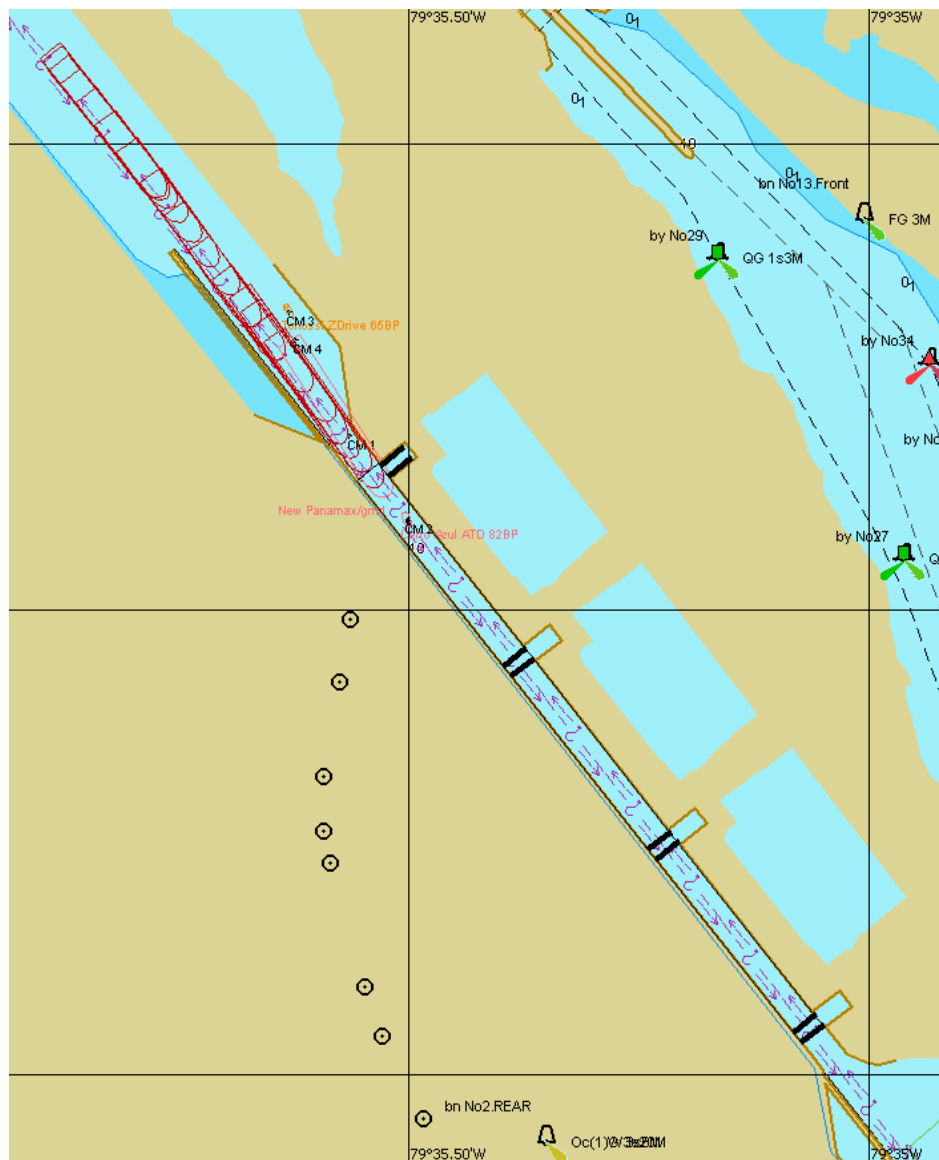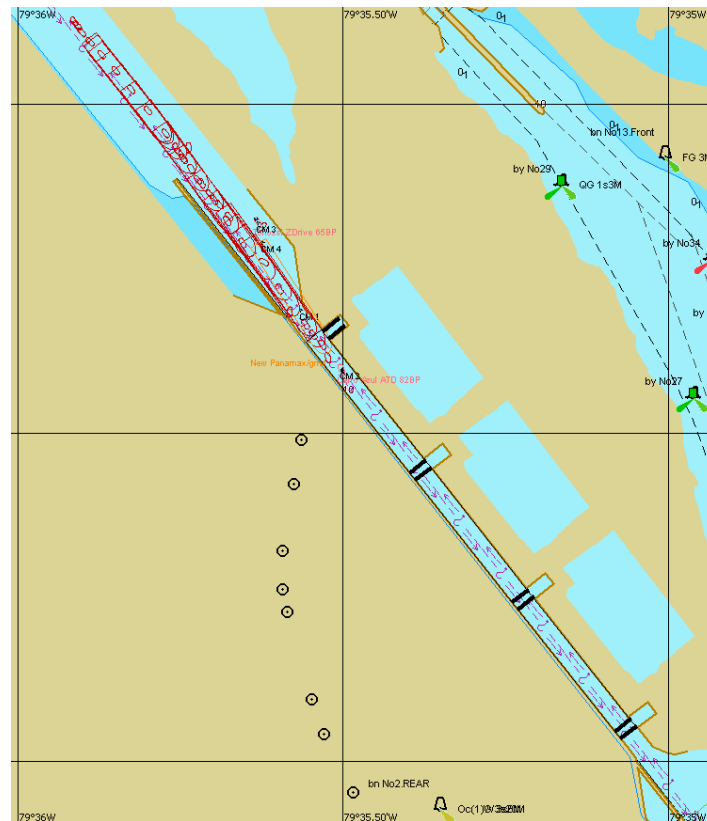

Figure 35: Vessel Type tracking in Manoeuvre 08.
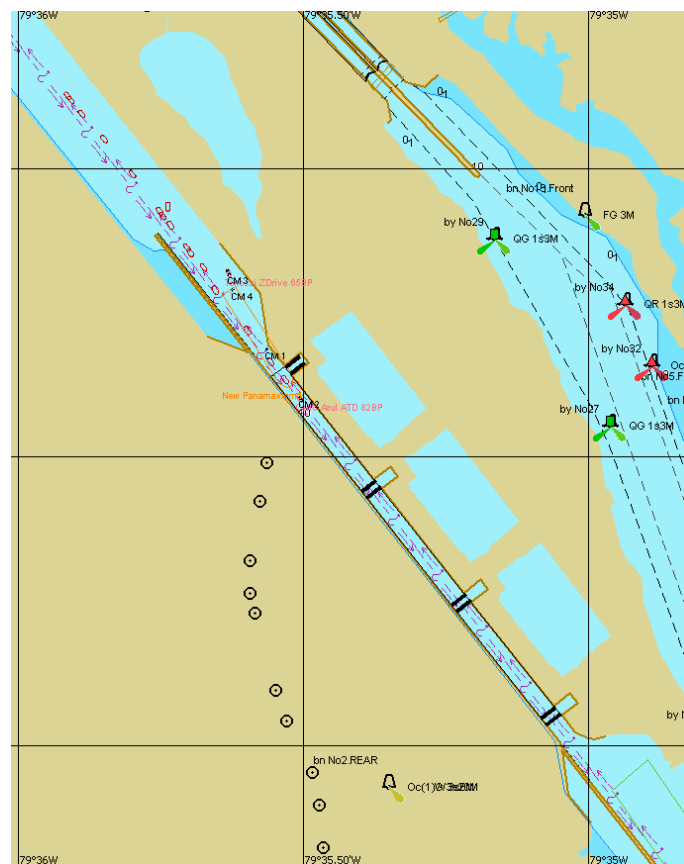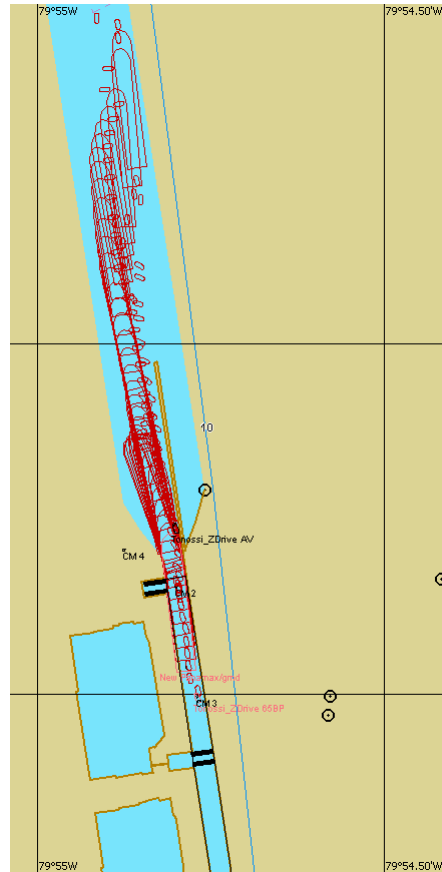
Figure 36: Vessel Type and Tugs tracking in Manoeuvre 08.
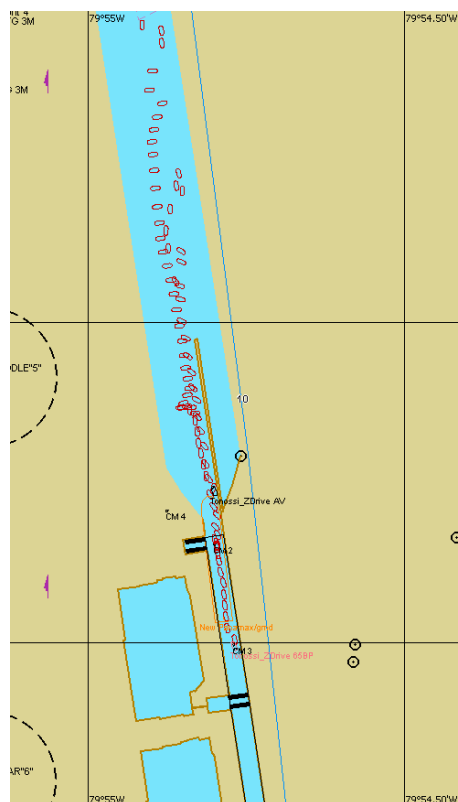
Figure 37: Tugs tracking in Manoeuvre 08.

Manoeuvre 09

The simulated situation was:

Manoeuvre	Wind (knots)	Current (knots)	Tugs
Atlantic Entrance	10 from NNO	0.0	1 de 65t 1 de 65t

Manoeuvre 09 – The Cerro Azul Tug was used in the bow, with two tied lines through the centre, and the tug Tonosi was used in the stern, with two tied lines. The tugs were controlled by Bridges 1 and 2, as Own Ship.

The Vessel Type was controlled by the instructor, also as Own Ship.

It was tried an entrance in locks sailing in astern.

The difficulty in control the Vessel Type sailing astern, in environmental conditions configured was higher than with the ship sailing ahead.

The conclusion was that is much more stable sailing ahead as astern, being, in this case, more difficult to maintain control of Vessel Type and tug use in stern.

Inside the first chamber the Vessel Type ran aground due to the wind force pushing it to over chamber internal wall and also due to the tug used in stern not having enough power to support the ship, even using its full force most of the time in manoeuvre.
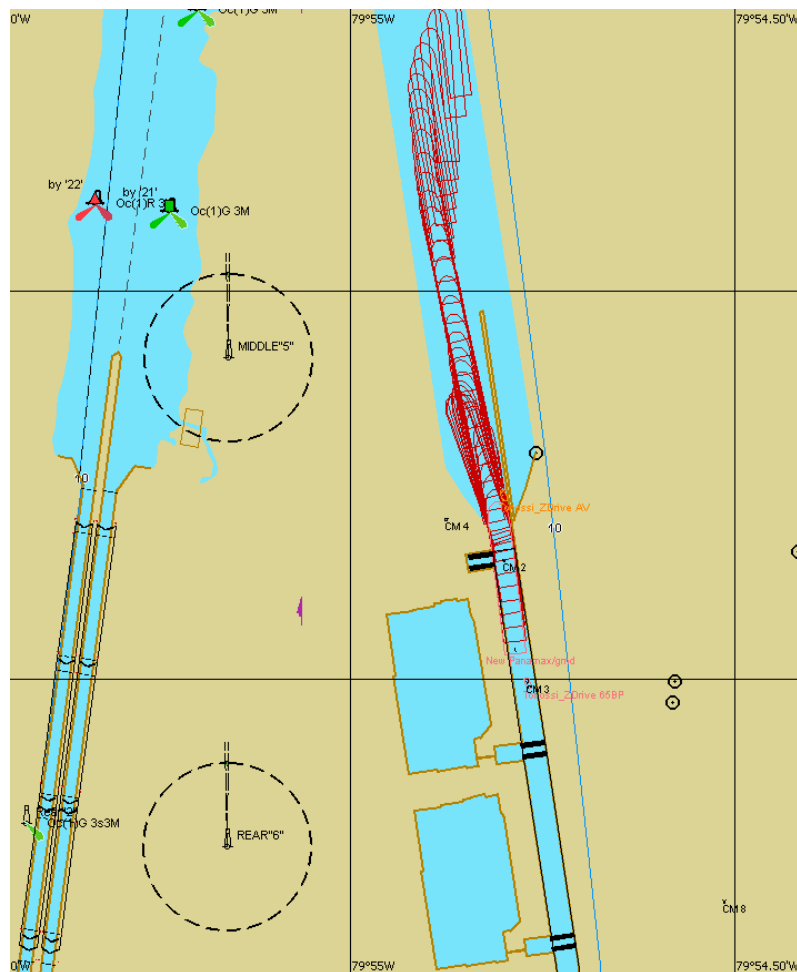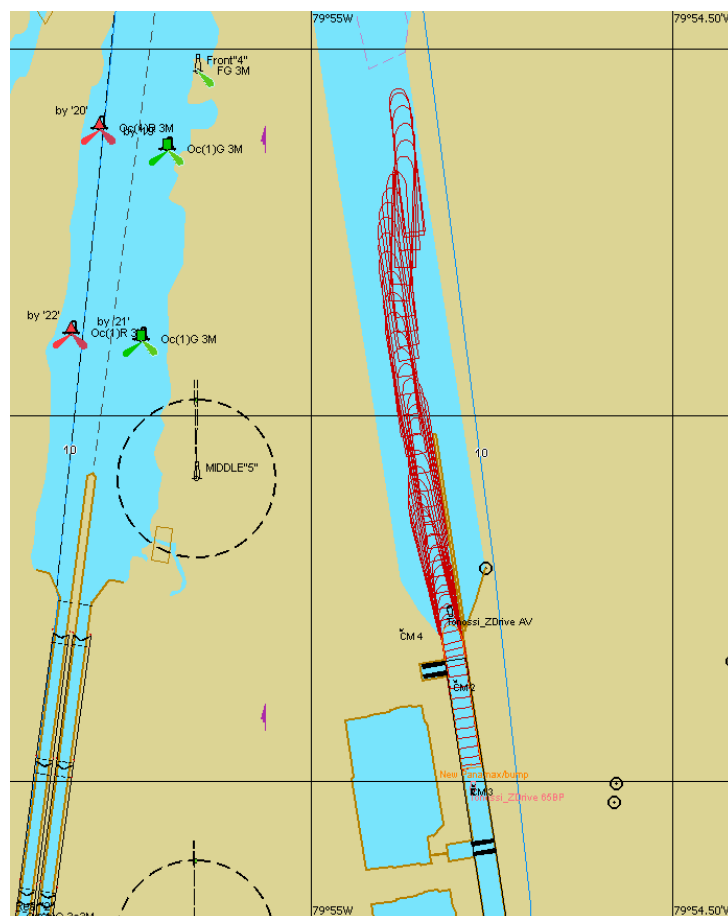

Figure 38: Vessel Type tracking in Manoeuvre 09.

Figure 39: Vessel Type and Tugs tracking in Manoeuvre 09.

Figure 40: Tugs tracking in Manoeuvre 09.

6.3.2 Manoeuvres carried out by FHM Team.

Manoeuvre 10

The simulated situation was:

Manoeuvre	Wind (knots)	Current (knots)	Tugs
Atlantic Exit	14.2 from NNE	1.3 to ENE	1 de 61t 1 de 54t

Manoeuvre 10 – The Los Santos Tug was used in the bow, with two tied lines and controlled as Own Ship in Bridge 2 by collaborator of CSA team. The Chiriqui III tug was used in the stern with one tied line and controlled as Own Ship by the instructor. The Vessel Type was also controlled as Own Ship by the instructor.

In this manoeuvre it wasn't possible to control the Vessel Type, even with the assistance of tugs using all its power.

Due to tugs' low power and metocean conditions, there is difficulty also in controlling tugs during manoeuvre.

The towline of tug used in stern broke and the Vessel Type ran aground.

Figure 41: Vessel Type and Tugs tracking in Manoeuvre 10.

Manoeuvre 11

The simulated situation was:

Manoeuvre	Wind (knots)	Current (knots)	Tugs
Atlantic Exit	14.2 from NNE	1.3 to ENE	1 de 65t 1 de 61t

Manoeuvre 11 – The Chiriqui III Tug was used in the bow, with two tied lines and controlled as Own Ship in Bridge 2 by collaborator of CSA team. The Tonosi tug was used in the stern with one tied line and controlled as Own Ship by the instructor. The Vessel Type was also controlled as Own Ship by the instructor.

In this manoeuvre it wasn't possible to control the Vessel Type, even with the assistance of tugs using all its power.

Due to tugs' low power and metocean conditions, there is difficulty also in controlling tugs during manoeuvre.

The towline of tug use in stern broke and affected all manoeuvre.

Figure 42: Vessel Type and Tugs tracking in Manoeuvre 11.

Manoeuvre 12

The simulated situation was:

Manoeuvre	Wind (knots)	Current (knots)	Tugs
Atlantic Exit	14.2 from NNE	1.3 to ENE	1 de 82t 1 de 65t

Manoeuvre 12 – The Cerro Azul Tug was used in the bow, with two tied lines and controlled as Own Ship in Bridge 2 by collaborator of CSA team. The Tonosi tug was used in the stern with one tied line and controlled as Own Ship by the instructor. The Vessel Type was also controlled as Own Ship by the instructor.

In this manoeuvre it wasn't possible to control the Vessel Type, even with the assistance of tugs using all its power.

Due to tugs' low power and metocean conditions, there is difficulty also in controlling tugs during manoeuvre.
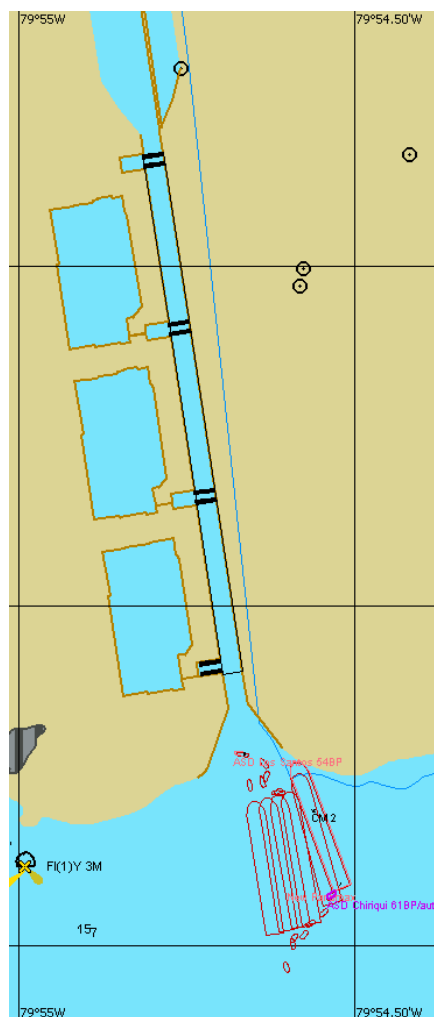

Figure 43: Vessel Type and Tugs tracking in Manoeuvre 12.

Manoeuvre 13

The simulated situation was:

Manoeuvre	Wind (knots)	Current (knots)	Tugs
Atlantic Exit	10 from NNE	1.0 to ENE	1 de 82t 1 de 65t

Manoeuvre 13 – The Cerro Azul Tug was used in the bow, with two tied lines and controlled as Own Ship in Bridge 2 by collaborator of CSA team. The Tonosi tug was used in the stern with one tied line and controlled as Own Ship by the instructor. The Vessel Type was also controlled as Own Ship by the instructor.

In this manoeuvre it wasn't possible to control the Vessel Type, even with the assistance of tugs using all its power.

Due to tugs' low power and metocean conditions, there is difficulty also in controlling tugs during manoeuvre.

Figure 44: Vessel Type and Tugs tracking in Manoeuvre 13.

Manoeuvre 14

The simulated situation was:

Manoeuvre	Wind (knots)	Current (knots)	Tugs
Atlantic Exit	05 from NNE	1.0 to ENE	1 de 82t 1 de 65t

Manoeuvre 14 – The Cerro Azul Tug was used in the bow, with two tied lines and controlled as Own Ship in Bridge 2 by collaborator of CSA team. The Tonosi tug was used in the stern with one tied line and controlled as Own Ship by the instructor. The Vessel Type was also controlled as Own Ship by the instructor.

In this manoeuvre, we reduced more the effects of wind and current, but it wasn't possible to control the Vessel Type, even with the assistance of tugs using all its power.

Due to tugs' low power and metocean conditions, there is difficulty also in controlling tugs during manoeuvre.
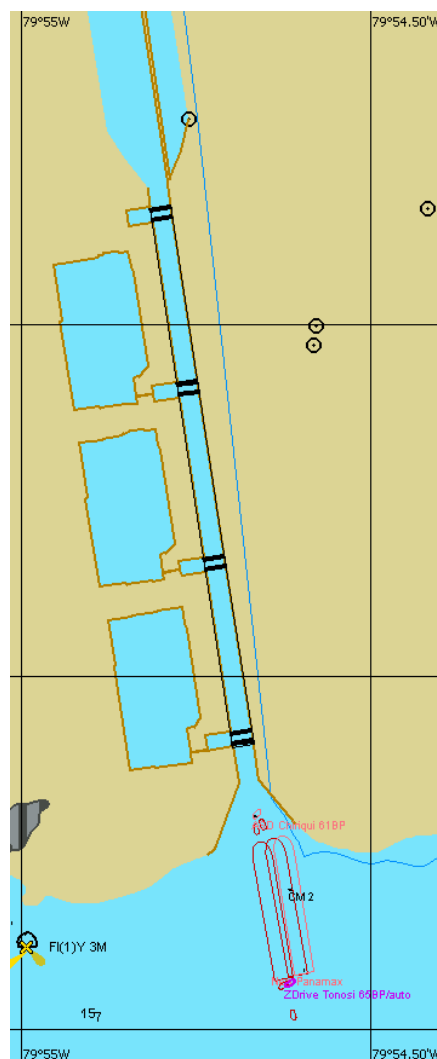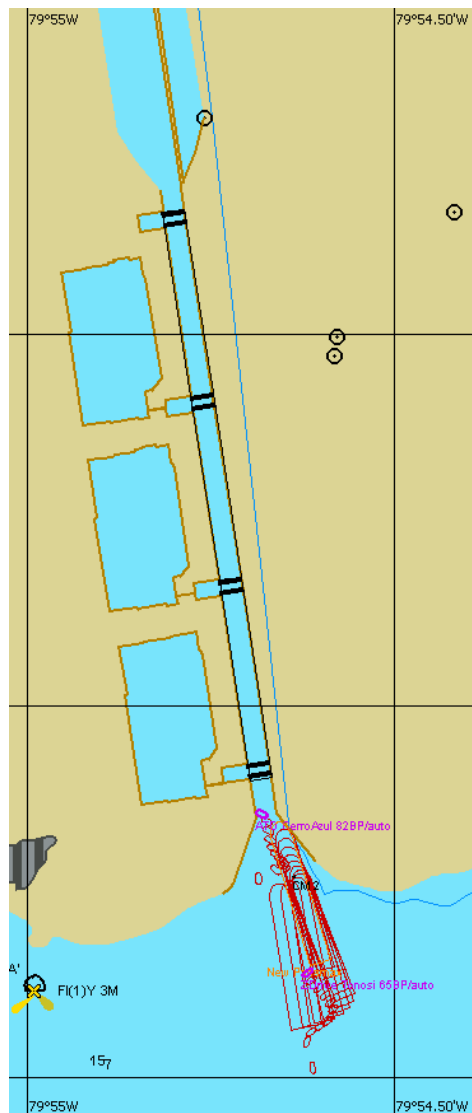

Figure 45: Vessel Type and Tugs tracking in Manoeuvre 14.

Manoeuvre 15

The simulated situation was:

Manoeuvre	Wind (knots)	Current (knots)	Tugs
Atlantic Exit	05 from NNE	0.5 to ENE	1 de 82t 1 de 65t

Manoeuvre 15 – The Cerro Azul Tug and Tonosi tug were used in the bow and in the stern, respectively, with one tied line and controlled as Own Ship by the instructor. The Vessel Type was also controlled as Own Ship by the instructor.

In this manoeuvre, after a few attempts, we reach a configuration less uncomfortable in relation to wind and current effects. However, although we could conduct and control the Vessel Type and tugs, the manoeuvre required much effort, making the tugs perform in its limits.

A ship with LOA of 366m, with tied lines about 30 meters to two tugs with LOA of 28.9 e 27.4, has its manoeuvrability very restricted in a chamber of 427 meters length. This fact entails constants situations of near miss.

Figure 46: Vessel Type tracking in Manoeuvre 15.

Figure 47: Vessel Type and Tugs tracking in Manoeuvre 15.

Figure 48: Tugs tracking in Manoeuvre 15.

Manoeuvre 16

The simulated situation was:

Manoeuvre	Wind (knots)	Current (knots)	Tugs
Atlantic Entrance	05 from NNE	0.5 to ENE	1 de 82t 1 de 65t

Manoeuvre 16 – The Cerro Azul Tug was used in the bow, with two tied lines and controlled as Own Ship in Bridge 2 by collaborator of CSA team. The Tonosi tug was used in the stern with one tied line and controlled as Own Ship by the instructor. The Vessel Type was also controlled as Own Ship by the instructor.

In this manoeuvre, even with the effects of wind and current reduced, there isn't facility to control the Vessel Type, even with the assistance of tugs using all its power. This fact and also the possibility of occur a human failure in manoeuvre can cause an accident. As well as occurred the collision of Tonosi Tug in third chamber entrance.

Figure 49: Vessel Type tracking in Manoeuvre 16.
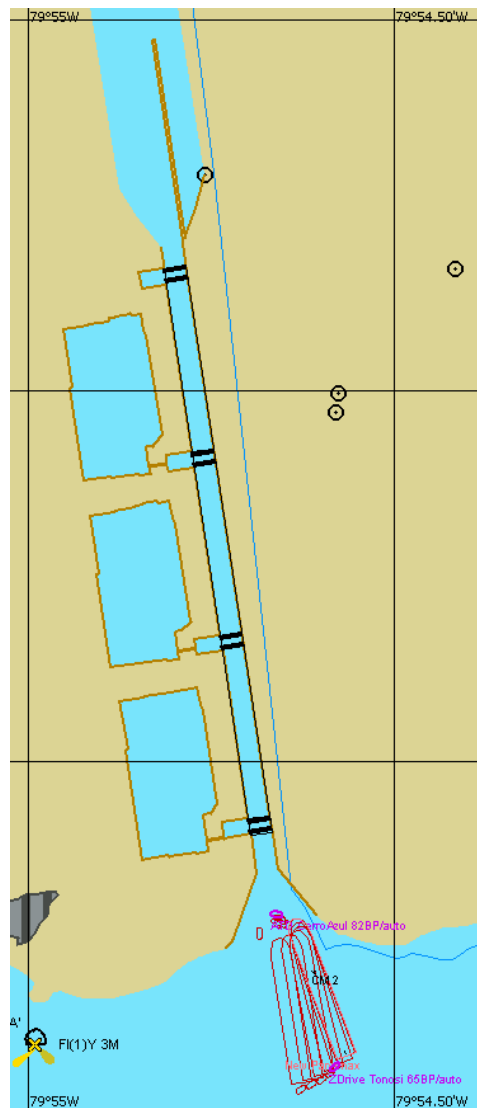
Figure 50: Vessel Type and Tugs tracking in Manoeuvre 16.

Figure 51: Tugs tracking in Manoeuvre 16.

Manoeuvre 17

The simulated situation was:

Manoeuvre	Wind (knots)	Current (knots)	Tugs
Atlantic Entrance	05 from NNE	0.5 to ENE	1 de 82t 1 de 65t

Manoeuvre 17 – The Cerro Azul Tug was used in the bow, with two tied lines and controlled as Own Ship in Bridge 2 by collaborator of CSA team. The Tonosi tug was used in the stern with one tied line and controlled as Own Ship by the instructor. The Vessel Type was also controlled as Own Ship by the instructor.

In this manoeuvre, even with the effects of wind and current reduced, there isn't facility to control the Vessel Type, even with the assistance of tugs using all its power.
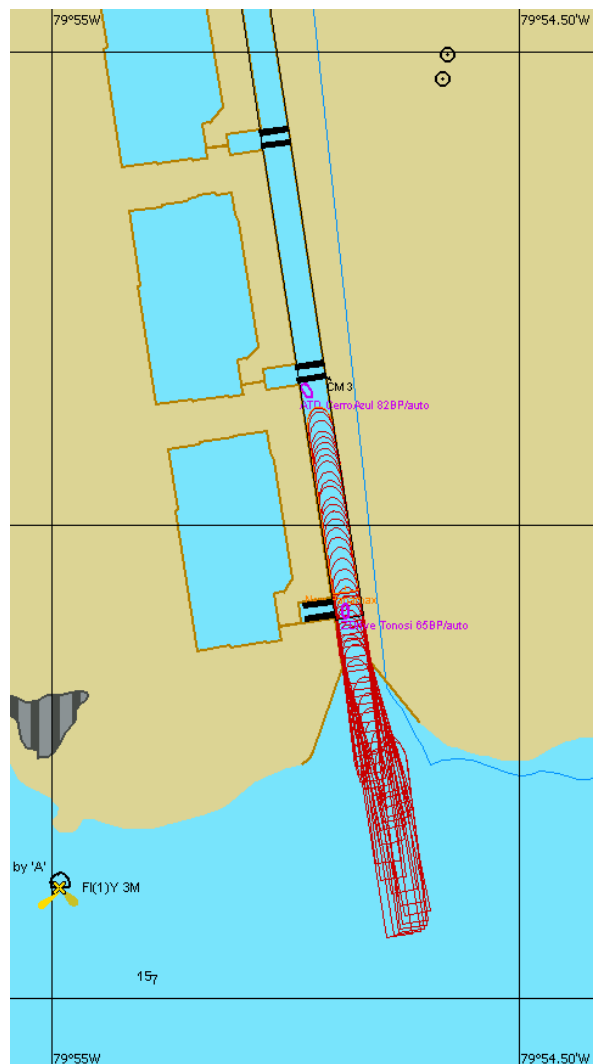

Figure 52: Vessel Type tracking in Manoeuvre 17.
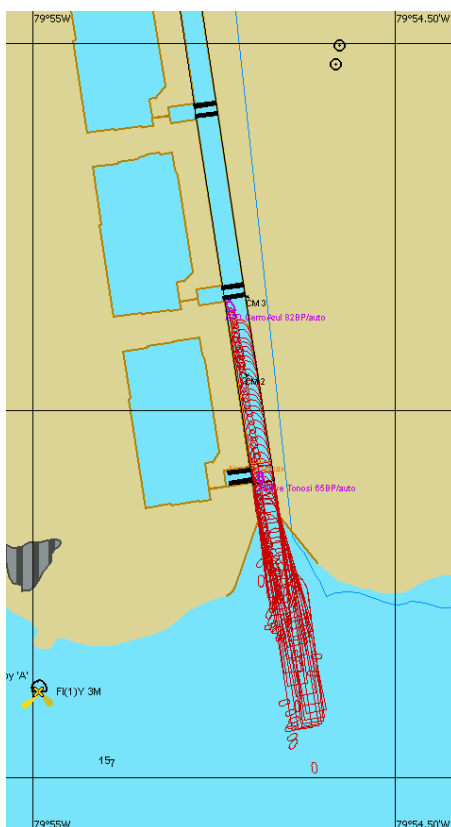
Figure 53: Vessel Type and Tugs tracking in Manoeuvre 17.
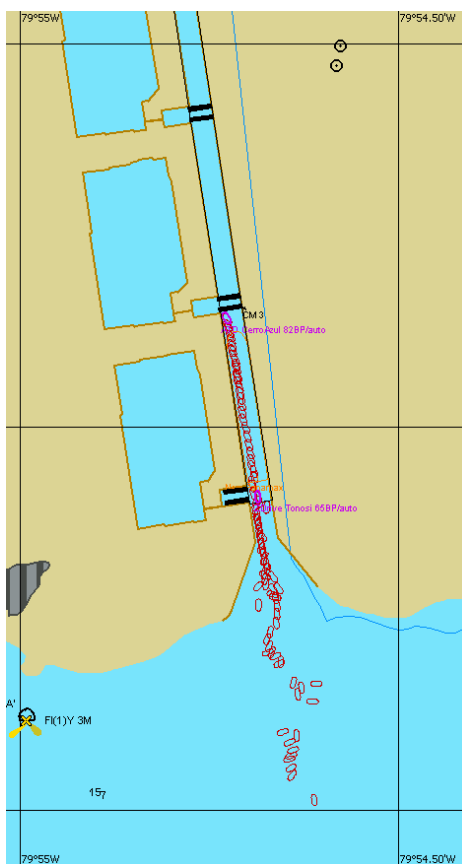

Figure 54: Tugs tracking in Manoeuvre 17.

Manoeuvre 18

The simulated situation was:

Manoeuvre	Wind (knots)	Current (knots)	Tugs
Atlantic Entrance	05 from NNE	0.5 to ENE	1 de 82t 1 de 65t

Manoeuvre 18 – The Cerro Azul Tug was used in the bow, with two tied lines and controlled as Own Ship in Bridge 2 by collaborator of CSA team. The Tonosi tug was used in the stern with one tied line and controlled as Own Ship by the instructor. The Vessel Type was also controlled as Own Ship by the instructor.

In this manoeuvre, even with the effects of wind and current reduced, there isn't facility to control the Vessel Type, even with the assistance of tugs using all its power.

The wind pushes the Vessel Type constantly in chamber internal wall.
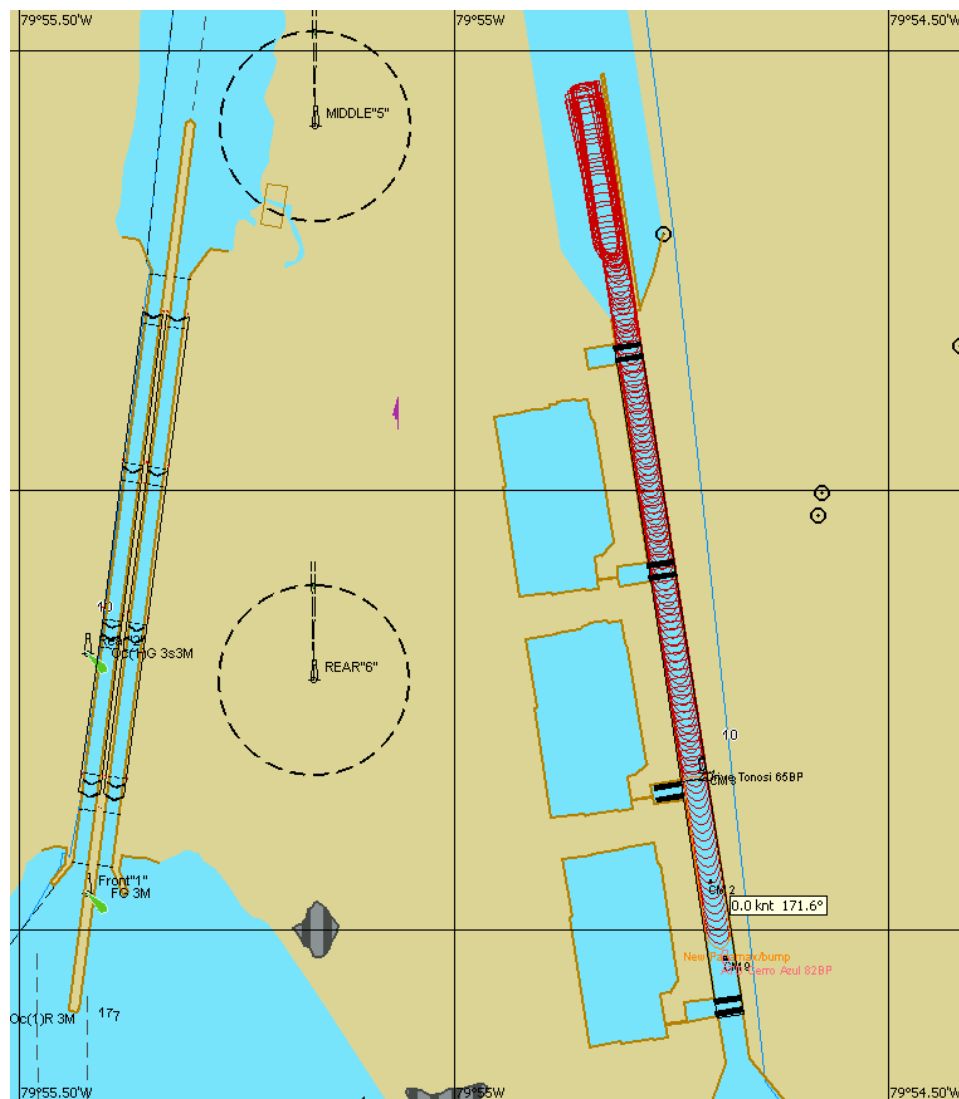

Figure 55: Vessel Type tracking in Manoeuvre 18.

Figure 56: Vessel Type and Tugs tracking in Manoeuvre 18.

Figure 57: Tugs tracking in Manoeuvre 18.

Manoeuvre 19

The simulated situation was:

Manoeuvre	Wind (knots)	Current (knots)	Tugs
Atlantic Entrance	05 from NNE	0.5 to ENE	1 de 82t 1 de 65t

Manoeuvre 19 – The Cerro Azul Tug was used in the bow, with two tied lines and controlled as Own Ship in Bridge 2 by collaborator of CSA team. The Tonosi tug was used in the stern with one tied line and controlled as Own Ship by the instructor. The Vessel Type was also controlled as Own Ship by the instructor.

In this manoeuvre, even with the effects of wind and current reduced, there isn't facility to control the Vessel Type, even with the assistance of tugs using all its power.

We obtained considerable difficult to control the Vessel Type using the tugs in the first chamber entrance.

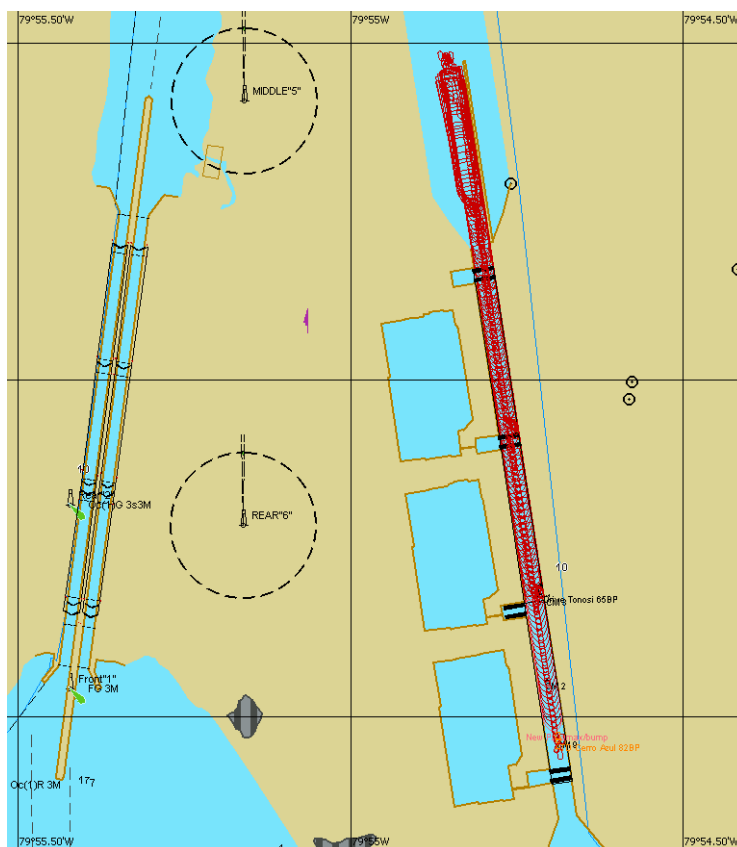Figure 58: Vessel Type tracking in Manoeuvre 19.

Figure 59: Vessel Type and Tugs tracking in Manoeuvre 19.

Figure 60: Tugs tracking in Manoeuvre 19.

Manoeuvre 20

The simulated situation was:

Manoeuvre	Wind (knots)	Current (knots)	Tugs
Pacific Exit	03.9 from NNO	2.8 to ENE	1 de 82t 1 de 65t

Manoeuvre 20 – The Cerro Azul Tug was used in the bow, with two tied lines and controlled as Own Ship in Bridge 2 by collaborator of CSA team. The Tonosi tug was used in the stern with one tied line and controlled as Own Ship by the instructor. The Vessel Type was also controlled as Own Ship by the instructor.

In this manoeuvre, even with the effects of wind and current reduced, there isn't facility to control the Vessel Type, even with the assistance of tugs using all its power.
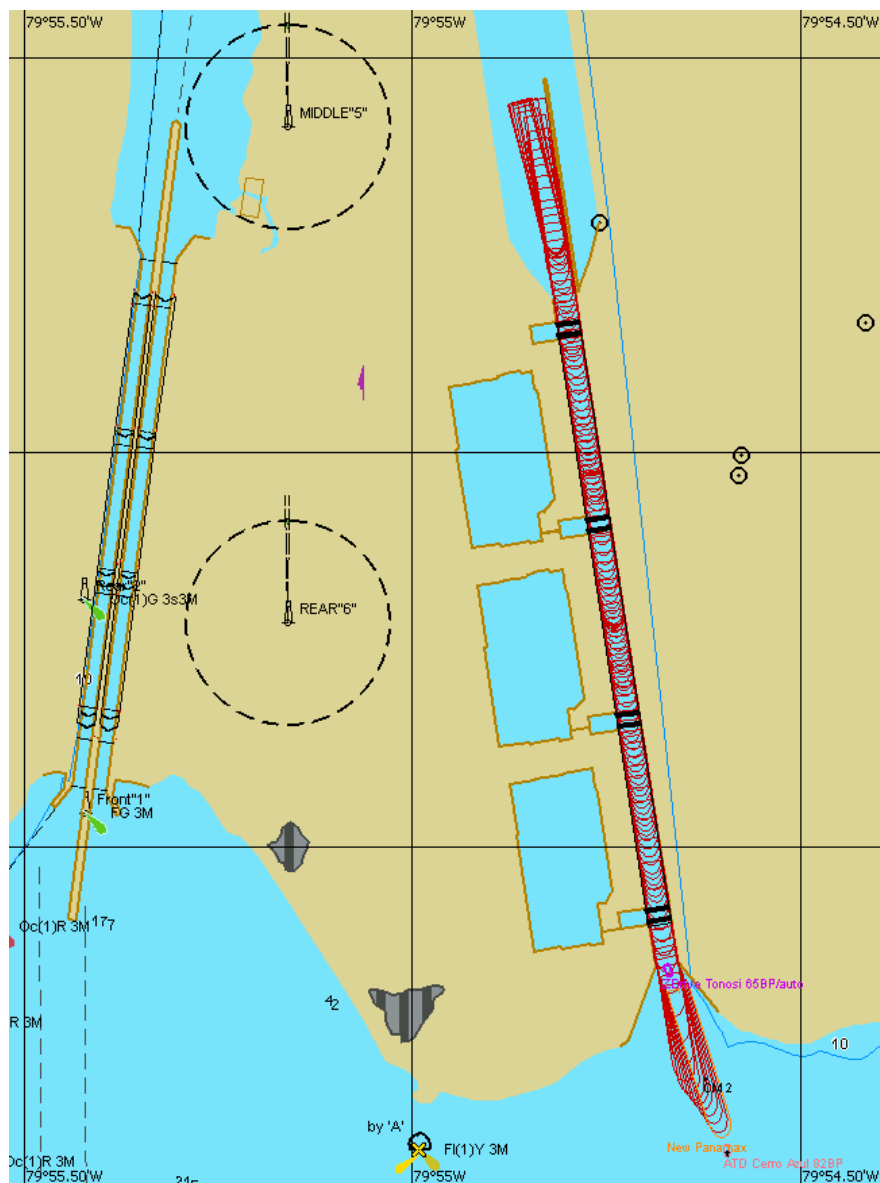

Figure 61: Vessel Type and Tugs tracking in Manoeuvre 20.

Manoeuvre 21

The simulated situation was:

Manoeuvre	Wind (knots)	Current (knots)	Tugs
Pacific Exit	03.9 from NNO	2.8 to ENE	1 de 82t 1 de 65t

Manoeuvre 21 – The Cerro Azul Tug was used in the bow, with two tied lines and controlled as Own Ship in Bridge 2 by collaborator of CSA team. The Tonosi tug was used in the stern with one tied line and controlled as Own Ship by the instructor. The Vessel Type was also controlled as Own Ship by the instructor.

In this manoeuvre, even with the effects of wind and current reduced, there isn't facility to control the Vessel Type, even with the assistance of tugs using all its power.

Figure 62: Vessel Type and Tugs tracking in Manoeuvre 21.

Manoeuvre 22

The simulated situation was:

Manoeuvre	Wind (knots)	Current (knots)	Tugs
Pacific Exit	03.9 from NNO	0.5 to ENE	1 de 82t 1 de 65t

Manoeuvre 22 – The Cerro Azul Tug was used in the bow, with two tied lines and controlled as Own Ship in Bridge 2 by collaborator of CSA team. The Tonosi tug was used in the stern with one tied line and controlled as Own Ship by the instructor. The Vessel Type was also controlled as Own Ship by the instructor.

In this manoeuvre, even reducing the current to 0.5 knots, it wasn't possible to control the Vessel Type with all available resources. So the Vessel Type ran aground.

Figure 63: Vessel Type and Tugs tracking in Manoeuvre 22.

Manoeuvre 23

The simulated situation was:

Manoeuvre	Wind (knots)	Current (knots)	Tugs
Pacific Exit	03.9 from NNO	0.5 to ENE	1 de 82t 1 de 65t

Manoeuvre 23 – The Cerro Azul Tug was used in the bow, with two tied lines and controlled as Own Ship in Bridge 2 by collaborator of CSA team. The Tonosi tug was used in the stern with one tied line and controlled as Own Ship by the instructor. The Vessel Type was also controlled as Own Ship by the instructor.

In this manoeuvre, even reducing the current to 0.5 knots, it wasn't possible to control the Vessel Type with all available resources. So the Vessel Type ran aground.
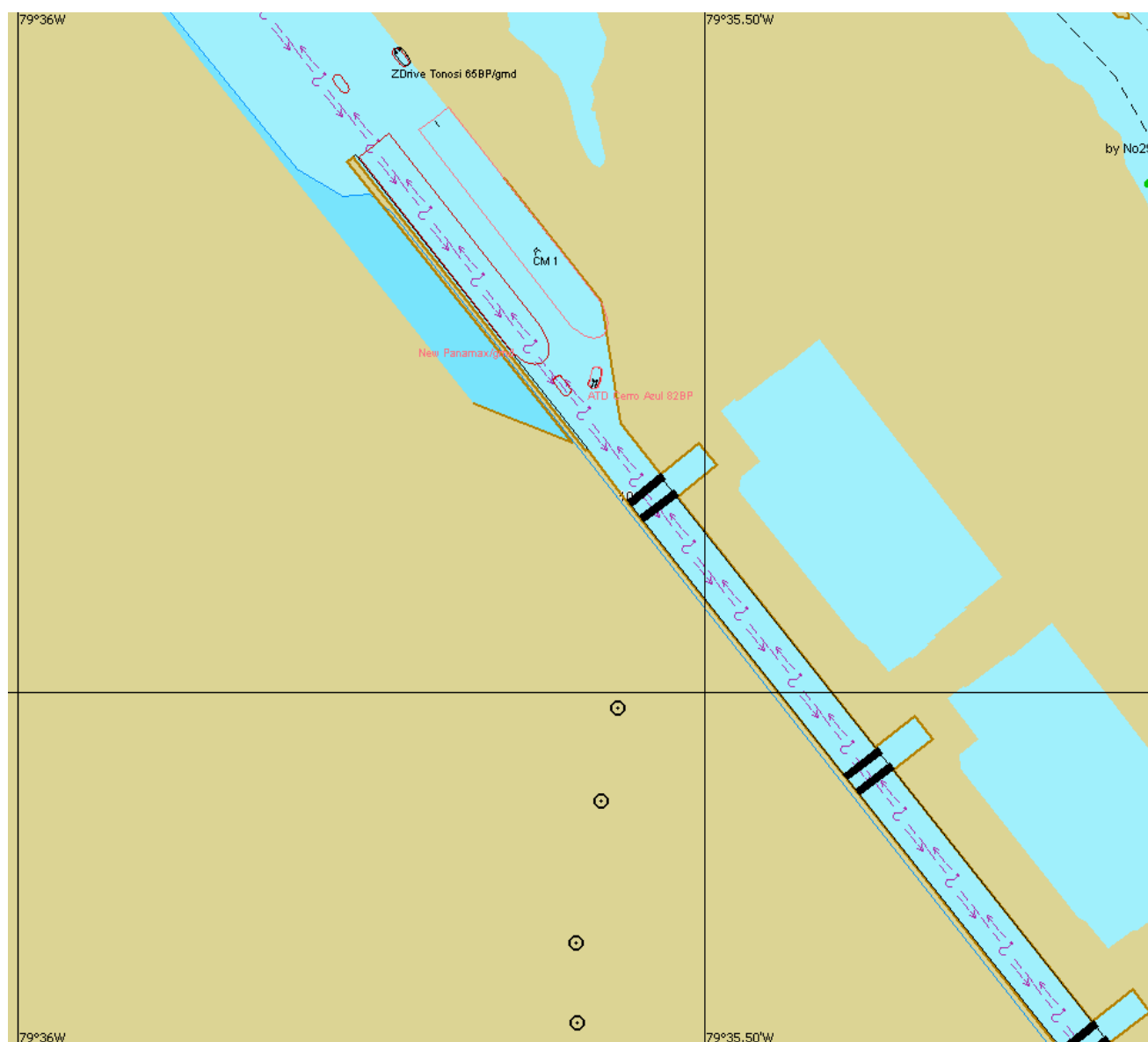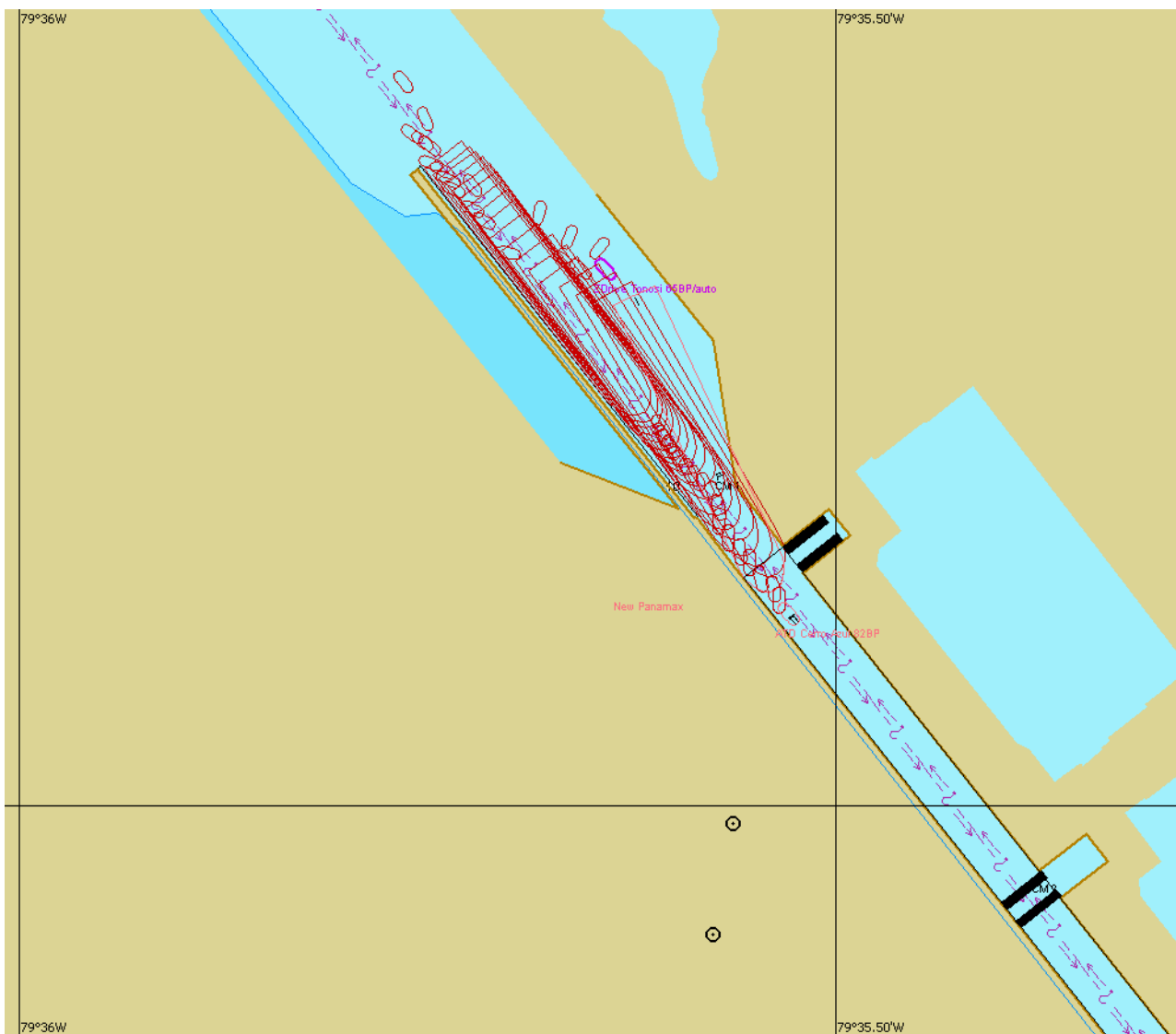

Figure 64: Vessel Type and Tugs tracking in Manoeuvre 23.

Manoeuvre 24

The simulated situation was:

Manoeuvre	Wind (knots)	Current (knots)	Tugs
Pacific Exit	03.9 from NNO	0.5 to ENE	1 de 82t 1 de 65t

Manoeuvre 24 – The Cerro Azul Tug was used in the bow, with two tied lines and controlled as Own Ship in Bridge 2 by collaborator of CSA team. The Tonosi tug was used in the stern with one tied line and controlled as Own Ship by the instructor. The Vessel Type was also controlled as Own Ship by the instructor.

In this manoeuvre, even reducing the current to 0.5 knots, it wasn't possible to control the Vessel Type with all available resources. So the Vessel Type ran aground.

The tugs using 60% of its power weren't able to affect the Vessel Type, in environmental conditions configured in this simulation. For that reason, it was even more reduced the current to the next manoeuvre in Pacific.

Figure 65: Vessel Type and Tugs tracking in Manoeuvre 24.

Manoeuvre 25

The simulated situation was:

Manoeuvre	Wind (knots)	Current (knots)	Tugs
Pacific Exit	03.9 from NNO	0.3 to ENE	1 de 82t 1 de 65t

Manoeuvre 25 – The Cerro Azul Tug was used in the bow, with two tied lines and controlled as Own Ship in Bridge 2 by collaborator of CSA team. The Tonosi tug was used in the stern with one tied line and controlled as Own Ship by the instructor. The Vessel Type was also controlled as Own Ship by the instructor.

In this manoeuvre, even reducing the current to 0.3 knots, it wasn't possible to control the Vessel Type with all available resources. The Vessel Type continued to drift to port side.
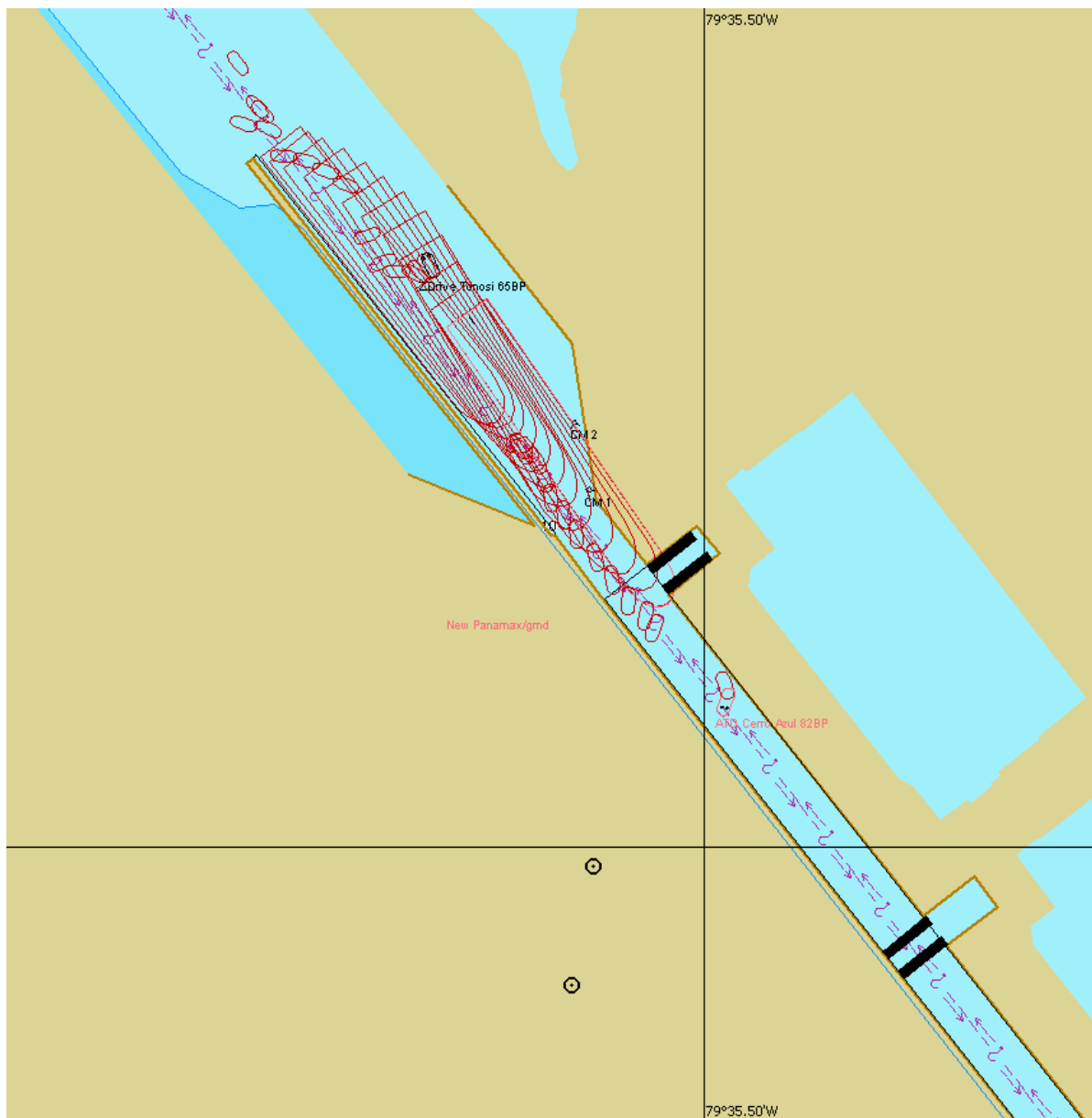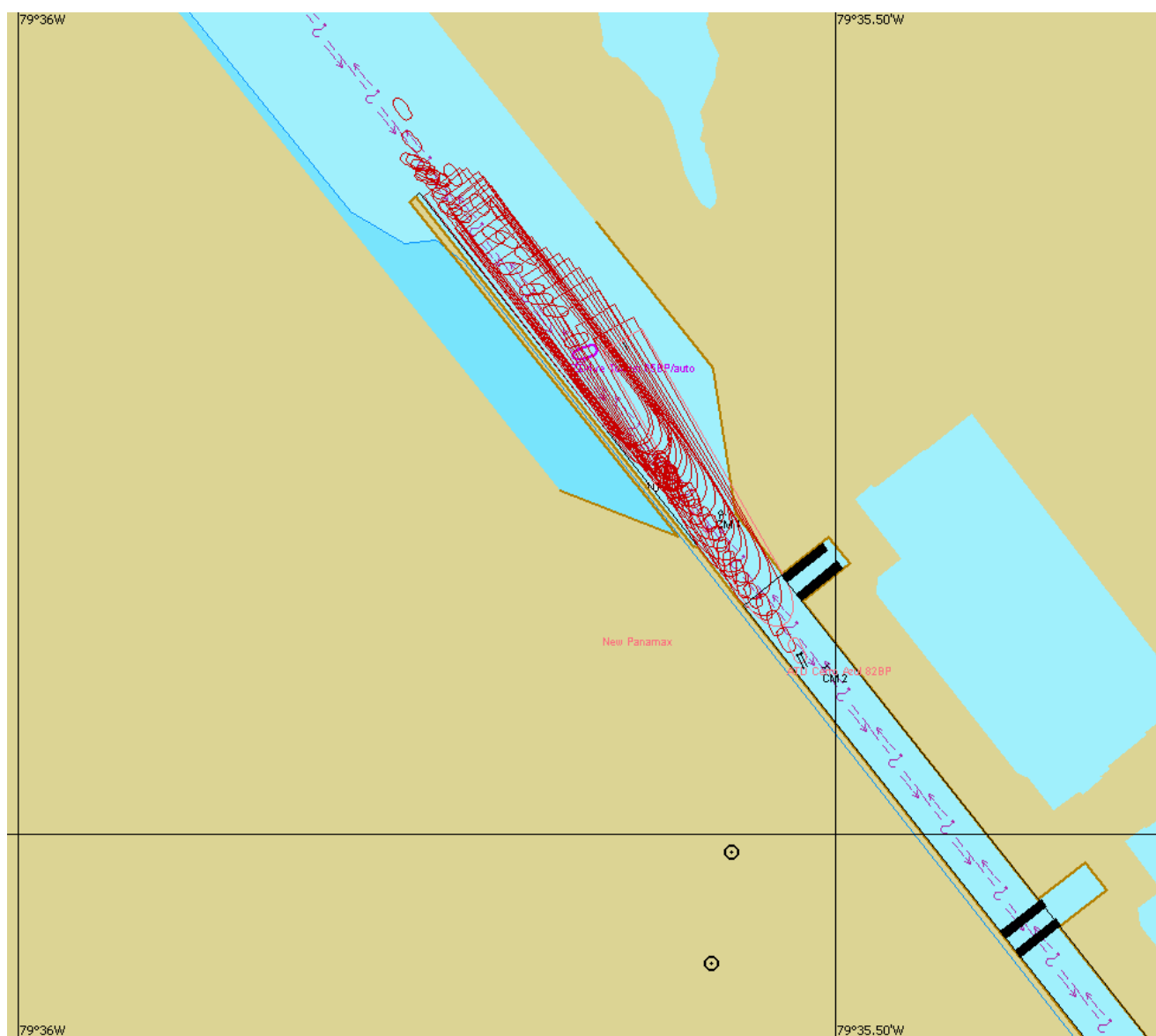
It was more reduce the current to the next manoeuvres in Pacific.

Figure 66: Vessel Type and Tugs tracking in Manoeuvre 25.

Manoeuvre 26

The simulated situation was:

Manoeuvre	Wind (knots)	Current (knots)	Tugs
Pacific Exit	03.9 from NNO	0.2 to ENE	1 de 82t 1 de 65t

Manoeuvre 26 – The Cerro Azul Tug was used in the bow, with two tied lines and controlled as Own Ship in Bridge 2 by collaborator of CSA team. The Tonosi tug was used in the stern with one tied line and controlled as Own Ship by the instructor. The Vessel Type was also controlled as Own Ship by the instructor.

In this manoeuvre, even reducing the current to 0.2 knots, it continued the difficult to control the Vessel Type with all available resources. The Vessel Type drifted a lot to port side.

From 30% of its power, the Cerro Azul Tug already could overcome the inertia of Vessel Type.
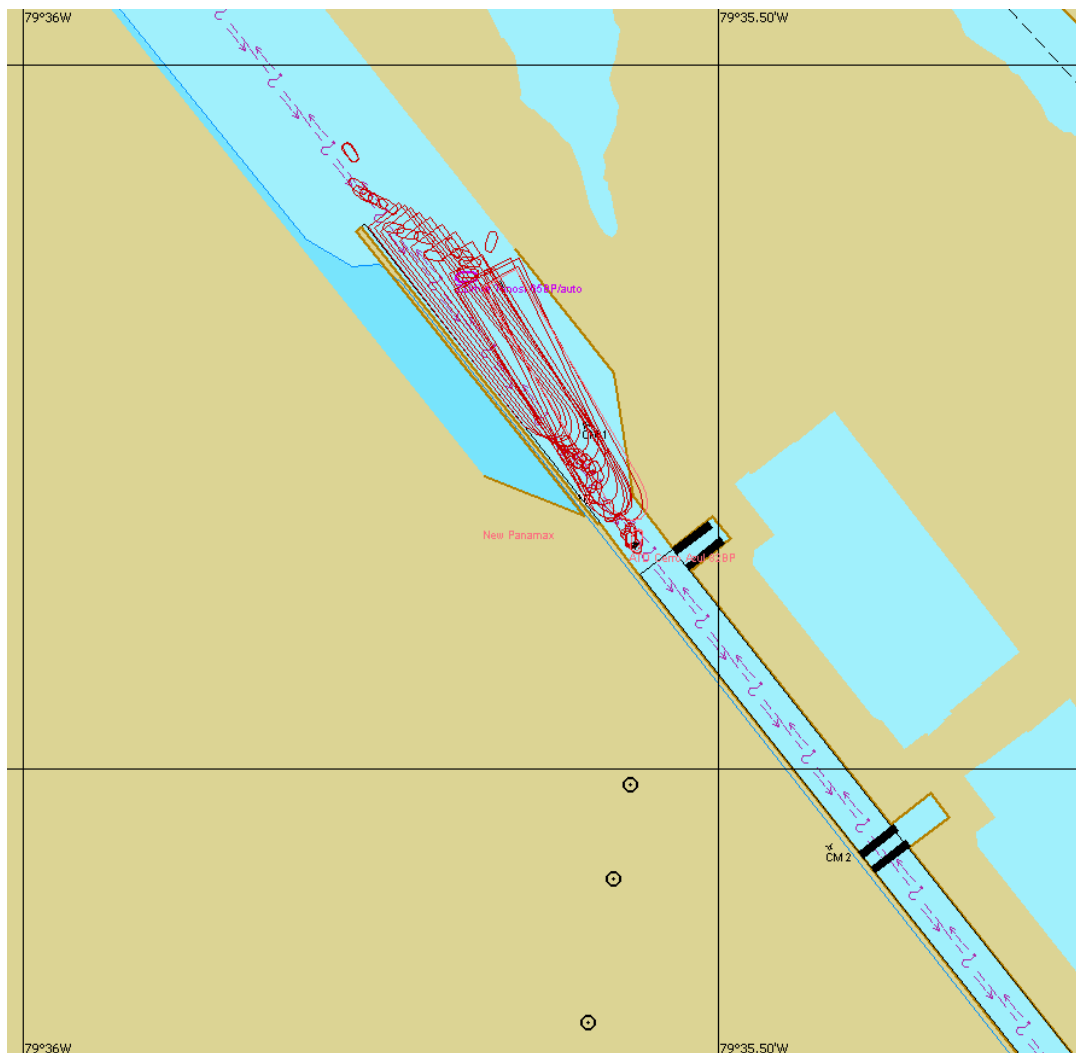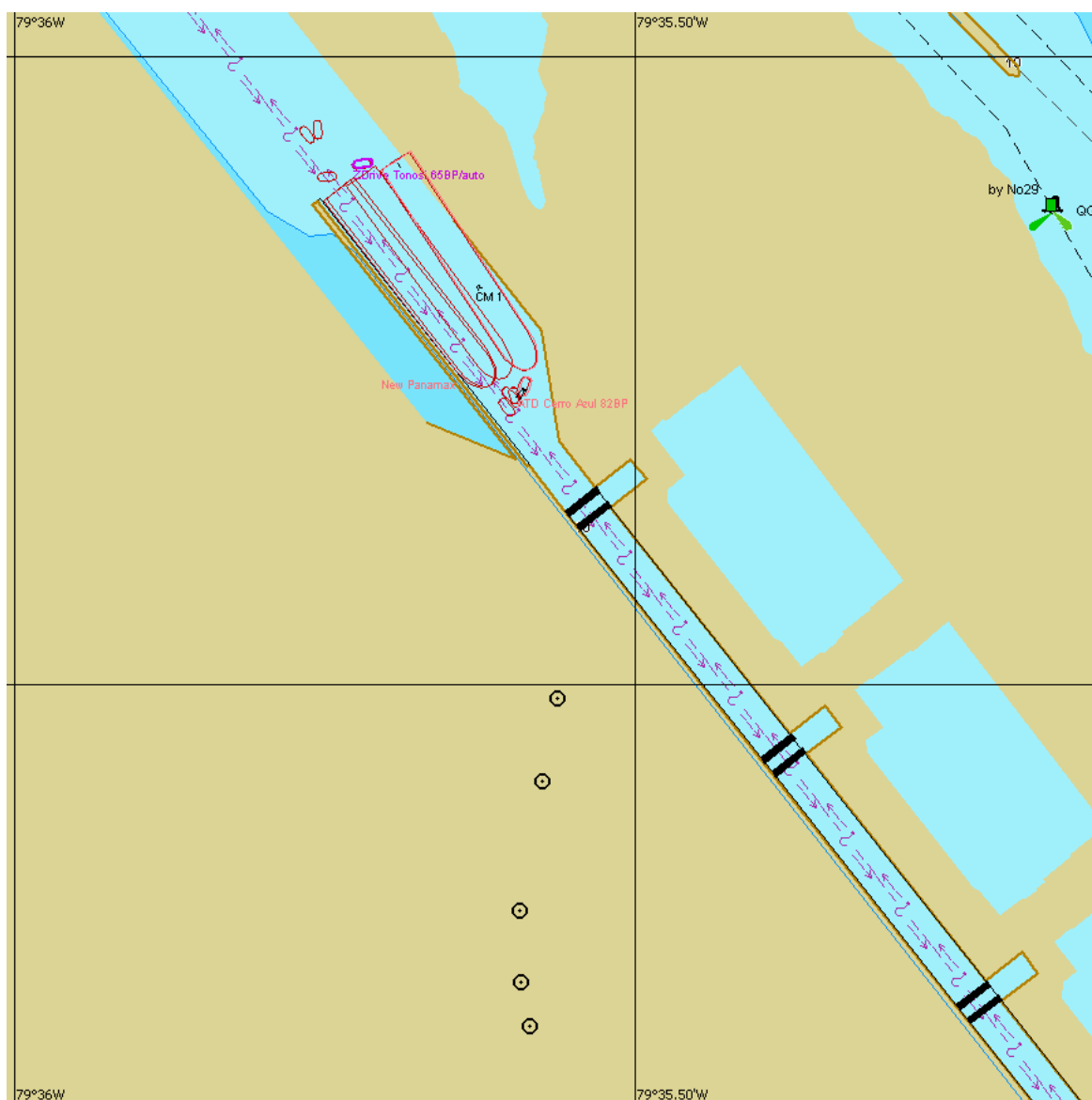

Figure 67: Vessel Type and Tugs tracking in Manoeuvre 26.

Manoeuvre 27

The simulated situation was:

Manoeuvre	Wind (knots)	Current (knots)	Tugs
Pacific Entrance	03.9 from NNO	0.2 to ENE	1 de 82t 1 de 65t

Manoeuvre 27 – The Cerro Azul Tug was used in the bow, with two tied lines and controlled as Own Ship in Bridge 2 by collaborator of CSA team. The Tonosi tug was used in the stern with one tied line and controlled as Own Ship by the instructor. The Vessel Type was also controlled as Own Ship by the instructor.

In this manoeuvre, even reducing the current to 0.2 knots, it continued the difficult to control the Vessel Type with all available resources. The Vessel Type drifted a lot to starboard side.

The difficulty in tie lines in the Vessel Type prejudiced excessively in ships' control before entering the chamber. This facts shows that any mistake, even minimum, can conduct to an accident.
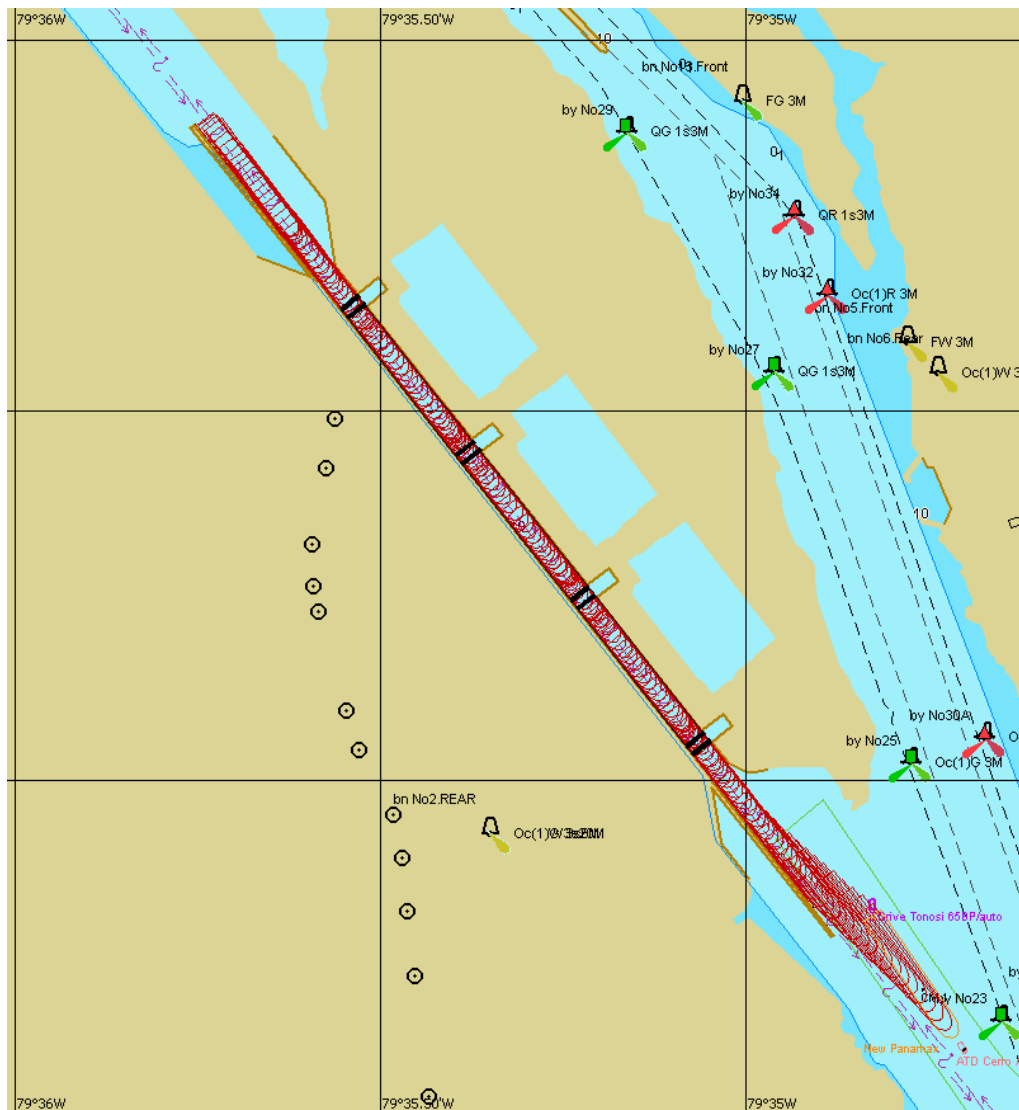
Figure 68: Vessel Type tracking in Manoeuvre 27.

Figure 69: Tugs tracking in Manoeuvre 27.

Manoeuvre 28

The simulated situation was:

Manoeuvre	Wind (knots)	Current (knots)	Tugs
Pacific Entrance	03.9 from NNO	0.2 to ENE	1 de 32t 1 de 54t

Manoeuvre 28 – The Cacique Tug was used in the bow, with two tied lines and controlled as Own Ship in Bridge 2 by collaborator of CSA team. The Los Santos tug was used in the stern with one tied line and controlled as Own Ship by the instructor. The Vessel Type was also controlled as Own Ship by the instructor.

With 40% of its power, the Cacique Tug already could overcome the inertia of Vessel Type. It have occurred two near miss situations which made the tug used in stern drop the line.

In the third chamber exit, when we simulated a possible distraction of those involved in the manoeuvre and forced the loss of control of the Vessel Type to restore after, it was difficult to go back to control the Vessel Type in constant environmental conditions in this manoeuvre.
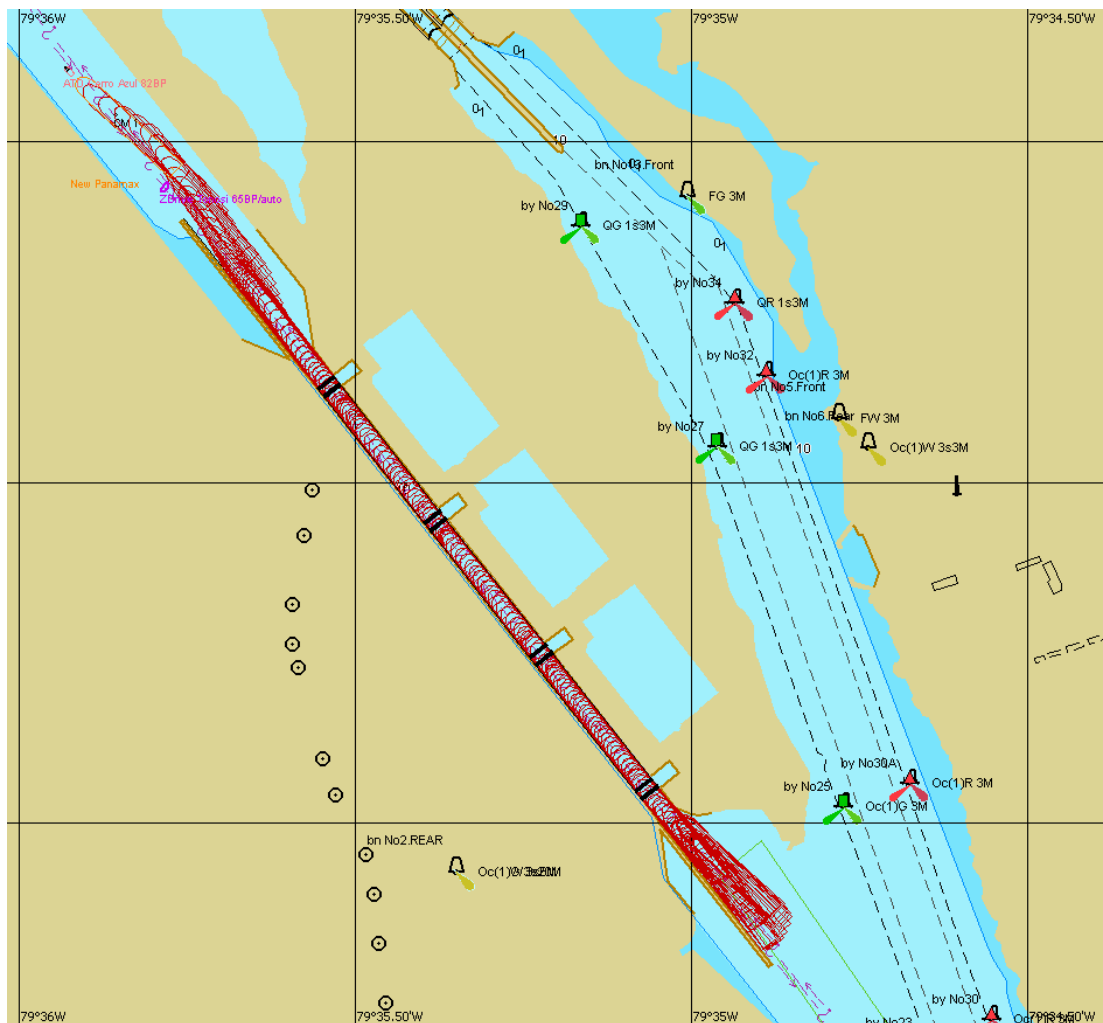
Figure 70: Vessel Type tracking in Manoeuvre 28.
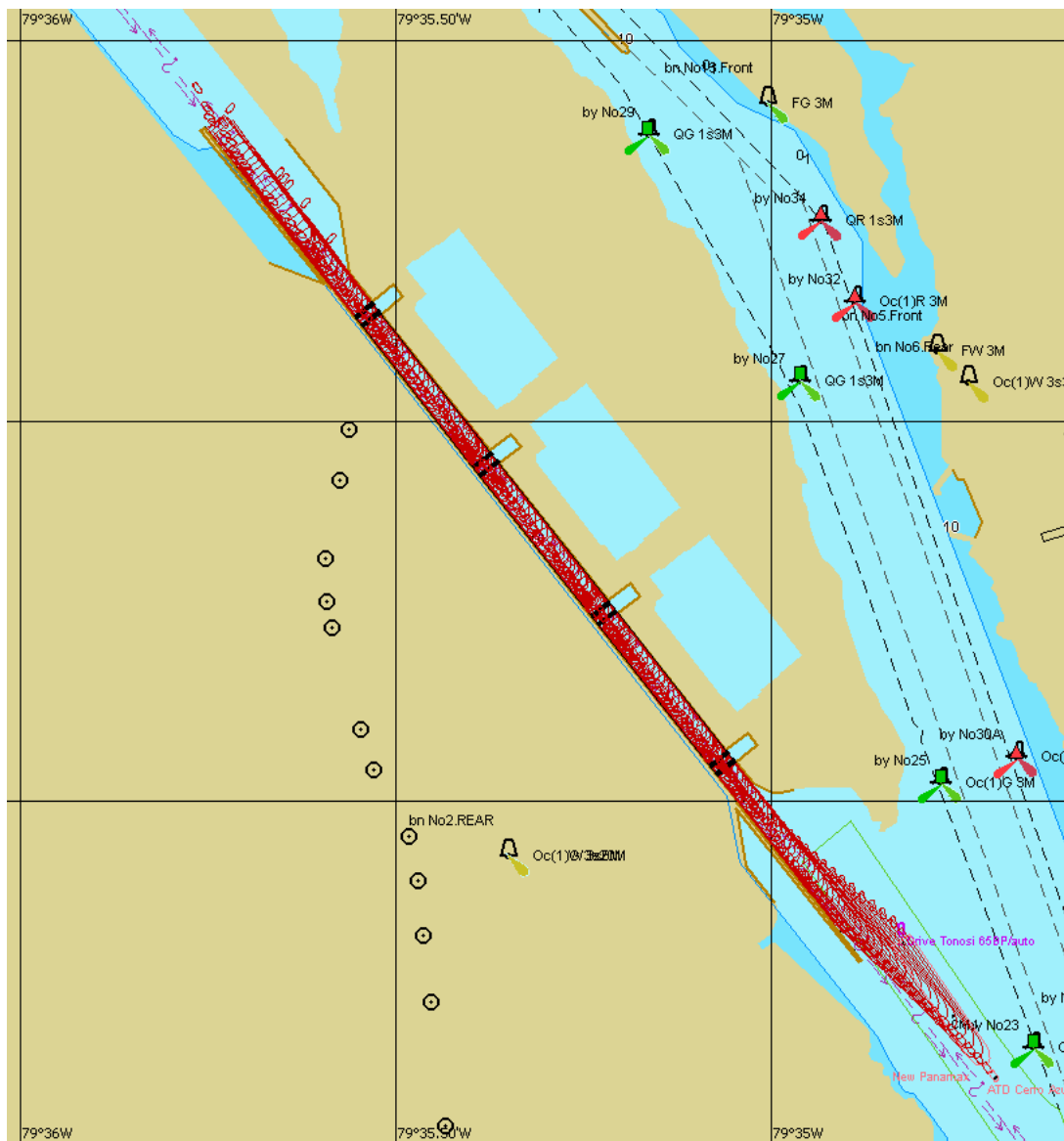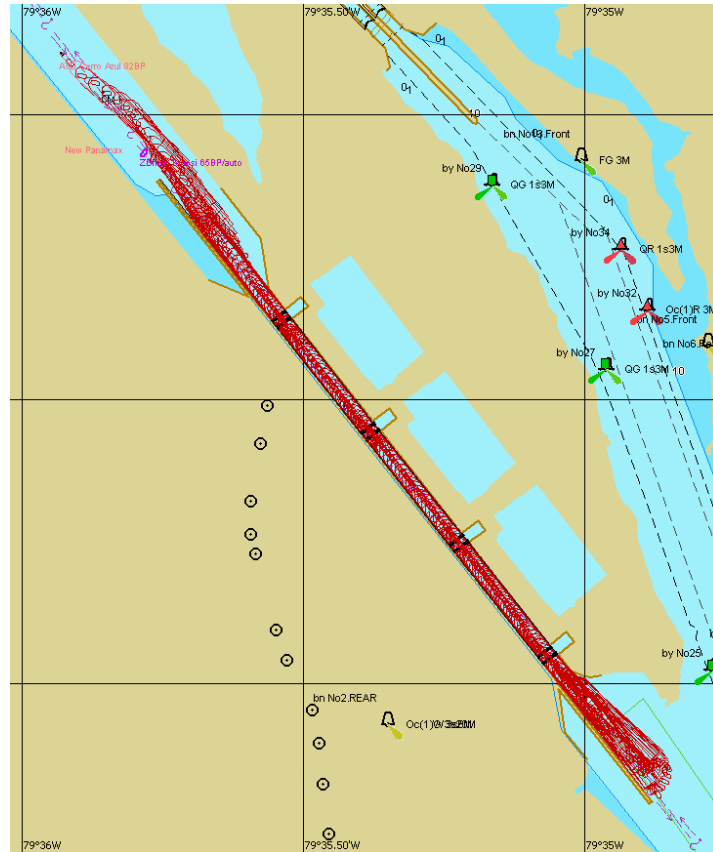
Figure 71: Vessel Type and Tugs tracking in Manoeuvre 28.
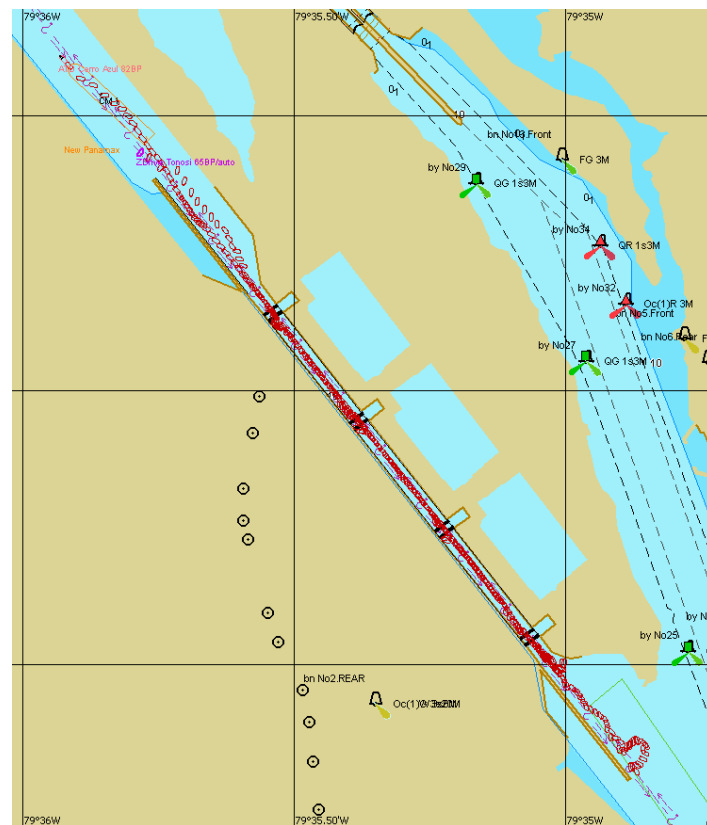
Figure 72: Tugs tracking in Manoeuvre 28.

Manoeuvre 29

The simulated situation was:

Manoeuvre	Wind (knots)	Current (knots)	Tugs
Pacific Exit	03.9 from NNO	0.2 to ENE	1 de 32t 1 de 54t

Manoeuvre 29 – The Cacique Tug was used in the bow, with two tied lines and controlled as Own Ship in Bridge 2 by collaborator of CSA team. The Los Santos tug was used in the stern with one tied line and controlled as Own Ship by the instructor. The Vessel Type was also controlled as Own Ship by the instructor.

It wasn't possible to control the Vessel Type, it did run aground.

Figure 73: Vessel Type and Tugs tracking in Manoeuvre 29.

Manoeuvre 30

The simulated situation was:

Manoeuvre	Wind (knots)	Current (knots)	Tugs
Pacific Exit	03.9 from NNO	0.2 to ENE	1 de 32t 1 de 54t

Manoeuvre 30 – The Cacique Tug was used in the bow, with two tied lines and controlled as Own Ship in Bridge 2 by collaborator of CSA team. The Los Santos tug was used in the stern with one tied line and controlled as Own Ship by the instructor. The Vessel Type was also controlled as Own Ship by the instructor.

It wasn't possible to control the Vessel Type, it did run aground.
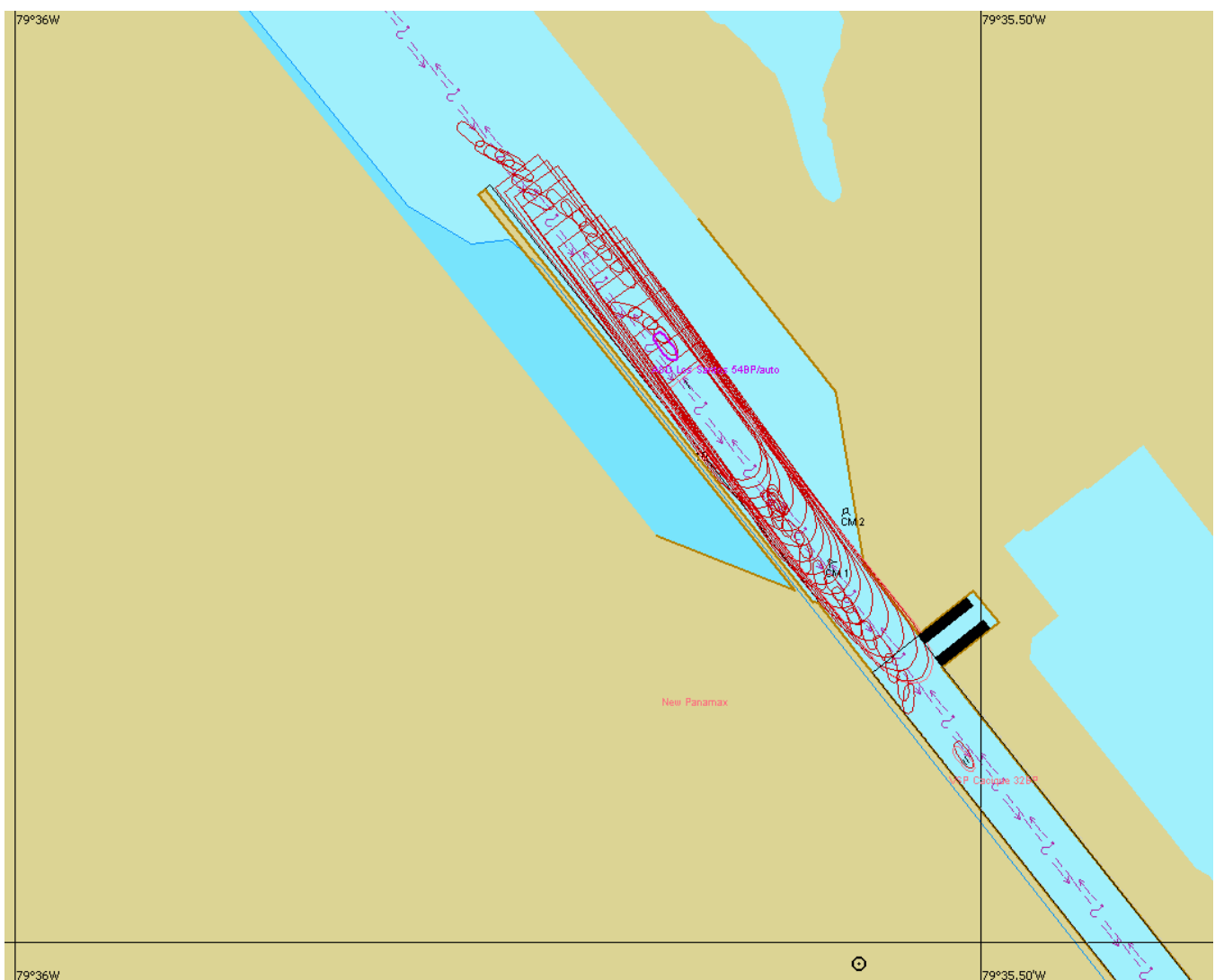
Figure 74: Vessel Type and Tugs tracking in Manoeuvre 30.

Manoeuvre 31

The simulated situation was:

Manoeuvre	Wind (knots)	Current (knots)	Tugs
Pacific Exit	03.9 from NNO	0.2 to ENE	1 de 32t 1 de 54t

Manoeuvre 31 – The Cacique Tug was used in the bow, with two tied lines and controlled as Own Ship in Bridge 2 by collaborator of CSA team. The Los Santos tug was used in the stern with one tied line and controlled as Own Ship by the instructor. The Vessel Type was also controlled as Own Ship by the instructor.

The manoeuvre was lost due to the difficulty to control the Vessel Type and the tugs in configured environmental conditions.
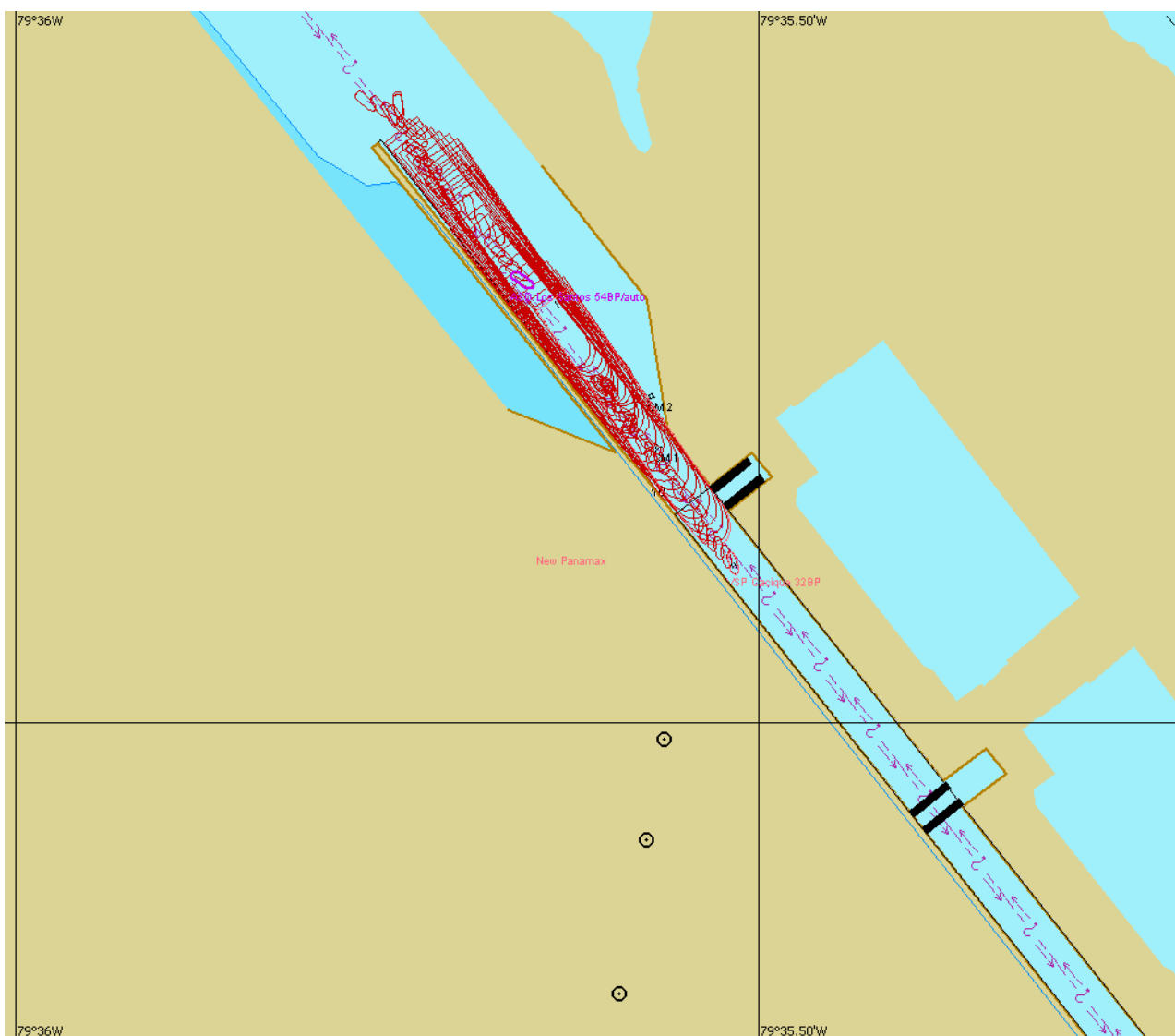

Figure 75: Vessel Type and Tugs tracking in Manoeuvre 31.

Manoeuvre 32

The simulated situation was:

Manoeuvre	Wind (knots)	Current (knots)	Tugs
Pacific Exit	03.9 from NNO	0.2 to ENE	1 de 32t 1 de 54t

Manoeuvre 32 – The Cacique Tug was used in the bow, with two tied lines and controlled as Own Ship in Bridge 2 by collaborator of CSA team. The Los Santos tug was used in the stern with one tied line and controlled as Own Ship by the instructor. The Vessel Type was also controlled as Own Ship by the instructor.

We could only control the ship using full power of tugs.

Figure 76: Vessel Type tracking in Manoeuvre 32.

Figure 77: Vessel Type and Tugs tracking in Manoeuvre 32.

Figure 78: Tugs tracking in Manoeuvre 32.

Manoeuvre 33

The simulated situation was:

Manoeuvre	Wind (knots)	Current (knots)	Tugs
Atlantic Exit	05.0 from NNE	0.5 to ENE	1 de 32t 1 de 54t

Manoeuvre 33 – The Cacique Tug was used in the bow, with two tied lines and controlled as Own Ship in Bridge 2 by collaborator of CSA team. The Los Santos tug was used in the stern with one tied line and controlled as Own Ship by the instructor. The Vessel Type was also controlled as Own Ship by the instructor.

It was very difficult to control the Vessel Type in first chamber entrance. The tugs worked with its maximum power.

In the last chamber exit, even using the maximum power of tugs, it wasn't possible to not lean the Vessel Type against the approaching zone.

It was necessary use the machinery of the Vessel Type to be able to exit the third chamber, because we weren't being able to control Vessel Type lateral movements without impeding its movement. However, this situation, made it achieve the speed of 0.9 knots and then the Vessel Type collided with the approaching zone.

Figure 79: Vessel Type tracking in Manoeuvre 33.
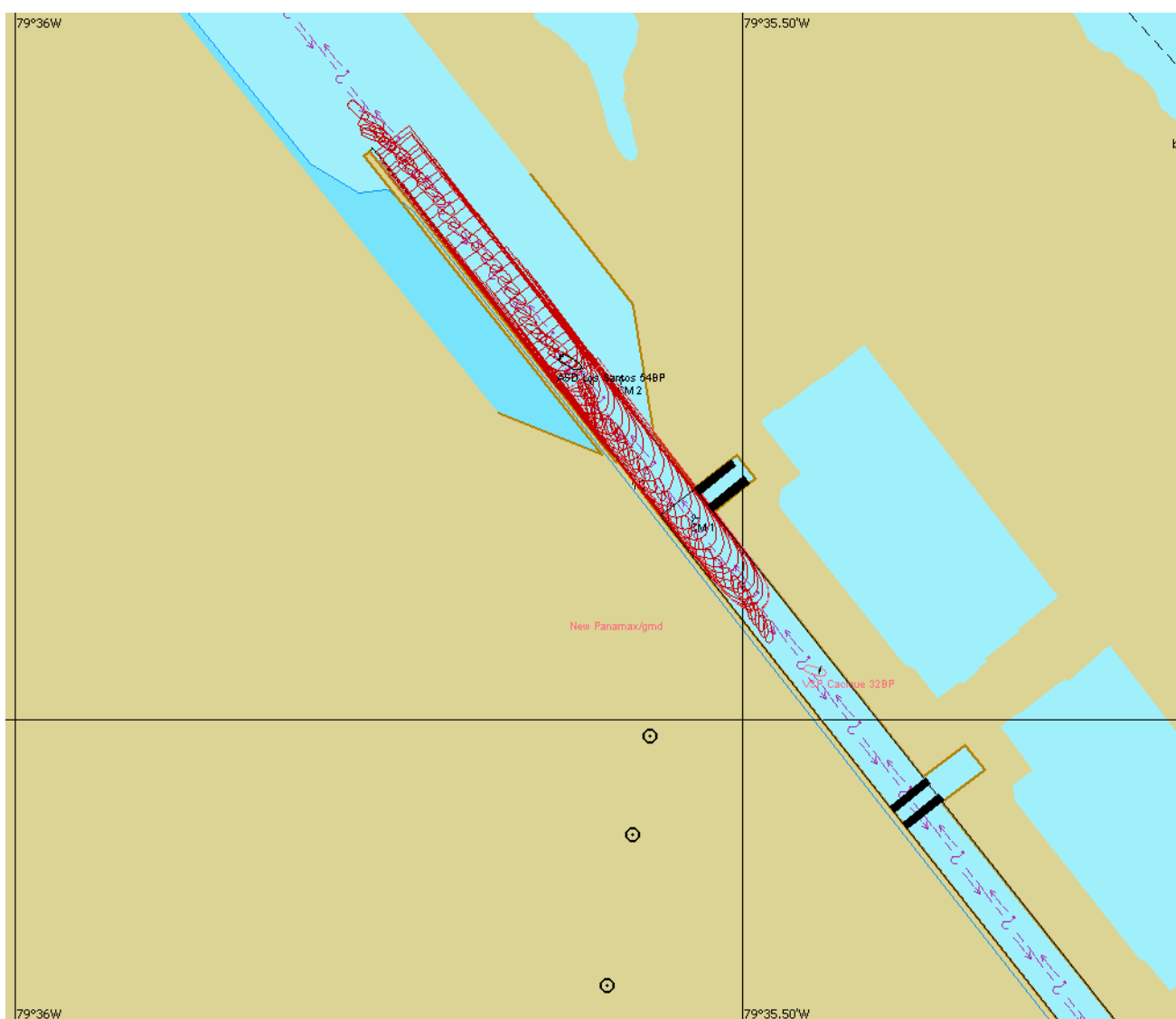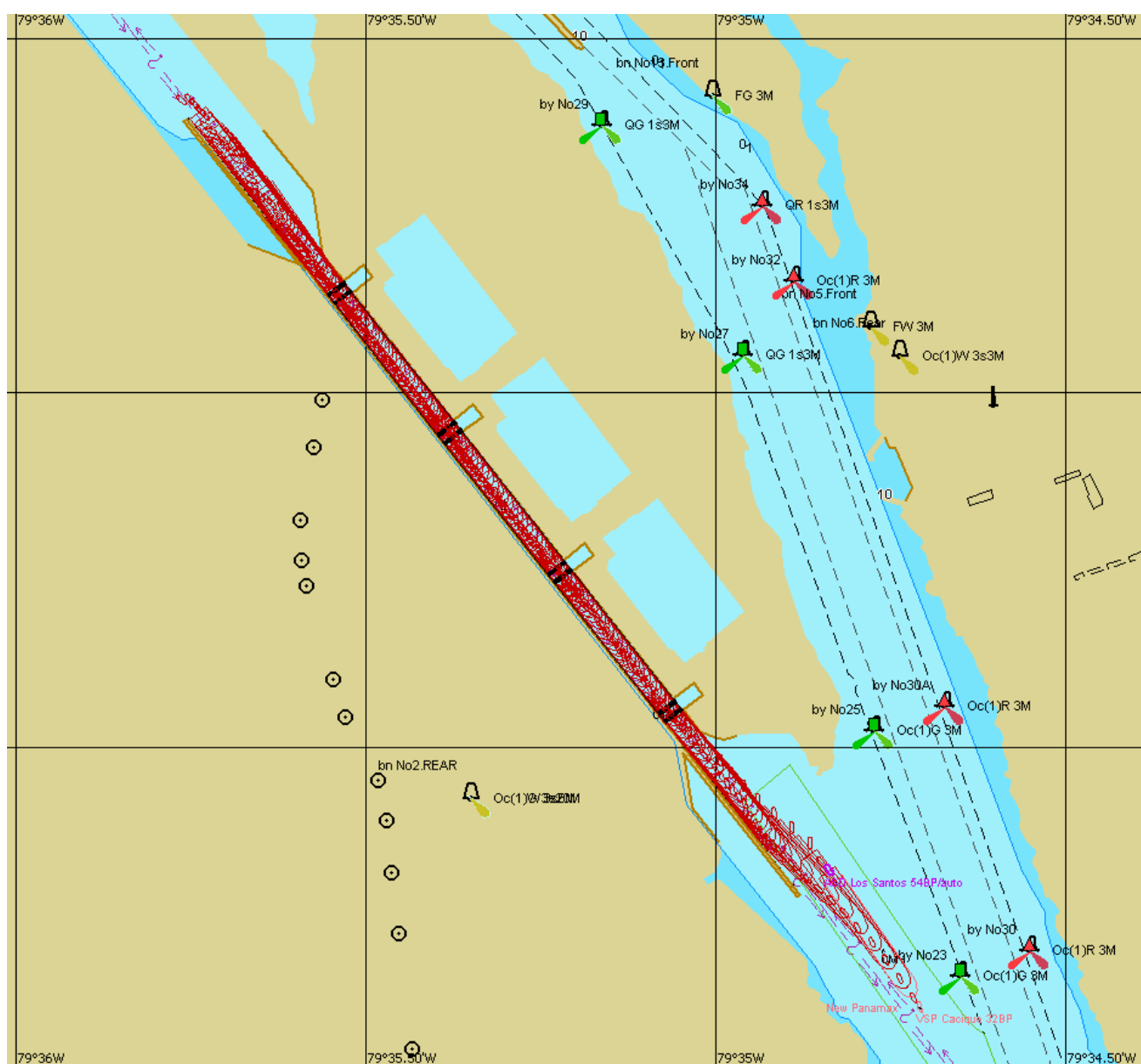
Figure 80: Vessel Type and Tugs tracking in Manoeuvre 33.

Figure 81: Tugs tracking in Manoeuvre 33.

Manoeuvre 34

The simulated situation was:

Manoeuvre	Wind (knots)	Current (knots)	Tugs
Atlantic Entrance	05.0 from NNE	0.5 to ENE	1 de 32t 1 de 54t

Manoeuvre 34 – The Cacique Tug was used in the bow, with two tied lines and controlled as Own Ship in Bridge 2 by collaborator of CSA team. The Los Santos tug was used in the stern with one tied line and controlled as Own Ship by the instructor. The Vessel Type was also controlled as Own Ship by the instructor.

It was very difficult to control the Vessel Type in first chamber entrance. The tugs worked with its maximum power.

The Cacique Tug worked close to the chamber wall and with a dangerous heading, considering the possibility of a broke line, a collision of great impact would be inevitable. Due to its proximity a collision occurred.

It's important to highlight that manoeuvring only in this way; we can control the Vessel Type behaviour according to our purpose.
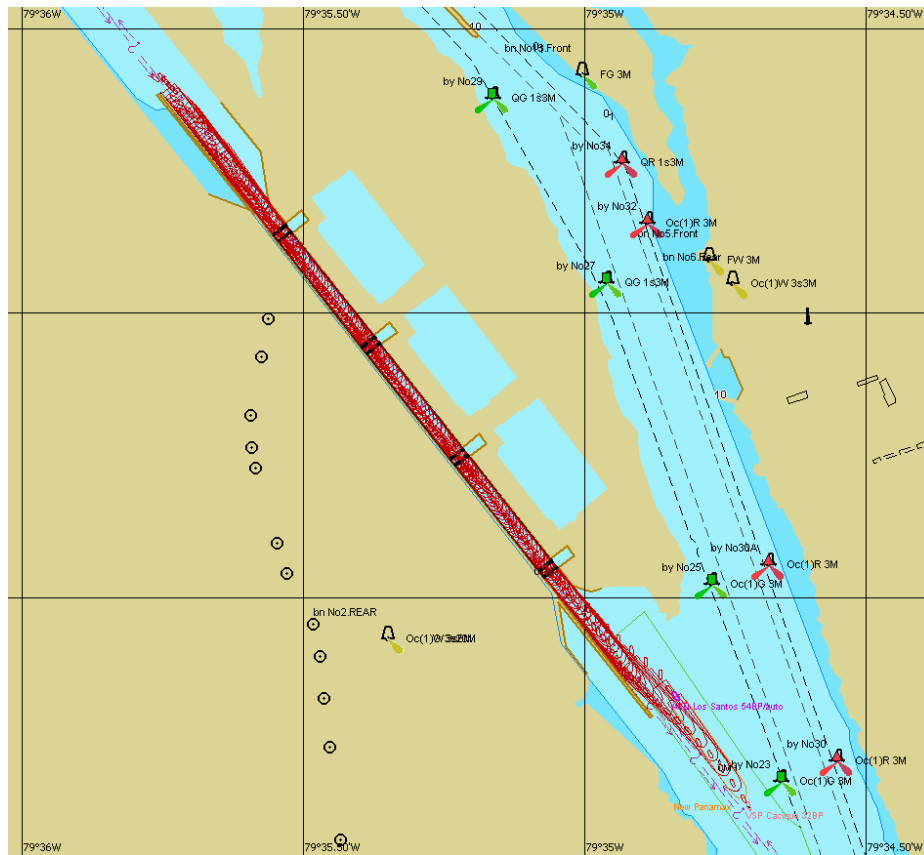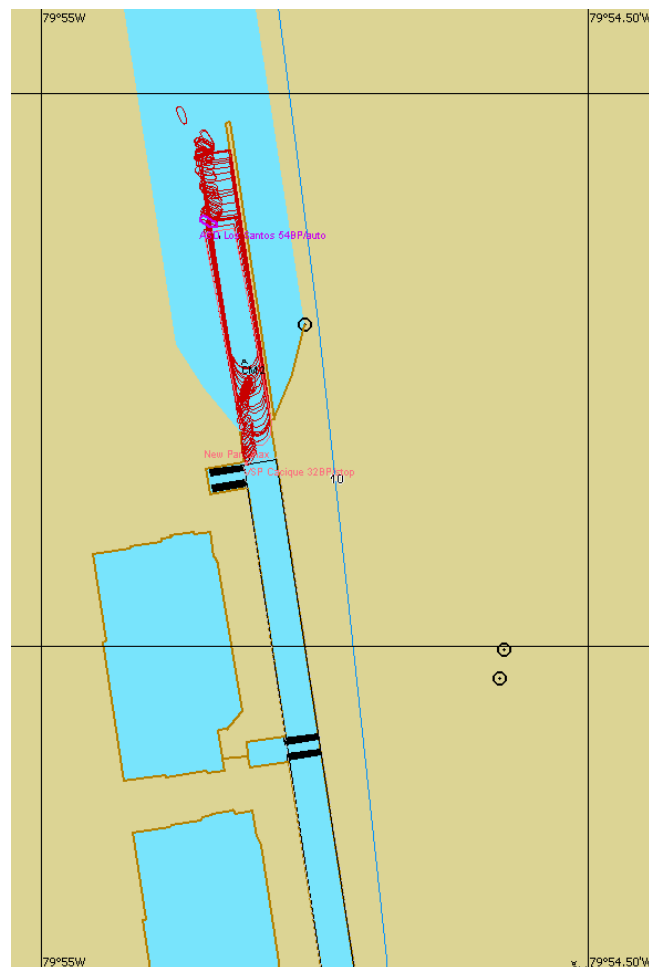

Figure 82: Vessel Type and Tugs tracking in Manoeuvre 34.
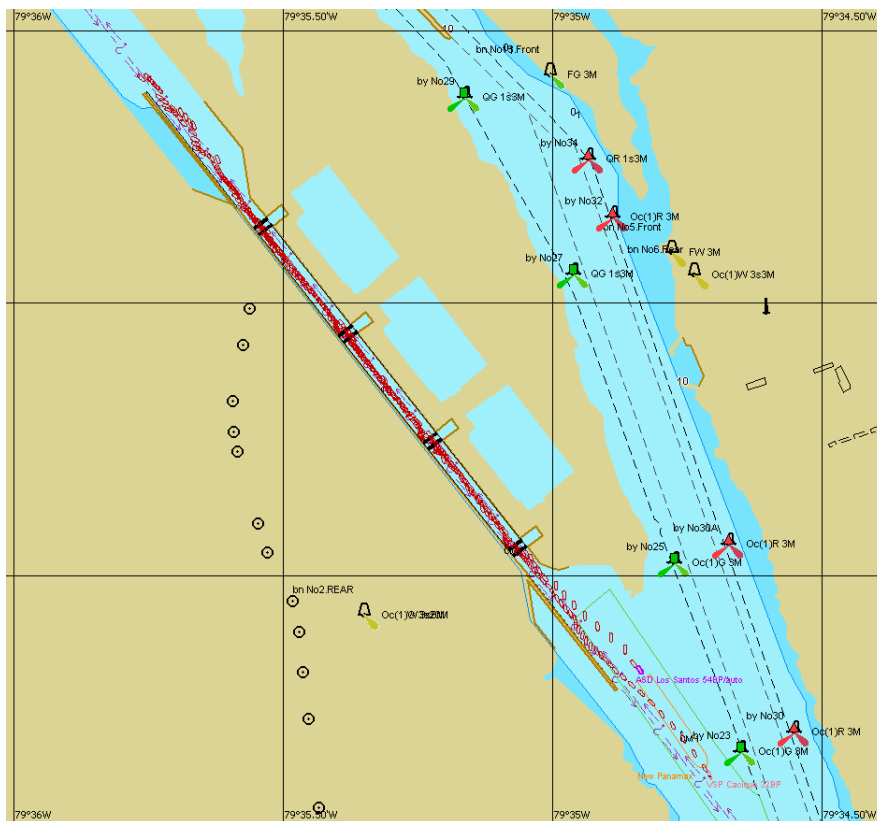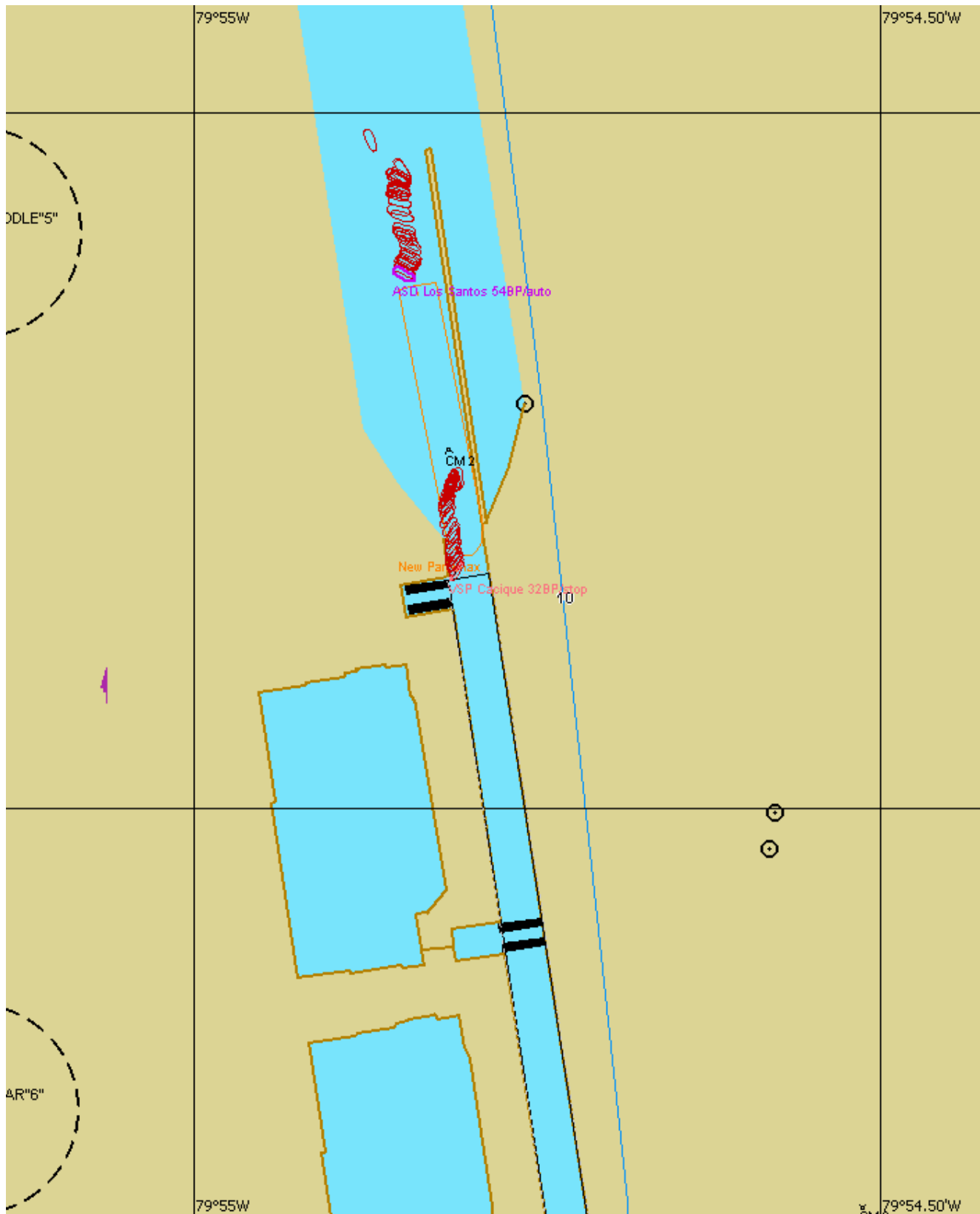
Figure 83: Tugs tracking in Manoeuvre 34.

Manoeuvre 35

The simulated situation was:

Manoeuvre	Wind (knots)	Current (knots)	Tugs
Atlantic Entrance	05.0 from NNE	0.5 to ENE	1 de 32t 1 de 54t

Manoeuvre 35 – The Cacique Tug was used in the bow, with two tied lines and controlled as Own Ship in Bridge 2 by collaborator of CSA team. The Los Santos tug was used in the stern with one tied line and controlled as Own Ship by the instructor. The Vessel Type was also controlled as Own Ship by the instructor.

It was very difficult to control the Vessel Type. The tugs worked within its maximum power almost constantly.

It is very complicated, inside the chamber, to control the Vessel Type only with tugs. This situation lead us to use the Vessel Type propulsion, a resource that we should avoid using because exposes the tug in stern to Vessel Type wake, which affect the tug safety.

Figure 84: Vessel Type tracking in Manoeuvre 35.

Figure 85: Vessel Type and Tugs tracking in Manoeuvre 35.

Figure 86: Tugs tracking in Manoeuvre 35.

7. PARTICIPANTS

The following collaborators participated in this report and in simulations carried out in CSA, ministered by FHM:

NAME Function	COMPANY
Ernesto de Sá Coutinho Junior Naval Architecture	Fundação Homem do Mar
Jeferson Ferreira de Almeida Carvalho Marine Consultant	Fundação Homem do Mar
Tamara di Maria Furtado Souza Project Designer	Fundação Homem do Mar
Sérgio Hamilton Sphaier PhD in Hydrodynamics	Fundação Homem do Mar
José Mario Santos Calixto General Coordinator	Fundação Homem do Mar
Gustavo Ayarza President of Consejo de los Metalurgicos del Canal de Panama	Consejo de los Metalurgicos del Canal de Panama
Ricardo Espada Vice president of Area Atlantica de la Union de Ingenieros Marinos	Union de Ingenieros Marinos
Roger Barahona Representative of Area del Pacifico Union de Capitanes y Oficiales de Cubierta	Union de Capitanes y Oficiales de Cubierta

8.   CONCLUSION

Several interactions exist, some influencing tugs performance and others tugs safety or even both. Interaction effects influencing tugs safety are the kind of interactions which occur between ships when close to each other. These interaction effects are more pronounced in shallow and narrow waters and when a tug is in the relatively close vicinity of a ship and increase sharply with increasing ship's speed.

Because tugs have to operate close to ships which are often underway at speed these effects should always be taken into account. Considering the interaction effects and all other risky situations that have been discussed, it is clear that the following aspects are essential for safe shiphandling with tugs:

- Experience in recognizing risky situations and knowing how to deal with them.
- Good knowledge of the limitations of tugs.
- Appropriate ship's speed taking account of interaction effects and tug limitations.
- Careful use of ship's propellers when tugs are operating close to the stern. Tug captains should be informed in good time about intended use of ship's propellers.
- Optimal communication, information exchange and cooperation between pilots, ship masters and tug captains. Pilots should inform tug captains well in advance of intended manoeuvres and should, as far as possible, keep an eye on assisting tugs. Tug captains should inform pilots about developing or suspected risky situations and contact the pilot whenever in doubt. Ship masters should inform the pilot about the manoeuvring capabilities of the ship, and relevant aspects of ship's mooring, anchoring and towline securing equipment. The pilot should inform the ship master about the tug assistance and manoeuvres to be executed.
- Tug should be fully appropriate for the assistance required and should comply with the following minimum requirements: sufficient bollard pull, high manoeuvrability and free running speed, good stability and sufficient freeboard, suitable towing equipment with a properly working quick release system and an optimal horizontal and vertical angle of view from the wheelhouse.
- Tugs operating at a ship's side should be sufficiently powerful and secured so that the risk of becoming jammed between ship and shore due to wind, current and/or wave forces can be avoided.
- Sufficient ship crew members should be available and well prepared on station to secure tugs with minimum delay.
- Ship's crews should not drop a tug's towline into the water but lower it gently onto the tug's deck.
- Ships should be designed so that sufficient towlines can safely and properly be secured for effective tug assistance.

Considering international literature and after the accomplishment of simulations studies with Vessel Type and with Tugs which assisted the Vessel Type in manoeuvres, described in Technical Report RS-034, it was concluded that seaworthiness of this Vessel Type entering and exiting the new locks of Panama Canal wasn't occurring in a safe way. As the following reasons:

•   The bollard pull needed to carry out these manoeuvres isn't enough;

•   The locks dimensions are small when compared with the ones of the Vessel Type and the Tugs, when operating together, with tied lines having average length equal to 30 meters, inside the locks;

•   There are no refuge areas and enough space to manoeuvre inside the locks. So errors can't be made; and

•   During simulations, it have occurred several events, already commented in this report, which affect tugs safety.

Situations as communication failures, broken lines and damages in Tugs or its equipments of direct use in manoeuvres must be taking into account. For example, in a few moments of simulations, the tug, trying to conduct the ship accordingly with the orders of the officer in charge of navigation, and having its maximum power used, navigated close to the chamber wall and with a heading that left the bow facing this wall; in case the line broke in one of this moments of manoeuvre, a collision would be inevitable.

We recommend that a risk analysis be made and that be offered a special training for those who are involved in these manoeuvres, principally pilots and tugs captains, because errors may lead us to loss of life and pollution.

In nautical aspect, during the manoeuvres was very difficult to maintain the control of Vessel Type and Tugs under environmental conditions, according to reports passed by the contracting party, recurrent in the area. The conditions were reconfigured to be milder. As the use of Tugs, the performance was unsatisfactory due to its low power.

9. BIBLIOGRAPHIC REFERENCES

1. PIANC. Permanent International Association of Navigation Congress. "Harbour Approach Channels – Design Guidelines" – Final Report 121, January 2014.

2. The Nautical Institute. "Squat Interaction Manoeuvring", 1995.

3. HENSEN, Captain Henk. "Tug Use in Port – A Practical Guide", Second Edition, 2003.

4. TECHNICAL REPORTS HID-011-2011 and HID-2013-06.

5. HYDRODYNAMIC MODELING STUDY – North East Breakwater Open Water Disposal.

6. FEASIBILITY STUDY OF PALO SECO – Technical Appendices.

7. CAJATY, Marcelo & FRAGOSO, Otávio A. Rebocadores Portuários, 1ª Edição, 2002.

8. IALA. International Association of Marine Aids to Navigation and Lighthouse Authorities – IALA Guideline No 1058. "On the Use of Simulation as a Tool for Waterway Design and Aton Planning", Edition 1, 2007.

9. MCCARTNEY, Bruce L.; EBNER, Laurie L.; HALES, Lyndell Z.; NELSON, Eric E. *Ship Channel and Design Operation – ASCE Manuals and Reports on Engineering Practice*. Illustrated Edition. 2005.

10. THORENSEN, Carl A. Port Designer´s Handbook: Guidelines and Recommendations. Thomas Telford Editors, 2003.

11. MAGAZINE, Programa de Ampliación (December 2014).

12. FILES, M-6120-30D.pdf and SK-H-1126_WGS84.dwg.

10. ANNEX – MATHEMATICAL MODELLING

DESCRIPTION OF TRANSAS
SHIP MOTION
MATHEMATICAL MODELING

(VERSION 02.11)

INTRODUCTION

This report includes short description of ship motion mathematical model. It includes motion equations and main forces: ship dynamics equations; hull forces (hydrodynamics and aerodynamics) at deep water; rudder, propeller and thruster forces; engine dynamics equations; shallow water effect; wind and wave models.

GENERAL

Coordinate Systems

The following coordinate systems are used for the description of the own ship's motion (all reference frames are Cartesian):

- $X_0Y_0Z_0$ earth-fixed reference frame with O_0 origin in a certain fixed point:

  X_0 axis is directed towards the north and lies in the plane parallel to the undisturbed water surface,

  Y_0 axis is directed towards the east and lies in the plane parallel to the undisturbed water surface;

  Z_0 axis is directed downward at a right angle to the undisturbed water surface.

- XYZ body-fixed frame with O origin in the vessel's center of gravity (CG):

  X axis is directed from aft to fore, lies in the central lateral plane and is parallel to the waterplane (longitudinal axis);

  Y axis is directed to starboard, is perpendicular to the central lateral plane and parallel to the waterplane (transverse axis);

  Z axis is directed from top to bottom at a right angle to the waterplane (normal axis).

- $X_1Y_1Z_1$ local frame with O origin in the vessel's center of gravity (CG) (axis obtained by translating $X_0Y_0Z_0$ earth-fixed coordinate system parallel to itself until its origin coincides with the origin of the body-fixed coordinate system):

  X_1 axis is directed towards the north and lies in the plane parallel to the undisturbed water surface,

  Y_1 axis is directed towards the east and lies in the plane parallel to the undisturbed water surface;

  Z_1 axis is directed downward at a right angle to the undisturbed water surface.

The coordinate systems in use are shown in Fig 1 and Fig 2.
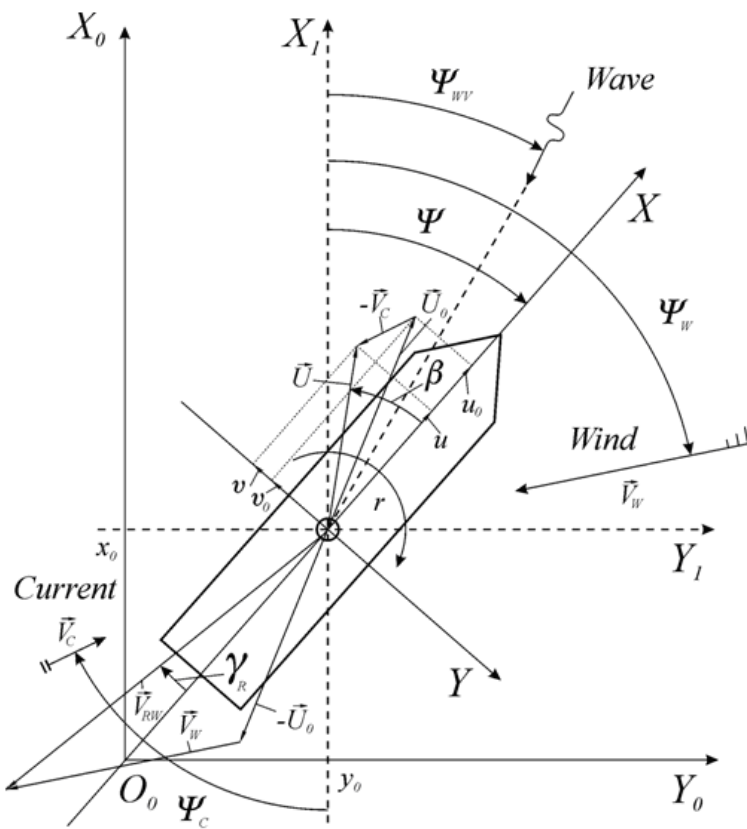
Fig 1. Coordinate systems (horizontal plane)
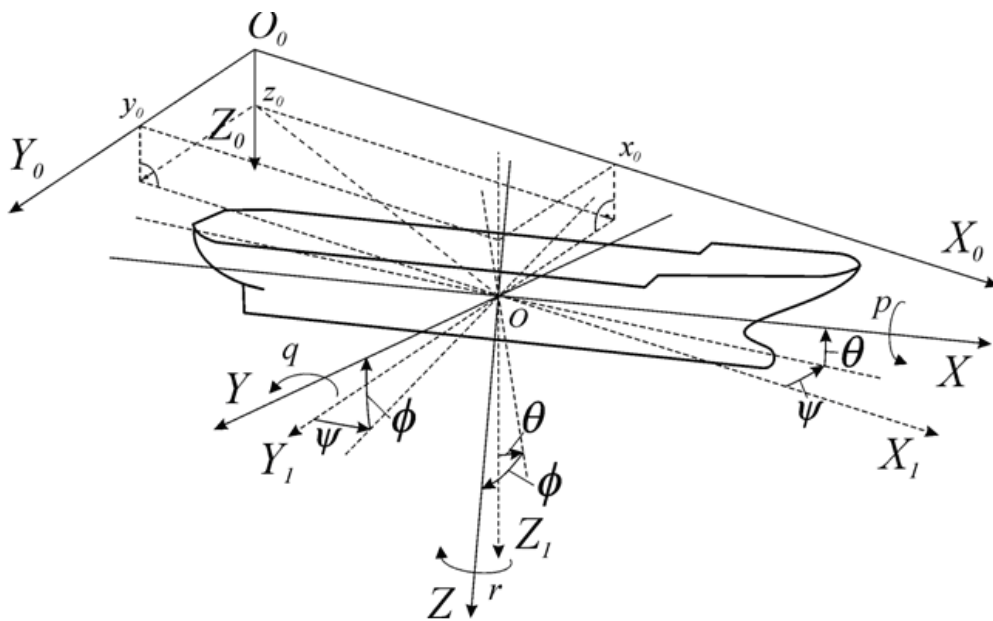
Fig 2. Coordinate systems

Kinematic Equations

Euler Kinematic Equations for the Roll, Pitch and Yaw Rates

Euler kinematic equations for the roll, pitch and yaw rates allow determining the roll, pitch and yaw rate vector projection on the axes of the Cartesian body-fixed frame via the vessel angle derivatives:

$$p = \dot{\phi} - \dot{\psi}\sin\theta\,;$$

$$q = \dot{\theta}\cos\phi + \dot{\psi}\cos\theta\sin\phi\,;$$

$$r = -\dot{\theta}\sin\phi + \dot{\psi}\cos\theta\cos\phi\,.$$

For these equations to be used in the integration of the vessel motion model, the equations should be solved relative to $\dot{\phi}, \dot{\theta}$ and $\dot{\psi}$.

As a specific case, in considering the motion with four degrees of freedom, these equations will be rewritten in the following form:

$$p = \dot{\phi}\,;$$

$$r = \dot{\psi}\cos\phi\,.$$

In considering the motion with three degrees of freedom we have only one equation:

$$p = \dot{\phi}\,.$$

The Kinematic Equations for the Linear Velocities

The kinematic equations for the linear velocities allow determining derivatives of the gravity center coordinates $\dot{x}_0 = U_{X_0}$, $\dot{y}_0 = U_{Y_0}$, $\dot{z}_0 = U_{Z_0}$ from the projections of the velocity vector on the body-fixed axes u_0, v_0, ω_0.

$$\dot{x}_0 = u_0\cos\psi\cos\theta + v_0(\sin\phi\cos\psi\sin\theta - \cos\phi\sin\psi) + \omega_0(\cos\phi\cos\psi\sin\theta + \sin\phi\sin\psi)\,;$$

$$\dot{y}_0 = u_0\sin\psi\cos\theta + v_0(\sin\phi\sin\psi\sin\theta + \cos\phi\cos\psi) + \omega_0(\cos\phi\sin\psi\sin\theta - \sin\phi\cos\psi)\,;$$

$$\dot{z} = -u_0\sin\theta + v_0\sin\phi\cos\theta + \omega_0\cos\phi\cos\theta\,.$$

As a specific case, in considering the motion with four degrees of freedom, these equations will be rewritten in the following form:

$$\dot{x}_0 = u_0\cos\psi - v_0\cos\phi\sin\psi\,;$$

$$\dot{y}_0 = u_0\sin\psi + v_0\cos\psi\,.$$

In considering the motion with three degrees of freedom:

$$\dot{x}_0 = u_0\cos\psi - v_0\sin\psi\,;$$

$$\dot{y}_0 = u_0\sin\psi + v_0\cos\psi\,.$$

Kinematic Equations for the Vessel's Velocity Relative to a Liquid

If there is a current (with a permanent homogeneous velocity field) the concept of the vessel's velocity relative to a liquid is also used:

$$\vec{U} = \vec{U}_0 - \vec{V}_C \ .$$

This vector's components are determined in the following way:

$$u = u_0 - V_{C_X} \ ;$$

$$\upsilon = \upsilon_0 - V_{C_Y} \ ;$$

$$\omega = \omega_0 - V_{C_Z} \ ;$$

With the vessel's actual roll and pitch angles, V_{C_Z} is negligibly small.

The calculations of forces on the hull use $\vec{U}$ vector components.

Another group of kinematic equations allows determining β drift and α attack angles from the projections of the vector of vessel's velocity relative to the liquid on the body-fixed axes u, υ, ω :

$$u = U \cos\beta \cos\alpha \ ;$$

$$\upsilon = -U \sin\beta \cos\alpha \ ;$$

$$\omega = -U \sin\alpha \ .$$

In the calculations of forces and moments acting on the vessel's hull β and α angles are used. For the equations to be used they should be solved relative to β and α. In considering the motion with four or three degrees of freedom

$$u = U \cos\beta \ ;$$

$$\upsilon = -U \sin\beta \ .$$

Kinematic Equations of the Apparent Wind

Calculations of the aerodynamic forces use the apparent wind speed V_{RW} and the apparent wind angle γ_{RW} .

The apparent wind speed vector $\vec{V}_{RW}$ and its components (projections on the vessel-fixed axes) are determined as follows:

$$\vec{V}_{RW} = -\vec{U}_0 + \vec{V}_W \ ;$$

$$V_{RW_X} = -u_0 + V_{W_X} \ ;$$

$$V_{RW_Y} = -\upsilon_0 + V_{W_Y} \ .$$

The vessel's actual roll and pitch angles being small V_{W_z} may be neglected. Then the apparent wind speed module and apparent wind angle are determined by the following equations:

$$V_{RW} = \sqrt{V_{RW_X}^2 + V_{RW_Y}^2} \; ;$$

$$V_{RW_X} = -V_{RW} \cos \gamma_{RW} \; ;$$

$$V_{RW_X} = V_{RW} \sin \gamma_{RW} \; .$$

Ship Motion Equations

In the body-fixed reference, equations of the vessel's spatial (6 degrees of freedom) motion will have the following form:

$$m(\dot{u}_0 - v_0 r + \omega_0 q) \qquad = X \; ; \qquad (1)$$

$$m(\dot{v}_0 + u_0 r - \omega_0 p) \qquad = Y \; ; \qquad (2)$$

$$m(\dot{\omega}_0 - u_0 q + v_0 p) \qquad = Z \; ; \qquad (3)$$

$$I_{x_C} \dot{p} + \left(I_{z_C} - I_{y_C} \right) qr \qquad = K \; ; \qquad (4)$$

$$I_{y_C} \dot{q} + \left(I_{x_C} - I_{z_C} \right) rp \qquad = M \; ; \qquad (5)$$

$$I_{z_C} \dot{r} + \left(I_{y_C} - I_{x_C} \right) pq \qquad = N \; . \qquad (6)$$

For determining the vessel's position, its gravity center coordinates in the Earth frame are used: x_0, y_0, z_0.

For determining the vessel's hull orientation, the vessel's roll ϕ, pitch θ and heading ψ angles are used.

Forces and moments are recorded in the body-fixed frame.

By integrating the motion equations, we obtain components of the velocity and rate-of-turn vectors in the body-fixed frame: u, v, ω, p, q, r.

Kinematic equations are used for determining derivatives of the gravity centre coordinates and vessel angles $\dot{x}_0, \dot{y}_0, \dot{z}_0, \dot{\phi}, \dot{\theta}, \dot{\psi}$.

By integrating kinematic equations we obtain the gravity centre coordinates and vessel angles at the following moment of time.

The summarized forces in the equations (1-6) are presented in the following form:

$$X = X_I + X_H + X_P + X_R + X_T + X_C + X_A + X_W + X_{EXT};$$

$$Y = Y_I + Y_H + Y_P + Y_R + Y_T + Y_C + Y_A + Y_W + Y_{EXT};$$

$$Z = Z_I + Z_H + Z_W + Z_{EXT};$$

$$K = K_I + K_H + K_P + K_R + K_T + K_C + K_A + K_W + K_{EXT};$$

$$M = M_I + M_H + M_P + M_W + M_{EXT};$$

$$N = N_I + N_H + N_P + N_R + N_T + N_C + N_A + N_W + N_{EXT};$$

where:

$X_I, Y_I, Z_I, K_I, M_I, N_I$	–	inertial forces and moments;
$X_H, Y_H, Z_H, K_H, M_H, N_H$	–	hydrodynamic forces and moments;
X_A, Y_A, K_A, N_A	–	aerodynamic forces and moments;
X_C, Y_C, K_C, N_C	–	current forces and moments;
X_R, Y_R, K_R, N_R	–	rudder forces and moments;
X_T, Y_T, K_T, N_T	–	thruster forces and moments;
X_P, Y_P, K_P, M_P, N_P	–	propeller forces and moments;
$X_W, Y_W, Z_W, K_W, M_W, N_W$	–	wave forces and moments;
$X_{EXT}, Y_{EXT}, Z_{EXT}, K_{EXT}, M_{EXT}, N_{EXT}$	–	external forces and moments which include the forces of interaction with other vessels, anchor forces, mooring lines etc.

The aforementioned system of equations (1-6) describes the motion of a vessel having 6 degrees of freedom. Simpler simulator versions can use a reduced vessel motion model (with fewer degrees of freedom). E.g., for the high speed craft the degrees of freedom may be reduced in number to four, and the motion equations will, therefore, have the following form:

$$m(\dot{u}_0 - v_0 r) \quad = X$$

$$m(\dot{v}_0 + u_0 r) \quad = Y$$

$$I_{x_C}\dot{p} \quad = K$$

$$I_{z_C}\dot{r} \quad = N$$

For the displacement type vessels the number of modeled degrees of freedom may be reduced to three. In this case the equations will assume the following form:

$$m(\dot{u}_0 - v_0 r) \quad = X$$

$$m(\dot{v}_0 + u_0 r) \quad = Y$$

$$I_{z_C}\dot{r} \quad = N$$

This report deals in what follows with the motion of displacement-type vessels.

Inertial Forces and Moments (Associated with "Ideal Fluid" Effects)

The addition hull masses in equations (1-6) are calculated with regard to the hull's shape. In the problem of modeling the vessel's spatial motion for the simulator, the cross members of the addition liquid masses matrix can be disregarded in view of their relative smallness. Accordingly, our model assumption forces and moments associated with "ideal fluid" effects have the following form:

$$X_I = X_{\dot{u}}\dot{u} - Y_{\dot{v}}vr + Z_{\dot{\omega}}\omega q ;$$

$$Y_I = Y_{\dot{v}}\dot{v} - Z_{\dot{\omega}}\omega p + X_{\dot{u}}ur ;$$

$$Z_I = Z_{\dot{\omega}}\dot{\omega} - X_{\dot{u}}uq + Y_{\dot{v}}vp ;$$

$$K_I = K_{\dot{p}}\dot{p} + \left(N_{\dot{r}} - M_{\dot{q}}\right)qr + \left(Z_{\dot{\omega}} - Y_{\dot{v}}\right)v\omega;$$

$$M_I = M_{\dot{q}}\dot{q} + \left(K_{\dot{p}} - N_{\dot{r}}\right)rp + \left(X_{\dot{u}} - Z_{\dot{\omega}}\right)\omega u;$$

$$N_I = N_{\dot{r}}\dot{r} + \left(M_{\dot{q}} - K_{\dot{p}}\right)pq + \left(Y_{\dot{v}} - X_{\dot{u}}\right)uv.$$

External Forces in Motion Equations

The external forces $F_{EXT}=[X_{EXT},\ Y_{EXT},\ Z_{EXT}]^T$ and moments $M_{EXT}=[K_{EXT},\ M_{EXT},\ N_{EXT}]^T$ e.g., forces from interaction with other vessels, are taken into account in a special way:

$$F_{EXT} = \frac{\Sigma P_{EXT}}{\Delta t};\ \ M_{EXT} = \frac{\Sigma L_{EXT}}{\Delta t},$$

where Δt is a step in the vessel's motion model integration,

$$\sum P_{EXT} = \sum_i \int_t^{t+\Delta t} F_{EXT\,i}(t)dt$$

– is a sum of external moments acting on the vessel over the integration step;

$$\sum L_{EXT} = \sum_i \int_t^{t+\Delta t} M_{EXT\,i}(t)dt$$

– is a sum of external angular moments acting on the vessel over the integration step. This method of considering the external forces allows the momentarily acting (during part of the integration step) as well as fast changing external forces to be taken into account.

HULL FORCES

Hydrodynamic Forces

In the vessel fixed axes, the hydrodynamic forces and moments can be presented in the following form:

$$X_H = \frac{\rho}{2} A_C U^2 C_{XH} ;$$

$$Y_H = \frac{\rho}{2} A_C (U^2 + L^2 r^2) C_{YH} ;$$

$$Z_H = -\left[N_{\dot{z}} w + \rho g A_{wp} z \right];$$

$$K_H = -\overline{HG}_y Y_H - \left[N_p p + mg \overline{GM}_T \phi \right];$$

$$M_H = -\left[N_q q + mg \overline{GM}_L \theta \right];$$

$$N_H = \frac{\rho}{2} A_C L (U^2 + L^2 r^2) C_{NH} ,$$

where C_{XH}, C_{YH}, C_{NH} are dimensionless coefficients of the hydrodynamic forces and yaw moment; A_C is area of the immersed part of center lateral plane; A_{wp} is water plane area; $N_p, N_q, N_{\dot{z}}$ are coefficients of roll, pitch and heave damping respectively; $\overline{HG}_z = z_G - z_H$ is distance between gravity center and center of hydrodynamic pressure; $\overline{GM}_T$ and $\overline{GM}_L$ are transverse and longitudinal metacentric height respectively.

Coefficients $N_p, N_q, N_{\dot{z}}$ are determined with regard to the hull shape, ship speed U and frequency of encounter σ.

Dimensionless coefficients C_{XH}, C_{YH}, C_{NH} are non-linear functions of the vessel's hull parameters, yaw rate (dimensionless rate of turn $\bar{r} = \frac{Lr}{U}$) and drift angle β.

Coefficient of the longitudinal hydrodynamic force $C_{XH}(V, \beta)$ is an even function of the drift angle and depends on the vessel's dimensions. Value $C_T(V) = C_{XH}(V,0)$ is determined by hull resistance at forward motion. The dependence of the characteristic on the speed allows the resistance non-quadratic at slow speeds to be taken into account. Ship resistance coefficient can be decomposed into viscous and wave components:

$$C_T(V) = C_T(Rn, Fn) = (1+k) C_F(Rn) + C_W(Fn),$$

where *Rn* is Reynolds number, *Fn* is a Froude number.

Coefficients C_{YH}, C_{NH} should best be decomposed as follows:

$$C_{YH} = C_{YHp} U^2 /(U^2 + L^2 r^2) + C_{YHd} ;$$

$$C_{NH} = C_{NHp} U^2 /(U^2 + L^2 r^2) + C_{NHd} ,$$

where $C_{YHp}(\beta), C_{NHp}(\beta), C_{YHd}(\beta, \bar{r}), C_{NHd}(\beta, \bar{r})$ are hydrodynamic coefficients, "p" index means "positional" (effect of drift without yaw rate), "d" means "damping" (effect of yaw rate). Thus, hydrodynamic Y-force and yaw moment are:

$$Y_H = \frac{\rho}{2} A_C \left[C_{YHp} U^2 + C_{YHd}(U^2 + L^2 r^2) \right];$$

$$N_H = \frac{\rho}{2} A_C L \left[C_{NHp} U^2 + C_{NHd}(U^2 + L^2 r^2) \right].$$

Coefficients $C_{YHp}(\beta), C_{NHp}(\beta)$ are functions of drift angle and vessel's dimensions. Coefficients $C_{YHd}(\beta, \bar{r}), C_{NHd}(\beta, \bar{r})$ are functions of yaw rate drift angle and ship dimensions. The range of $\bar{r}$ being infinite, we use $\bar{r}/\sqrt{1 + \bar{r}^2}$ parameter; its counterpart is yaw rate angle $\gamma = \arctan(\bar{r})$.

Aerodynamic Forces

Surge, sway, yaw and roll aerodynamic forces are expressed by the non-dimensional aerodynamic characteristics as follows:

$$X_A = -C_{XA}(\gamma_R) \frac{\rho_A V_{RW}^2}{2} A_T;$$

$$Y_A = C_{YA}(\gamma_R) \frac{\rho_A V_{RW}^2}{2} A_L;$$

$$N_A = C_{NA}(\gamma_R) \frac{\rho_A V_{RW}^2}{2} A_L L;$$

$$M_A = \overline{AG}_z Y_A,$$

where V_{RW} is apparent (relative) wind speed, γ_R is apparent wind angle, A_T and A_L are the transverse and lateral projected wind areas. Here the wind speed is at the height of 6 meters, set as a parameter of disturbances acting on the vessel, is reduced to the height of the vessel's sail area centre over the sea level.

Non-dimensional coefficients C_{XA}, C_{YA}, C_{NA} are calculated as functions of the apparent wind angle γ_R taking into account the configuration of vessel's over-water part.

Determining of Hydrodynamic and Aerodynamic Coefficients

Hydrodynamic Coefficients

To obtain $C_{XH}(\beta), C_{YH}(\beta, \bar{r}), C_{NH}(\beta, \bar{r})$ or its components $C_{YHp}(\beta), C_{NHp}(\beta), C_{YHd}(\beta, \bar{r}), C_{NHd}(\beta, \bar{r})$ we use tank test results in tabulated form in the whole range of drift angle and yaw rate.

As an example, hydrodynamic coefficients of a container ship (length overall 203 m, breadth 25.4 m, draft middle 9.8 m) are shown in Fig 5, Fig 6. Ship view is shown in Fig 3. A photograph of tank tests (self-propelled model, controllability tests) is shown in Fig 4.
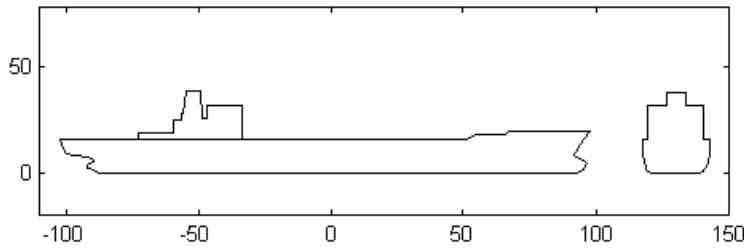
Fig 3. Container ship view
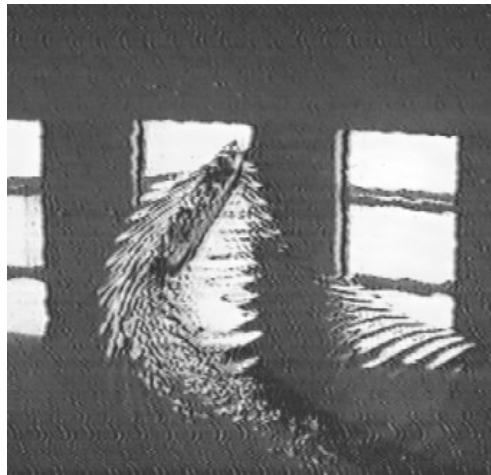
Fig 4. Tank tests (photo)

Position coefficients $C_{XH}(\beta)$, $C_{YHp}(\beta)$ and $C_{NHp}(\beta)$ for container ship are shown in Fig 5.
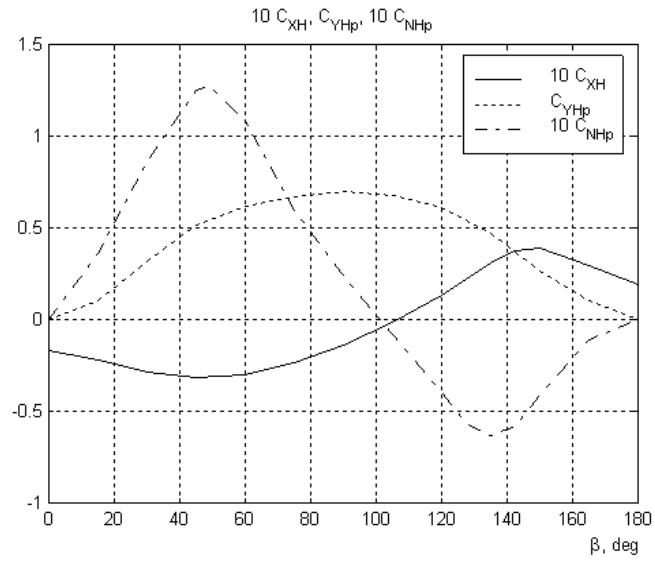
Fig 5. Hydrodynamic coefficients of a container ship (position coefficients).

Tank test results

Full hydrodynamic coefficients $C_{YH}(\beta, \overline{r})$ and $C_{NH}(\beta, \overline{r})$ are shown in Fig 6 and Fig 7.
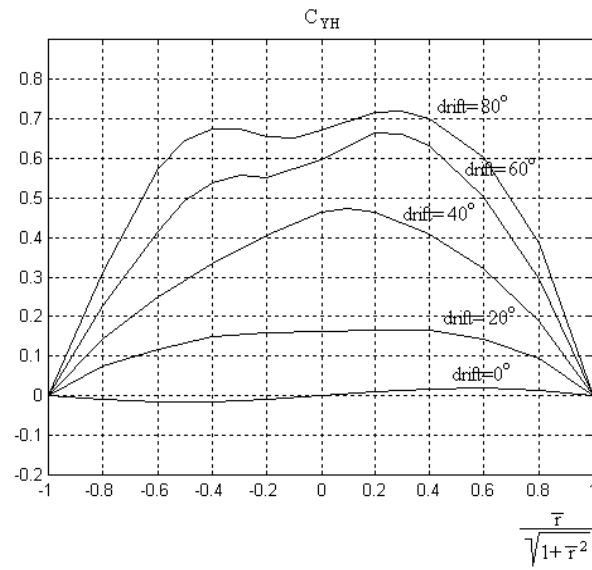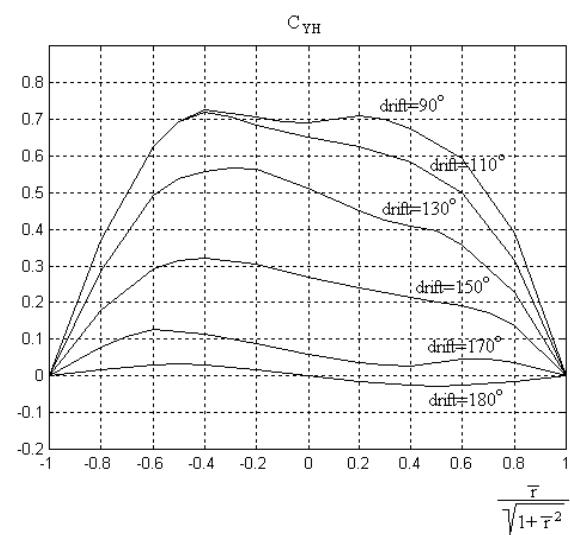
Fig 6. Hydrodynamic coefficient of a container ship, tank test results
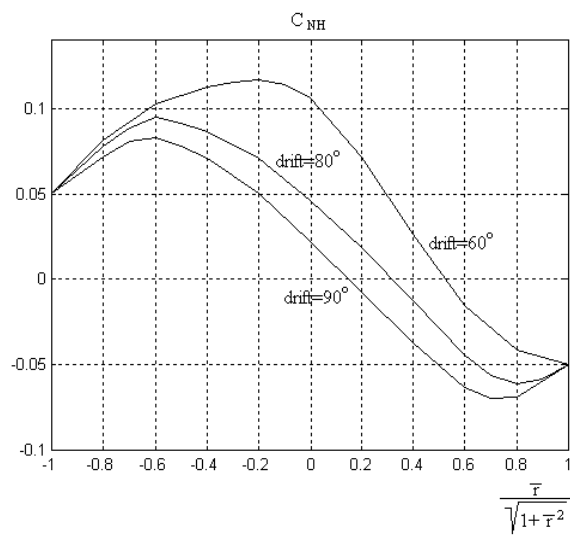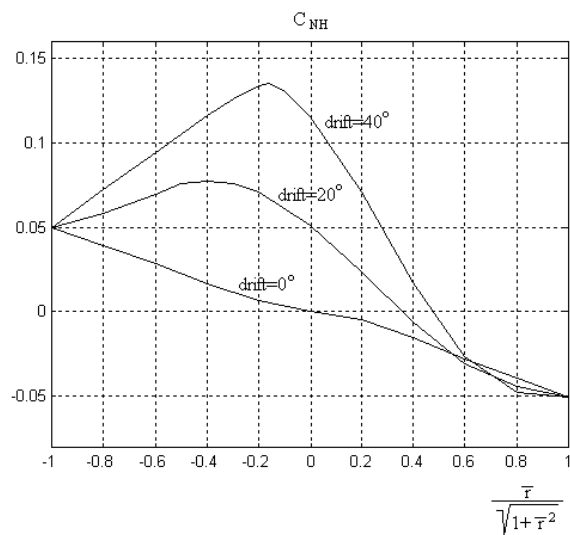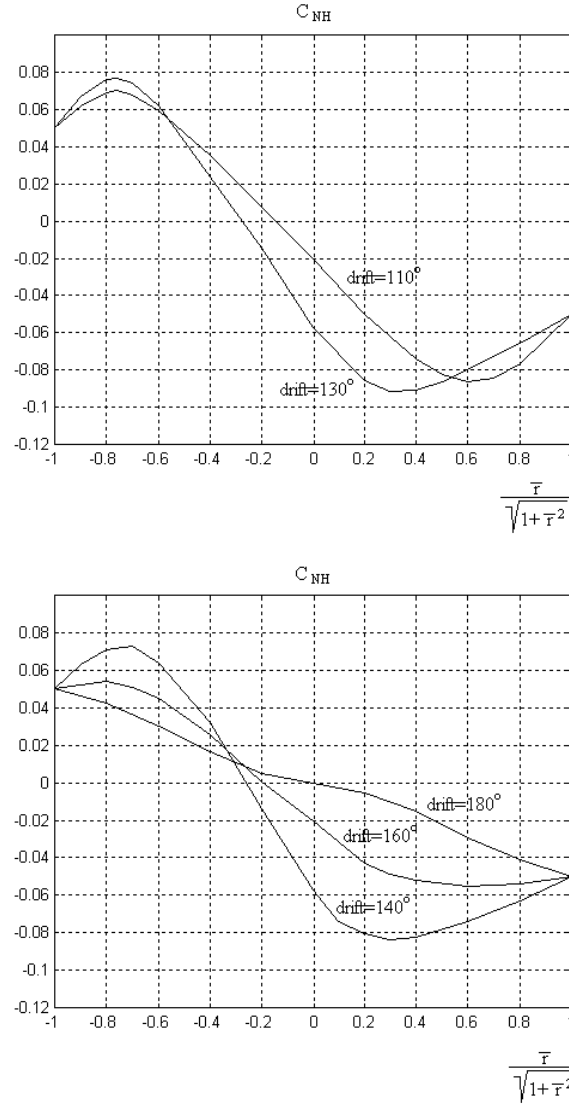
Fig 7. Hydrodynamic coefficient of a container ship, tank test results

Where tank test results are not available, $C_{YHp}(\beta), C_{NHp}(\beta)$ calculations use trigonometric series expansion with coefficients depending on the ship dimensions; $C_{YHd}(\beta, \overline{r}), C_{NHd}(\beta, \overline{r})$ calculations use interpolation formulas with coefficients depending on the ship dimensions. For verification of approximations, tank tests are compared to the results of calculations. E.g., hydrodynamic coefficients $C_{XH}(\beta)$, $C_{YHp}(\beta)$ and $C_{NHp}(\beta)$ for the trawler (tank tests and calculations) are shown in Fig 8. Vessel's principal particulars are follows: length overall 56 m, breadth 10 m, draft middle 3.15 m.
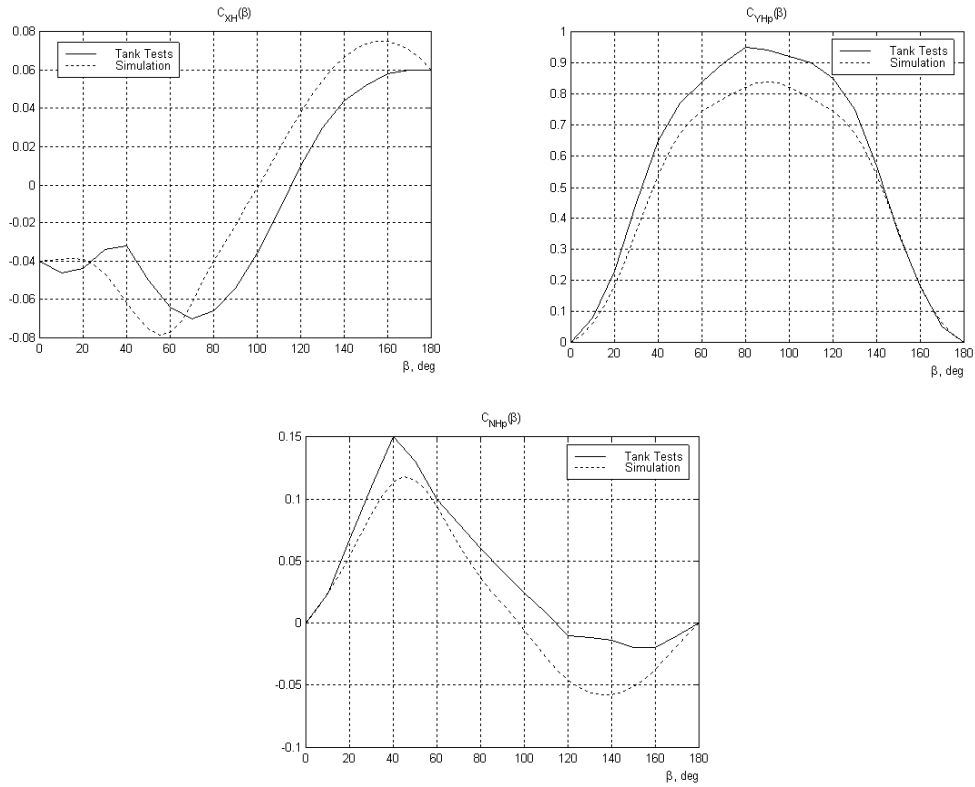
Fig 8. Hydrodynamic coefficients for a trawler (tank test and simulation)

Aerodynamic Coefficients

For a specific ship with known wind-tunnel results, C_{XA}, C_{YA}, C_{NA} are given in tabulated form in the entire range of wind angle γ_R . Comparison of the model prediction and wind tunnel test data for the tanker is shown in Fig 10. Tanker view is shown in Fig 9. The vessel's principal particulars are as follows: length overall 295 m, breadth 45 m, draft 17 m.
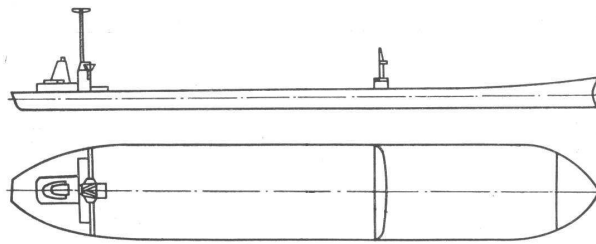
Fig 9. Tanker view
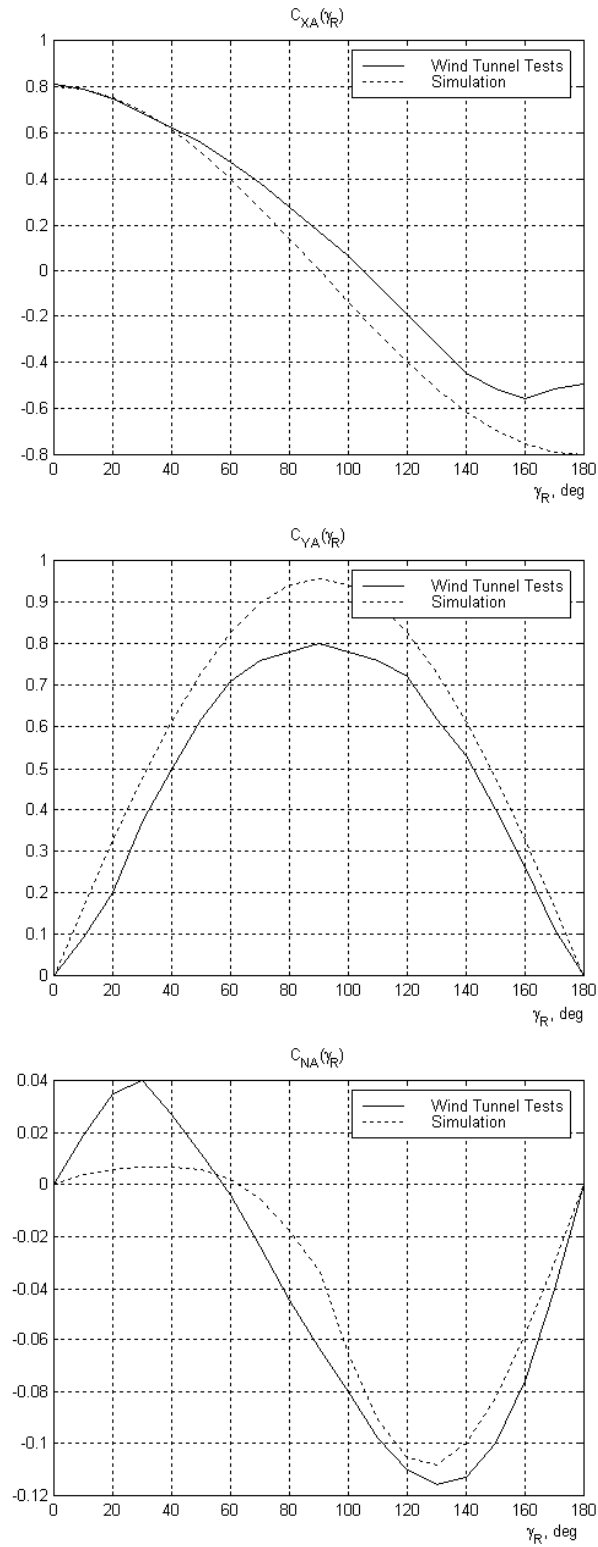
Fig 10. Aerodynamic coefficients of tanker, wind tunnel test and simulation.

Wind Forces and Moments Due to the Localized Wind

The wind model provides distribution of aerodynamic forces along the ship hull. Transas mathematical model allows distribution of wind forces along the ship length at least at seven sections. This refining of wind modeling allows the determination of aerodynamic forces and moments taking into consideration sections of over water hull, superstructure and deck equipment exposed to wind (see Fig 11).
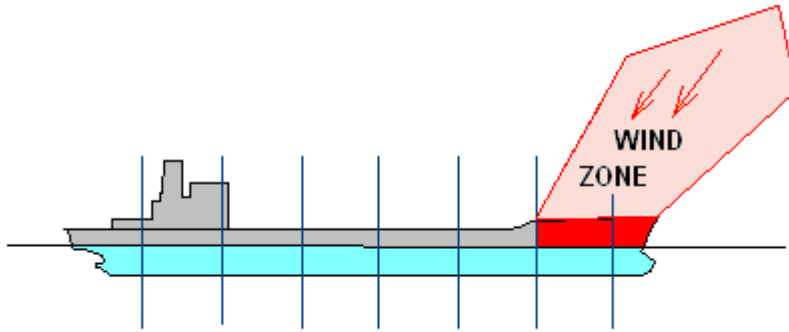
Fig 11. Container ship hull exposed to the wind load at bow

PROPELLERS

FP and CP Propellers

The mathematical model takes into account the longitudinal X_P, transverse Y_P and vertical Z_P forces, yawing moment N_P, heeling moment K_P and trimming moment M_P created by the CPP or FPP, and the moment on shaft Q_P.

The affected propeller thrust T_e, lateral force Y_P, and torque on the shaft Q_P are determined in the following way (for each propeller):

$$T_e = \rho n^2 D^4 (1 - \bar{t}) K_T(J, P/D) \,;$$

$$Y_P = \rho n^2 D^4 K_{YP}(J, P/D) \,;$$

$$Q_P = \rho n^2 D^5 K_Q(J, P/D) \,,$$

where P/D is propeller pitch ratio, J is propeller advance, n is propeller shaft frequency, K_T, K_Q and K_{YP} are non-dimensional coefficients.

Longitudinal and vertical forces are as follows:

$$X_P = T_e \cos \theta_P \,;$$

$$Z_P = T_e \sin \theta_P \,,$$

where θ_P is the shaft angle of inclination.

Yaw moment for single-screw ship is:

$$N_P = Y_P x_P \,,$$

for twin-screw ship is:

$$N_P = \sum_{i=1}^{2} (Y_{Pi} x_{Pi} + X_{Pi} y_{Pi}) \,.$$

Heeling moment K_P is produced by the propeller, and the trimming moment M_P is determined by propeller's relative coordinates x_P, y_P and z_P.

The propeller operation diagrams $K_T(J)$, $K_Q(J)$ are determined by the use of these B series propellers (Troost propellers), T4 series propellers (Titov propellers) and modern geometry propellers (M, Z, T6, T7 series propellers).

An example of FPP operation diagrams is shown in Fig 12, for the CPP – in Fig 13.
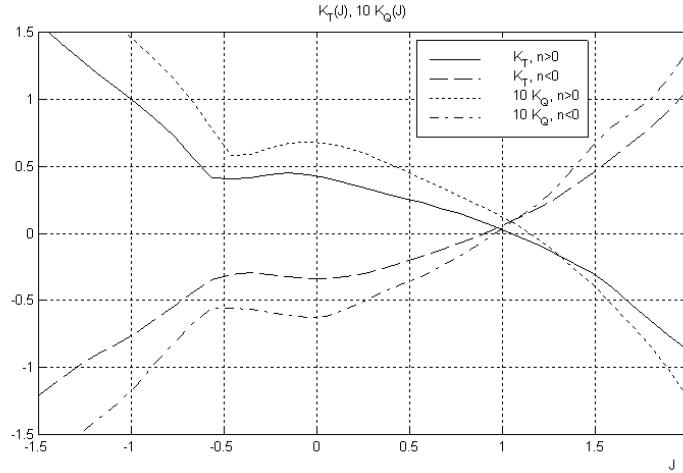
Fig 12. Example of FPP operation diagrams. Number of blades is 4, disc area ratio = 0.67,

P/D pitch ratio = 1
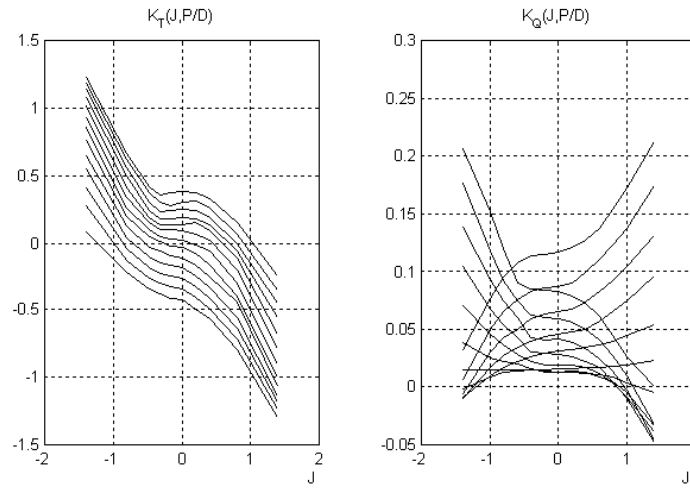
Fig 13 Example of CPP operation diagrams. Number of blades is 4, disc area ratio = 0.7,

P/D pitch ratio varies from -1 to 1.4

The relative propeller advance is determined by:

$$J = \frac{u_P(1-W)}{nD},$$

where u_P is a geometrical speed of water flow on the propeller in the axial direction.

Propeller interaction with the vessel hull is taken into account by using wake coefficients $W = W(U)$ and thrust deduction coefficient $\bar{t} = \bar{t}(J/J^*)$, where J^* is a steady value of the propeller advance at the given RPM value. Parameters of these dependencies are the propeller diameter, type of propeller fixture, fullness of displacement, vessel dimensions.

Hydrodynamic characteristics of propellers of high-speed vessels depend on cavitation number æ:

$$æ = \frac{2(P_{atm} + \rho gh - P_{vap})}{\rho u_P^2}$$

where P_{atm} = 101300Pa is atmospheric pressure, h is propeller's axle sinkage relative actual water surface, in meters and P_{vap} is vapor pressure, in Pascal. An example of propeller operation diagrams $K_T(J)$, $K_Q(J)$ for high-speed vessels is shown in Fig 14.
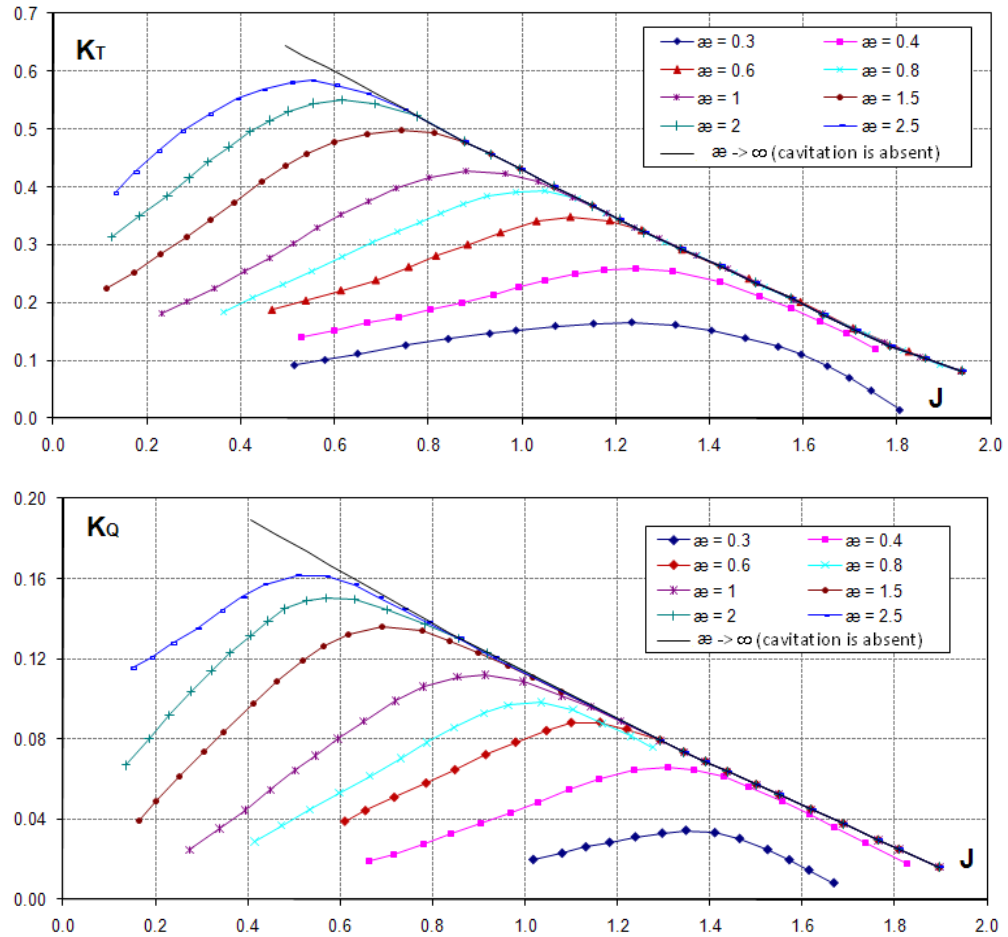
Fig 14. Example of propeller operation diagrams for high-speed vessels.

Disc area ratio = 1.35, P/D pitch ratio = 1.9

As the propeller is reversed, a significant transverse force occurs on the vessel's hull. This force is caused by the asymmetry of the ship stern geometrical shape in height and a difference in the limiting conditions of the propeller jet flowing around the hull next to the free surface and bottom edge. A non-dimension coefficient of the transverse force $K_{YP}(J, n, P/D)$ depends on the relative advance, RPM, pitch and geometric characteristics of the propeller and hull's stern part. Calculations of the coefficient of the transverse force occurring in the vessel's reversing use the experimental data and the theoretical calculation procedures.

This kind of $K_Y(J)$ dependence for a FPP (during the reversing to the full speed astern) is shown in Fig 15.
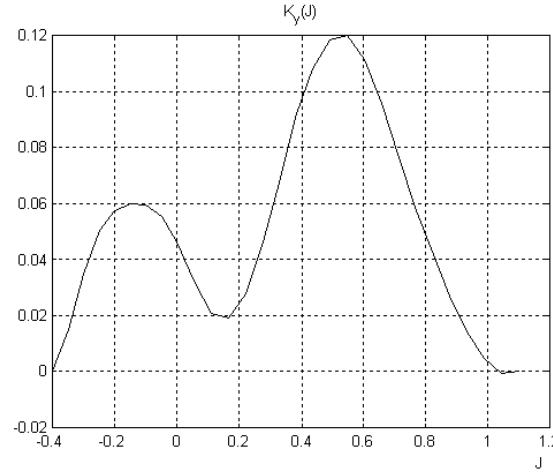
Fig 15. Coefficient of transverse force (FPP, reverse to Full Astern)

The transverse force occurring in single propeller vessels due to the non-uniform distribution of the wake over the propeller disk is taken into account by using an additional rudder angle $\delta_0 = \delta_0(J, P/D)$.

When a vessel is moving with a drift, and during the vessel's curvilinear motion, there is some change in the velocity field next to the propeller, which brings about changes in the propeller traction. This effect is taken into account by determining the speed of the water inflow on the propeller in the axial direction with regard to the side wash angle and a correction to the wake coefficient:

$$J = \frac{u'_P}{nD},$$

where $u'_P = u_P(1 - W')\cos(\kappa\beta_P)$ is a velocity of inflow on the propeller in the axial direction, β_P is geometrical angle of inflow on the propeller, $W' = W'(W, \beta_P)$ is wake coefficient with the correction taken into account, $\kappa = \kappa(\beta_P)$ is side wash angle coefficient.

Propeller Inside Turning Nozzle

The mathematical model takes into account the longitudinal X_P and transverse Y_P forces, yawing moment N_P, heeling moment K_P and trimming moment M_P created by the Vane Propeller. These forces are the following:

$$X_{PN} = T_e + X_N + \Delta X_{PN};$$
$$Y_{PN} = Y_P + Y_N + \Delta Y_{PN};$$
$$K_{PN} = K_P + K_N + \Delta K_{PN};$$
$$M_{PN} = M_P + M_N + \Delta M_{PN};$$
$$N_{PN} = N_P + N_N + \Delta N_{PN},$$

Components marked with *'PN'* correspond to the combined effect from propeller and nozzle, components marked with '*P'* and '*N'* correspond to the separated effect, T_e is effective propeller thrust whilst additional parameters (Δ) are due to interaction of propeller and nozzle.

In considering of geometric parameters of a particular ship's hull, propellers and nozzles, the curves of nozzle effect are transformed into following relations:

$$X_N = C_{XN}(C_{Te},\beta)f(D_N,\ell_N,u_P,C_{Te},\delta_N);$$
$$Y_N = C_{YN}(C_{Te},\beta)f(D_N,\ell_N,u_P,C_{Te},\delta_N),$$

where C_{XN} (Fig 16) and C_{YN} are peripheral hydrodynamic nozzle characteristics, f is function taking into account the nozzle dimensions and current ship operation parameters, C_{Te} is propeller thrust load coefficient, D_N is nozzle diameter, ℓ_N is nozzle length, u_N is incoming flow velocity, δ_N is angle of nozzle setting.
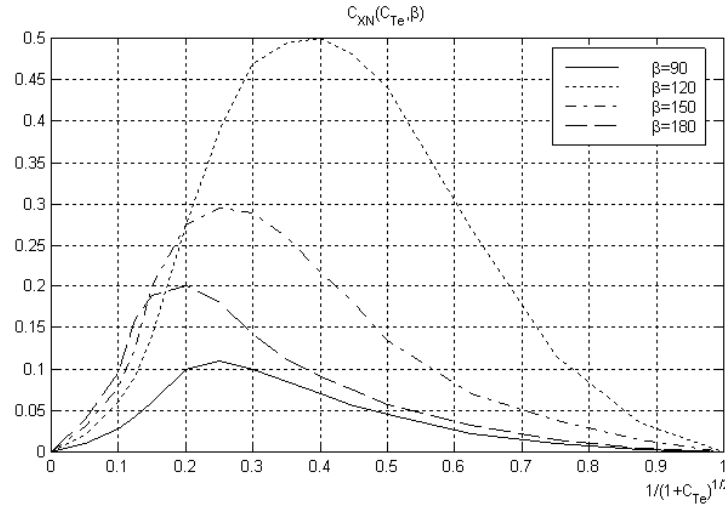
Fig 16. Effect of the nozzle on longitudinal force in propeller-nozzle complex

Vane Propeller (Voith Schneider)

The mathematical model takes into account the longitudinal X_{VSP} and transverse Y_{VSP} forces, yawing moment N_{VSP}, heeling moment K_{VSP} and trimming moment M_{VSP} created by the Vane Propeller and torque on the propeller axis Q_{VSP}.

The thrust and torque of a Vane propeller when ship is running along a curved trajectory is calculated as follows.

$$X_{VSP} = C_{VSPx}(J,\alpha)\frac{\rho F_P u_{VSP}^2}{2};$$
$$Y_{VSP} = C_{VSPy}(J,\alpha)\frac{\rho F_P u_{VSP}^2}{2};$$
$$Q_{VSP} = C_{VSPq}(J,\alpha)\rho F_P n^2 D^3,$$

where C_{VSPx} and C_{VSPy} are non-dimensional thrust coefficients in longitudinal and transversal directions, C_{VSPq} is non-dimensional torque coefficient, $u_{VSP} = \pi nD$ is blades peripheral velocity, $F_P = DL$ is hydraulic section area, D is blade orbit diameter and L is blade length.

Propeller thrust and torque coefficients are determined from the model tests of vane propellers, geometrical characteristics of particular propeller and effect of a ship's hull taken into account. Fig 17 presents an example of thrust coefficient curves for a vane propeller with pivot kinematics and eccentricity=*0.75* as a function of adjusted

direction of thrust α and relative advance J (its projection onto incoming flow direction).

$K_{VSPx}(J,\alpha)$
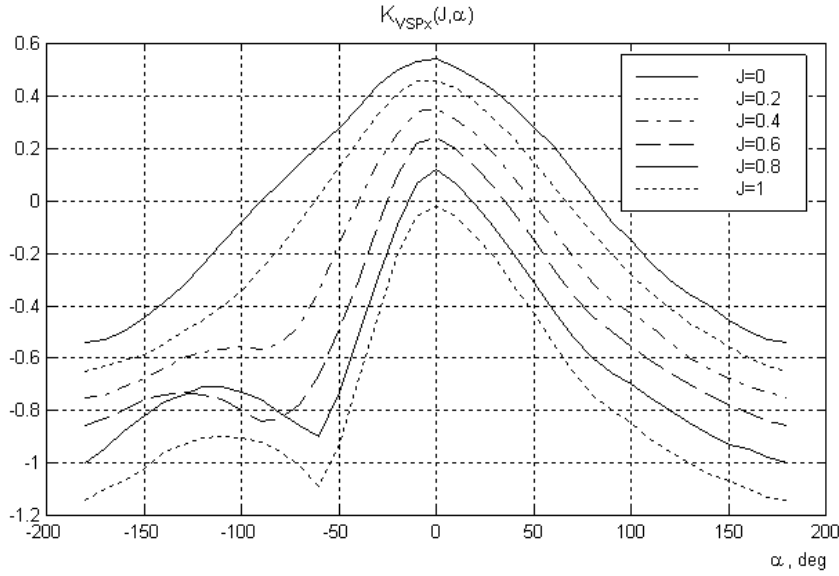
Fig 17. Vane propeller thrust coefficient in the longitudinal direction

(in flow frame of reference)

The relative propeller advance is determined by:

$$J = \frac{u_p}{u_{VSP}} ,$$

where u_p is inflow velocity on the propeller.

For a commanded steering direction θ and a given local drift angle at the position of the propeller β, the adjusted direction of thrust for the propeller coefficients is

$$\alpha = \theta + \beta .$$

VSP also creates a heeling moment K_{VSP}, trimming moment M_{VSP} and yawing moment N_{VSP} which are determined by VSP coordinates relative to the ship's centre of gravity x_{VSP}, y_{VSP} and z_{VSP}.

Mutual impact of vane propellers on each other is also considered.

Waterjet

The mathematical model takes into account the longitudinal X_{WJ} and transverse Y_{WJ} forces, as well as yawing moment N_{WJ}, heeling moment K_{WJ} and trimming moment M_{WJ} created by the waterjet.

Calculations of these forces and moment use the model of a waterjet as a vane pump. It is also possible to model a water jet as a propeller within a tunnel.

The waterjet thrust (in the axial direction) is determined from the following formula:

$$P = \frac{\rho}{2} \pi \frac{D^2}{4} u_{WJ}^2 C_T ,$$

where $u_{WJ} = u(1-W)$ is geometrical speed of water flow on the waterjet propeller in the axial direction C_T is waterjet load coefficient.

The load coefficient C_T and outflow speed (speed at the waterjet outlet) u_1 is determined by the head H and onflow speed u_{WJ}. In its turn, head H is connected to flow Q by means of the head/flow characteristic. An example of the waterjet head/flow characteristic is shown in Fig 18.
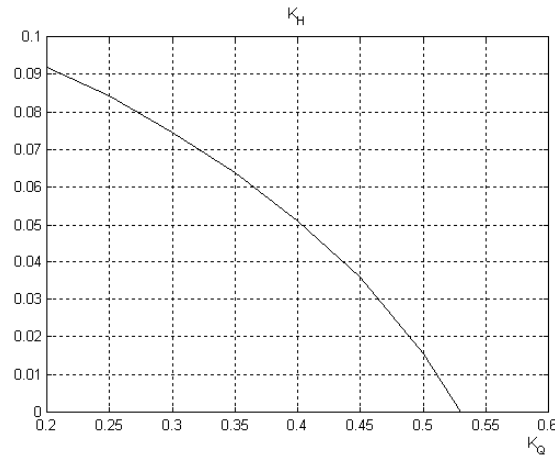
Fig 18. Waterjet head / flow characteristic

Steering is performed by turning the waterjet thrust to angle δ_{WJ}. As this is done, the waterjet develops the following forces:

$$X_{WJ} = P \cos k\delta_{WJ} \; ;$$

$$Y_{WJ} = P \sin k\delta_{WJ} \, ,$$

where $k\delta_{WJ}$ − is angle which the waterjet thrust turns to when the waterjet turns to angle δ_{WJ}.

Coefficient k depends on the onflow speed u_{WJ}, which is essential where the waterjet nozzle is turned (reverse-steering gear) rather than the waterjet itself.

The waterjet also develops yawing moment N_{WJ}, heeling moment K_{WJ} and trimming moment M_{WJ} which are determined by the waterjet coordinates x_{WJ}, y_{WJ} and z_{WJ} relative to the ship's center of gravity.

Some of the waterjets are fitted out with a reversing bucket which allows the ahead/astern reversing of thrust.

On the reversing bucket (as it is lowered), some additional resistance and transverse force are developed, which are determined by the speed of the jet at the waterjet outlet and the immersed bucket area.

Azimuth Propellers

Azimuth propellers ensure high manoeuverability of ships, which is particulary important in the slow-speed maneuvering, towing, dynamic positioning, etc. This up-to-date propulsion type if used both, as an auxiliary control, and as the main propulsion. The mathematical model of an azimuth propeller models operate with

the azimuth propellers by well known manufacturers like Azipod, Aquamaster, Schottel, KaMeWa, Niigata, Kawasaki, Ulstein and Brunvoll.

The mathematic model takes into account longitudinal X_{AP} and transverse Y_{AP} forces, yawing moment N_{AP}, heeling moment K_{AP} and trimming moment M_{AP} created by the azimuth propeller fitted out with a CPP or FPP in a nozzle or without it, and also moment Q_P on the shaft. This section describes a mathematic model of an azimuth propeller using an azimuth propeller with an FPP in the nozzle as an example.

The longitudinal and transverse forces from the azimuth propeller in the ship body axes coordinate system are calculated as follows:

$$X_{AP} = X'_{AP} \cos(\delta_{AP}) + Y'_{AP} \sin(\delta_{AP});$$

$$Y_{AP} = -X'_{AP} \sin(\delta_{AP}) + Y'_{AP} \cos(\delta_{AP}),$$

where δ_{AP} is a turn angle of the Azimuth propeller, whilst X'_{AP} and Y'_{AP} are projections of the force in the azimuth propeller body axes coordinate system, determined from the following expressions:

$$X_{AP} = R_{AP} \cos(\gamma_{AP});$$

$$Y_{AP} = R_{AP} \sin(\gamma_{AP}),$$

where R_{AP} is resulting thrust defined as:

$$R_{AP} = k_{AP} T_{AP}.$$

The values of coefficient $k_{AP} = f(\alpha_{AP}, C_{TeAP})$ and turn angle of the resulting force relative to the propeller shaft axis $\gamma_{AP} = f(\alpha_{AP}, C_{TeAP})$ are determined from the data of serial tests of nozzle propellers with a circular range of onflow angles as a function of onlflow angle $\alpha_{AP} = \delta_{AP} - \beta_{AP}$ and thrust load coefficient C_{TeAP}, β_{AP} here being the local drift angle in the azimuth propeller position.

The thrust value $T_{AP} = \rho n^2 D^4 K_T(J, P/D)$ is determined in accordance with "FP and CP propellers" section, assuming that onflow angle α_{AP} is equal to 0, and the onflow speed in the determining of propeller advance J is equal to the actual onflow speed.

Fig 19 presents an example of the turn angle of the resulting force $\gamma_{AP} = f(\alpha_{AP}, C_{TeAP})$ from the onflow angle and thrust load coefficient according to the data of serial tests of nozzle propellers with the circular range of onflow angles.
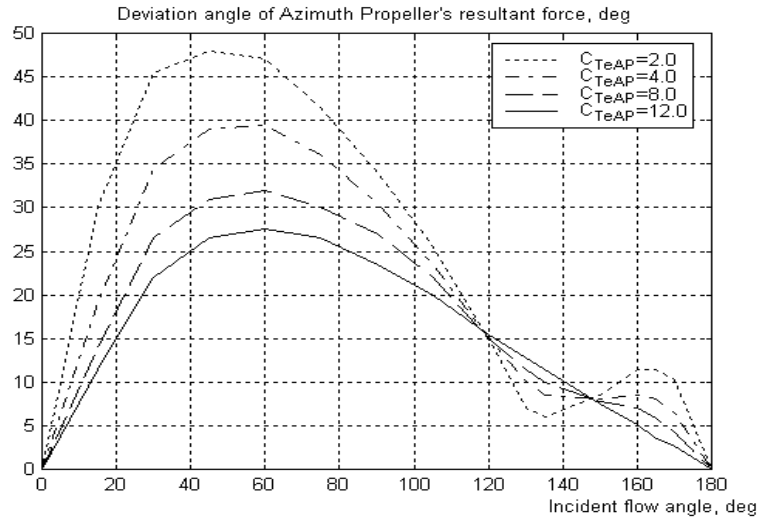
Fig 19. *Experimental onflow angle and thrust load coefficient dependence of the turn angle*

of the resulting force on the azimuth propeller

The heeling moment K_{VSP} , trimming moment M_{VSP} and yawing moment N_{VSP} are determined by the coordinates of the azimuth propeller position relative to the ship centre of gravity x_{AP} , y_{AP} and z_{AP} . Moment on the shaft Q_P is determined according to "FP and CP Propellers" section with regard to the data on the largest possible moment on the shaft depending on the onflow angle and thrust coefficient.

Calculations of the onflow angle and speed, of the resulting forces and moments from the azimuth propeller, take into account interaction with the hull according to "FP and CP Propellers" section. The mutual effect of the azimuth propellers is also taken into account as a modification of thrust deduction and wake factors depending on the relative positions, propeller turn and operating mode.

RUDDERS AND THEIR ACTUATORS

Balanced Rudder

The mathematical model takes into account longitudinal X_R and transverse Y_R forces, yawing moment N_R and heeling moment K_R developed by the rudder.

These forces and moments are the following:

$$X_R = C_{XR} \frac{(\bar{u}_R^2 + v_R^2)}{2} A_R \, ;$$

$$Y_R = C_{YR} \frac{(\bar{u}_R^2 + v_R^2)}{2} A_R \, ;$$

$$N_R = C_{NR} \frac{(\bar{u}_R^2 + v_R^2)}{2} A_R L \, ;$$

$$K_R = (z_R - z_G) Y_R$$

where C_{XR}, C_{YR} and C_{NR} are non-dimensional coefficients, u_R and v_R are rudder inflow velocities, $\bar{u}_R$ is average longitudinal flow velocity, A_R is total area of the rudder.

Rudder inflow velocities are:

$$u_R = u(1 - W_R) \, ;$$

$$v_R = v + x_R r \, ,$$

where W_R is wake coefficient.

Average longitudinal flow velocity $\bar{u}_R$ is

$$\bar{u}_R^2 = \frac{A_{RP} u_{RP}^2 + (A_R - A_{RP}) u_R^2}{A_R} \, ,$$

where A_{RP} is rudder area swept by propeller area, $u_{RP} = f(C_T, u_R)$ is axial flow velocity at the location of the rudder, C_T is propeller thrust load coefficient.

Non-dimensional coefficients C_{XR}, C_{YR} and C_{NR} depend on the rudder angle δ_R, drift angle β, yaw rate r and the propeller thrust load coefficient C_T:

$$C_{XR} = C_{XR}(\beta, r, \delta_R, C_T)$$

$$C_{YR} = C_{YR}(\beta, r, \delta_R, C_T)$$

$$C_{NR} = C_{NR}(\beta, r, \delta_R, C_T)$$

This dependence is expanded to δ_R series as follows:

$$C_{XR} = C_{XR}^0 + C_{XR}^{\delta_R} \delta_R + C_{XR}^{\delta_R^2} \delta_R^2 + C_{XR}^{\delta_R^3} \delta_R^3$$

The kind of dependence $C_{YR}^{\delta_R}(\beta, C_T, r = 0)$ for a twin propeller vessel with two rudders is shown in Fig 20.
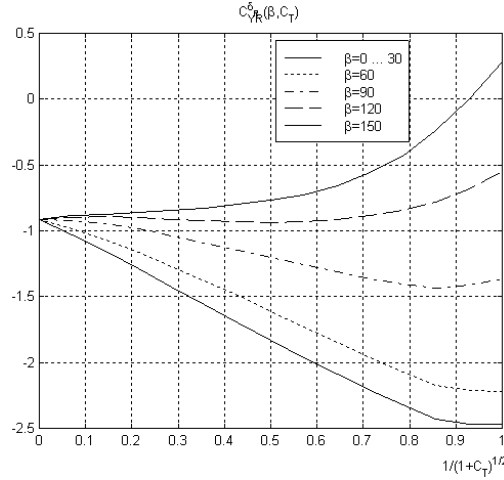

Fig 20. $C_{YR}^{\delta_R}(\beta, C_T, r = 0)$ *characteristic for twin-rudder twin-propeller ship*

Flanking Rudder

The mathematical model of flanking rudders is currently being developed.

The mathematical model of the ship motion will take into account the longitudinal X_{FR} and transverse Y_{FR} forces, yawing moment N_{FR} and heeling moment K_{FR} created by a flanking rudder.

Tugs (single screw and twin screw) are sometimes fitted out with flanking rudders. Flanking rudders are installed in front of the tug propeller. Flanking rudders are often installed in conjunction with other rudder systems, like a single rudder behind the propeller or rudder systems and most commonly used in conjunction with fixed nozzles.

Forces and moments are the following:

$$X_{FR} = C_{XFR} \frac{(\overline{u}_{FR}^2 + v_{FR}^2)}{2} A_{FR};$$

$$Y_{FR} = C_{YFR} \frac{(\overline{u}_{FR}^2 + v_{FR}^2)}{2} A_{FR}$$

$$K_{FR} = (z_{FR} - z_G)Y_{FR};$$

$$N_{FR} = C_{NFR} \frac{(\overline{u}_{FR}^2 + v_{FR}^2)}{2} A_{FR}L,$$

where C_{XFR}, C_{YFR} and C_{NFR} are non-dimensional coefficients, u_{FR} and v_{FR} are flanking rudder inflow velocities, $\overline{u}_{FR}$ is average longitudinal flow velocity, A_{FR} is total area of the flanking rudder.

Non-dimensional coefficients C_{XFR}, C_{YFR} and C_{NFR} depend on the rudder angle δ_R, flanking rudder angle δ_{FR}, drift angle β, yaw rate r and the propeller thrust load coefficient C_T.

High Lift Rudders (Becker and Shilling)

Some modern ships are equipped with high lift rudders, e.g., Becker and Shilling rudders.

The Becker rudder is a rudder with a flap. Its design incorporates a section shape similar to airfoil section but with a flap at the trailing edge. The flap deflects twice the angle of the main body of rudder and causes the rudder act as a high lift airfoil section at smaller rudder angles; at larger rudder angles the Becker rudder appears to be a thrust deflecting scoop for the propeller jet.

For Becker rudders, non-dimensional coefficients C_{XR}, C_{YR} and C_{NR} depend on the rudder angle δ_R, flap angle δ_F, drift angle β, yaw rate r and the propeller thrust load coefficient C_T.

Shilling MonoVec rudder consists of one-piece balanced rudder with slipstream guide plates at the top and bottom to control the flow over the rudder edges, and a special hydrodynamic profile, which allows for extreme rudder angles (up to 75 degrees). For Shilling rudder, formulae for a conventional rudder are suitable, but non-dimensional coefficients C_{XR}, C_{YR} and C_{NR} are special.

Wind tunnel comparison test between high lift rudder and conventional rudder is presented in Fig 21. The hydrodynamic profile of high lift rudder delays the stall angle and maximum lift (rudder force) is rapidly approached at around 30 degrees.
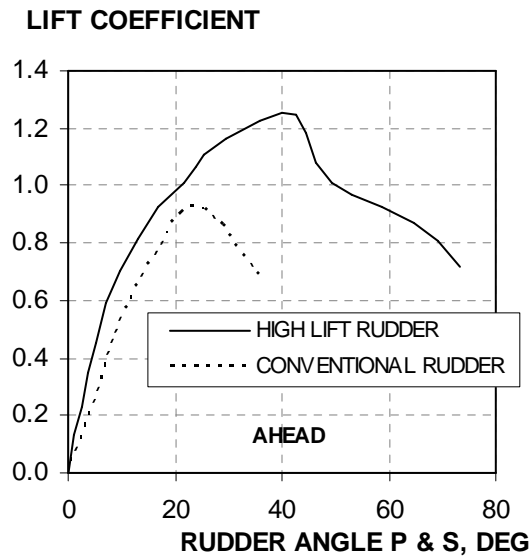
LIFT COEFFICIENT

Fig 21. High lift rudder coefficient in comparison with conventional rudder lift coefficient

Results of Transas model tests are presented in Fig 22 and Fig 23.
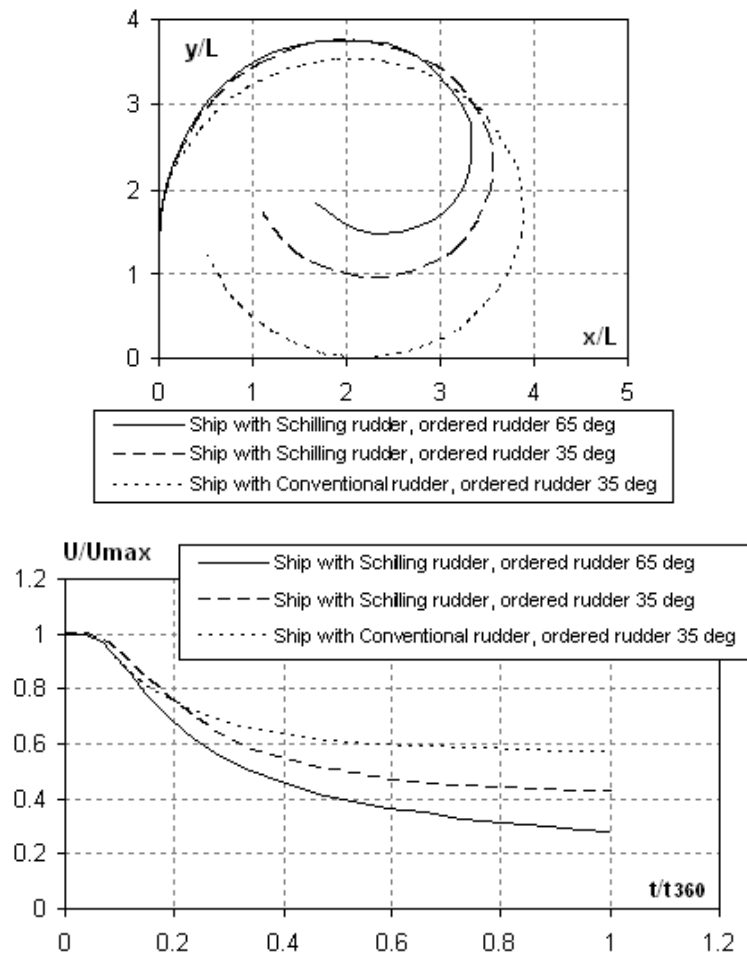
Fig 22. Starboard turning through 360 degrees

In Fig 22 the track plot of starboard turning circle on deep water and corresponding to it time history of speed are presented. Here L is ship length, U is current ship speed, Umax is full ship speed ahead, t is current time, t360 is time at 360 degrees change of heading.

Fig 23. Starboard turning through 90 degrees

Table 1. Principal dimensions for the ship with conventional rudders and ship with Becker rudders

Model name	Ship with conventional rudders	Ship with Becker rudders
Displacement, t	31585	25598
Loa, m	183.8	179.6
Breadth, m	30.3	29.4
Draft, m	9.8	8.0
Number of rudders, profile rudder area, sq. m.	2 x 12	2 x 10

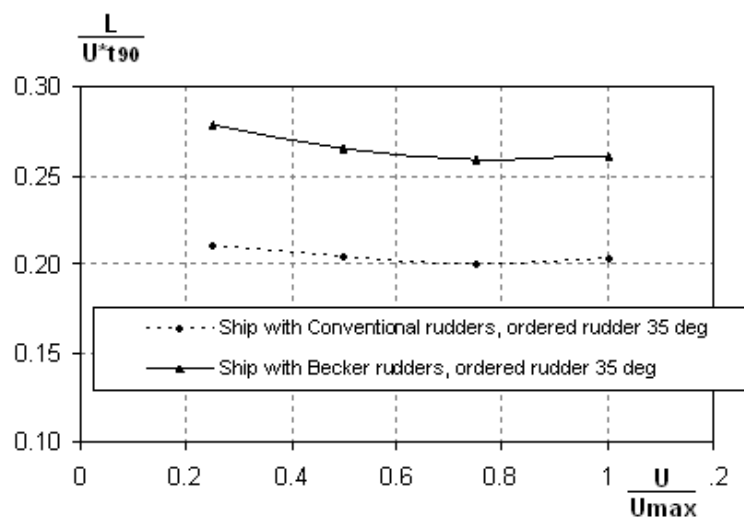From the diagrams shown (Fig 21–Fig 23) the improved performance of high lift rudder is evident.

Steering Gear

The model of the electro-hydraulic steering gear is included in the ship motion model. It introduces additional nonlinearity into steering dynamics as shown in Fig 24.
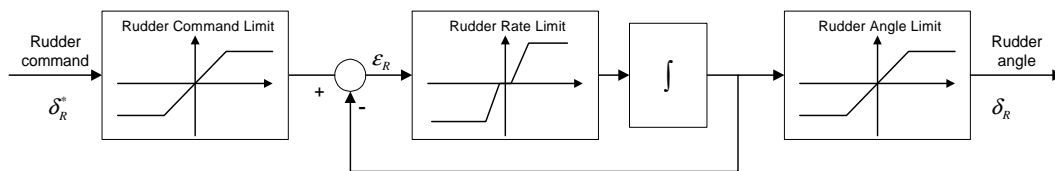
Fig 24. Steering gear model

The steering gear model includes 3 pumps (2 pumps and standby pump, only 2 pumps can operate simultaneously). The rudder rate limit depends on the number of active pumps.

The following faults are simulated:

• control failure (rudder command signal fault);

• mechanical rudder jamming;

• power failure (it causes rudder erratic behavior determined by the inflow);

• hydraulic oil pressure reduction (it causes reduction of rudder rate);

• malfunction of any pump.

THRUSTERS

Tunnel Thrusters (Bow and Stern)

The vessel's mathematical model takes into account the lateral force Y_T, yaw moment N_T and roll moment K_T created by thrusters. For each thruster, these forces and moments are the following:

$$Y_T = T_0 C_{YT}(\beta, u_T, u);$$

$$K_T = (z_T - z_G)Y_T$$

$$N_T = T_0 C_{NT}(\beta, u_T, u)x_T$$

where T_0 is the value of the thrust of thruster at $u = 0$; u_T is the water jet velocity at the thruster's output. The coefficients of the effect of hull $C_{YT}(\beta, u_T, u)$, $C_{NT}(\beta, u_T, u)$ are determined by the number of simultaneously operating thrusters and the position of thruster (bow or stern).

For a single bow and a single stern thruster coefficients $C_{YT}(\beta, u_T, u)$ and $C_{NT}(\beta, u_T, u)$ are shown in Fig 25 and Fig 26.
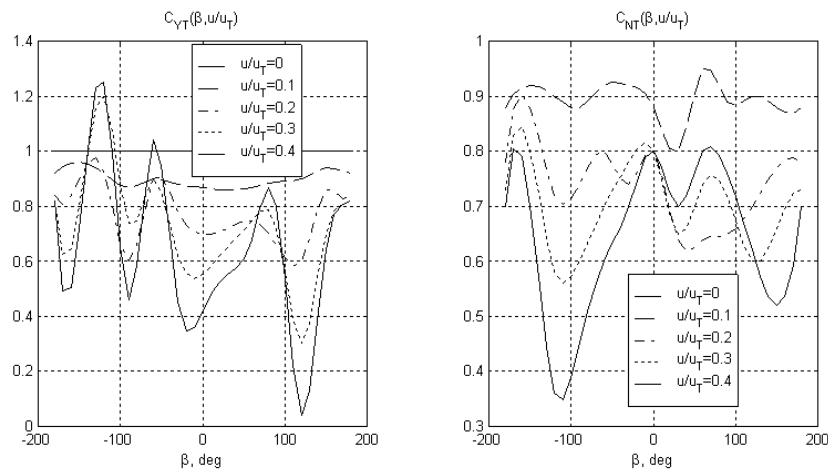

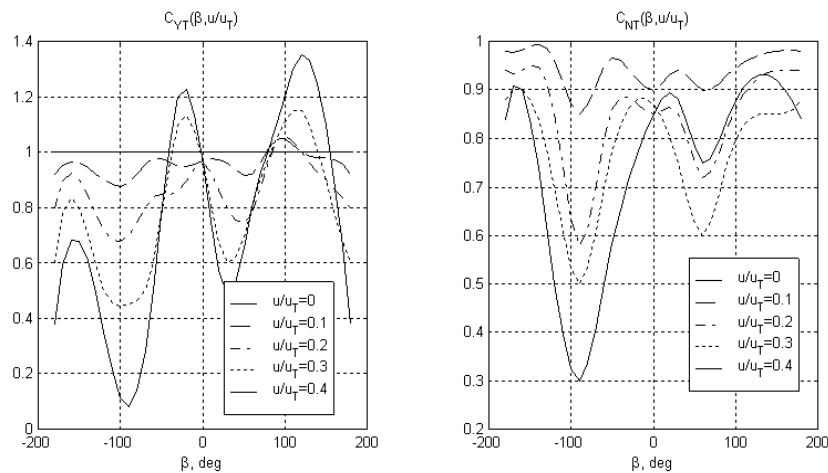Fig 25. Coefficients $C_{YT}(\beta, u_T, u)$ and $C_{NT}(\beta, u_T, u)$ for a single bow thruster

Fig 26. Coefficients $C_{YT}(\beta, u_T, u)$ and $C_{NT}(\beta, u_T, u)$ for a single stern thruster

MAIN ENGINE

Introduction

The mathematical model of the main engine allows simulating low- and medium-speed reversible diesels (which are started and reversed by the compressed air), as well as the non-reversible medium- and high-speed diesels (where the propeller is reversed by means of reversing gear). Steam and gas turbines are also included in the mathematical model.

Diesel engines with FPP, CPP, Voith Schneider, Z-Drive and waterjets are simulated.

Gas Turbines are simulated with CPP and waterjets.

Steam Turbines are simulated with CPP.

Diesel electrical propulsion is simulated with CPP.

Engine Dynamics

Propeller shaft RPM is obtained from:

$$2\pi J_E^* \frac{dn}{dt} = Q_e - Q_P - Q_f \,,$$

where $Q_e(n,h)$ is the engine output torque, determined from the family of the engine characteristics (an example of these characteristics for low-speed diesel is shown in Fig 27); $Q_P(n,V,P/D)$ the torque absorbed by propeller (in case of Voith Schneider $Q_P(n,V,\lambda_0)$) and $Q_f(n)$ is friction torque. Friction torque plus propeller torque is load torque.
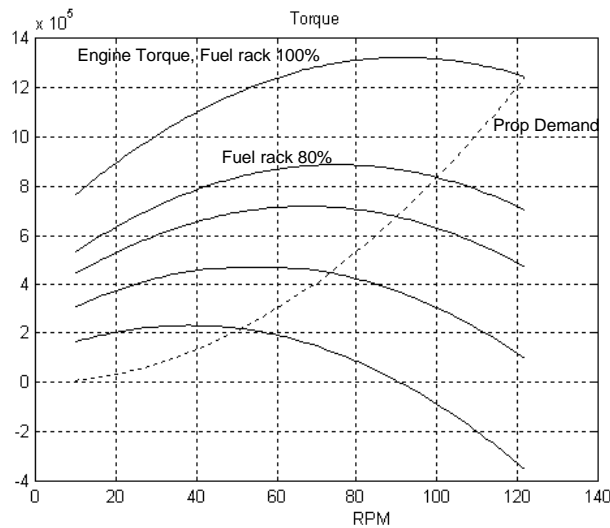
Fig 27. Low-speed diesel torque characteristics

Engine Telegraph

Steady dependence between engine RPM, propeller pitch and engine telegraph order is given by combinator diagram (Fig 28).
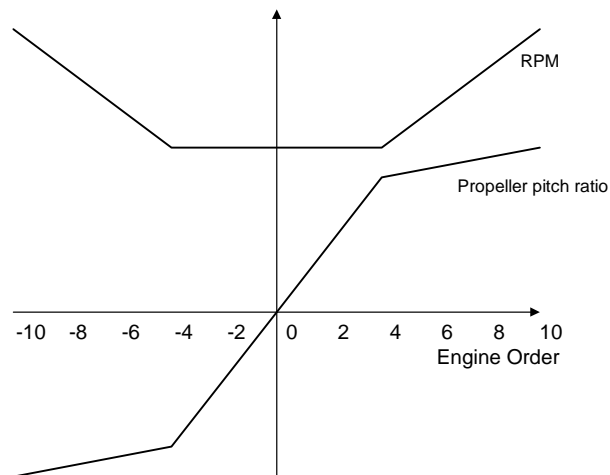
Fig 28. Example of a combinator diagram

Engine Remote Control System

The model of the main engine includes the model of the remote control system (RCS). RCS diagram is shown in Fig 29.
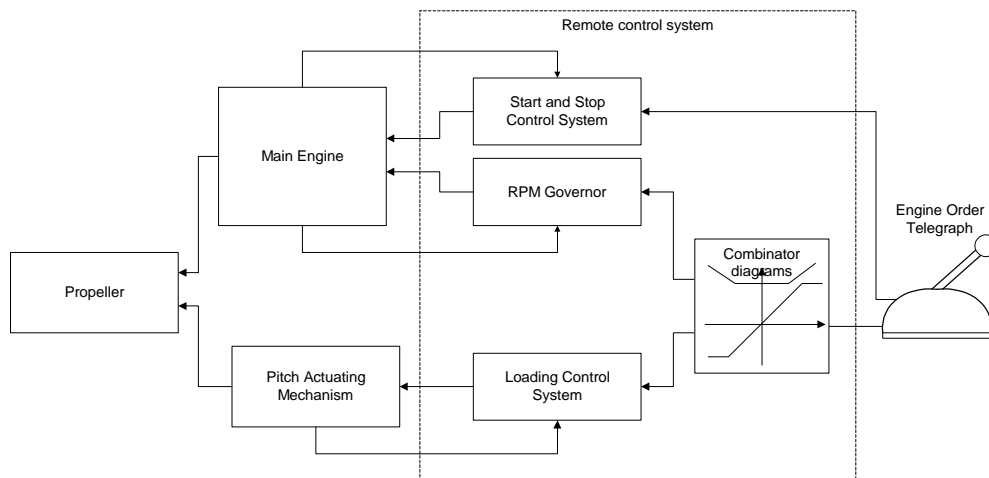
Fig 29. RCS diagram

RCS includes RPM governor. RPM governor can be switched off; in this case the remote control system controls the fuel rack directly. The RCS controls position of the diesel fuel rack h via the RPM governor or by acting directly on the actuator when the diesel is stopped or reversed.

RCS ensures changes of the diesel settings in accordance with either of the following programs: normal and emergency (Fig 30).

Fig 30. Example of RCS programs

For some ships with CPP, RCS includes loading control system as well.

RCS also includes starting, stopping and reversing systems. For the reversible FPP diesels, which are started and reversed with compressed air, calculations of torque created by the compressed air in the process of starting are made.

RPM Governor

Diesel engine is normally fitted with a hydraulic governor. The Woodward governor is an example of a commonly fitted type. RPM governor is simulated as a fully-variable (proportional-integral) RPM governor with a limiting characteristic.

Starting Air

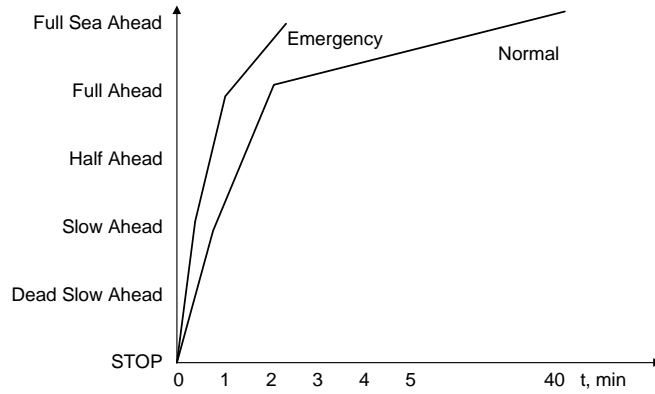For low and medium-speed reversible diesels (which are started and reversed by compressed air) at the stage of starting and reversing, torque is $Q_A(n, P_A)$, where P_A is starting air pressure. Starting air pressure dynamics is simulated as follows:

$$\frac{dP_A}{dt} = q_C - q_{start},$$

where q_C is filling of starting air cylinders, q_{start} is inflow when starting and reversing (can be determined from number of engine consecutive starts).

Clutch and Gear

Clutches and clutch control systems are modeled as part of medium- and high-speed diesel plants.

Propeller shaft rpm is obtained from:

$n = k_C n_e,$

where k_C is clutch and gear reduction coefficient (when the clutch is disconnected, reduction ratio is with "+" sign, or "–" when clutch is connected), n_e is engine shaft rpm.

Clutch control system for some ships can take into consideration some limitations (e.g., the clutch is not engaged unless the engine load is minimum: the propeller pitch is zero).

Gas Turbines

Gas turbine dynamics are simulated (start, stop, control by throttle lever).

Different versions of gas turbine connection with the propeller or waterjet shaft are simulated (an example is shown in Fig 31).
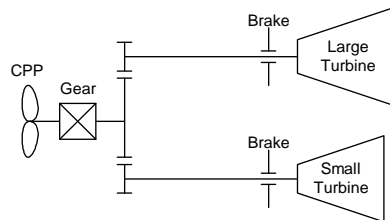
Fig 31. Connection of two gas turbines to the propeller shaft

Steam Turbines

Steam turbine dynamics are simulated (start, stop, control by throttle lever). Steam turbine is simulated with CPP.

For steam turbines, 2 modes are simulated – "Harbor" and "Sea", corresponding to different output RPM (output RPM in Sea mode can be 150-200% of output RPM in Harbor mode, transient time between Harbor and Sea modes is about 10-30 min).

Diesel Electric Propulsion

Electric propulsion is used mainly for special purpose vessels (tugs, trawlers, cable ships, ice breakers, etc.). Diesel electric propulsion can include d.c. or a.c. diesel-generator and d.c. or synchronous a.c. propulsion motor.

An example of diesel-electrical propulsion diagram is shown in Fig 32. Here the output current from a.c. generators is delivered at constant voltage and frequency, for the manoeuvring or slow speeds, however, the current is passed on to propulsion motors at a lower frequency and with voltage adjusted. The speed of a synchronous motor is dictated by the frequency of the current supplied.

Fig 32. Diesel-electrical propulsion diagram

Prevalent Faults Model

Diesel engine model includes following models of faults:

• engine RPM reduction;

• air compressor failure;

• increased air consumption during the start;

• clutch on fault.

WIND

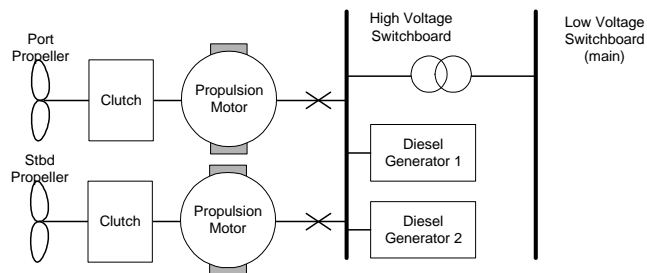The model of wind disturbances includes a model of constant wind $\overrightarrow{V_{W0}}$ determined by wind direction and speed (at 6 meters), and superimposed gusting random winds $\overrightarrow{V_{WG}}$ and squalls $\overrightarrow{V_{WS}}$:

$$\overrightarrow{V_W}(t) = \overrightarrow{V_{W0}} + \overrightarrow{V_{WS}}(t) + \overrightarrow{V_{WG}}(t) .$$

Squall

Squall model is determined by the maximum wind speed V_{max} and squall duration t_{max} :

$$\overrightarrow{V_{WS}}(t) = \overrightarrow{f}(V_{max}, t_{max}, t) .$$

Relation between the average wind speed and maximum speed in the squall is determined by Beaufort scale. Example of $V_{WS}(t)$ process is shown in Fig 33.
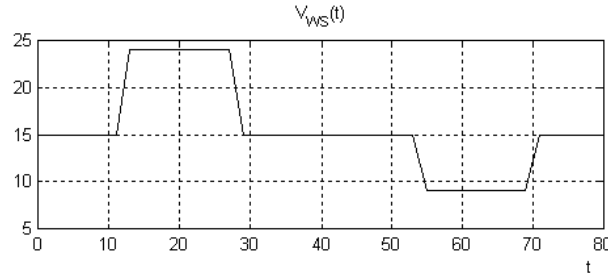
Fig 33. Sample of wind velocity in a squall

Gusting Random Wind

Model of the gusting variable wind component is based on spectral characteristics of turbulent and wave variable wind components:

$$S_{GW}(\omega) = S_{GWturb}(\omega) + S_{GWwv}(\omega) ,$$

where $S_{GWturb}(\omega) = \dfrac{D\alpha}{\omega^2 + \alpha^2}$ is spectrum of the turbulent component:

$$S_{GWturb}(\omega) = \frac{D\alpha}{\omega^2 + \alpha^2} ,$$

$S_{GWwv}(\omega)$ is spectrum of the wave component:

$$S_{GWwv}(\omega) = A\omega^{-5}\exp(-B\omega^{-4}) ,$$

Coefficients A, B, D and α are parameters of spectra depending of wind gust intensity.

Wind forces and moments acting on a ship are described in section "Aerodynamic forces".

WAVES

Introduction

The mathematical model allows simulation of the ship motions in irregular sea waves, at deep and shallow water. Wave surface model allows the wave elevation to be simulated in accordance with wave spectrum in various conditions. Wave-induced forces and moments include surge, sway and heave wave forces and roll, pitch and yaw wave moments $X_W(t)$, $Y_W(t)$, $Z_W(t)$, $K_W(t)$, $M_W(t)$, $N_W(t)$.

Wind-Generated Waves

The process of wave generation due to the wind starts with small wavelets appearing on the water surface. Short waves continue to grow until they finally break and their energy is dissipated. A storm, which has been blowing for a long time, is said to create a fully developed sea.

Wind generated waves are usually represented as a sum of a large number of wave components. Wave surface is determined by the following formula:

$$\zeta(x, y, t) = \sum_{i=1}^{N} \zeta_i(x, y, t) = \sum_{i=1}^{N} A_i \cdot \text{trochoid}(k_{xi} x + k_{yi} y - \omega_i t + \varphi_i),$$

where N is the number of components (harmonics), A_i is amplitude of a component, k_i are wave numbers of components, ω_i are frequencies of components, θ_i are directions of harmonics (relative the θ_{WV}), ϕ_i are phases. Wave parameters N, A_i, ω_i, k_i, θ_i $(i = 1...N)$ can be calculated on the basis of wave spectrum. Typically, total number of harmonics N is about 20.

Gerstner showed that that the motion of each fluid particle is a circle of radius r around a fix point (x_0, z_0):

$$\begin{cases} x = x_0 + r \sin(kx_0 - \omega t) \\ z = z_0 - r \cos(kx_0 - \omega t) \end{cases}.$$
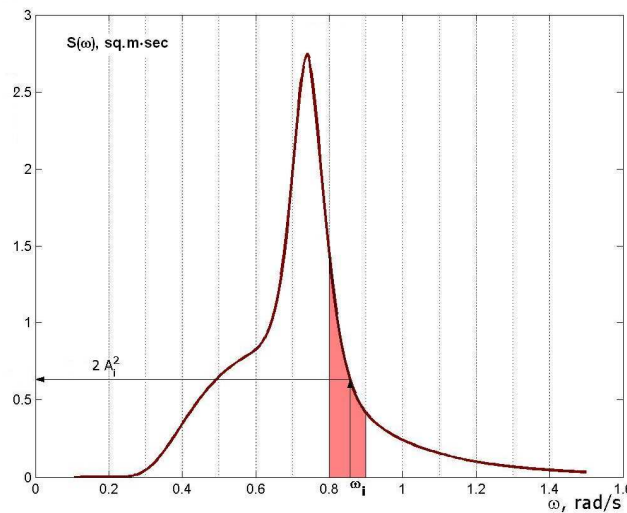
Fig 34. Frequency spectrum of wind waves

The wave amplitude A_i of i-wave component is related to the wave 2d-spectral density function $S(\omega)$, corresponding to the direction of i - wave component θ_i :

$$A_i^2 = 2S(\omega_i)\Delta\omega,$$

where ω_i is the wave frequency of i-wave component and $\Delta\omega$ is difference between successive frequencies (Fig 34). The wave phase ϕ_i is random phase uniformly distributed in range $[0, 2\pi)$.

The connection between wave number $k_i = 2\pi / \lambda_i$ and wave frequency ω_i (dispersion relationship) is:

$$\omega_i^2 = k_i g \operatorname{th}(k_i H)$$

where H denotes the water depth, g - acceleration due to gravity. At deep water dispersion relationship is $\omega_i^2 = k_i g$.

Examples of wave surface simulation are presented below.

Fig 35. Wave surface simulation

Wave Spectrum

There are many standard wave spectra: Neumann one-parameter spectrum, Bretschneider spectrum, Pierson-Moskowitz spectrum, Phillips spectrum, ITTC spectrum, etc.
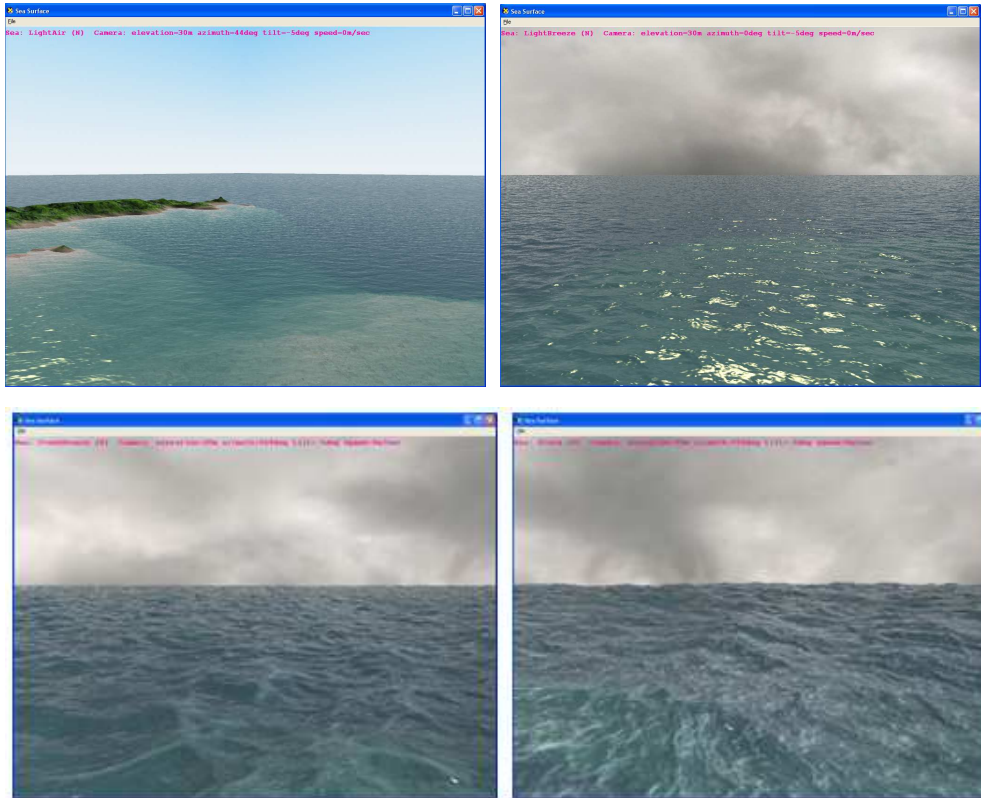
Pierson and Moskowitz assumed that if the wind blew steadily for a long time over a large area, the waves would come into equilibrium with the wind. (this is the concept of a *fully developed sea*). They calculated the wave spectra for various wind speeds and found that the spectra were of the form:

$$S(k) = \frac{0.0081}{4k^3} \exp\left(-\frac{0.74g}{|k|^2 V^4}\right),$$

where V is the wind speed.

Average wave parameters for different sea states are presented in table 2:

Table 2. Sea State Table

Sea State	Wave Height H_3% (m)	Wave Height H_1/3 (m)	Wave Length (m)	Period (s)	Beaufort force	Wind speed (m/s)
1	0.1 – 0.25	0.08 – 0.19	1 – 2.5	1 – 2	2	1.8 – 3.3
2	0.25 – 0.75	0.19 – 0.57	2.5 – 7.5	2 – 3	2 – 3	1.8 – 5.2
3	0.75 – 1.25	0.57 – 0.95	7.5 – 14	3 – 4	3	3.4 – 5.2
4	1.25 – 2.0	0.95 – 1.52	14 – 26	4 – 5	4	5.3 – 7.4
5	2.0 – 3.5	1.52 – 2.65	26 – 58	5 – 6.5	5 – 6	7.5 – 12.4
6	3.5 – 6.0	2.65 – 4.5	58 – 115	6.5 – 8.5	7	12.5 – 15.2
7	6.0 – 8.5	4.5 – 6.44	115 – 190	8.5 – 10	8	15.3 – 18.2
8	8.5 – 11.0	6.44 – 8.3	190 - 270	10 -13	9	18 – 21

Hasselmann *et al*. after analyzing data collected during the Joint North Sea Wave Observation Project JONSWAP proposed a spectrum in the form (Fig 36):

$$S(\omega) = \frac{\alpha g^2}{\omega^5} \exp\left(-\frac{5}{4}\left(\frac{\omega_p}{\omega}\right)^4\right) \gamma^{\psi(\omega)}$$

where $\omega_p = 2\pi / T_p$ is the frequency of the peak of the JONSWAP spectrum,

$\alpha = 0.0076\left(\frac{U_{10}^2}{Fg}\right)^{0.22}$, U_{10} is wind speed at a height of 10.0 m above the sea surface, F is the distance from a lee shore, called the fetch, or the distance over which the wind blows with constant speed, $\gamma = 3.3$ is constant,

$$\psi(\omega) = \exp\left(\frac{(\omega - \omega_p)^2}{2\sigma^2 \omega_p^2}\right), \quad \sigma = \begin{bmatrix} 0.07, & \omega \le \omega_p \\ 0.09, & \omega > \omega_p \end{bmatrix}$$
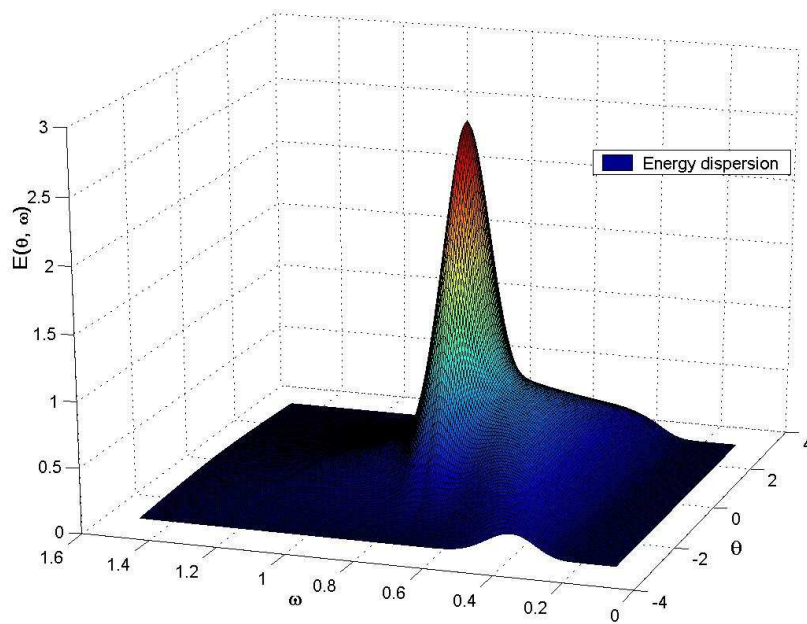
Fig 36. JONSWAP Spectrum (U_{10} =25m/s)

Sea Waves in Shallow and Coastal Waters

Sea waves are propagating over shallow or coastal water typically turning their wave front, e.g. the wave refraction is taking place. The waves are moving in more or less regular ridges developing so-called coastal swell. Wave's transformation appears due to damping of smaller waves with lower energy over the sea bottom. In physical terms, at shallow waters the waves look like long or solitary waves.

In addition to the refraction, shallow-water waves change other characteristics: wave height h rises at lower depth, while length and speed c reduce (as shown in Fig 37). Here h_0 is wave height at deep water, c_0 is wave speed at deep water.
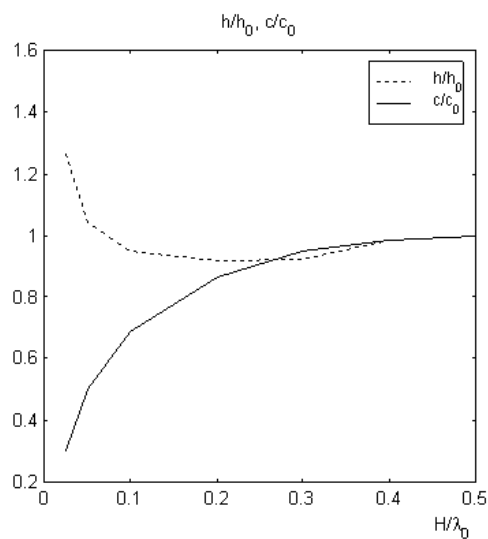

Fig 37. Change of wave parameters at shallow water

The incorporation of these effects into math model will be completed in the immediate future.

Wave-Induced Forces and Moments

Wave-induced forces and moments include 1st order wave forces (oscillator motion, index "1") and 2nd order wave forces (wave drift, index "2"):

$$X_W(t) = X_1(t) + X_2$$

$$Y_W(t) = Y_1(t) + Y_2$$

$$Z_W(t) = Z_1(t)$$

$$K_W(t) = K_1(t)$$

$$M_W(t) = M_1(t)$$

$$N_W(t) = N_1(t) + N_2$$

Angle of Wave Approach and Frequency of Encounter

For a ship moving with forward speed U, the wave frequency ω will be modified according to frequency of encounter ω_e:

$$\omega_e = \omega(1 - \omega/gU\cos\chi) ,$$

where $\chi = \psi_{WV} - \psi$ is angle of wave approach, $\chi = 0$ corresponds to head sea, $\chi = \pm 90$ corresponds to beam sea, $\chi = 180$ corresponds to following sea.

1st Order Wave Forces and Moments

When calculating 1st order wave forces and moments, we use the generalized, non-dimensional reduction coefficients $\kappa_i(\omega_i, \chi_i)$ which are functions of vessel draft (Smith effect), wave length /ship length ratio (wave distribution along the hull), angle of wave approach. Typically $\kappa_i(\omega_i, \chi_i)$ is less than 1, see Fig 38.

Sway wave force is:

$$Y_1(t) = \sum_{i=1}^{N} \kappa_{iy}(\omega_i, \chi_i) mg \frac{\partial \zeta_i(x,y,t)}{\partial l_i} ,$$

where l_i is direction of i harmonic propagation, χ_i is angle of i wave component approach, κ_{iy} is reduction coefficient, $s_i(x,y,t) = \frac{\partial \zeta_i(x,y,t)}{\partial l_i}$ is wave slope angle of i-component.
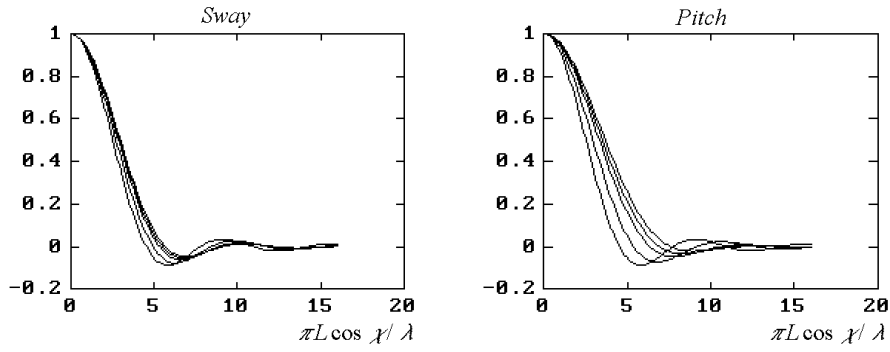
Fig 38. The generalized reduction coefficients in surge and pitch

versus ship length/wave length ratio

2nd Order Wave Forces and Moments

2nd order wave forces and moments are constant forces depending on angle of wave approach, wave height and ship speed.

$$X_2(t) = I_X(\chi, H_{1/3})\rho g L H_{1/3}^2 + \Delta X(U, \chi, H_{1/3})3$$

$$Y_2(t) = I_Y(\chi, H_{1/3})\rho g L H_{1/3}^2$$

$$N_2(t) = I_N(\chi, H_{1/3})\rho g L^2 H_{1/3}^2,$$

where $I_{X,Y,N}(\chi, H_{1/3})$ are non-dimensional coefficients depending on ship dimensions, $\Delta X(V, \chi, H_{1/3})$ is additional resistance at rough sea.

Results of Ship Motion Simulation

Ship yawing simulation and sea trials results are shown in Fig 39–Fig 41.

Conditions:

- River-sea ship, displacement: 3510 t (see photo in Fig 39);
- Speed: 10 knots;
- Initial ship heading: 255 degrees;
- Wave direction: 120 degrees;
- Significant wave height: about 0.5 m;
- Autopilot is turned on.

Yaw rate implementation (fragment) is shown in Fig 40. Yaw rate spectrum is shown in Fig 41.

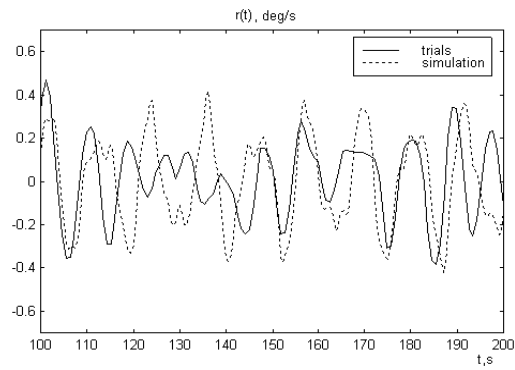*Fig 39. Photo of river-sea ship in waves*

Fig 40.   Yaw rate (fragment). Simulation and trials result
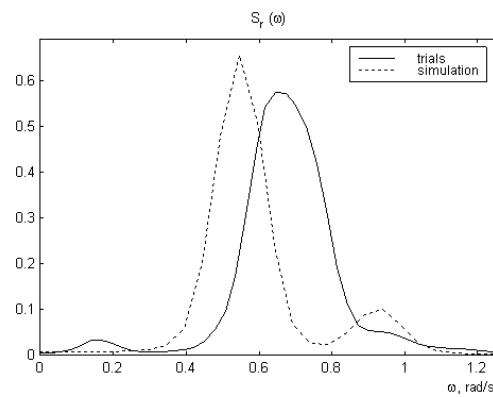
Fig 41.   Spectrum of yaw rate. Simulation and trials result

Ship rolling and pitching simulation and sea trials results are shown in Fig 42–Fig 46.

Conditions:

• Offshore supply vessel, displacement: 2200 t (see photo in Fig 42);

• Speed: 5 knots;

• Initial ship heading: 90 degrees;

• Wave direction: 120 degrees;

• Significant wave height: about 1.7 m;

• Autopilot is turned on.

Pitch angle implementation (fragment) is shown in Fig 43. Pitch angle spectrum is shown in Fig 44.

Roll angle implementation (fragment) is shown in Fig 45. Roll angle spectrum is shown in Fig 46.

Fig 42. Offshore supply vessel

Fig 43. Pitch angle implementation (fragment). Simulation and trials result

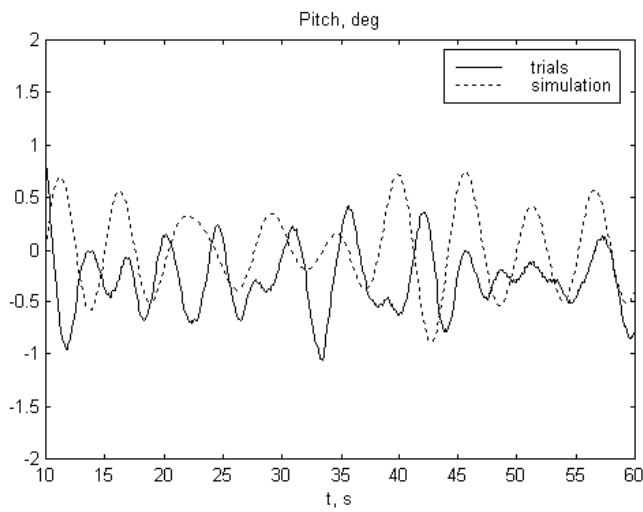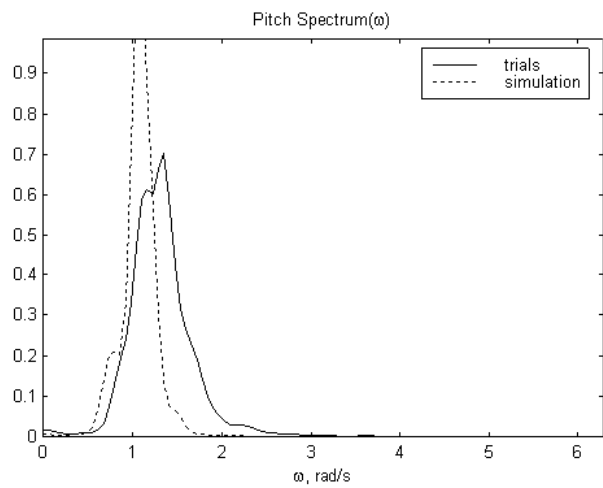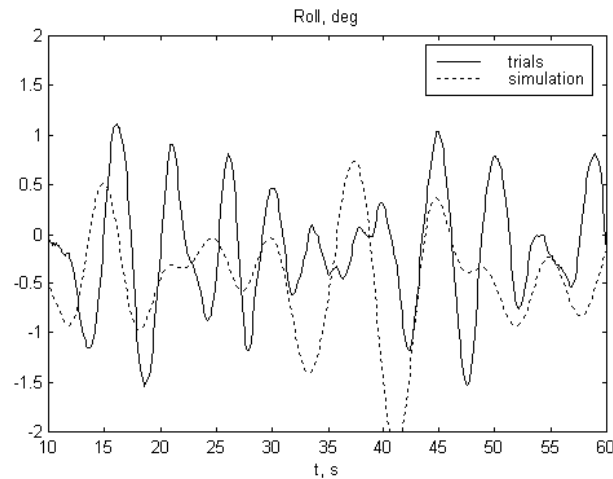*Fig 44. Pitch angle spectrum. Simulation and trials result*

Fig 45. Roll angle implementation (fragment). Simulation and trials result
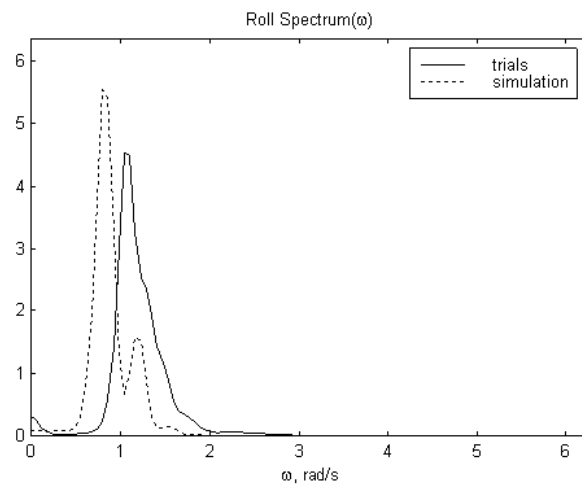
Fig 46. Roll angle spectrum. Simulation and trials result

Slamming, Surface Broach and Turnover

In addition to the existing mathematical model of the ship roll/pitch, being developed are some additional components of disturbing forces and moments, enabling modeling of slamming, surface broaching and actual capsizing on the waves.

Effects of Waves on Propeller and Rudder Operations

Additional loads on rudder and propeller due to waves will be included in the new Transas model. The model will predict variable periodical propeller loads which affect the main engine operation and steering.

Effect of Technical and Natural Obstacles on Wind and Wave Disturbances

When estimating the effect of wind and sea on the ship, it is important to consider the shadow zones from various technical and natural objects (shore, harbour facilities, other ships, etc.). This effect is particularly important during the mooring of the ship and sailing in rough weather, whilst cross-winds are a source of considerable concern for container ship operations.

SEA TRIALS

<u>Principal Goals of Sea Trials:</u>

The present-day requirements to the mathematical models of the controlled ship motion developed for the manoeuvring simulator, have called for the soft- and hardware facility, which would allow obtaining high-accuracy results of the ships' seaworthiness and manoeuvring trials.

The obtained data is used for checking the adequacy and improving the quality of the developed mathematical ship motion models.

<u>Examples of ships sea trials:</u>

The results of trials involving a sea-river ship (North and Baltic Sea, 1997) can serve as an example of vessels' sea trials. The ship has the following principal characteristics: displacement – 3510 t, length – 95 m, breadth – 13 m, draft – 3.7 m, power plant output – 2x640 KWt, speed – 11.1 knots.

Fig 47. Sea-river ship
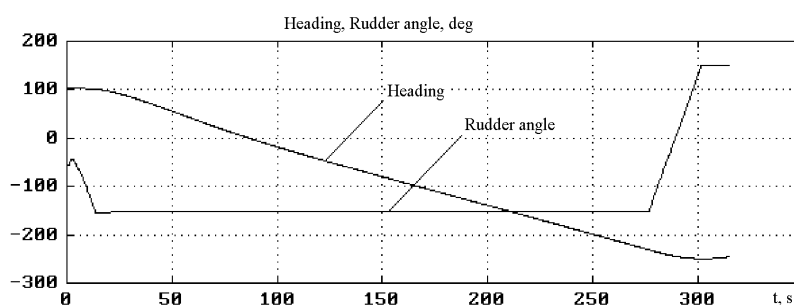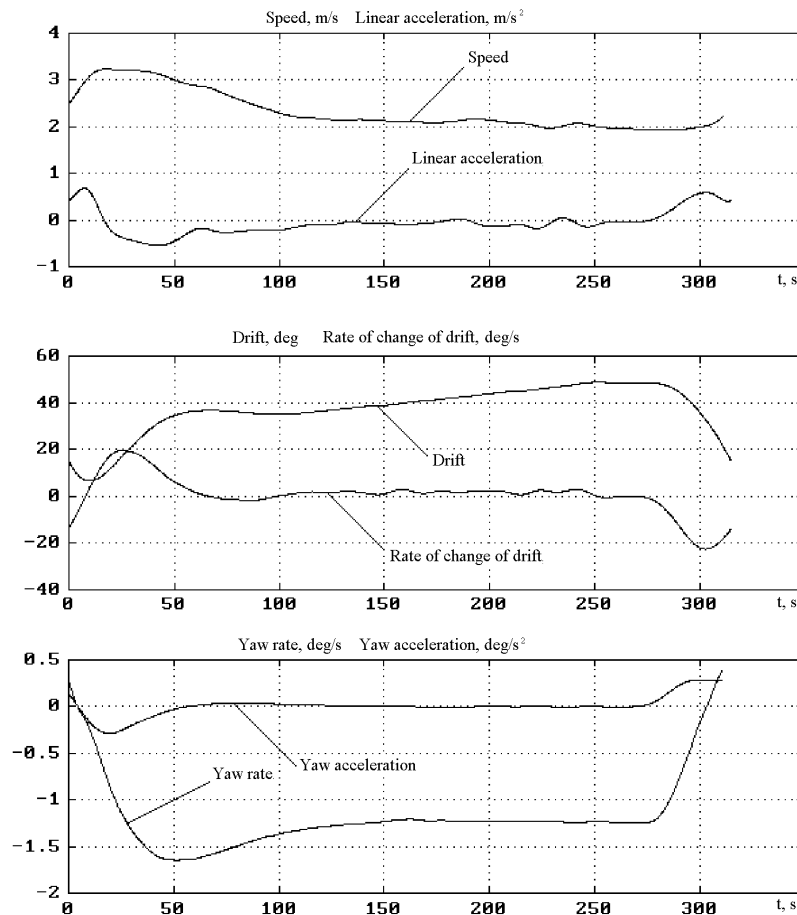
Fig 48. Change of the ship's motion parameters ("STB 30° Turning Circle" Manoeuver)

Note: The value of the rudder angle is increased 5 times; of the motion speed derivative – 10 times, derivative of the drift angle and rate of turn – 5 times.

The ship's seaworthiness and manoeuvring trials were held. During the trials, the following manoeuvres were recorded:

• ship's motion on the rough sea under the control of the helmsman (at various wave encounter angle values);

• ship's motion on the rough sea under the control of the autopilot;

• inertia and reversing characteristics;

• turning circles, zigzags, spiral;

• ship's motion under the thrusters effect.

The results of processing of "STB 30° Turn" and "Full Ahead-Full Astern" manoeuvre recordings are provided as examples.
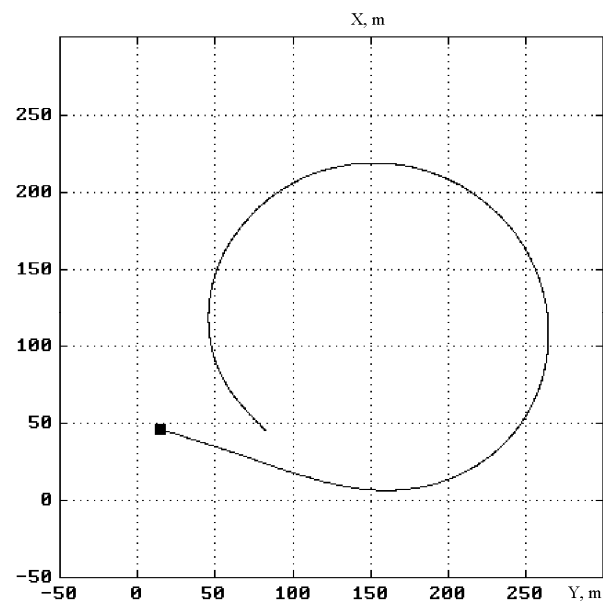
Fig 49. Ship track («STB 30° Turn» manoeuvre)
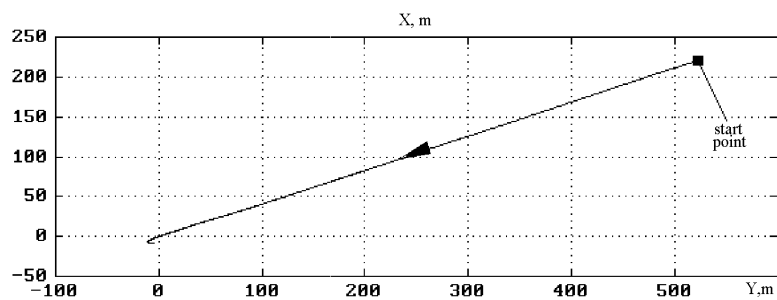
Fig 50. Ship track ("Full Ahead-Full Astern Reversing" manoeuvre)
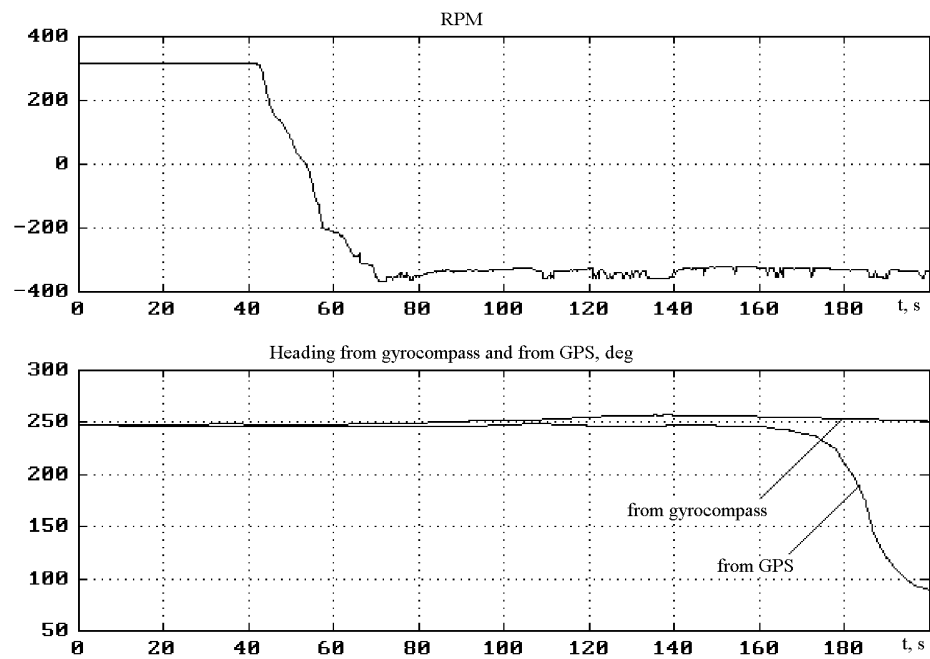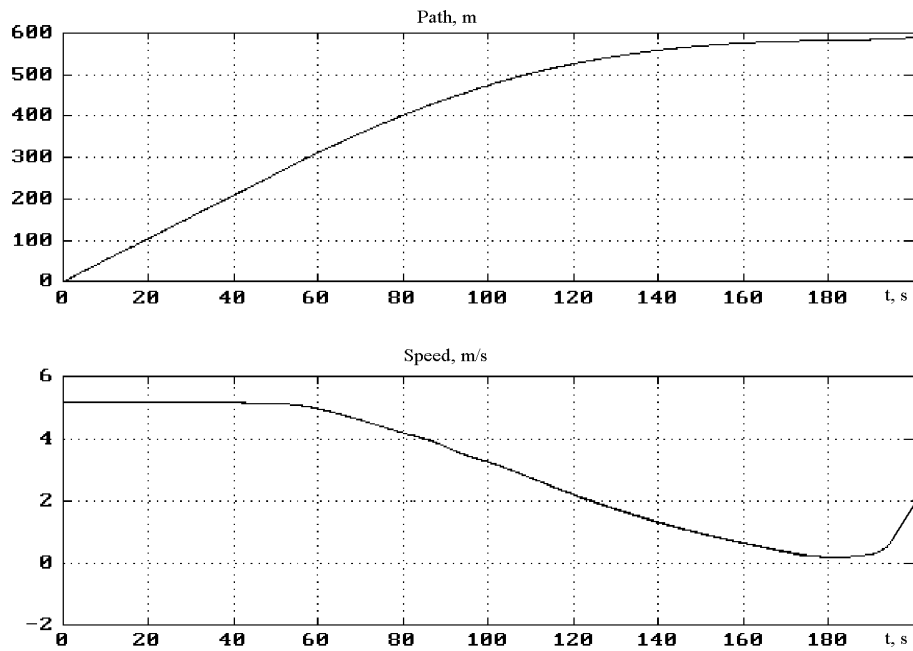
Fig 51. *Change of the ship motion parameters*

("Full Ahead-Full Astern Reversing" manoeuvre)

The mathematical model of the ship should be corrected to take into account the results of the completed seaworthiness and manoeuvring trials. Specifically, manoeuvring trials showed that the ship has an unstable diagram of controllability, and this is taken into account during the model adjustment. Fig 52 a) shows a ship's diagram of controllability before the correction of the model, whilst Fig 52 b) shows the results of processing of "Spiral" manoeuvre recording and the mathematical model's diagram of controllability re-adjusted accordingly.
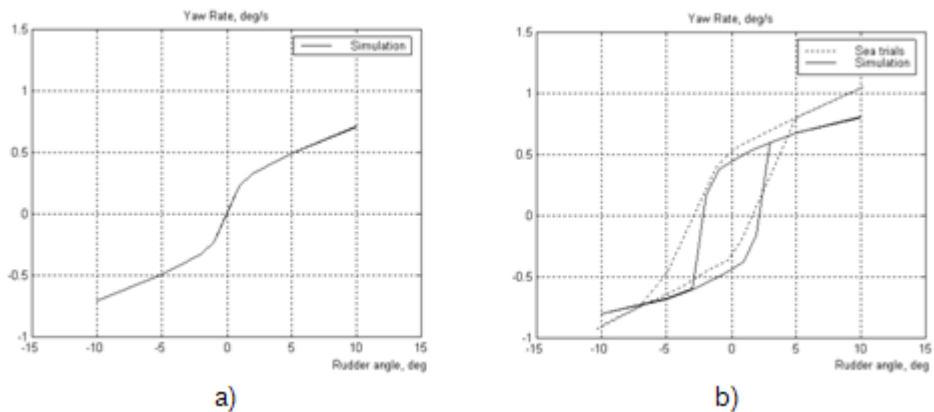
Fig 52. *Sea-river ship's diagram of controllability*

In the last few years sea trials of more than five ships have been conducted.

The seaworthiness and manoeuvring trials of the next ship are scheduled for summer 2001.

SHALLOW WATER EFFECT

General Description of Shallow Water Effect

The shallow water effect manifests itself typically in the increasing of inertia and damping hydrodynamic forces of the hull, changes in the propeller and rudder operation parameters and their interaction with the vessel's hull. Besides, propulsion in shallow water gives rise to forces acting in a vertical plane and bringing about considerable changes in the vessel's stability and trim. Shallow water also causes significant changes in the vessel's roll/pitch parameters.

The effect of reduced underwater clearance manifests itself most noticeably by the ratio of water depth h to vessel's draft T, e.g., $\bar{h} = \dfrac{h}{T}$ is less than 2. The degree of the shallow water effect depends on the vessel's relative speed through the depth Froude number in $Fn_h = \dfrac{V}{\sqrt{gh}}$, where V is ship speed, g - is gravity acceleration.

For Froude number, Fn_h, of more than 0.3, the effect of the hydrodynamic forces and squat is significant. The shallow water effect, change of trim and stability and other related phenomena increase dramatically after Froude number Fn_h of 0.8 and reach the maximum at Froude number, Fn_h around 1.0 which corresponds to the "critical" speed $V_{cr} = \sqrt{gh}$.

Effect of Shallow Water on Hull's Hydrodynamic Forces

The effect of shallow water on hydrodynamic coefficients C_{XH}, C_{YHp}, C_{YHd}, C_{NHp}, C_{NHd} manifests itself in a considerable increase of the separation force components and a change in the wave formation pattern. It can be taken into account by means of appropriate coefficients, obtained experimentally with regard to the degree of water shallowness as a function of $\bar{h}$.

The change of hydrodynamic coefficients will be taken into account through the input of correction coefficients $k_{XH}^{\bar{h}}$, $k_{YHp}^{\bar{h}}$, $k_{YHd}^{\bar{h}}$, $k_{NHp}^{\bar{h}}$ and $k_{NHd}^{\bar{h}}$.

The resulting hydrodynamic hull coefficients are determined by the following simple dependencies:

$$C_{XH} = C_{XH}^{\infty} k_{XHp}^{\bar{h}} ;$$

$$C_{YHp} = C_{YHp}^{\infty} k_{YHp}^{\bar{h}} ;$$

$$C_{YHd} = C_{YHd}^{\infty} k_{YHd}^{\bar{h}} ;$$

$$C_{NHp} = C_{NHp}^{\infty} k_{NHp}^{\bar{h}} ;$$

$$C_{NHd} = C_{NHd}^{\infty} k_{NHd}^{\bar{h}}$$

As an example, Fig 53 shows shallow water correction coefficients $k_{YHp}^{\bar{h}}$ and $k_{NHp}^{\bar{h}}$ on the lateral force and turning moment for moderate Froude numbers.

Hull sway/yaw shallow water coefficients
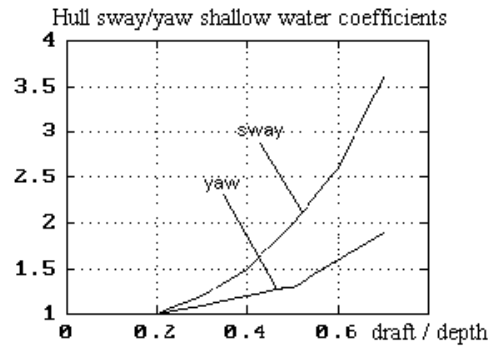
Fig 53. Shallow water effect on lateral force coefficients $k_{YHp}^{\bar{h}}$

and yaw moment coefficients $k_{NHp}^{\bar{h}}$

Shellow water coefficients on added masses
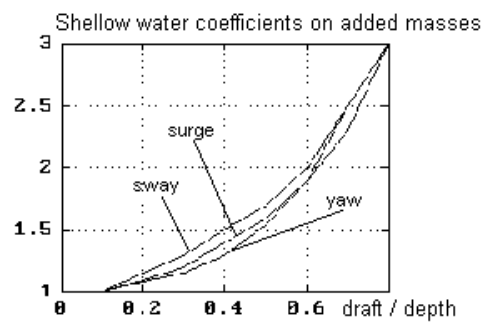
Fig 54. Shallow water coefficients effect on added masses in surge sway and yaw

The effect of shallow water on the vessel added masses $-X_{\dot{u}}$, $-Y_{\dot{v}}$ and $-N_{\dot{r}}$ (surge, sway and yaw respectively) is determined by $k_{X_{\dot{u}}}^{\bar{h}}$, $k_{Y_{\dot{v}}}^{\bar{h}}$, $k_{N_{\dot{r}}}^{\bar{h}}$ coefficients, which are functions of draft/depth ratio $\bar{h}$ and hull block coefficients C_B.

The resulting added masses in shallow water conditions are determined by a multiplication of the deep water values and corresponding shallow water coefficients, e.g. $X_{\dot{u}} = X_{\dot{u}}^{\infty}\ k_{X_{\dot{u}}}^{\bar{h}}$, $Y_{\dot{v}} = Y_{\dot{v}}^{\infty}\ k_{Y_{\dot{v}}}^{\bar{h}}$ and $N_{\dot{r}} = N_{\dot{r}}^{\infty} k_{N_{\dot{r}}}^{\bar{h}}$.

Shallow water correction coefficients on added masses in surge, sway and yaw for 77,000-ton displacement tankers are shown in Fig 54.

Effect of Shallow Water on Propeller Hydrodynamic Forces

Changes in the propeller's hydrodynamic forces (thrust and torque) on the shallow water are taken into account indirectly via the change of the wake coefficient $W = W^\infty (1 + k_W^{\bar{h}})$ and thrust deduction coefficient $\bar{t} = \bar{t}^\infty (1 + k_{\bar{t}}^{\bar{h}})$ depending on the degree of water shallowness $\bar{h}$.
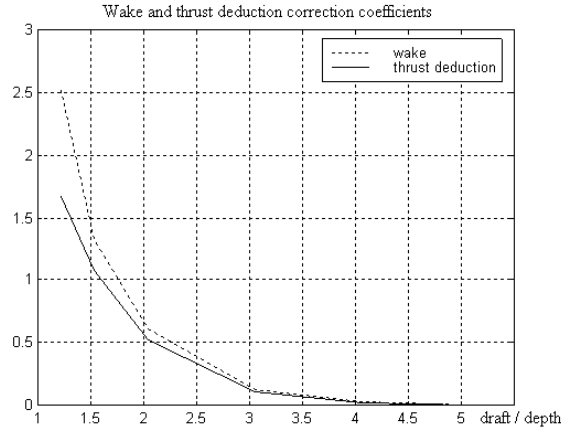
Fig 55. Shallow water effect on wake and thrust deduction

(ship middle draft is 9.8 m)

Effect of Shallow Water on Rudder Hydrodynamic Forces

The effect of shallow water on the rudder's non-dimensional hydrodynamic characteristics: surge, sway and yaw (C_{XR}, C_{YR}, C_{NR}) is calculated by applying the rudder shallow water correction $k_{xr}^{\bar{h}}$, $k_{YR}^{\bar{h}}$, $k_{NR}^{\bar{h}}$ coefficients which are also a function of water depth/draft ratio $\bar{h}$. The rudders operating in the propeller race are indirectly affected by the propeller wake and thrust coefficients (see above). Fig 56 shows the dependence of $k_{YR}^{\bar{h}}$ on the shallow water.
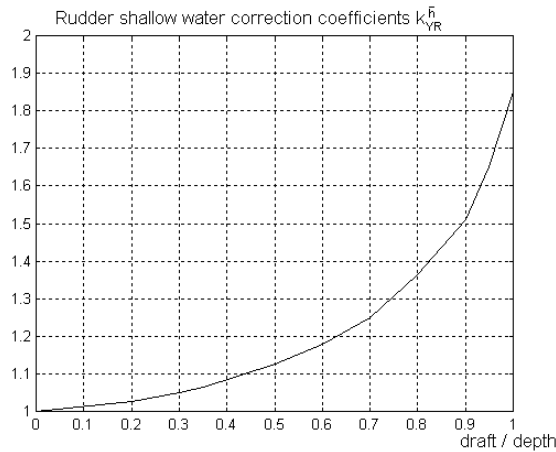
Fig 56. Shallow water effect on rudder lateral force

Effect of Shallow Water on Manoeuvring Characteristics

The shallow water effect will change steering, manoeuvring and stability parameters, compared with those in deep water conditions. Fig 57 illustrates the change in steering diagram (non-dimensional yaw rate $r' = \dfrac{rL}{u'}$, versus rudder angle spiral test) for the river-sea ship in different depth conditions. Four steering diagrams are shown: for deep water and for relative depth $\bar{h}$ 2.0 and 1.2.
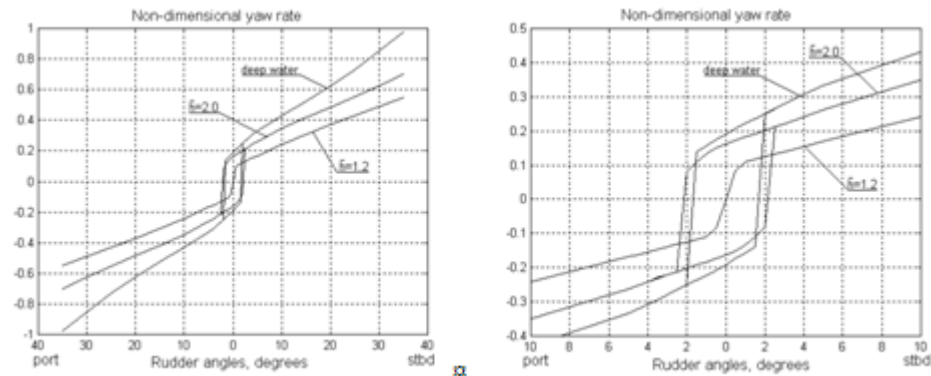
Fig 57. Ship steering diagrams spiral test curve at different depth values

Shallow Water Effect on Ship's Sinkage and Trim, Squat Phenomenon

When the ship operates on shallow water there is an increase in the speeds of liquid particles in the region between the ship bottom and the seabed (Fig 58), which results to decreasing in the pressure under the ship bottom and hull sinkage (increase of ship draft).
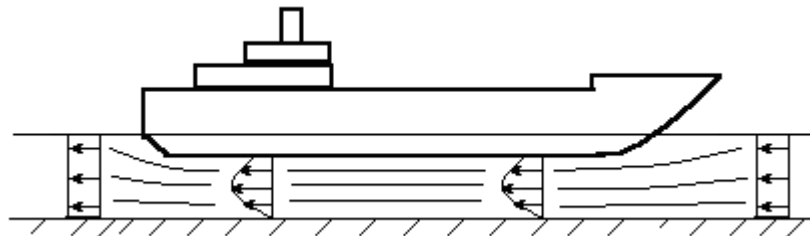
Fig 58. Distribution of speeds in the region between the ship bottom and the seabed

In this case the redistribution of hydrodynamic pressures along the ship hull occurs (Fig 59).
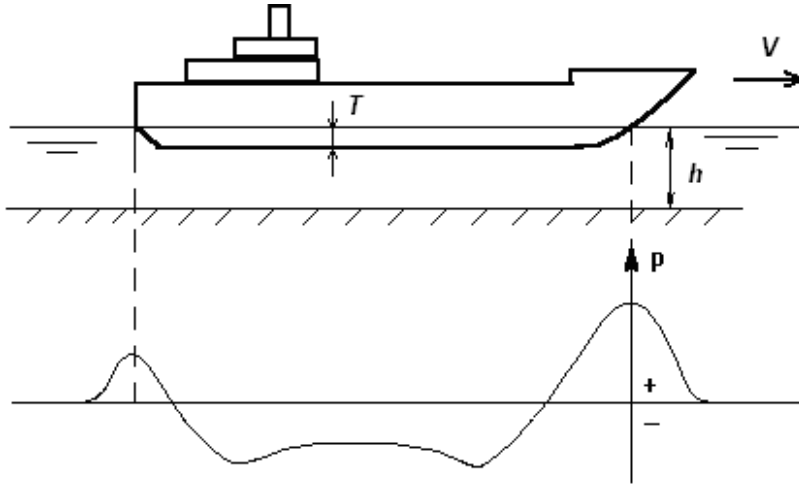
Fig 59. Distribution of hydrodynamic pressures along the ship hull during

the motion on the shallow water

As a result of the asymmetry of pressure field along the ship hull the sinkage accompanies with a change in the trim. The combination of vertical movement (sinkage) and rotation movement (trim angle) is referred to as squat phenomenon.

The effect of shallow water on the ship's sinkage and trim is determined on the basis of regular model testing results conducted in a wide range of speeds for the representative ship hull.

Sinkage and dynamic trim are functions of the initial trim, depth/draft ratio $\bar{h}$, depth

Froude number Fn_h , block coefficient C_B and length/beam ratio $\dfrac{L}{B}$. Fig 60 shows

a typical variation at the forward and aft drafts as function of the depth Froude number Fn_h and depth/draft ratio $\bar{h}$.
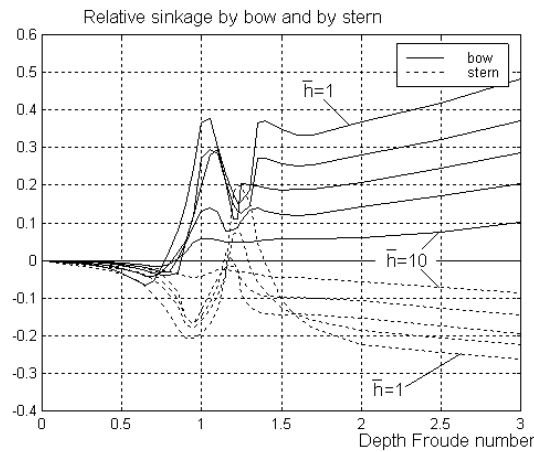
Fig 60. Relative sinkage by the bow and by the stern in shallow water

The results of sea trials and model tests show that the most of fine ships without bow bulb moving on shallow water sink with bow up while the ships with full form and block coefficient value $C_B \geq 0.8$ sink more by bow than by the stern.

MODELLING SHIPS OPERATION IN ICE-COVERED WATER

General Description

The simulator reproduces ships operation in ice-covered water. To enable this, procedures for entering ice-covered zones in the gaming area are provided. The mathematical ship model receives information on ice parameters and arrangement. The detection of a ship-contact-with-ice event actuates the mechanism of determining the ice force impact on the ship. These ice effects are summed with other force components of the mathematical ship model. This ensures manifestation of special features of the ship's behavior in ice-covered waters and a response to the excessive loads on the ship hull and on the propulsion units

Ice arrangement and Parameters

The outlines of areas occupied with ice are set with an aggregate of polygons, ice parameters designated in each of them. These outlines remain stationary and are not subject to the effect of currents, wind or waves.

There is a capability to use broken ice of various types, solid unbroken ice and ice in the channel formed by the ship while moving through the solid unbroken ice. For the broken ice parameters, the thickness (considered to be constant) and compacting are taken. Thickness is taken to be the parameters of unbroken flow ice (ice field). Parameters of ice in the channel are: ice consolidation, closure, freeze-up and accretion degree.

Mathematical Ship Model Ice Class

The mathematical ship model can be assigned with an ice class which permissible ice loads are set with regard to, and which the response to them when exceeded depends on.

Ice Impacts

The quasi-static approach is used, i.e., taken into account are those averaged ice impacts effects which correspond to the instant values of the ship kinematic parameters and set ice parameters.

The starting point for calculating ice impacts on the ship is the assumption that they are applied in the ship hull contact-with-ice areas which are determined from the geometric considerations. Several such areas can be singled out for the arbitrary ship motion in the horizontal plane (see Fig 61). They are all considered to be within the ice thickness and coincident with the ship hull plating.
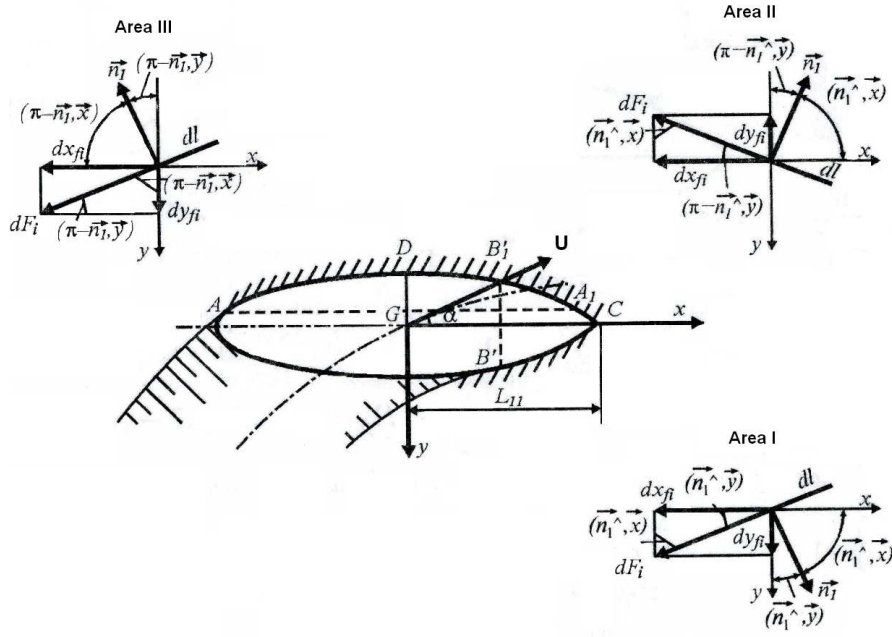
Fig 61. Ship hull contact-with-ice areas

It is assumed that with the ice parameter constancy, the elementary (linear) ice impact within the contact area depends on the direction of the normal to the ship plating unit in its centre, the current speed of the plating unit and ice relative motion, the effective hull half-breadth B_{ef} in the place where the contact area element is located. The determining of this effective half-breadth is shown in Fig 62.
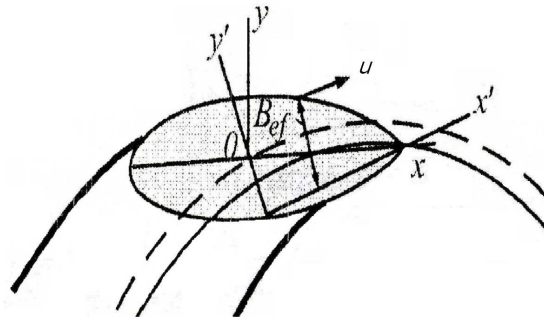
Fig 62. Effective hull half-breadth determination

This approach allows the two-dimensional ice impact during the ship sailing in the broken ice to be presented as follows.

$$X_{ICE} = F * Kx * \cos\beta,$$

$$Y_{ICE} = F * Ky * \sin\beta,$$

$$N_{ICE} = Concentration^{pc} * Thickness^{pt} * \frac{\rho_{ice}}{2} * L^4 * r^2 * Kn,$$

where $F = Kf\left(Thickness, Concentration\right) * \rho_{ice} * U^2 * L * Thickness * Fn^{fnp}$,

X_{ICE} – longitudinal ice force,

Y_{ICE} – lateral ice force,

N_{ICE} – yawing ice moment,

Kx, Ky, Kf, Kn - force and moment dimensional coefficients; tabular and empirical dependencies taking into account the field and test tank testing in the ice research,

Fn – Froude number,

frp, pt, pc – power exponents reflecting certain experience,

L – ship length along the waterline,

β – drift angle at the ship centre of gravity,

r – ship rate of turn,

U – ship centre-of-gravity speed,

ρ_{ice} – ice compactness.

During the sailing in the floe ice where the impacts are exceedingly sensitive to the particulars of the ship's shape, determine the possibility of breaking into the ice, for exiting from the ice channel in particular, dependencies are presented as follows.

– Normal horizontal impact on the contact area element:

$$dFn = dL * Un^{nu} * Fnu * \rho_{ice} * Thickness^{nt} ,$$

where dL – element length; Un – normal speed of the contact area element and ice relative motion; Fnu – coefficient taking into account the field experience testing; nv, nt – power exponent taking into account the field and text tank testing.

– Tangent horizontal impact on the contact area element:

$$dFt = dFn * Kfric ,$$

where $Kfric$ – empirical friction coefficient depending on the contact area element location on the ship.

In the course of modelling, the ship-and-ice contact area is checked on each time step, and the elementary ice impact within this area are integrated and re-calculated to the origin of the body-based frame of reference.

HYDRODYNAMIC INTERACTION BETWEEN THE SHIP AND WATERWAY BOUNDARIES

Typically a channel bottom and walls have various irregularities, such as way boundaries, under water shoals, jetties, channel walls and traffic ships. The pressure field induced by these irregularities models effects of these factors. For a running vessel the field parameters are governed by the underwater hull geometry, depth under the keel, propulsion and bow thruster performance and the current.

An example of pressure field induced by a river-sea ship running straight ahead is shown in Fig 63. Positive pressure forward and aft, low pressure zone amidships, as well as the effect of rotating propeller in the aft zone realistically reflect the pressure field of the propeller driven vessel.
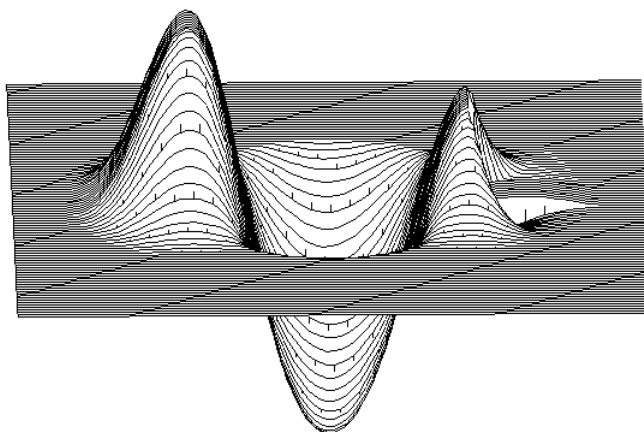

Fig 63. The example of pressure field induced by a river-sea ship

The mathematical model of the ship motion calculates changes in the pressure field and resulting hydrodynamic forces induced by factors listed above. Interaction forces and moments are determined as integral characteristics of the resulting pressure distribution along the hull surface. Hydrodynamic forces due to the ship's interaction with the channel are calculated numerically and validated by the model experiments.

Effects of the Channel and Jetty Boundaries

The effect of the channel or piers is estimated by additional forces X_{PR}, Y_{PR} and moments N_{PR} calculated as hydrodynamic components of a vector of forces and moments affecting the vessel. The effect of the wall or channel on the inertia forces is also modeled. The principal parameters in ship/channel interaction are beam/draft and length beam ratios, distance between the vessel centreplate sides and channel boundaries, defined as y_{ch} and e_{ch} distances in Fig 64, an angle between the vessel's centreline plane and the line of the wall, vessel's speed U and rate of turn r, as well as the channel's width B_{ch} and depth h, channel wall slope α_{ch}.

The effect of these parameters on the vessel hydrodynamic forces is calculated on the basis of analysis of various model testing result.
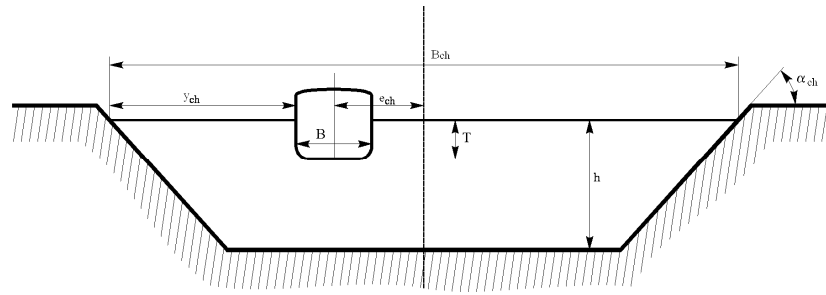
Fig 64. Main geometric parameters determining ship motion in the channel

As an example, Fig 65 shows the dependence of the coefficient of the transverse force on the vessel's hull during the motion in a channel, on the relative distance from the wall on the ship beam S/B and the relative width of the channel to the ship beam $B_{channel}/B$ for the specific depth/draft ratio equal 1.4.
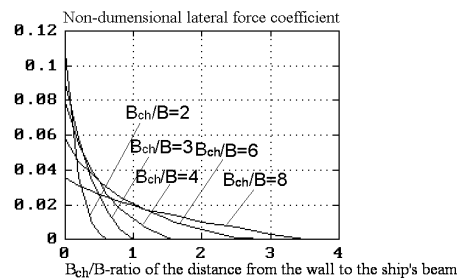
Fig 65. Channel effect on lateral force

Short Banks Effect and Its Modeling

In the interaction with the piers, the ship hydrodynamic force and moment are functions the distance between the piers and the vessel's gravity centre defined as distance y_{pr} on Fig 67, distance between the piers and the tangent to the vessel's hull contour parallel to the wall line defined as e_{pr} on Fig 67, angle between the vessel's centreline plane and wall line γ_{pr}, water depth h and ship motion parameters, such as yaw rate r and ship speed U.

The ship hydrodynamic forces to the short bank or pier are derived from the results of the regular model testing in a wide range of bank and ship types. A relative increase of the lateral force coefficient in the presence of a short bank and restricted depth as compared to the deep-water conditions for a pure motion is shown on Fig 66. The increase of the lateral force is shown here as a function of draft/depth ratio T/h for several distances from the bank.
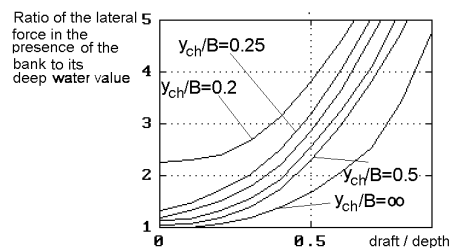
Fig 66. Increase of the lateral force due to the shallow water and bank effect
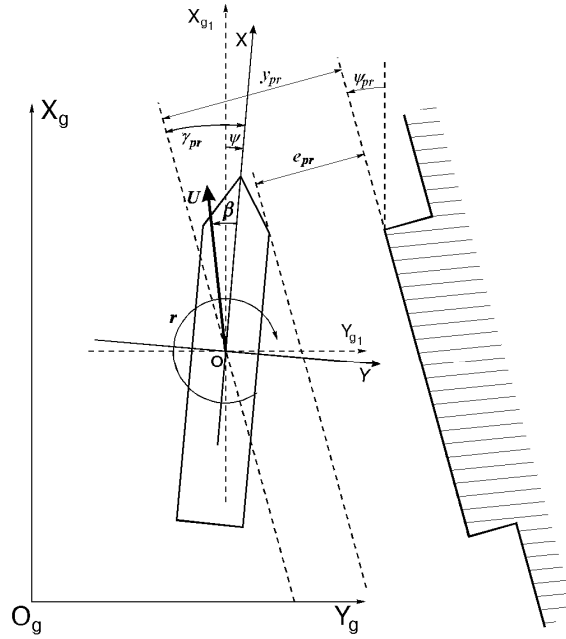
Fig 67. Definitions in modelling of the effects of short banks or piers

Effect of the Vertical Wall on Thrusters Performance

The thruster's efficiency will vary with the vessel approaching the pier because of the thruster jet interaction with the wall (Fig 68). This interaction is governed by the relative distance e_{thr} / D_{thr} between the thrusters outlet and the piers (in this context e is a distance to the pier, D_{thr} is the inner diameter of the thrusters tunnel).
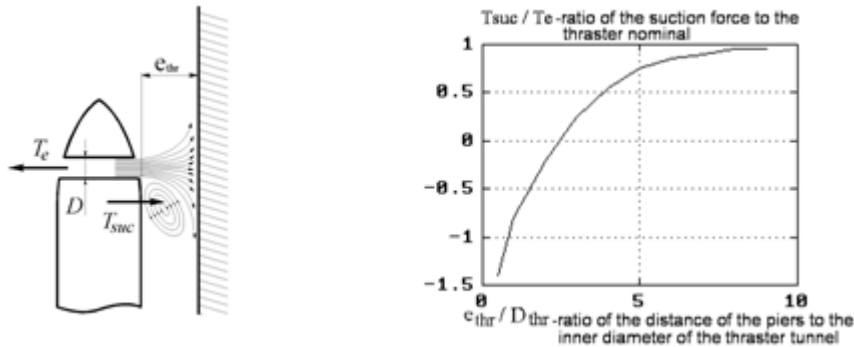
Fig 68. Thruster interaction with the pier

A reduced pressure from the thruster jet generates the suction force T_{suc} acting in the direction opposite to the thruster traction. This force increases as the vessel is approaching the pier and may exceed the thruster rated T_e shown in the left-hand side of Fig 68 as a ratio of T_{suc} / T_e versus e / D_{thr}. There is an additional hydrodynamic force pulling to piers when the vessel is moving astern at the berth, due to the propeller wake between the hull and the pier.

The ship motion modeling calculates this hydrodynamic component (lateral force and yaw moment) on the basis of the regular test data involving a large model and operating propellers.

Effect of the Inclined Bottom (Sloping Bank)

The slope of a sea bed will give a rise to an additional hydrodynamic lateral force and a moment typically turning a ship bow towards "free water" side.
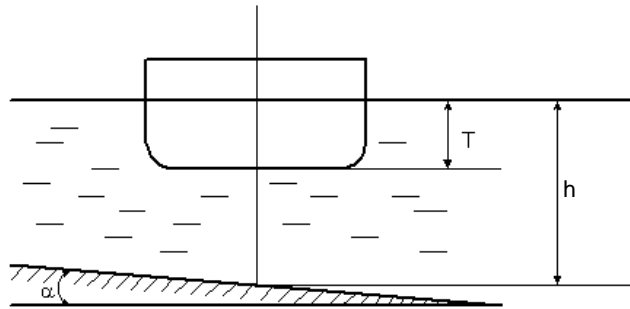
Fig 69. Ship over inclined sea bottom

The hydrodynamic forces on a ship near the sloping bank are determined by the hull particulars, relative depth, speed (Froude number at given depth) and slope angle. Even for small slopes of 5-6 degrees the values of turning forces and moments are rather larger, and therefore often it is quite difficult to keep the ship on course parallel to the water edge. Fig 70 illustrates the relation of the rudder angle, needed to keep the ship on a straight course when running over inclined bottom parallel to the bank as a function of water depth/draft ratio. The relation is predicted for the river-sea ship and is in a good agreement with the full-scale trial measurements.
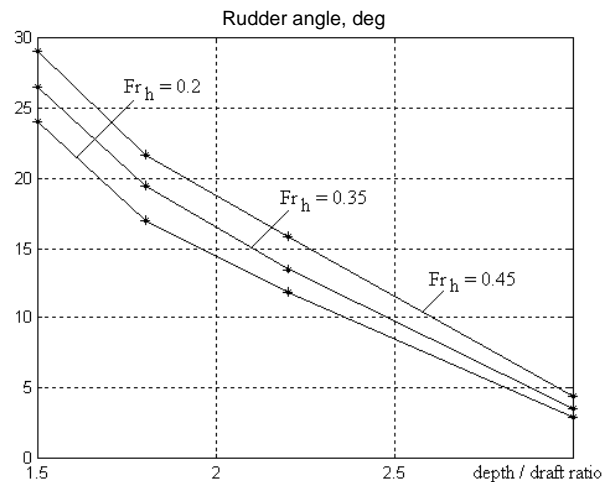
Fig 70. The rudder angle needed to keep the ship on a straight course parallel

to the bank with the inclined bottom

Ship-to-Ship Interaction Effect and Its Modeling

Forces and moment of the vessels' hydrodynamic interaction are determined in the Cartesian body-fixed frame as shown in Fig 71, with distances x_{int} and y_{int} characterizing relative positions of the vessels. The passing vessel is marked with prime, (accent) symbols.

Ship-to-ship interaction hydrodynamic forces on the own and passing vessels are modeled on the basis of formulas obtained from systematic tests.
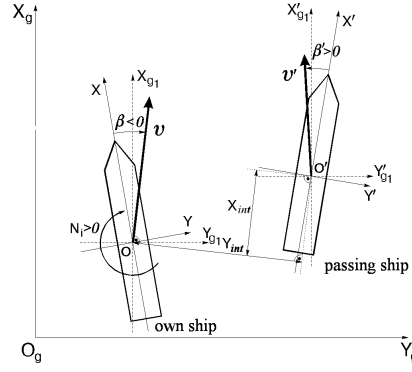
Fig 71. Definitions in ship-to-ship interaction modeling

Ship-to-ship interaction equations take into account the changes in the hull flow-around conditions due to the constrained stream between the partner vessels, the vessels' wave systems overlaying each other's shallow water effect. The modeling is done for the cases of passing, head-on encounter, overtaking, and includes interaction of the oncoming vessels and effect of the passing vessel on the unmoving vessel.

The general expressions for the longitudinal and transverse components of the interaction force and turning moment are as follows:

$$X_{INT} = C_{XINT}\left(Fn, (y_{\text{int}} - 0.5B - 0.5B')/(0.5B), \frac{2x_{\text{int}}}{L'}, \psi, \psi', \beta, \beta', \frac{H}{T}, \frac{V'}{V}, \frac{L'}{L}, \frac{B'}{B}, \frac{T'}{L'} \right) \frac{\rho U^2}{2} LT;$$

$$Y_{INT} = C_{YINT}\left(Fn, (y_{\text{int}} - 0.5B - 0.5B')/(0.5B), \frac{2x_{\text{int}}}{L'}, \psi, \psi', \beta, \beta', \frac{H}{T}, \frac{V'}{V}, \frac{L'}{L}, \frac{B'}{B}, \frac{T'}{L'} \right) \frac{\rho U^2}{2} LT;$$

$$N_{INT} = C_{NINT}\left(Fn, (y_{\text{int}} - 0.5B - 0.5B')/(0.5B), \frac{2x_{\text{int}}}{L'}, \psi, \psi', \beta, \beta', \frac{H}{T}, \frac{V'}{V}, \frac{L'}{L}, \frac{B'}{B}, \frac{T'}{L'} \right) \frac{\rho U^2}{2} L^2 T;$$

Predictions of the turning moments on small and large vessels shown in Fig 72 are in good agreement with the test results.

Fig 72. Ship-to-ship interaction turning moments (collision avoidance manoeuvre

of vessels on reciprocal courses) on a small and large vessel in head-on encounter

MOORING WALLS

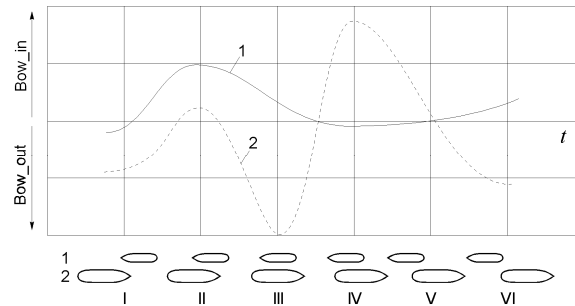## Specific Features of the Ship's Motion Close to the Mooring Wall

As the ship is moving close to a solid vertical wall, the ship's motion parameters change. Some additional forces and moments originated by interaction between the ship and the wall arise on the ship hull (Fig 73).

Specific features of the ship's motion under such conditions consist in the following:

- As the ship is moving parallel to the vertical wall with a zero or small positive drift angle (the ship's bow is farther from the wall than the stern), the speed of the water passing between the ship and the wall will grow due to the local constraint of the stream, the pressure will drop down. As a result, developed on the ship are a transverse force directed to the wall and a moment working to swing the ship's bow from the wall ("free water effect"). The centre of hydrodynamic forces pressure is in the ship's stern most point.

- As the ship is proceeding along the wall with a large positive drift angle, the nature of the flow around the ship hull changes. The speed of the stream in the area between the ship hull and the wall gets smaller that the speed of the ship, and the pressure in this area becomes positive. The transverse force reverses the sign changing its direction to that from the wall, whilst its point of application moves to the foremost position of the ship. The moment, therefore, retains its direction causing the "free water effect" as before.

The mooring wall effect is taken into account in the mathematical model of the ship's motion on the basis of information on the distance from the ship's bow and the ship's stern to the nearest point of the mooring wall, on the ship's motion kinematic parameters. In the ship modeling, the effect of the wall on the ship's motion is normally started to be taken into account when the distance between the ship and the wall is less than four hull breadths.

Description of the Ship/Mooring Wall Interaction Mathematical Model

The mathematical model of the ship/mooring wall interaction takes into account forces and moments acting horizontally (longitudinal and transverse forces, yawing moment).

Equations for the calculations of forces have the following form:

$$X_{pr} = k_{1Fn}(0.5v^2 a_{22\,pr} \cos\alpha - a_{11\,pr}(0.5u^2 \cos\alpha + uv\sin\alpha));$$

$$Y_{pr} = k_{2Fn}(0.5u^2 a_{11\,pr} \sin\alpha - a_{22\,pr}(0.5v^2 \sin\alpha + uv\cos\alpha));$$

$$N_{pr} = k_{3Fn}\left(0.5r^2 a_{33\,pr} + \left(1 - \frac{1}{m_{1pr}}\right)(\lambda_{11} - \lambda_{22})uv\right),$$

where u, v, r are longitudinal, transverse and angular velocities in the fluid axes reference system;

α – is angle between the ship centerline plane and the wall;

$$a_{11\,pr} = f(\lambda_{11}, L_{oa}, B_{oa}, b), \ a_{22\,pr} = f(\lambda_{22}, L_{oa}, B_{ao}, b), \ a_{33\,pr} = f(\lambda_{66}, L_{oa}, B_{oa}, b)$$

are coefficients depending on the added ship masses, length and breadth of the hull and the distance from the ship to the wall;

λ_{11}, λ_{22}, λ_{66} are added ship masses;

coefficients k_{1Fn}, k_{2Fn}, k_{3Fn} depend on the ship's Froude number.
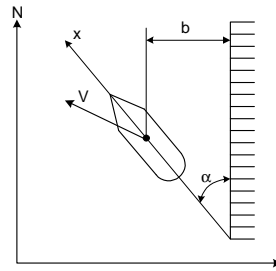
Fig 73. Ship's motion at the mooring wall

Results of Principal Effects Modeling

By way of example of the ship/mooring wall interaction modeling, the modeling of an 11046 ton car-passenger ferry's motion close to the wall will be considered.

Three most illustrative situations will be looked into:

- the ship is proceeding parallel to an "endless" vertical wall, close to it;
- the ship is proceeding parallel to an "endless" vertical wall, at a larger distance from it;
- the ship is proceeding parallel to a "limited" vertical wall, close to it.

In all the three cases the ship is initially moving at a speed of 1 m/s, with a zero drift angle, parallel to the wall (on the manoeuvre diagrams, distances are specified in cables).

Fig 74. Modeling of an 11046 ton car-ferry's motion close to the wall

The manoeuvres shown above indicate that the a "longer" wall has a greater effect on the ship track; the closer the ship approaches the wall, the more its track changes; as the ship is sailing close to the wall, its track deviates from the wall, i.e., the model implements the aforementioned "free water" effect. The obtained results are in full conformance with ship handling practice.
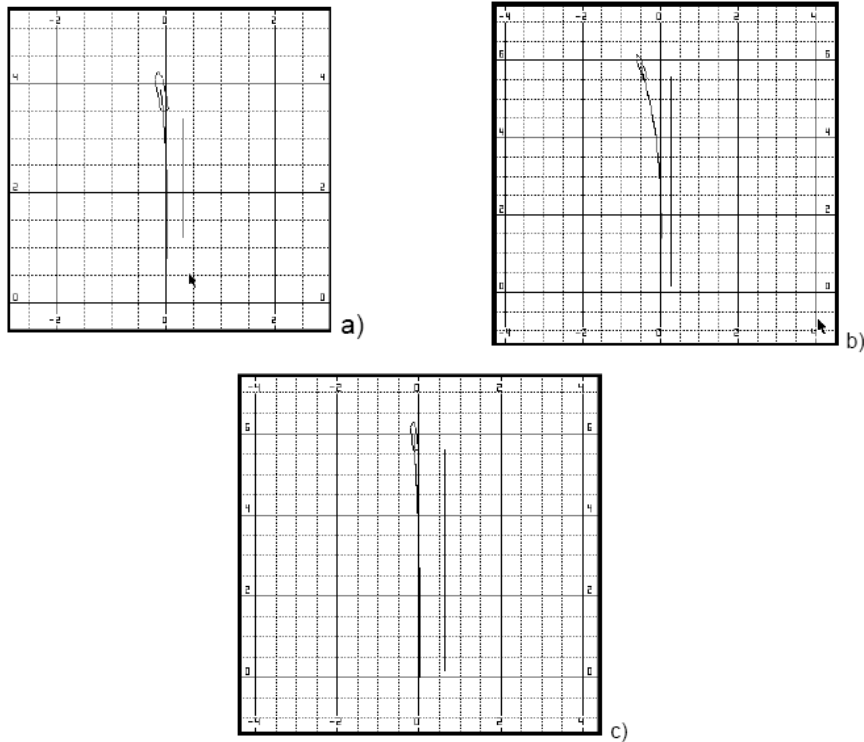
Examples of Comparing Modeling Results with the Results of Tank Testing

The quality of the ship/mooring wall interaction model has been checked by using the results of tank tests carried out for the radio-controlled model of a medium fish trawler.

Photographs of the model tank testing results are shown in Fig 75.

Fig 76 and Fig 77 show, for comparison purposes, tracks of the medium fish trawler model in the tank and results of mathematical modeling made for the motion of a seiner similar in dimensions to the model of the medium fish trawler.

Table 3. Principal dimensions and their ratios for the model of a medium fish trawler and a seiner

Model	L_{oa}	B_{oa}	T_f	T_a	L_{oa}/B_{oa}	B_{oa}/T_m
Seiner	54.7m	9.78 m	3.88 m	3.88 m	5.6	2.5
Medium Fish Trawler Model	650 mm	120 mm	48 mm	48 mm	5.4	2.5

For an easier comparison, ship motion coordinates on the diagrams are shown in relative units: hull lengths.
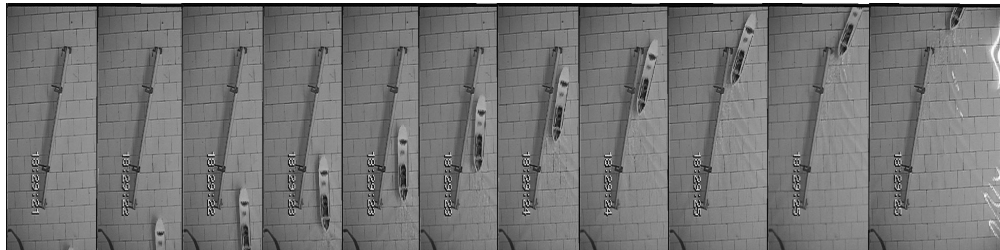
Fig 75. Photographs of tank testing results. Motion of the medium fish trawler model close to a vertical wall

a) b)
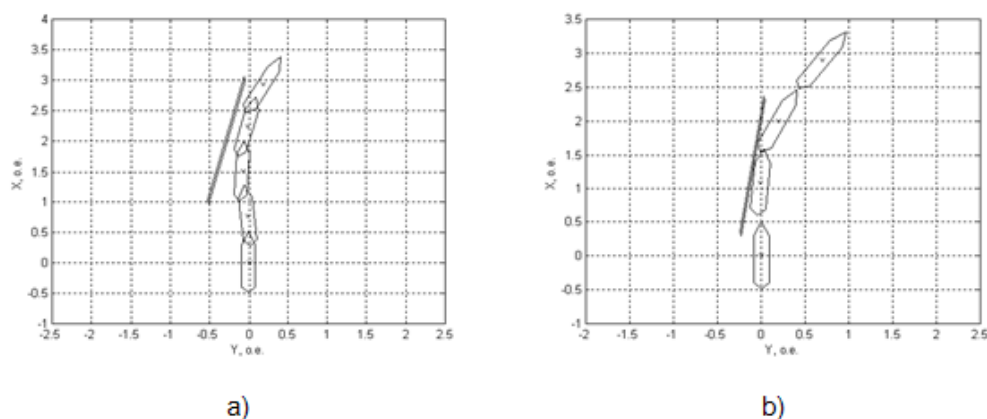
Fig 76. Motion of the medium fish trawler model to the starboard close to a rectilinear vertical wall: a) without touching the wall; b) with a touch

a)   b)
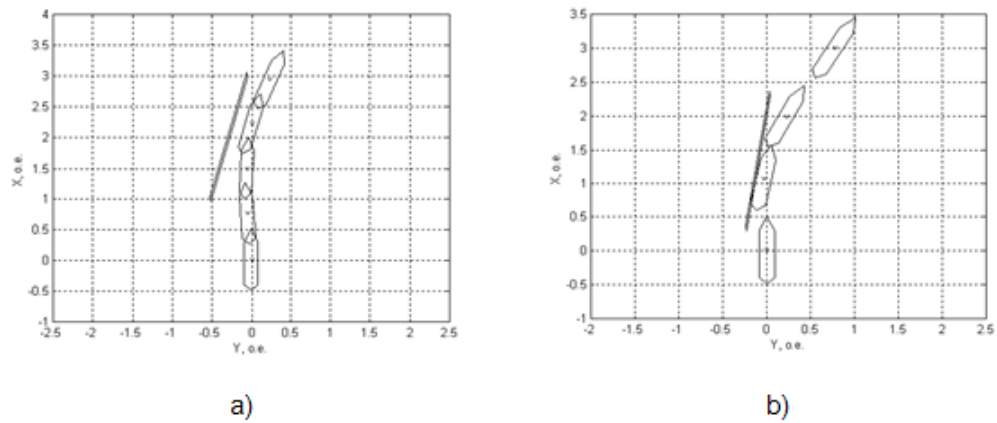
Fig 77. Results of mathematical modeling of seiner motion close to the mooring wall:

a) without touching the wall; b) with a touch

It can be seen from the comparison of tracks shown in Fig 76 and Fig 77 that there is a high-quality matching between the results of mathematical modeling and results of tank tests.

CURRENT

Introduction

In a mathematical model of ship motion, the current is set as steady liquid flow, variable in horizontal and vertical directions (see page 73). Parameters of the current are determined by the speed V_C and direction ψ_C of the current set in reference point on the chart. Such approach allows the ship's motion to be modeled in complex hydrographic conditions: at the bends of river beds and channels, and the port approaches and within the port areas with tidal currents, in the channel junction areas, etc.

To reduce the amount of information on the chart, parameters of a current are set in areas intended for conducting the exercises as shown in Fig 78 (the selected area is delineated with bold lines). There is no current beyond the selected area on the chart. In the selected area, current vectors are interpolated by the set reference points.
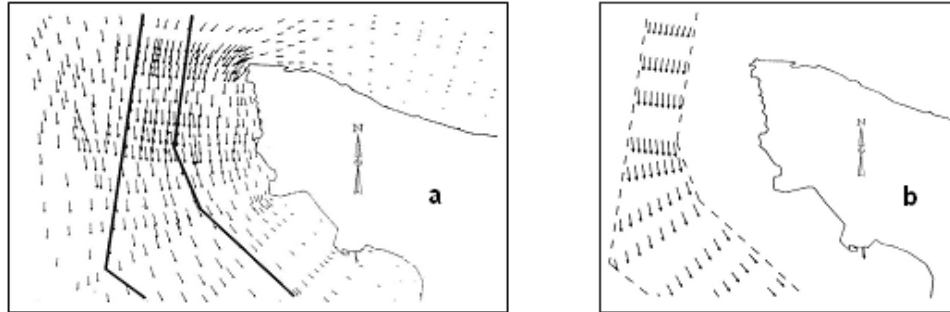

Fig 78. Example of setting currents in the vessel traffic area (b) on a general current chart (a)

Current Forces and Moments

Forces and moments originated by the currents are represented with two components in the mathematical mode. The first component is part of hydrodynamic forces and moments on the ship hull depending on the speed of current $\vec{V}_C$ in the origin of the ship axes system of reference. In this case, the speed of current is considered to be constant along the entire ship length. This component is taken into account in the ship motion equation in the part of hydrodynamic forces and moment on the hull. The second component takes into account the non-uniformity in the distribution of the current speed side component along the ship's length $v_C(x)$ (Y-component of current speed in body-fixed frame). The transverse force and swinging moment for this component are determined in accordance with the strip method (side force and yaw moment for this term/component are modeled according to a strip theory along the lines). So the total side force and yaw moment can be expressed as follows:

$$Y_C = -\frac{\rho}{2}\int\limits_{-l_a}^{l_f}T(x)C_{CFD}(x)\big(v_C(x)-v_C(0)\big)\big|v_C(x)-v_C(0)\big|dx\,;$$

$$N_C = -\frac{\rho}{2}\int\limits_{-l_a}^{l_f}T(x)C_{CFD}(x)\big(v_C(x)-v_C(0)\big)\big|v_C(x)-v_C(0)\big|xdx\,,$$

where l_a and l_f are length of afterbody and forebody, $T(x)$ is variable draft along the hull, $C_{CFD}(x)$ is variable cross-flow drag coefficient along the hull and $v_c(0)$ is side component of current speed in the origin of body-fixed frame. The cross-flow drag coefficient along the hull $C_{CFD}(x)$ is determined by calculation methods with regard to the shape of the ship frames. An algorithm has been implemented for the numerical integration of the side force and swinging moment as per the above expressions, and for determining the heeling moment K_C resulting from the current. The hull is divided into ten sections along its length (see Fig 79).
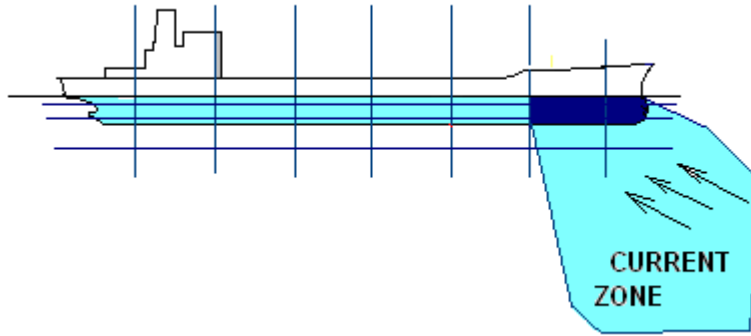

Fig 79. Ship hull in the current velocity flow varying in horizontal direction

Fig 80 and Fig 81 show a calculated sample of the autopilot-controlled ship passing through the area of a local crossflow (V_C=2 knots, ψ_C=90°– the flow area is shown with hatching).
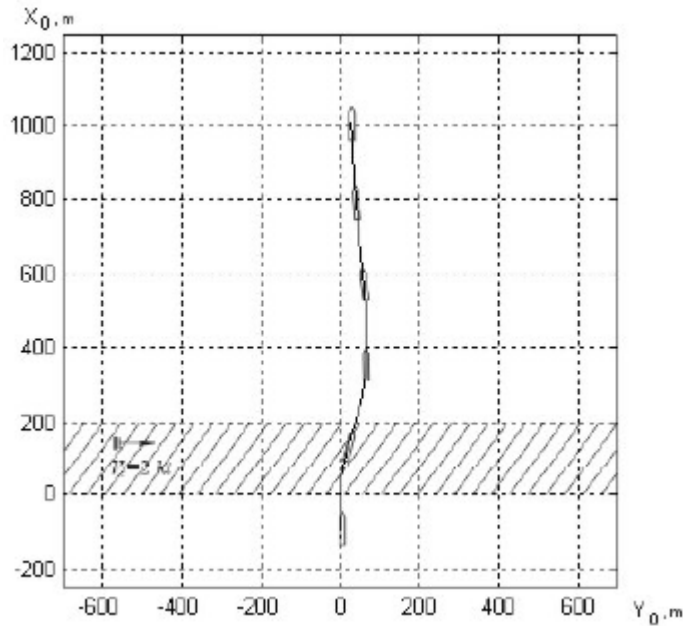
Fig 80. Autopilot-controlled ship passing through the local crossflow area

(simulated motion path)
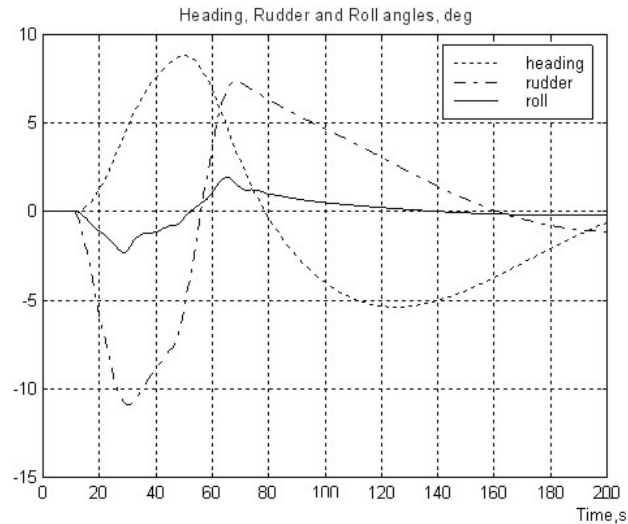
Fig 81. Changes of course, rudder angle and heel angle as the autopilot-controlled ship is

passing through the local crossflow area

Current Forces and Moments Due to Non-uniform Distribution of Current in the Vertical Directions

The latest version of current model accounts of the current velocity distribution and corresponding current forces acting on the ship hull in vertical direction. The program allows any numbers of sections exposed to local current loads along the ship draught. This model improvement provides more accurate calculation of the current forces and moments for vessels sailing in the variable in depth current field (Fig 82).
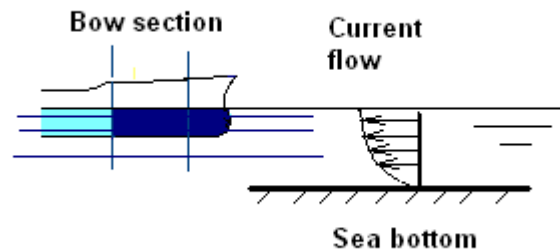
Fig 82. Ship hull in the current velocity flow varying in vertical direction

ANCHORS, MOORING LINES, MOORING BUOYS

Anchors

The mathematical model of the anchor chain effect consists of the anchor chain model, anchor motion model and the model of changes in the anchor chain length which includes the anchor winch model.

Mathematical Model of an Anchor Chain

An anchor chain is modeled as an elastic stretchable heavy thread. The shape and length l_{chn} of the chain are determined from the transcendental equation

$$T_{CHN}(l_{chn}, \xi_1, \zeta_1) = k_{chn} \frac{l_{chn} - L_{chn}}{L_{chn}},$$

where (ξ_1, ζ_1) are coordinates of the hawse in the anchor fixed frame (see Fig 83), L_{chn} is the length of unstretched chain, k_{chn} is the chain's elasticity coefficient, $T_{CHN}(l, \xi, \zeta)$ is a non-linear function determining the tension in the catenary curve along its length and coordinates of the end points.
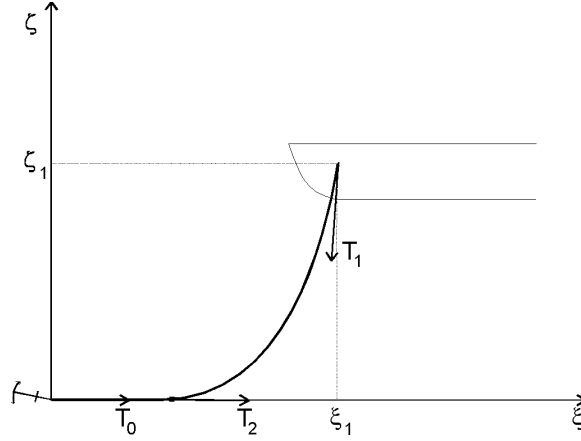
Fig 83. Anchor chain forces

The tensile stresses in the top and lowermost points of the chain are determined from a catenary curve equation

$$T_{1CHN}(l_{chn}, \xi_1, \zeta_1), \qquad T_{2CHN}(l_{chn}, \xi_1, \zeta_1),$$

Force T_{0CHN} acting on the anchor is determined by the sum of T_{2CHN}, and the cohesive force between the chain and the bottom. The tension force in the chain's top point T_{2CHN} is applied to the ship's hawser. It is reduced to $X_{CHN}, Y_{CHN}, Z_{CHN}$ forces and $K_{CHN}, M_{CHN}, N_{CHN}$ moments relative to the vessel's gravity center.

Mathematical Model of the Anchor Motion

The anchor motion is described with the following equation

$$m_{anch} \frac{dv_{anch}}{dt} = \begin{cases} X_{0CHN} - X_{ANCH} & \text{- if the vessel is moving} \\ 0 & \text{- if the vessel is immobile} \end{cases}$$

where m_{anch} is the anchor mass, X_{0CHN} is a projection of T_{0CHN} on ξ axis, $X_{ANCH} = -k_{anch}m_{anch}gv_{anch}/|v_{anch}|$ is the anchor holding power which has a nature of dry friction, g is gravity acceleration, k_{anch} is anchor holding power coefficient or friction coefficient which depends on the ground type, angle of the force application T_{0CHN}, as well as on the character of motion (static friction is greater than the motion friction). Dependence on the angle T_{0CHN} of force application has a non-linear character and is drastically reduced as the anchor chain reaches an angle at which the anchor is torn off from the holding ground.

Anchor holding power coefficients in dependence on anchor type and bottom ground type are shown in table below.

Table 4. Anchor holding power coefficients

Bottom ground type	Stokes anchor	Hall anchor	Gruson anchor	Standard Stockless Anchor
Rock	19	8.6	8.8	48
Gravel	17	8.2	8.4	45
Mud	16	6.8	7.0	43
Sand	9	2.5	2.7	32

Mathematical Model of Change in the Anchor Chain Length

The process of changes in the anchor chain length is described by the following equation

$$m_{chn}(L_{chn})\frac{dv_{chn}}{dt} = T_{1CHN} - F_{V\_CHN} - F_{F\_CHN} - F_{STP\_CHN} - F_{WINCH} \; ;$$

$$\frac{dl_{chn}}{dt} = v_{chn} \; ,$$

where m_{chn} – is mass of the hanging part of the chain, T_{1CHN} is tension of chain in the hawser, F_{V_CHN} is force of viscous friction of chain and anchor on the water, F_{F_CHN} is force of dry friction of chain in the hawser which depends on the chain's angle of inclination and the chain tensile stress, F_{STP_CHN} is stopping dry frictional force, F_{WINCH} is force from the anchor winch.

The winch is operating in the heaving mode and ensures the set rate of heaving the anchor chain, the winch's limited power taken into account.

Mooring Lines

Calculation of forces from the mooring lines use a mathematical model of a mooring line as an elastic stretchable thread, as well as a mathematical model of the winch and a model of mooring line/mooring gear interaction.
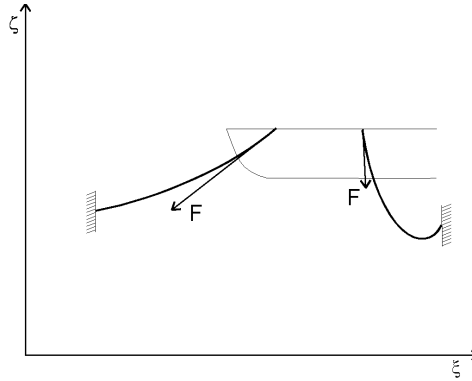
Fig 84. Mooring line forces

The mathematical model of mooring line/mooring gear interaction allows modeling of:

• break of a rigidly fastened mooring line when the limit tensile stress is exceeded;

• free heaving;

• picking up the slack on the mooring line.

The mathematical model of a mooring winch allows: heaving a mooring line at a permanent speed (the winch power taken into account); providing a set stress of the mooring line.

A mooring line is modeled as an elastic stretchable heavy thread with sag. The transient oscillatory processes or the wind effect are not taken into account. The force acting on the vessel from the side of a mooring line is calculated on the assumption of the line's spatial configuration along a catenary curve, with the mooring line's non-linear elasticity stretching determined by the following expression:

$$F_{ML} = F_{ML}(r_{1ml}, r_{2ml}, l_{ml}) = \Phi(\varepsilon),$$

where: r_{1ml}, r_{2ml} are vectors setting the coordinates of mooring line fastening points, l_{ml} is length of heaved mooring line, ε is relative stretching of the mooring line.

Fig 85. Rope nonlinear force

A view of Φ (ε) function is shown in Fig 85. The stretching modeling uses a non-linear dependence of the tensile stress on a linear zone, saturation zone and break zone. A 3-D configuration of a mooring line (Fig 84) is determined from the catenary curve equation.

Mooring Buoys

There are mathematical models of two types of mooring buoys: Single Anchor Leg Mooring (SALM) and Catenary Anchor Leg Mooring (CALM) for the solution of problems of mooring to a buoy.
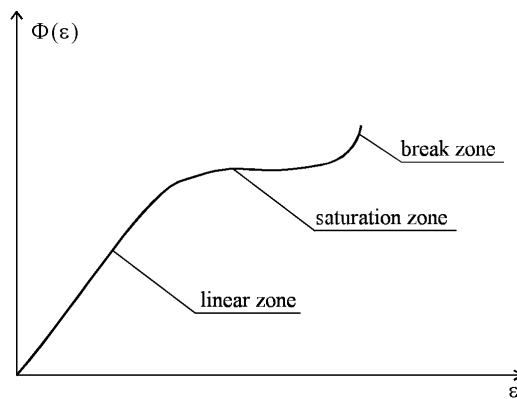
SALM. The buoy is fixed on a single "dead" anchor so that it is oriented vertically. The buoy has two degrees of freedom, for the generalized coordinates the buoy's deviation from the anchor in a horizontal plane $(\vec{r}_{mb})$ is used. When a buoy deviates from the origin of coordinates, due to the presence of the anchor chain it sinks a bit thus originating buoyancy force which ensures the anchor cable tension. The projection of the tensile stress on the horizontal plane is directed from the buoy to the origin of coordinates and is in fact the buoy's restoring force which is determined by the following expression:

$$\vec{F}_{REST\_MB} = \vec{F}_{REST\_MB}(\vec{r}_{mb}, h, h_w),$$

where $\vec{r}_{mb}$ is the buoy's deviation from the anchor; h is sea depth, h_w is wave ordinate, F_{RES_MB} .is part from the restoring force.

The force of hydrodynamic resistance caused by the buoy's motion and current is described by the following equation:

$$\vec{F}_{RES\_MB} = -0.5\rho C_{Xmb} S_{mb} (\vec{v}_{mb} - \vec{v}_c)|\vec{v}_{mb} - \vec{v}_c|,$$

$$\frac{d\vec{r}_{mb}}{dt} = \vec{v}_{mb},$$

where ρ is water density; S_{mb} is an area of side projection of the submerged part of the buoy, C_{Xmb} is hydrodynamic resistance coefficient, v_{mb} is the buoy's speed, v_c is the speed of the current.

As a result, the equation of SALM motion looks as follows:

$$m_{mb} \frac{d\vec{v}_{mb}}{dt} = \vec{F}_{REST\_MB} + \vec{F}_{RES\_MB} + \vec{F}_{ML},$$

where m_{mb} is the mass of the buoy.

CALM is a cylindrical buoy fit with the anchor chains with "dead" anchors on the ends. The number of modeled anchors may be from 4 to 8. The mathematical model describes motion in the vertical and horizontal planes. The rotation around the vertical axis and the motions in the list and trim angles are not modeled.
The following factors are taken into account in the modeling.

• external force from the mooring line;

• speed and direction of current;

• sea state.

Equations of a Buoy's Motion in a Vertical Plane

The buoy is affected by the following forces:

1. Vertical component of the anchor chains' tensile stress:

$$Z_a = \sum_{i=1}^{n} Z_i ,$$

   where $Z_i = Z(l_{i\_chn}, \varsigma_{mb} - \varsigma_{i\_anch}, \xi_i)$ is a vertical projection of the anchor chain tensile stress determined by the chain length l_i, vertical $\varsigma_0 - \varsigma_{ai}$ and horizontal ξ_i distances between the buoy's gravity centre and the anchor. Calculations of vertical and horizontal projections of the anchor chain tensile stresses use the mathematical model of the chain as a heavy stretchable thread.

2. Buoy's buoyancy force:

$$Z_{B\_MB} = -g\rho S_{mb}(T_{mb}(\varsigma) - T_{0mb} + h_w) ,$$

   depending on the difference between the current T_{0mb} and static $T_{mb}(\varsigma)$ drafts, and on the wave ordinate.

3. The force of hydrodynamic resistance to the motion in the vertical plane.

   Due to the negligible magnitude of the buoy's vertical speed, the hydrodynamic resistance is considered to be linear:

$$Z_{RES\_MB} = \rho C_{Zmb} S_{mb} \left(\frac{d\varsigma}{dt} - \frac{dh_w}{dt}\right) .$$

   As a result, the mathematical model of the buoy's vertical motion is described by the following equation:

$$m_{mb}\frac{d^2\varsigma}{dt^2} = Z_{B\_MB} + \sum_{i=1}^{n} Z_i - Z_{RES\_MB} .$$

Equations of Buoy's Motion in a Horizontal Plane

A buoy's motion in the horizontal plane is described in the fixed coordinate system whose origin is in the buoy's gravity center in the equilibrium position. Each of n anchors has $\vec{r}_{i\_anch}$ coordinates and l_{i_anch} chain length. As the buoy deviates from the origin of coordinates $\vec{r}_{mb}$, there is a change in the anchor chain configuration, and a resulting force is originated: the sum of horizontal components of the chains tensile stresses. The resulting force is directed towards the origin of coordinates and is a restoring force

$$F_{REST\_MB} = \sum_{i=1}^{n} \frac{\vec{r}_{i\_anch} - \vec{r}_{mb}}{\left|\vec{r}_{i\_anch} - \vec{r}_{mb}\right|} Z(l_{i\_chn}, \varsigma_{mb} - \varsigma_{i\_anch}, \left|\vec{r}_{i\_anch} - \vec{r}_{mb}\right|) ,$$

where $Z(l_{i\_chn}, \varsigma_{mb} - \varsigma_{i\_anch}, \left|\vec{r}_{i\_anch} - \vec{r}_{mb}\right|)$ is a horizontal component of the anchor chain tensile stress.

Apart from the restoring force, modeling takes into account the mooring line's tensile stress F_{ML} and the hydrodynamic resistance force:

$$\vec{F}_{RES\_MB} = -0.5\rho C_{Xmb} S_{mb} (\vec{v}_{mb} - \vec{v}_c) \left| \vec{v}_{mb} - \vec{v}_c \right|.$$

As a result, the mathematical model of a buoy's motion in the horizontal plane looks as follows:

$$m_{mb} \frac{d\vec{v}_{mb}}{dt} = \vec{F}_{REST\_MB} + \vec{F}_{RES\_MB},$$

$$\frac{d\vec{r}_{mb}}{dt} = \vec{v}_{mb}.$$

SHIP MOTION CONTROL SYSTEMS

Autopilot

The mathematical model of the ship's motion includes an autopilot with characteristics described below.

Control modes:

- Stabilization of the set course;

- Turning in to a new course. In this mode, the autopilot turns the ship smoothly onto a new course at a set rate of turn.

Settings:

- Maximum rudder angle: Rudder Lim 0…35°;

- Maximum course deviation: Course Lim 5…30°. When this deviation is exceeded, "Alarm" indicator lights up, in case of triple deviation, the autopilot switches to "Manual" mode;

- Set rate of turn (when steering to a new course): 0…240°/min;

- Sensitivity 1…10.

Alarms:

- Course error beyond the set limits ("Off Course");

- Speed is too low: the rudder is ineffective ("LowShipSpeed").

Control algorithms:

- Algorithm for ship stabilization on the set course ("stabilizing course control") allows the number of rudder-over to be minimized when sailing on the rough sea. This algorithm is based on the PID law with the wave disturbance filtration. This algorithm is parameterized with a single parameter which is "sensitivity", rather than with three like in most of the autopilots, allowing an easy trimming;

- Algorithm for steering to a new course ("manoeuvring course control") develops the required rate of turn so as to ensure this switchover without re-adjustment. This algorithm is activated automatically as a new course is entered.

Dynamic Positioning System

The operation of the Dynamic Position (DP) System is related to the fundamental ship axes of horizontal motion – surge (alongship), sway (athwartship) and yaw (rotation around the selected rotation point). By automatic control of the propulsion system, thruster forces in surge and sway as well thruster moment in yaw will be applied in order to achieve the desired vessel motion, position, heading or path. DP System principles overview is illustrated on Figure below.

Ship Motion Control Systems
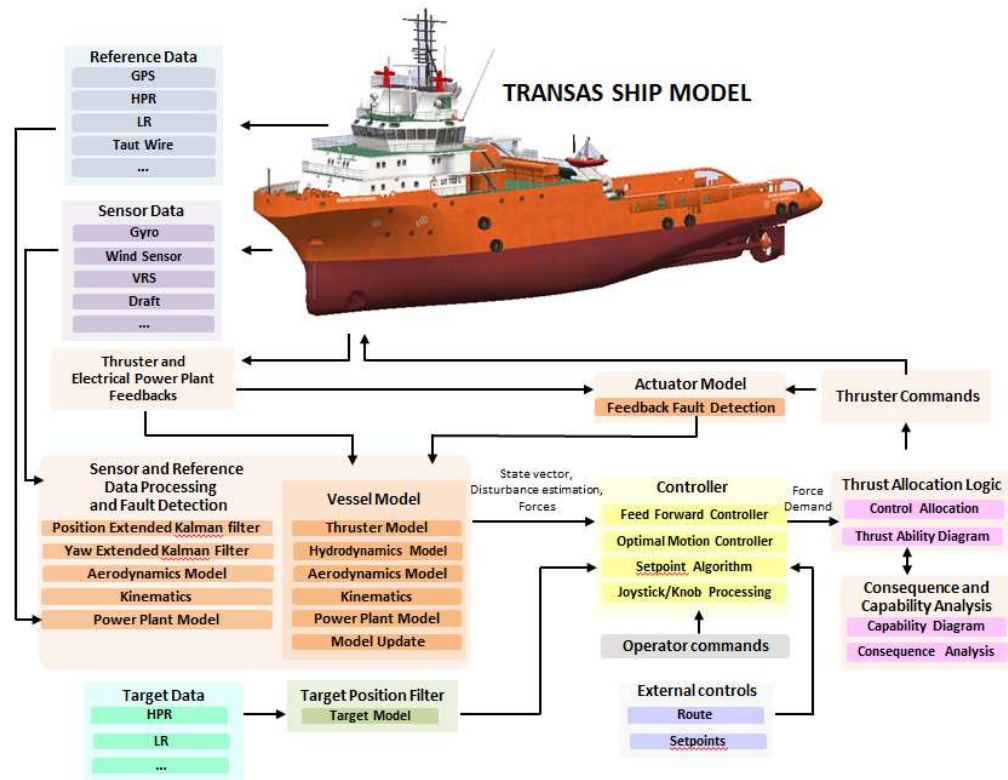
## The List of Transas Ship Models with On-Board Dynamic Positioning System

Name	Image	Displ. (t)	Dimensions (Loa x B x Tmax)	Design Power (kW)	Service Speed (knots)	Propeller	Rudder	Thrusters, Bow/Stern (kW)
OSV1		5334	79.3 x 18.3 x 5.2	Diesel, 2 x 2530	14.5	2 CPP	1 Suspended rudder	2 x 880 / 2 x 468
OSV2		4179	66.5 x 16.8 x 5.2	Diesel, 2 x 1771	13.20	2 Azimuth FPP	–	1 x 716 / –
OSV3		5291	80.4 x 18 x 6.6	Diesel, 2 x 6166	16.2	2 CPP in nozzles	2 Becker rudders	1 x 883, 1 x 1120 drop-down / 1 x 883
OSV5		8637	87.7 x 20.1 x 6.4	Diesel, 2 x 2797	14	2 CPP	2 Schilling rudders	1 x 1120, 1 x 880 drop-down / 1 x 1120
OSV6		5500	85.3 x 18.2 x 4.88	Diesel, 2 x 2685	12.4	2 CPP	2 Schilling rudders	1 x 1400, 1 x 810 swing-down / 1 x 1400
OSV7		4040	73.1 x 17 x 4.57	Diesel, 2 x 1193	12.8	2 Azimuth FPP	–	1 x 236, 1 x 883 drop-down / –
OSV9		5291	80.4 x 18 x 6.6	Diesel, 2 x 6166	16.2	2 CPP	2 Becker rudders	1 x 883, 1 x 1120 swing down / 1 x 883
OSV11		5291	80.4 x 18 x 6.6	Diesel, 2 x 3500	16.2	2 Azimuth FPP	–	1 x 883, 1 x 1120 drop down / 1 x 883
FSV1		812.7	53.3 x 10.4 x 2.9	Diesel, 4 x 1342	23	4 FPP	2 Suspended rudders	Azimuthal 1 x 186.4 / –
Shuttle Tanker 1		160529	277.4 x 46 x 15.85	Diesel, 1 x 16870	17	1 CPP	1 Schilling rudder	1 x 2200, Azimuthal 1 x 2200 / Azimuthal 1 x 2200
Shuttle Tanker 1		118133	277.4 x 46 x 12.4	Diesel, 1 x 16870	17.9	1 CPP	1 Schilling rudder	1 x 2200, Azimuthal 1 x 2200 / Azimuthal 1 x 2200
Shuttle Tanker 1		75737	277.4 x 46 x 8.91	Diesel, 1 x 16870	18.7	1 CPP	1 Schilling rudder	1 x 2200, Azimuthal 1 x 2200 / Azimuthal 1 x 2200
Semi Submersible 1		35700	130 x 79.6 x 10	Diesel, 4 x 4100	10	4 Azimuth FPP	–	–

ANNEX

COMPARISON OF TRANSAS SIMULATIONS AND SEA TRIAL TEST RESULTS

Ship Particulars

|	
Ship type	Fisher
Loading condition	full load
Displacement, t	1676.3
Number of main engines	1
Power of main engines, kW	840
Service speed, knots	12.6
Length overall, m	65.5
Length waterline, m	61.1
Breadth overall, m	10.4
Draft forward, m	3.9
Draft after, m	5.4
Type of propellers	FPP
Number of propellers	1
Diameter of propeller, m	3.5
Direction of propeller rotation	right
Number of rudders	1
Area of rudder, m^2	7.1
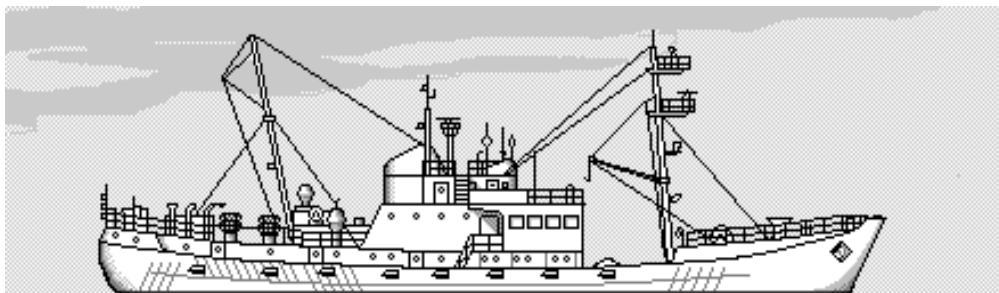
Turning Manoeuvring Characteristics. Turning 5 Degrees Starboard

Turning manoeuvring characteristics are shown in the table below:

Initial speed, m/s	5.3			
Rudder angle, deg			5	
Course, deg	90	180	270	360
Time, s	207.0	405.0	602.5	800.5
X, m	721.5	123.3	-538.0	60.1
Y, m	601.1	1263.5	666.6	3.9
Speed V, m/s	5.0			
Steady drift angle, deg	3.1			
Diameter of steady turning, m	1191.8			
Ship speed at steady turning, m/s	5.0			
Maximum X, m	688.1			
Maximum Y, m	1195.0			

Turning circles trajectories at 5 degrees of rudder angle, port and starboard, are shown in the figures below:
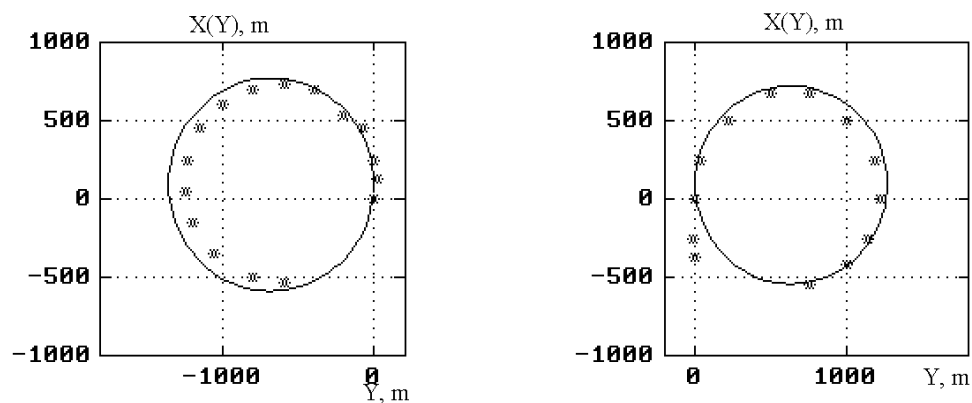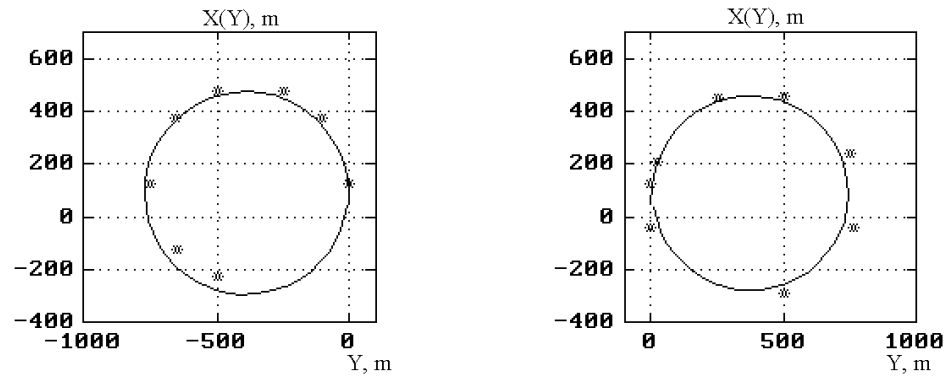

Sea trials data is marked with '*'.

Turning Manoeuvring Characteristics. Turning 10 Degrees Starboard

Turning manoeuvring characteristics are shown in a table below:

Initial speed, m/s	5.3			
Rudder angle, deg	10			
Course, deg	90	180	270	360
Time, s	124.5	240.5	356.5	472.5
X, m	439.6	121.7	-256	60.6
Y, m	325.3	703.6	386.2	7.7
Speed V, m/s	4.7	4.7	4.7	4.7
Steady drift angle, deg	5			
Diameter of steady turning, m	698.6			
Ship speed at steady turning, m/s	4.7			
Maximum X, m	440.9			
Maximum Y, m	704.9			

Turning circles trajectories at 10 degrees of rudder angle, port and starboard, are shown in the figures below:
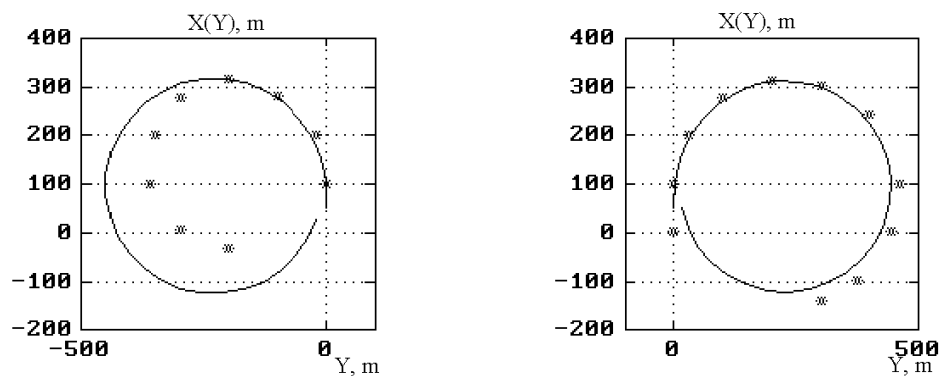

Sea trials data is marked with '*'.

Turning Manoeuvring Characteristics. Turning 20 Degrees Starboard

Turning manoeuvring characteristics are shown in a table below:

Initial speed, m/s	5.3			
Rudder angle, deg	20			
Course, deg	90	180	270	360
Time, s	84.0	160.0	236.5	312.5
X, m	301.6	124.5	-111.	65.9
Y, m	188.3	423.9	246.4	12.6
Speed V, m/s	4.4	4.3	4.3	4.3
Steady drift angle, deg	7.8			
Diameter of steady turning, m	415.4			
Ship speed at steady turning, m/s	4.3			
Maximum X, m	303.5			
Maximum Y, m	425.9			

Turning circles trajectories at 20 degrees of rudder angle, port and starboard, are shown in the figures below:


Sea trials data is marked with '*'. In port turning the trial measurements were subjected to the effects of environment.

Turning Manoeuvring Characteristics. Turning 30 Degrees Starboard

Turning manoeuvring characteristics are shown in a table below:

| Initial speed, m/s	5.3			
Rudder angle, deg	30			
Course, deg	90	180	270	360
Time, s	69.5	130.0	190.5	251.1
X, m	253.0	131.4	-41.7	78.0
Y, m	135.2	310.7	190.3	17.1
Speed V, m/s	4.0	3.9	3.9	3.9
Steady drift angle, deg	10.4			
Diameter of steady turning, m	298.2			
Ship speed at steady turning, m/s	3.9			
Maximum X, m	255.4			
Maximum Y, m	313.0			

Turning circles trajectory at 30 degrees of rudder angle, starboard, is shown
in the figure below:
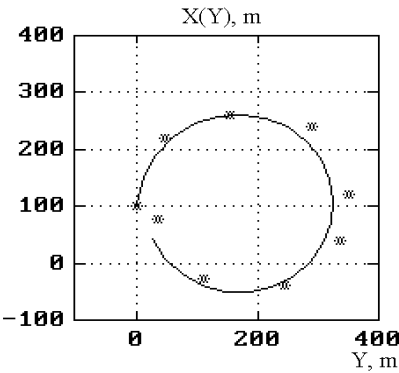
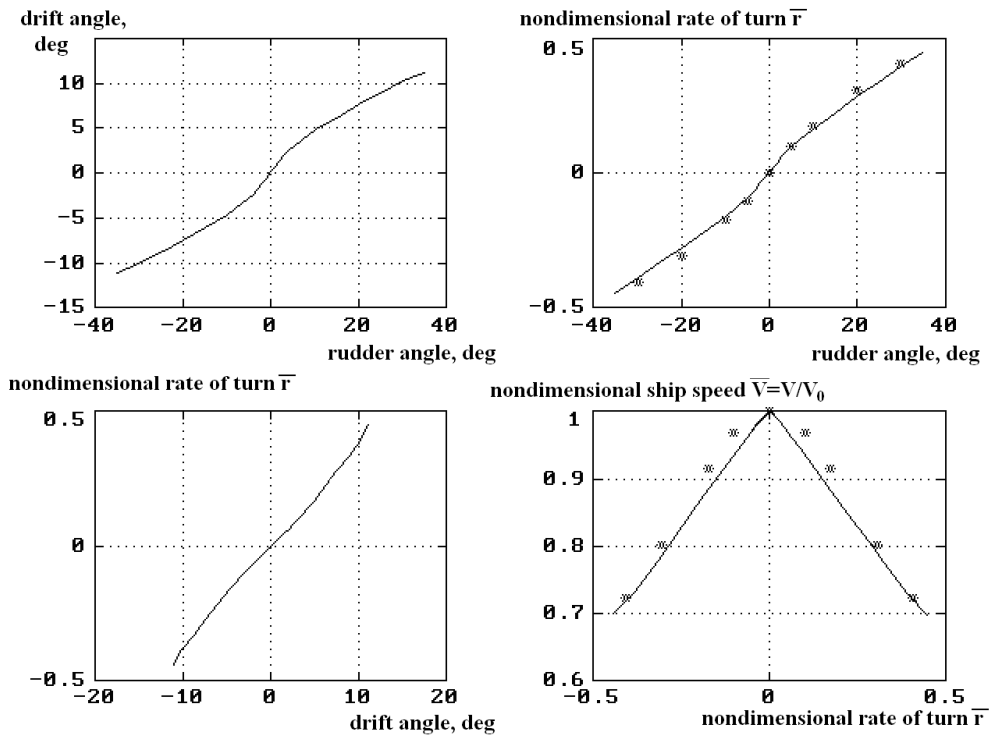Sea trials data is marked with '*'.

Pull Out Manoeuvre

In forward motion the ship is stable. Results of the pull out manoeuvre are shown in
the figure below:
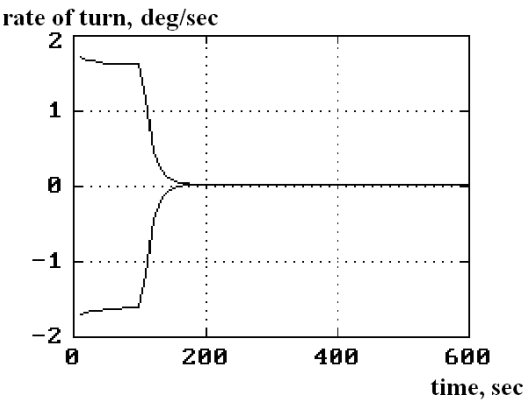
Controllability Diagram

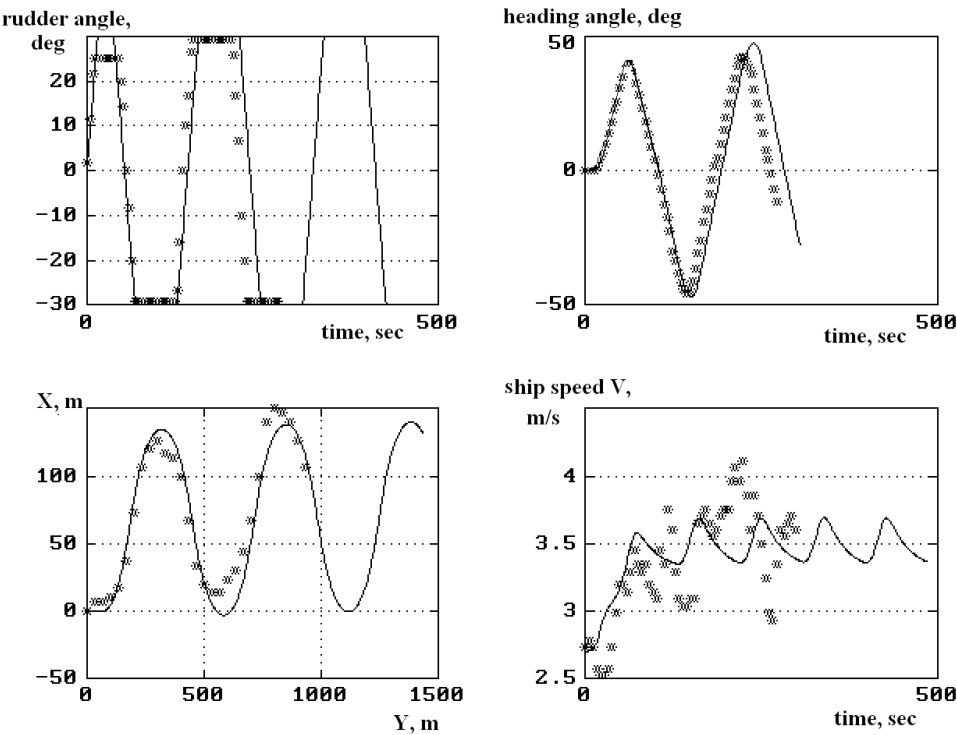Controllability diagram in deep water is shown in the drawings below:

Sea trials data is marked with '*'.

"Zigzag" Manoeuvre

Manoeuvring characteristics of right 10-10, 20-20, and 30-30 Zigzag Manoeuvres are shown in the table below:

	Rudder angle, deg		
	10	20	30
Period, s	105	130	162
Maximum heading angle value, deg	15.5	32.2	49
Maximum drift angle value, deg	5.0	7.8	10.4

The predicted and measured results of the right 30-30 Zigzag Manoeuvre are shown on the figures below, initial conditions are as follows: initial ship speed is 2.7m/s, telegraph order is at Half Ahead:

Sea trials data is marked with '*'.